UNITED STATES DEPARTMENT OF THE INTERIOR

GEOLOGICAL SURVEY

Examples of Active Faults in the Western United States: A Field Guide

By

Robert C. Bucknam *and* Kathleen M. Haller

Open-File Report 89-528

Prepared in cooperation with the International Geological Correlation Program
Project 206 -- A Worldwide Comparison of the Characteristics of Major Active Faults

Co-organizers: Robert C. Bucknam, U.S. Geological Survey, U.S.A.
Ding Guoyu, State Seismological Bureau, PRC
Zhang Yuming, State Seismological Bureau, PRC

Denver, Colorado

1989

CONTENTS

TABLES

FIGURES

Examples of Active Faults in the Western United States -- A Field Guide

By Robert C. Bucknam *and* Kathleen M. Haller

INTRODUCTION

This field guide has been prepared as a part of the final meeting of International Geological Correlation Program (IGCP) Project 206--"A Worldwide Comparison of the Characteristics of Major Active Faults." IGCP is a joint undertaking of the International Union of Geological Sciences (IUGS) and the United Nations Educational, Scientific and Cultural Organization (UNESCO). The project was begun in 1984 to synthesize current knowledge on the characteristics of selected major active faults on a worldwide basis. Major active faults undergoing contemporary or geologically recent deformation are a focus of study in many parts of the world, and studies of these faults provide critical insight into the nature and rates of tectonic processes. As potential seismogenic sources, active faults are major keys to the evaluation of seismic hazards of the regions in which they occur.

This field trip provides an opportunity to observe a variety of active faults occurring in diverse geologic environments in the Western United States. Many of these faults have undergone displacements in historic time in a generally semi-arid climate, which results in frequently spectacular preservation of geomorphic features associated with active faults. The trip begins at the western margin of the North American plate, traverses the Basin and Range province, and ends at the boundary between the Basin and Range and Middle Rocky Mountains-Colorado Plateaus provinces (fig. 1-1*B*), passing through portions of the most seismically active regions of the United States (fig. 1-2).

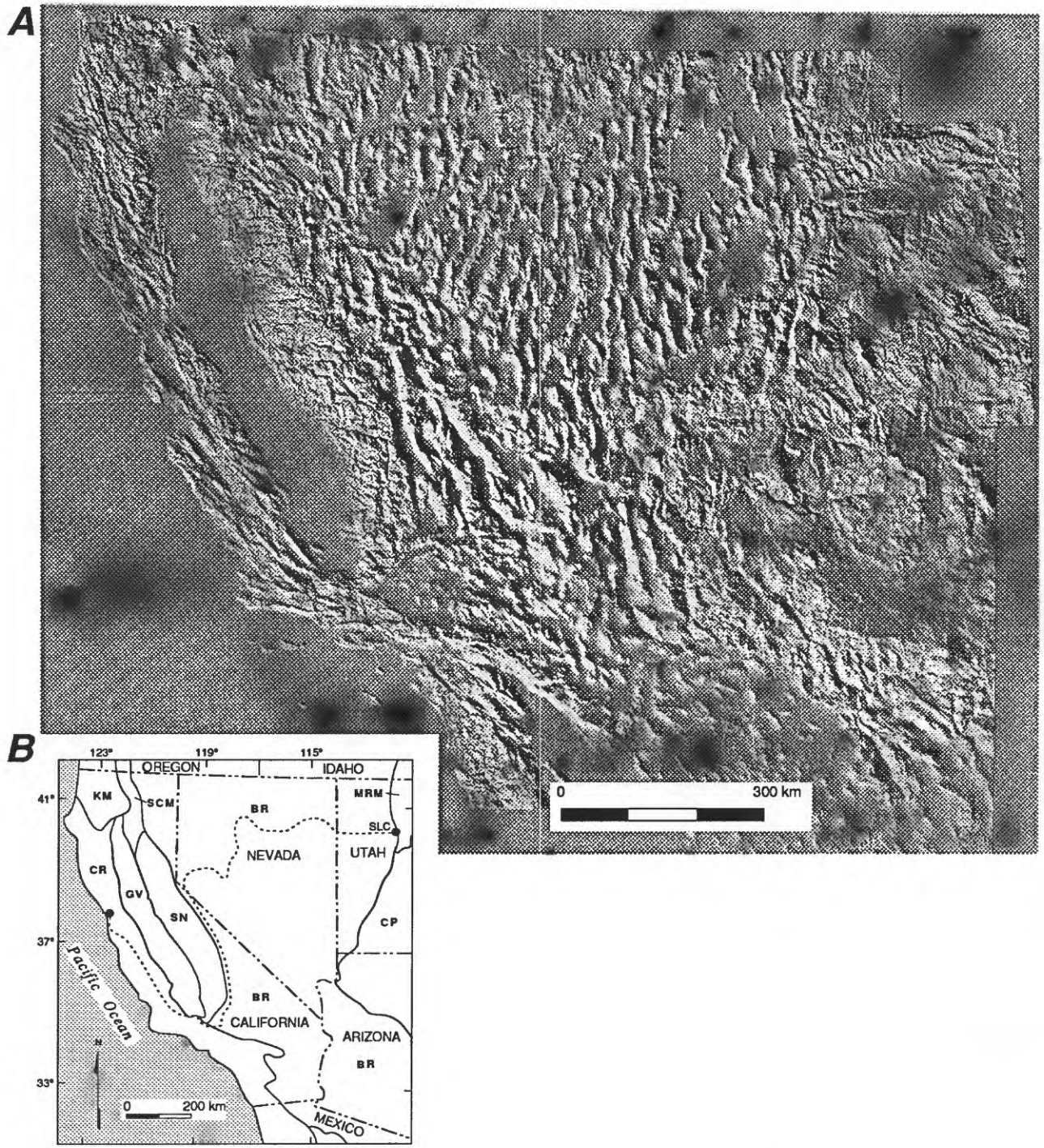

Figure 1-1. ***A***, Computer-generated shaded relief map of region along field-trip route. The map was produced from digital elevation data using method described by Batson and others (1975). Courtesy of Gerald Schaber, U.S. Geological Survey, Flagstaff, Arizona. ***B***, Physiographic provinces of the Western United States. Field-trip route shown by dashed line with dot at ends, San Francisco (SF) and Salt Lake City (SLC). Province shown are Basin and Range (BR), Colorado Plateaus (CP), Coast Ranges (CR), Great Valley (GV), Klamath Mountains (KM), Middle Rocky Mountains (MRM), Southern Cascade Mountains (SCM), and Sierra Nevada (SN).

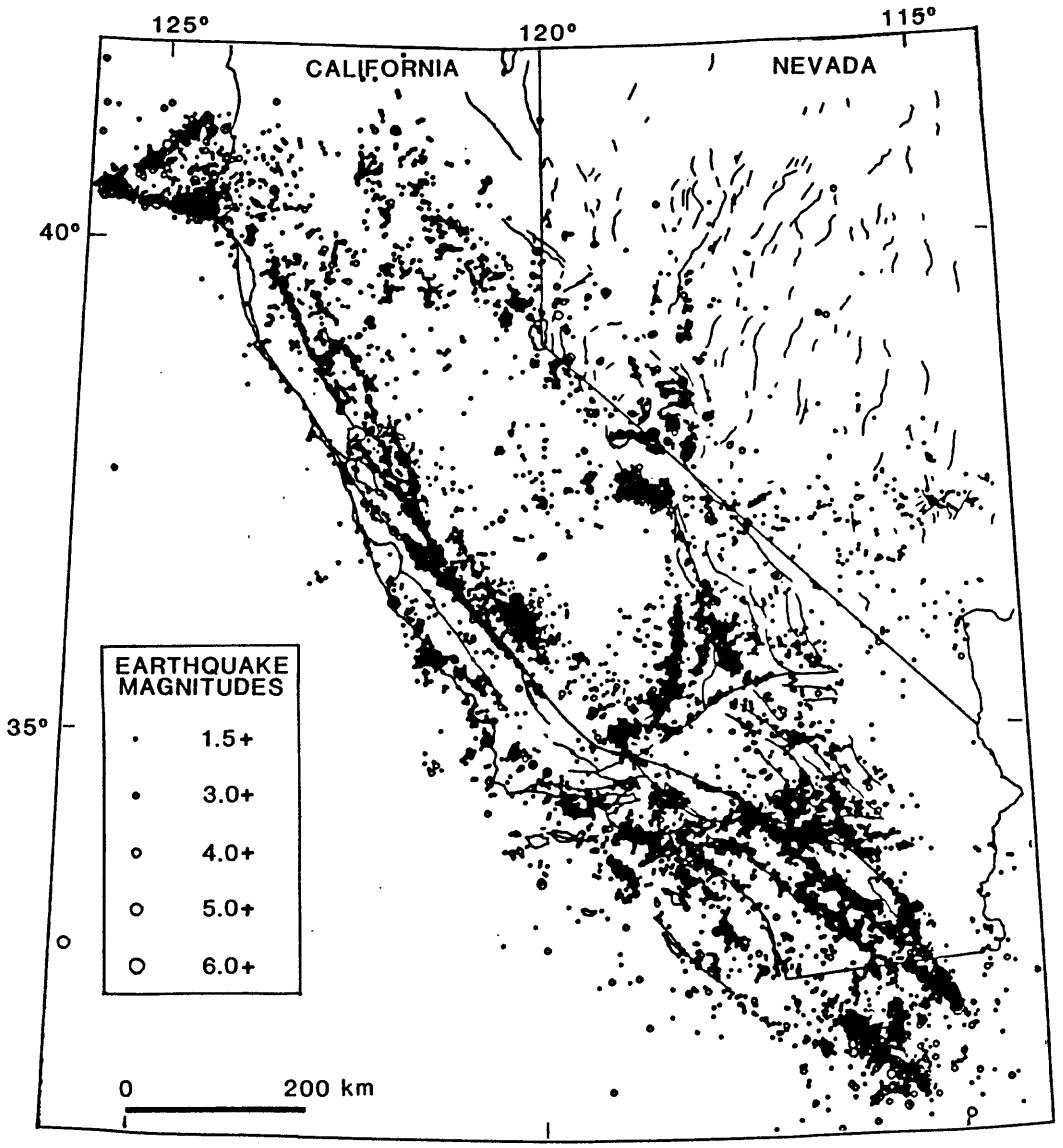

Figure 1-2. Earthquakes (M > 1.5) in California and Nevada, 1980 - 1984 (from Hill and Eaton, 1987).

DAY 1--SAN BRUNO TO PASO ROBLES, CALIFORNIA

Summary

During the first two days through the California Coast Ranges (fig. 1-1) the field trip will focus on the geomorphic expression of the fault, its geologic setting, and historic deformation along the San Andreas and other major active faults in the region. The trip starts near the locality for which the San Andreas fault was named by Lawson (1895), close to the epicenter of the 1906 San Francisco earthquake, and follows the fault nearly 300 km southeasterly to the Parkfield-Cholame area, site of a major ongoing experiment in earthquake prediction.

Tectonic Setting of the San Andreas Fault

Many important geologic relations in the Coast Ranges are closely linked to the evolution of the San Andreas fault, and an understanding of many important characteristics of the present behavior of the San Andreas fault ultimately depends on an understanding of the local and regional geologic setting of the fault. Current models of the evolution of the continental margin of California view the presently active San Andreas fault as an integral feature of the evolving margin between the North American and Pacific plates. Many of the stages in the evolution of the California continental margin also were critical in the evolution of areas far to the east, in the region of the present Great Basin. Because the focus of this trip is on active faults, only brief summaries of some major elements of the regional geologic setting are given in this guidebook to provide an appropriate context for more detailed discussions at individual stops. For an extensive review of the tectonic evolution of the region refer to papers in Ernst (1981) and the extensive bibliography of that work.

The North American continental margin in California has evolved through four basic types of tectonic configurations since late Precambrian time (fig. 1-3) as summarized by Dickinson (1981). The San Andreas transform system formed during the last of these four stages, and intraplate deformation during this fourth stage also produced the Basin and Range province.

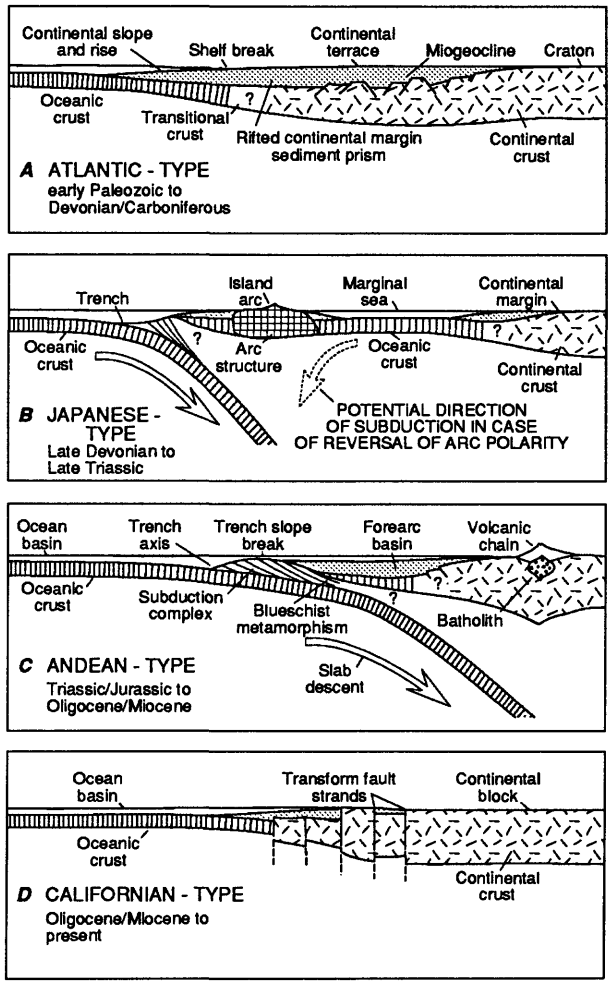

Figure 1-3. Basic continental-margin tectonic regimes which have affected California continental margin (modified from Dickinson, 1981). ***A***, An Atlantic-type passive margin was present following rifting in late Precambrian time. ***B***, A Japanese-type margin, characterized by offshore island arcs, formed in Late Devonian time. Extensive eugeosynclinal terranes of the western Cordillera were accreted to the continent during the Antler and Sonoma orogenies (discussed under Day 7) while this tectonic regime was active. ***C***, An Andean-type margin, which formed in Late Triassic - Early Jurassic time, was part of a circum-Pacific subduction system. Most of the California Coast Ranges terrane was accreted while this type of margin was active. ***D***, A California-type margin, characterized by a transform boundary between ocean-basin and continental rocks, began to form in early Neogene time (see fig. 1-4) and is the present continental-margin tectonic regime. Intraplate deformation during Neogene time also formed the Basin and Range province to the east. Reprinted by permission of Prentice Hall, Inc., Englewood Cliffs, New Jersey.

The major rock units of the California Coast Ranges, the Franciscan complex and the Great Valley sequence, and the Sierran rocks to the east, are regarded as related elements of a late Mesozoic arc-trench system that was oriented roughly parallel to the present California coast. Subduction of sea-floor lavas and sediments produced the melanges and sheared rocks of the Franciscan complex, whereas sedimentation of detritus derived from volcanic and plutonic rocks produced the largely coeval Great Valley sequence (Dickinson and Rich, 1972; Dickinson, 1981). The Sierra Nevada batholith is the intrusive root of a magmatic arc associated with the arc-trench system. Tectonic events in Paleogene time reflect a change in character of the subduction, perhaps reflecting a decrease in dip of the subduction zone. Although abundant Paleogene clastic sediments in the Franciscan indicate that subduction continued, magmatism in the Sierra Nevada ceased by this time (Dickinson, 1981). By Miocene time the Pacific and American plates came into contact as the intervening Farallon plate was subducted under the continental margin (fig. 1-4*B*), and strike-slip movement began on the San Andreas transform (Atwater, 1970). Dickinson (1981) points out that during Miocene time much of the transform movement was on faults other than the San Andreas fault, probably offshore, but since Pliocene time the transform movement has been primarily along the presently active trace of the San Andreas fault.

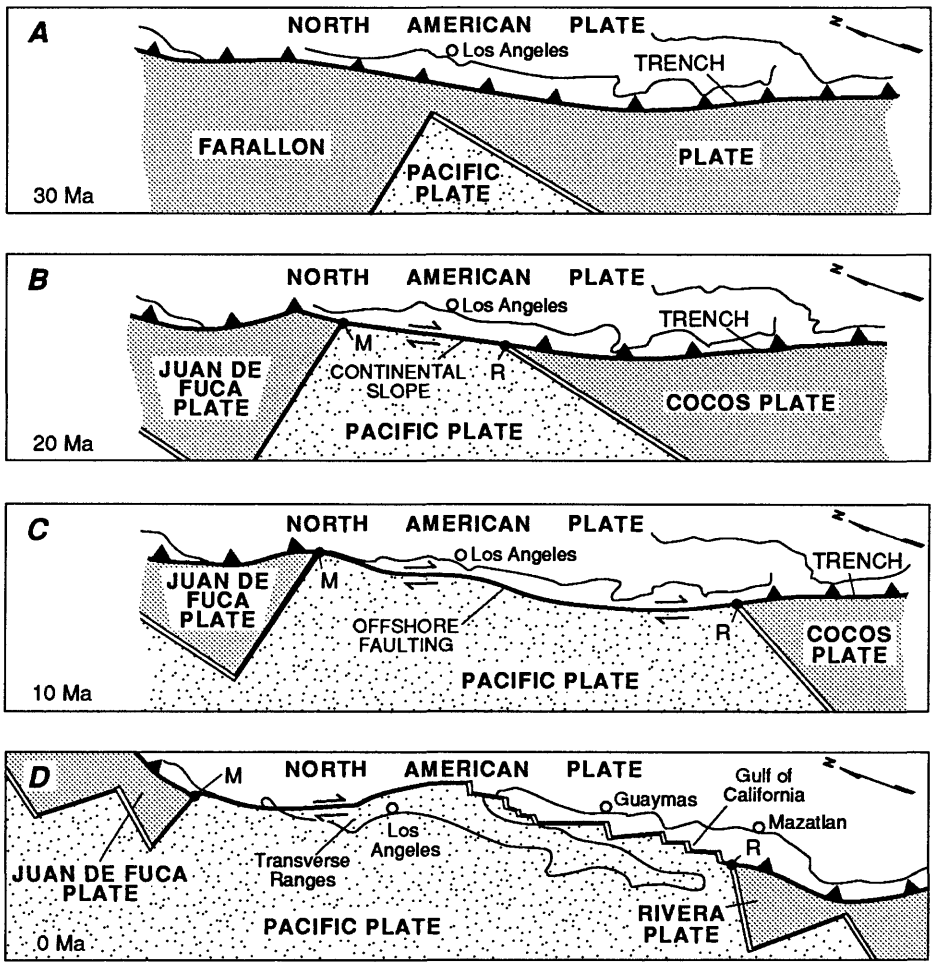

Figure 1-4. Evolution of the San Andreas fault since 30 Ma (modified from Dickinson, 1981). Heavy lines are faults, double lines are spreading ridges, fine lines are continental margin, and M and R are Mendocino and Rivera triple junctions, respectively. Reprinted by permission of Prentice Hall, Inc., Englewood Cliffs, New Jersey.

Within the California Coast Ranges the San Andreas fault juxtaposes primarily clastic sedimentary rocks that form the upper and lower plates of the Coast Range fault northeast of the San Andreas fault against crystalline rocks of the Salinian block (fig. 1-5). The lower plate of the Coast Range fault is composed of rocks of the Franciscan complex, and the clastic Great Valley sequence forms the upper plate. The primary components of the Franciscan are clastic sedimentary rocks, primarily graywacke, but minor amounts of shale, siltstone, and conglomerate are present. Altered mafic volcanic rocks (greenstones), bedded chert, ultramafic rocks (primarily serpentinite) and sparse, but distinctive assemblages of metamorphic rocks, including blue glaucophane schists (Bailey and others, 1964) are secondary but important components of the Franciscan. Shearing of the complex is nearly ubiquitous at outcrop scale and melange is developed widely.

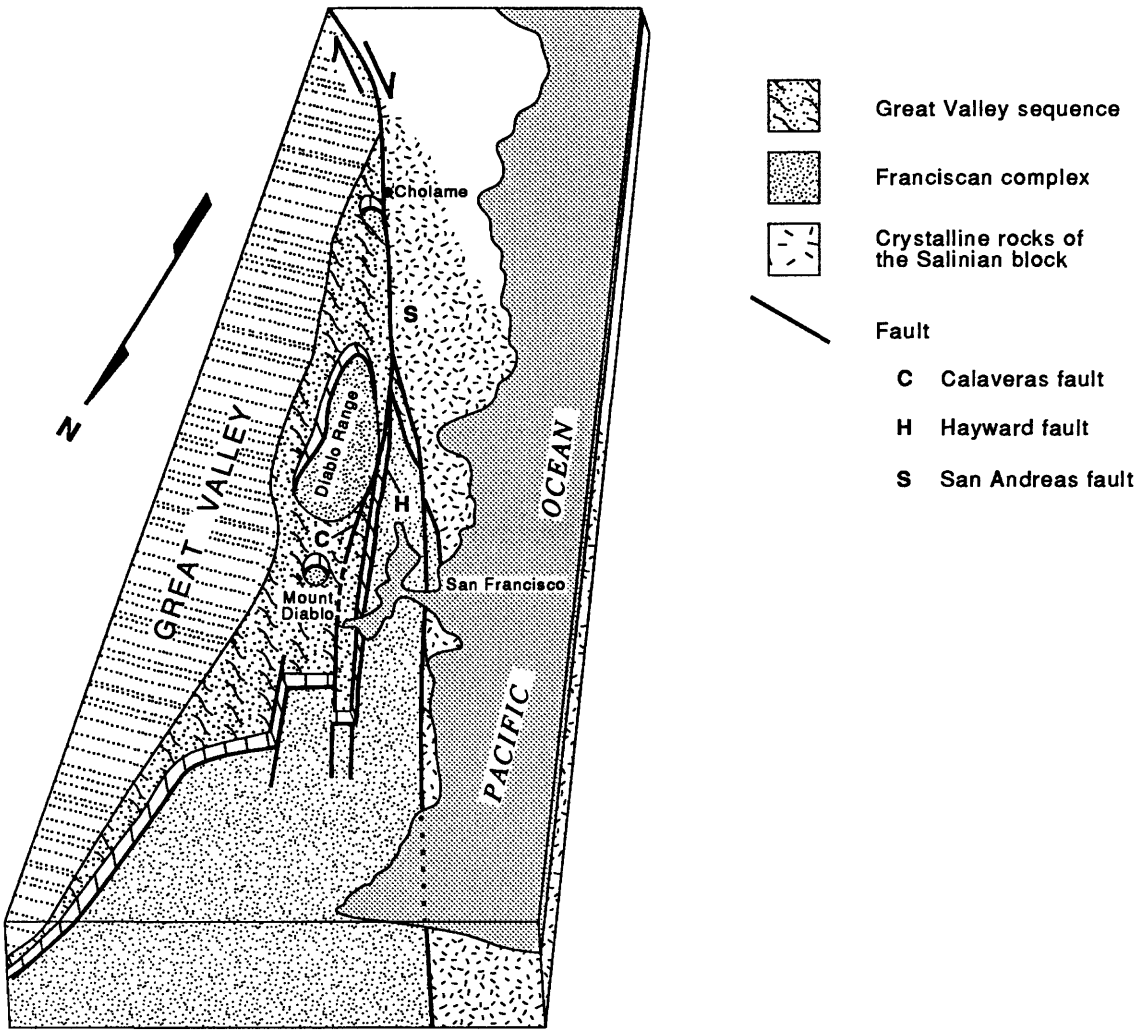

Figure 1-5. Major structural elements along the San Andreas fault in the Coast Ranges (modified from Irwin and Barnes, 1975). The Salinian block lies west of the fault and the Franciscan complex and Great Valley sequence lie on the east side. The Coast Range fault is the regional contact between the Franciscan rocks and the serpentinite at the base of the Great Valley sequence. Vertically-ruled areas are where parts of the Great Valley sequence has been removed to view subsurface relations.

The Great Valley sequence consists of a moderately deformed, predominantly clastic sequence (Bailey and others, 1964) that is largely coeval with the Franciscan complex. Shale locally comprises more than half of the section, but well-bedded sandstone and locally thick lenses of conglomerate are also major components. An ophiolite consisting of serpentinized ultramafic and volcanic rocks, interpreted as former oceanic crust, lies at the base of the Great Valley sequence in the California Coast Ranges (Hopson and others, 1981). Intensely sheared serpentinite at the base of the sequence, which marks the tectonic contact with the underlying Franciscan complex, is interpreted by Ernst (1970) as the result of underthrusting on a former Benioff zone. Jayko and others (1987) have argued that, although in some places the contact between the two units may be a thrust fault, it is generally a low-angle normal fault (detachment) related to uplift of the Franciscan complex; they have proposed that it be referred to as the Coast Range fault.

West of the San Andreas fault, basement rocks of the Salinian block are granitic plutons, largely Cretaceous in age, and metasedimentary host rocks genetically unrelated to the Franciscan complex which is exposed to the east and west of the block (Ross, 1978). The Salinian block is anomalous in the context of the subduction that gave rise to the rocks of the Franciscan complex and Great Valley sequence, and there currently is no widespread agreement on the source of the preplutonic rocks of the Salinian block. Page (1981) believes that plutons of the Salinian block represent a former southern continuation of the Sierra Nevada batholith and infers that the block was moved several hundred kilometers toward its present position in Paleocene time and an additional 300 km northward in in the Neogene. Relatively thin sections of Tertiary marine and nonmarine clastic sedimentary and volcanic rocks locally overlie a late Cretaceous erosion surface on the Salinian basement rocks. Correlation of one of these volcanic units, the Pinnacles rhyolite, with the Neenach volcanics in the Mojave Desert provide some of the best evidence that about 315 km of right-lateral slip has occurred on the San Andreas fault since the early Miocene (Page, 1981; Sims, 1989). Additional details of the Cenozoic chronology of slip on the fault are discussed at *Stop 1.3*.

Historical Surface Faulting on the Central San Andreas Fault

The San Andreas is a well-defined single fault zone for over 1,100 km in length. About 840 km of that distance has broken during historical earthquakes (Allen, 1981). Two great historic earthquakes--the 1857 Fort Tejon earthquake and the 1906 San Francisco earthquake -- produced most of the historical surface faulting (fig. 1-6). Each earthquake was associated with several hundred kilometers of surface rupture that had as much as 6 m of right-lateral slip. Some sections of the fault have ruptured repeatedly in historic time. A striking example of repeated slip is along the part of the fault adjacent to the San Francisco Bay area. A large earthquake that occurred on the San Andreas fault in that area in 1838 produced surface faulting from at least San Francisco to the latitude of San Jose, a distance of 64 km. The same section of the fault broke again during the 1906 San Francisco earthquake (Louderback, 1947).

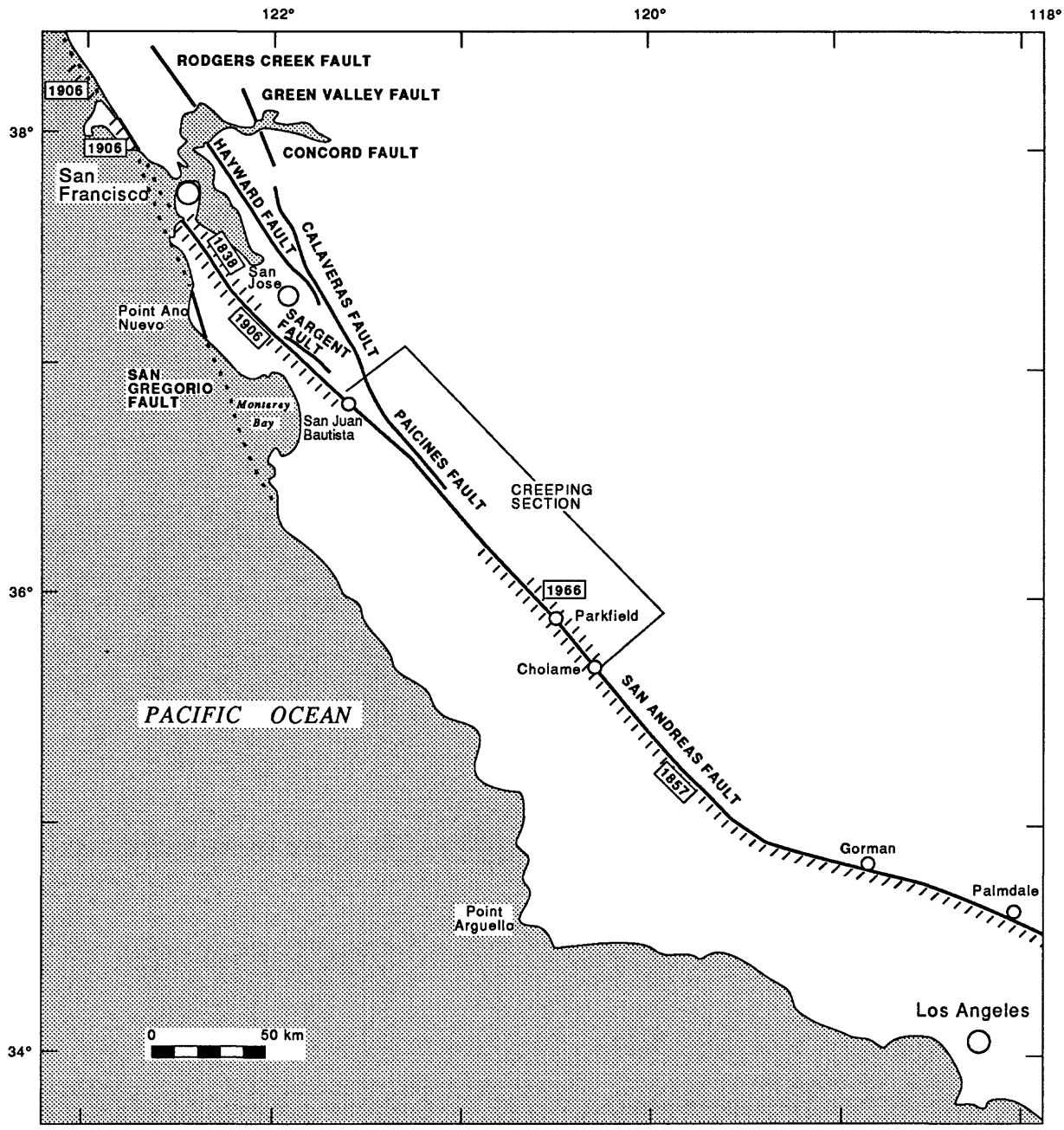

Figure 1-6. Map of central San Andreas and related faults, California. Patterned intervals show extent of surface rupture associated with 1838, 1857, 1906, and 1966 earthquakes on the San Andreas fault.

To the south, surface faulting has occurred along the section of the San Andreas fault near Parkfield during four historic earthquakes with magnitudes of 5.5 to 6.5 in 1901, 1922, 1934, and 1966. The rupture from the 1966 earthquake was 38 km long (Brown and Vedder, *in* Brown and others, 1967) and corresponds to a part of the fault that had broken earlier during the great 1857 earthquake (Sieh, 1978a). The regularity and similarity of characteristics of the earthquakes has led to the selection of the Parkfield area as the site of an earthquake-prediction experiment (Bakun and Lindh, 1985).

The Working Group on California Earthquake Probabilities (1988, p. 12) has subdivided the San Andreas fault into 10 segments that are expected to slip independently in large earthquakes. The segments are characterized by: 1) elapsed time since the last earthquake to rupture the segment, 2) recurrence interval, 3) amount of slip per event, and 4) the long-term slip rate. One of the segments, from San Juan Bautista to Cholame, is characterized by creep, at rates as high as 30-34 mm/yr in the central part of the segment, and is regarded as an unlikely site for a magnitude 7 or greater earthquake.

San Francisco Earthquake of 1906

On April 18, 1906 a major earthquake (M_s = 8.3) and an ensuing fire devastated the city of San Francisco, California. Soon afterward, the California Earthquake Commission under the direction of A.C. Lawson prepared a detailed report on the effects of the earthquake (Lawson, 1908). Detailed study of the faulting associated with the earthquake, combined with analysis of geodetic surveys of the region made before and after the earthquake, led to Reid's (1910) elastic rebound theory of earthquakes and to the subsequent ongoing interest in the geological nature of the fault. The earthquake may have been the largest historical earthquake in the continental United States, inasmuch as it produced a nearly continuous surface rupture (fig. 1-6) from Point Arena to San Juan Bautista, over 300 km to the south (Lawson, 1908). The total length of faulting, including offshore regions, is believed to have been more than 400 km and right-lateral horizontal displacements were locally as much as 6 m (Bonilla and others, 1984).

The southern part of the surface break intersected the Pacific coast at Mussel Rock, about 8 km northwest of the starting point for this trip. The trace of the fault in the 25-km-long interval southeast of Mussel Rock was described by Lawson (1908) as ". . . marked by a belt of upturned earth resembling a gigantic mole-track. . . The typical occurrence in turf-covered fields is a long, straight, raised line of blocks of sod broken loose and partly overturned." It was also noted that the break commonly followed valley margins, rather than following valleys bottoms.

Although parts of the surface trace commonly appeared relatively simple with slip confined to a narrow zone, a comparison of measured displacements at the fault with geodetic estimates of the coseismic fault slip by Thatcher and Lisowski (1987) showed that deformation occurred over a zone ranging from about 20 m to 2 km in width. Measured displacements at the fault average only about 70 percent of the total displacement (fig. 1-7) across the fault zone.

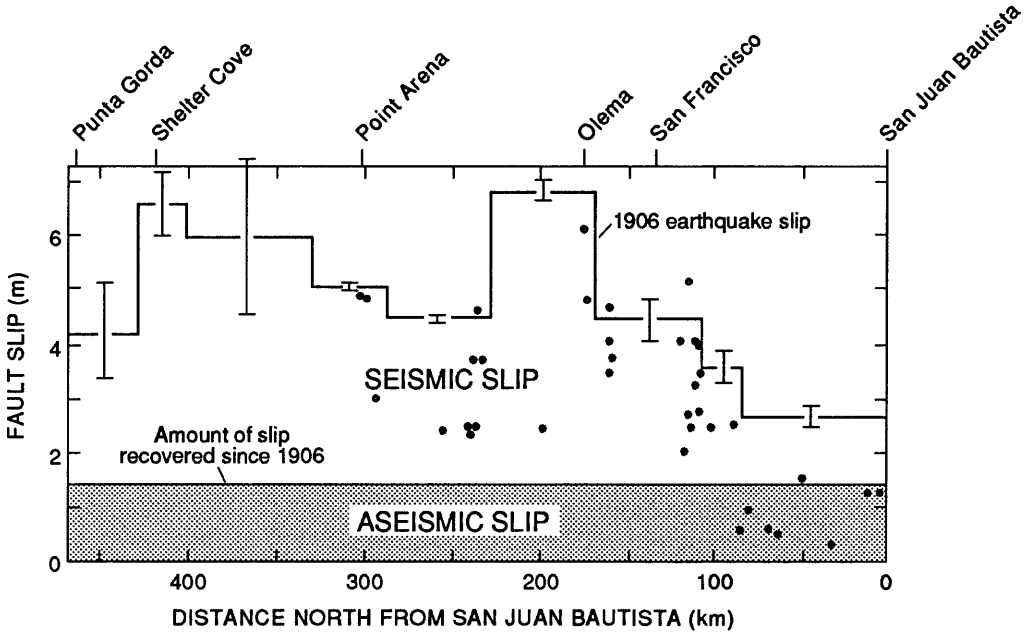

Figure 1-7. Slip on the San Andreas fault associated with the 1906 San Francisco earthquake (modified from Working Group on California Earthquake Probabilities, 1988). Solid dots show fault slip reported by Lawson (1908); straight line segments are geodetic measurements of 1906 fault slip with one-standard-deviation error bars shown for each determination (Thatcher and Lisowski, 1987). Patterned rectangle at bottom of graph indicates amount of slip recovered by elastic-strain accumulation since 1906.

Thatcher (1975a) reexamined geodetic data from surveys, made as early as 1853, of an approximately 100-km-wide region affected by the 1906 earthquake to determine the mechanism of strain accumulation and release associated with the earthquake. His analysis showed that the earthquake was preceded by about 50 years or more of relatively rapid preseismic strain accumulation, which he postulated followed an earlier period of slow accumulation of shear strain over a broad region. Seismic slip during the 1906 earthquake, which averaged about 4 m, appears to have been confined to the upper 10 km of the crust and was followed by at least 30 years of relatively rapid aseismic deformation near the fault. This postearthquake rebound is consistent with an additional 3-4 m of slip on the San Andreas fault at depths between about 10 and 30 km. Since 1950, the rate of shear-strain accumulation around San Francisco Bay has been comparatively low and has been uniformly distributed across an 80-km-wide zone immediately east of the fault and may reflect a shift in slip at depth to the Hayward-Calaveras fault systems (Thatcher, 1975b).

Segment 1A--San Bruno to San Jose (43 Miles)

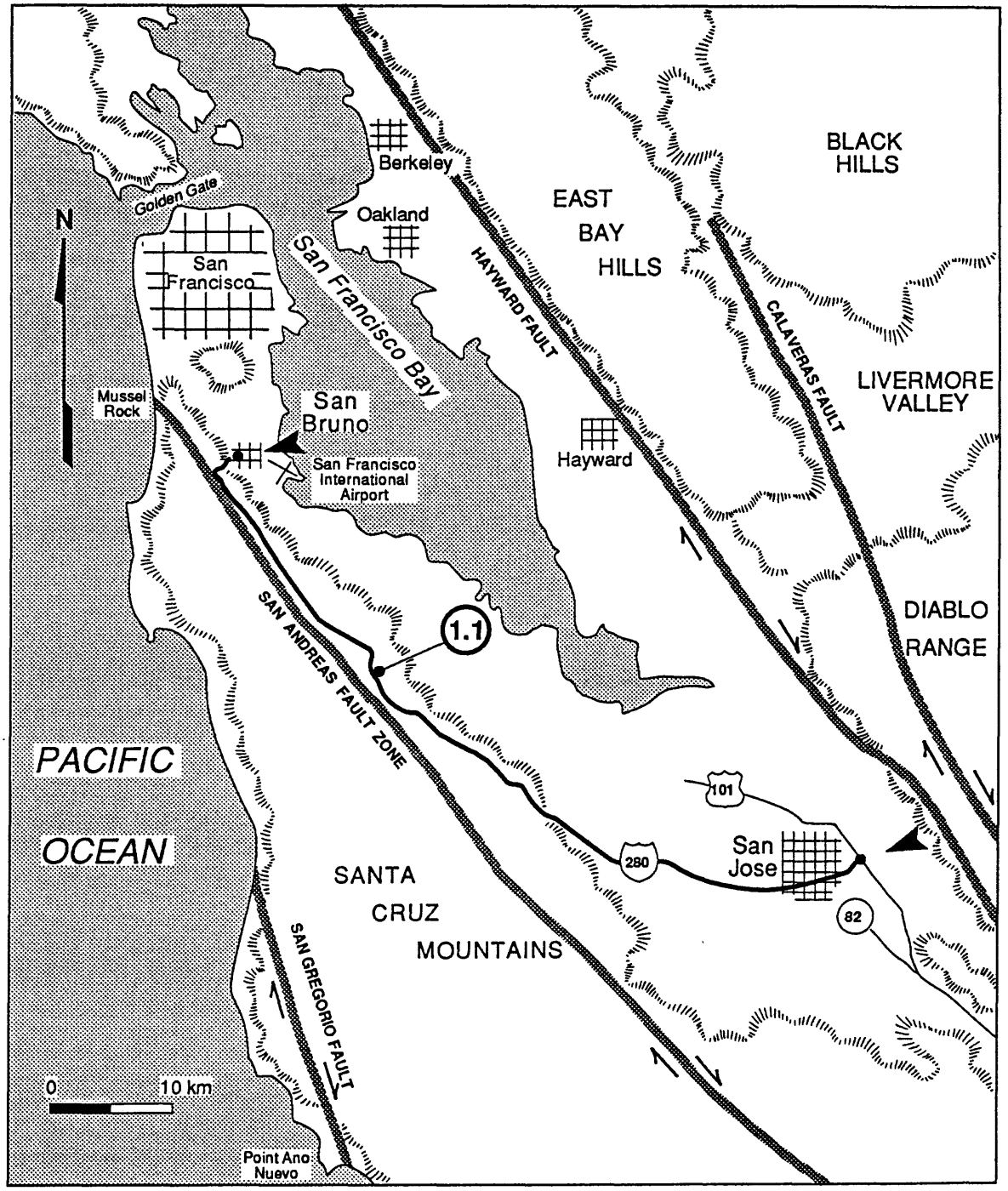

Figure 1-8. Route map for Segment 1A, San Bruno to San Jose, California. On this and remaining route maps, solid arrowheads mark endpoints of field-trip segments, open circles with numbers show locations of field-trip stops.

Route Narrative--The field trip begins in San Bruno near the locality in San Andreas Valley for which Lawson (1895, 1908) presumably named the San Andreas fault. We leave from the intersection of California Highway 82 (El Camino Real -- The King's Road) and San Bruno Avenue and drive southwest on San Bruno Avenue, climbing up into the low hills that border the coastal zone of the bay; our route intersects the San Andreas fault at Skyline Boulevard. The low hills are formed primarily on poorly consolidated sandstones of the lower Pleistocene and upper Pliocene Merced Formation, which locally contains beds of white volcanic ash dated as about 500,000 years old by Andrei Sarna-Wojcicki (Brabb and Pampeyan, 1983).

Turn left onto Skyline Boulevard at about 1.6 miles from El Camino Real and head southeast along a linear ridge overlooking the valley of the San Andreas rift (on the right). The road is virtually on the trace of the San Andreas fault for the first 0.5 mile, beyond which the fault gradually trends down the hillslope to the southwest. Soon after turning onto Skyline Boulevard you can get glimpses of San Andreas Lake, which is impounded by an earthfill dam built in 1870. Highly sheared Franciscan rocks in the eastern abutment of the dam were offset about 3 m (Hall, 1984) across a narrow zone of surface faulting from the 1906 earthquake, but the dam did not fail. The trace of the active fault lies about 100 m northeast of the axis of the valley, on the lower part of the slope between the valley floor and the ridge that we are traversing.

At about Mile 7.5 we pass the interchange for Black Mountain Road and Hayne Road, and a mile beyond that we cross a high bridge across San Mateo Creek. Lawson (1895) considered San Mateo Creek to be a superimposed stream because it cuts across and through the broadest part of the high plateau (Buri-buri plateau) that we have generally been driving on. The plateau, at an elevation of about 215 m, is the lower of two prominent geomorphic surfaces in the area. The upper surface is at an elevation of about 350 m, at the level of the flat-topped ridges several kilometers southwest of the rift, in the area between San Andreas Lake and Lower Crystal Springs Reservoir. Lawson believed the plateaus are erosional features which developed during relatively stable intervals separating periods of uplift.

Continue southeast on Interstate 280 another 6 miles and exit at Edgewood Road. Drive under the Interstate, turn left onto the entrance ramp for northbound Interstate Highway 280, drive 0.5 mile north, exit right on road marked "Vista", and continue to the parking area on the hilltop.

Stop 1.1--San Andreas Rift

The vista point is near the contact of Eocene Butano(?) sandstone to the north and sheared fine-grained graywacke, siltstone, and shale of the Franciscan complex to the south. To the southwest, beyond the linear valley of the San Andreas rift, you can see the Santa Cruz Mountains, which are underlain, on this side, by Eocene Butano sandstone. On the other side of the Santa Cruz Mountains, near the Pacific coast, the San Gregorio fault trends roughly parallel to the San Andreas (fig. 1-8). In the opposite direction, you can look to the northeast across San Francisco Bay, toward Oakland and the East Bay Hills, which are visible on a clear day. The Hayward and Calaveras faults trend roughly parallel to the San Andreas fault along and within the East Bay Hills, respectively. Much of the movement between the Pacific and North American plates is distributed across a broad zone that includes four major faults: the San Gregorio, the San Andreas, the Hayward, and the Calaveras (fig. 1-8).

Based on geodetic measurements made between 1970 and 1980 in the San Francisco Bay area, Prescott and others (1981) determined a relative horizontal deformation rate of 32 mm/yr across a nearly 100-km-wide zone eastward from the Pacific coast. They did not detect localized slip on faults on the San Francisco peninsula but did find evidence that deformation is occurring over a broad zone near the San Andreas fault, consistent with about 12 mm/yr slip on the fault at depths greater than a few kilometers. To the east, across the bay, rigid-block slip is occurring at a rate of 7 mm/yr on the Hayward fault, and an additional 7 mm/yr of slip is oc-

curring on the Calaveras fault, about half of which is distributed over a zone a few kilometers wide (fig. 1-9). The net slip rate across the entire zone parallel to the plate boundary is noticeably less than the 56 mm/yr for the rigid plate tectonic model of Minster and Jordan (1978).

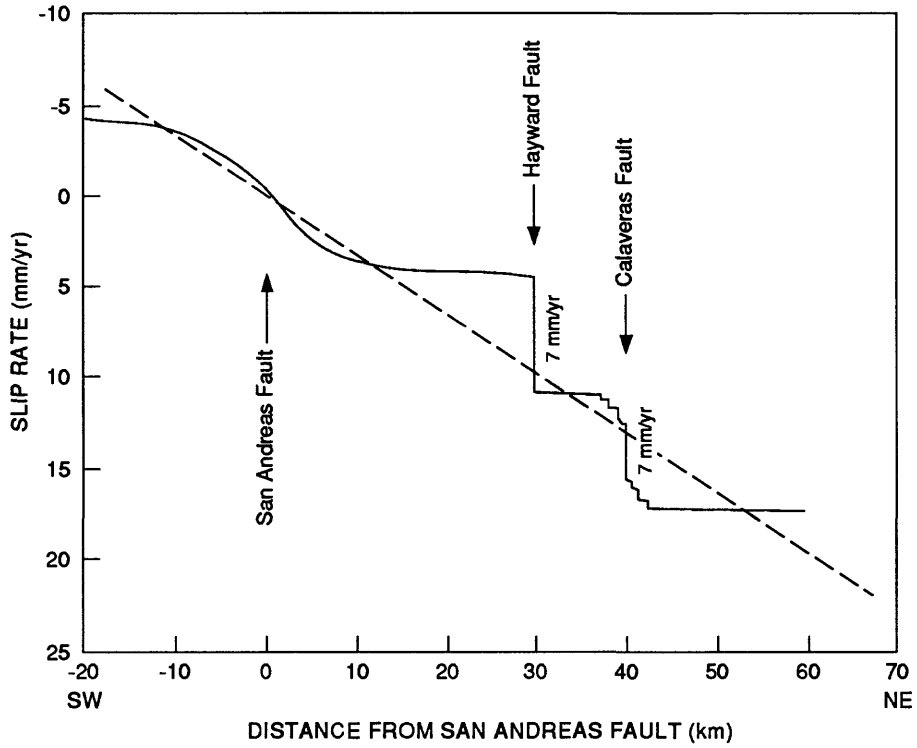

Figure 1-9. Distribution of slip parallel to faults in the San Francisco Bay region (from Prescott and others, 1981).

Geologic estimates of the long-term slip rate on faults in this area are sparse, but Hall (1984) determined a minimum rate of 12 mm/yr for the past 1,100 years for the San Andreas fault in the vicinity of this stop. Right-lateral offset of marine terraces along the San Gregorio fault indicate an average slip rate of 6-13 mm/yr during the past 200,000 years (Weber and Lajoie, 1977).

Route Narrative (continued)--Reenter Interstate Highway 280 northbound. Drive 1.7 miles to the marked exit on the right to the next vista point. Turn left under the Interstate Highway, and then turn left again onto the entrance ramp to southbound Interstate Highway 280. Proceed south to the intersection of Interstate Highway 280 and U.S. Highway 101 at San Jose (Mile 43).

Segment 1B--San Jose to Hollister (43 Miles)

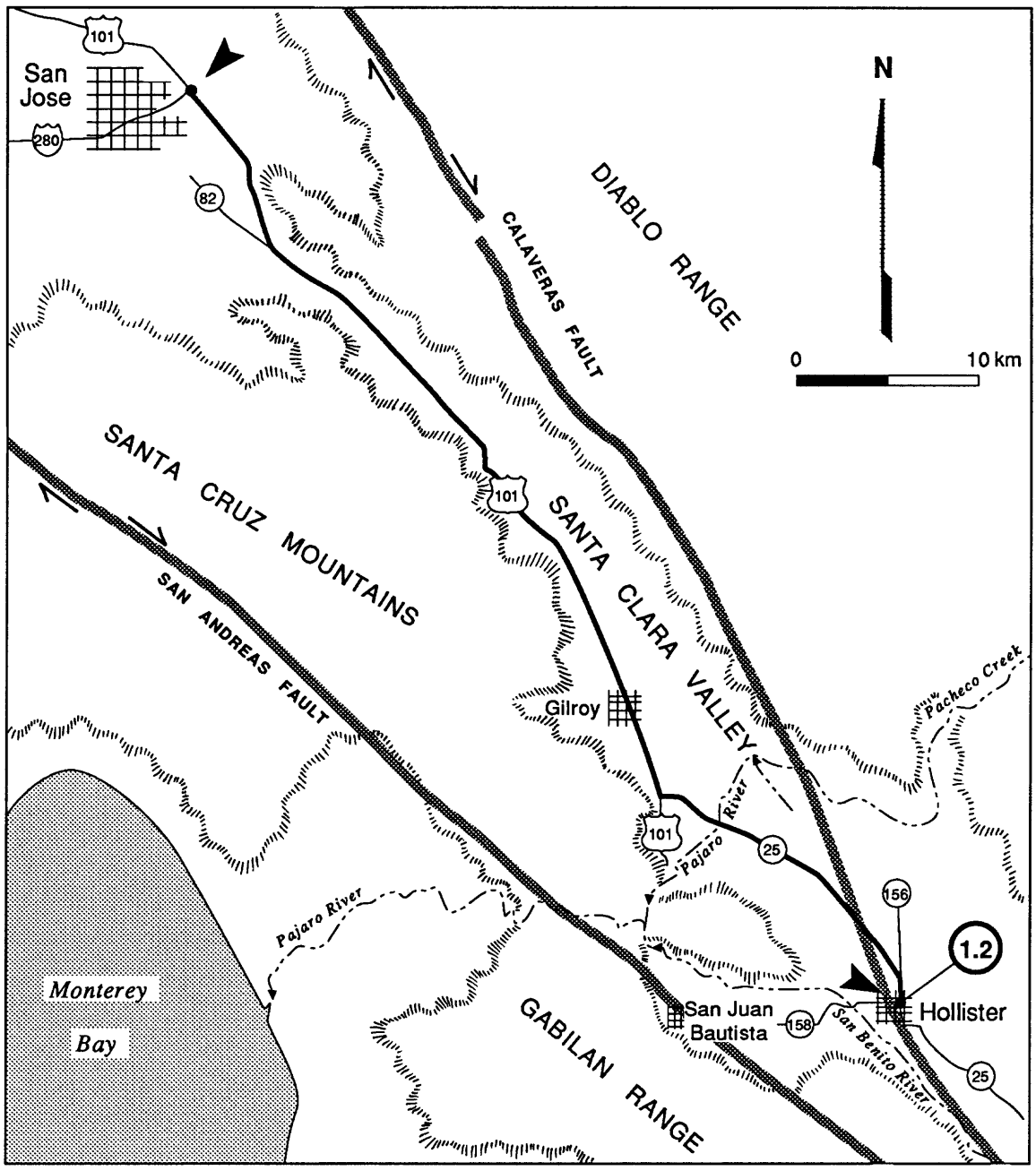

Figure 1-10. Route map for Segment 1B, San Jose to Hollister. San Juan Bautista marks the southern end of the surface rupture of the 1906 earthquake and the approximate northern end of the creeping segment of the fault.

Route Narrative--From the intersection of Interstate Highway 280 and U.S. Highway 101 at San Jose proceed southeast on Highway 101 to Gilroy (about Mile 29). About 2 miles south of Gilroy turn left off Highway 101 onto California Highway 25. Drive south toward Hollister across the plain formed by Lake San Benito, a late Pleistocene-Holocene lake dammed by a landslide across the narrows of the San Benito River to the west.

In about 5 miles (Mile 37) there is a conspicuous low hill in the valley directly ahead. It is a horst between two strands of the Calaveras fault which intersects our course from the left (fig. 1-11). Several miles further, the highway passes a few hundred meters to the west of the hill. The active trace of the fault is at the break in slope at the base of the hill and passes beneath the house and barn to the east which are being deformed by fault creep (Radbruch and Rogers, 1969). The active trace diverges from the hill at about this point, crosses the road about a mile ahead, and then follows the western side of a second, echelon hill (horst block). In about a mile (Mile 40), you will see sag ponds on both sides of the road where it crosses the southern end of the horst. These ponds lie on strands of the fault that currently have little or no creep.

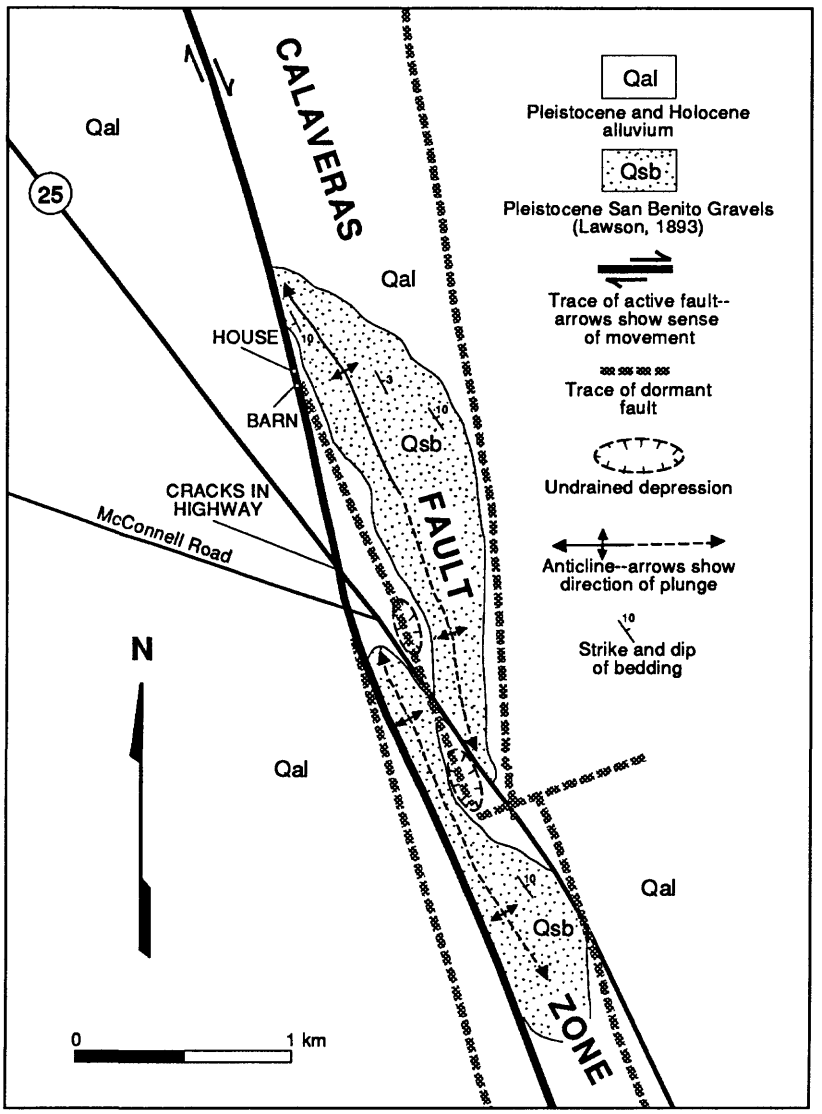

Figure 1-11. Horst blocks, cored by early Pleistocene San Benito formation, along the Calaveras fault north of Hollister, California (modified from Radbruch and Rogers, 1969).

About a mile beyond the dry sag ponds, a hill topped by a water tank is visible through a gap in the hills at 2 o'clock. The hill, Park Hill, is the western of 3 horst blocks within the Calaveras fault zone. Field-trip *Stop 1.2* is near the foot of the far (west) side of Park Hill.

Turn right on California Highway 156; as we drive into Hollister, we will pass exposures of the San Benito gravel of Lawson (1893) in the north end of Park Hill on the right. The southern end of surface faulting from the 1906 San Francisco earthquake is about 10 km to the west, at the town of San Juan Bautista. This locality is nearly coincident with the northern end of the creeping section of the San Andreas fault, which extends from a few kilometers north of San Juan Bautista to near Cholame, 180 km to the south (Burford and Harsh, 1980; Lisowski and Prescott, 1981).

In Hollister turn right at Third Street and stop at the intersection of Virginia Drive and Locust Avenue, three blocks to the west (fig. 1-12).

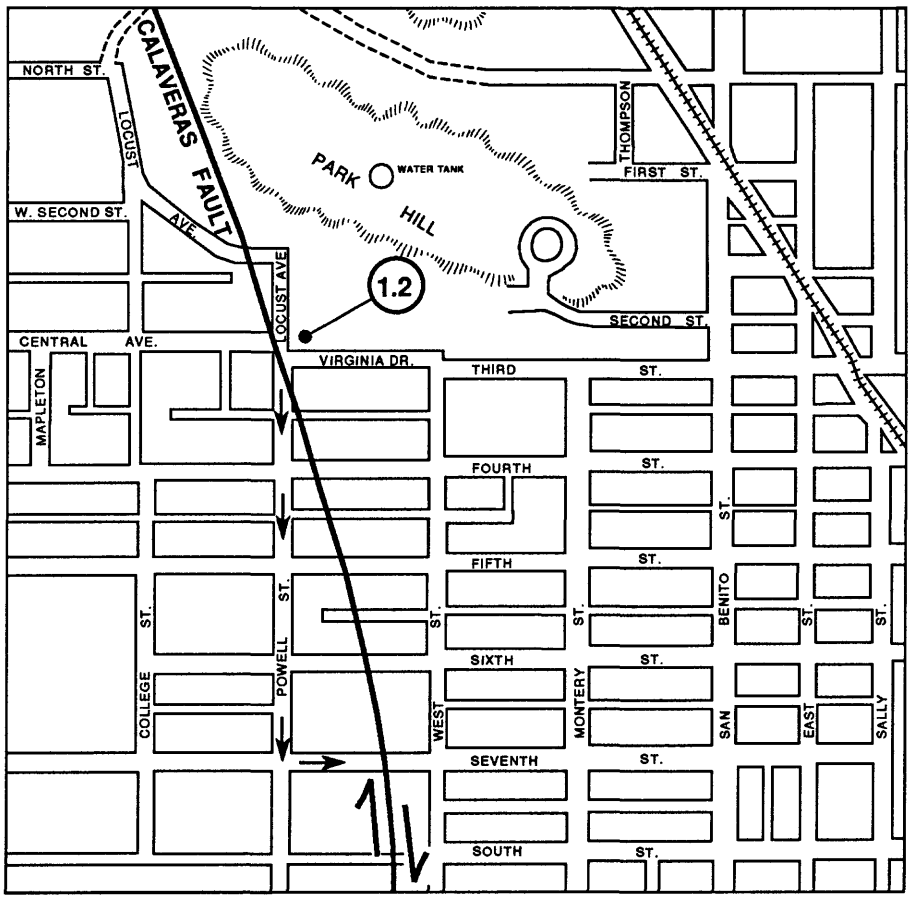

Figure 1-12. Map showing location of Calaveras fault at *Stop 1.2* in the city of Hollister, California (modified from Radbruch and Rogers, 1969).

Stop 1.2--Calaveras Fault at Hollister

The Calaveras fault extends about 120 km from about the latitude of San Francisco (fig. 1-6) to a point several kilometers southeast of Hollister (Jennings, 1975), where it swings southeast and becomes parallel to the San Andreas fault as two closely spaced branches, the Calaveras and Paicines faults (Dibblee, 1980). Slip on the Calaveras fault occurs primarily by aseismic creep (Prescott and others, 1981), but several earthquakes as large as magnitude 6 have occurred on the fault (Working Group on California Earthquake Probabilities, 1988). The effects of creep on cultural features is particularly conspicuous in Hollister, where the fault trends through residential neighborhoods. Schulz and others (1982) have determined a slip rate of about 7-10 mm/yr for the Calaveras fault at Hollister.

This stop is a walking tour that begins at the northwest corner of the intersection of Central Avenue and Locust Avenue where there is a conspicuous right-lateral offset of the sidewalk and curb and an echelon series of cracks in the asphalt to the south. Walk south along Locust Avenue as far as Seventh Street, and note offset curbs, sidewalks, and house foundations where the fault crosses streets to the east of Locust Avenue and Powell Street (fig. 1-12).

Segment 1C--Hollister to Peachtree Valley (62 Miles)

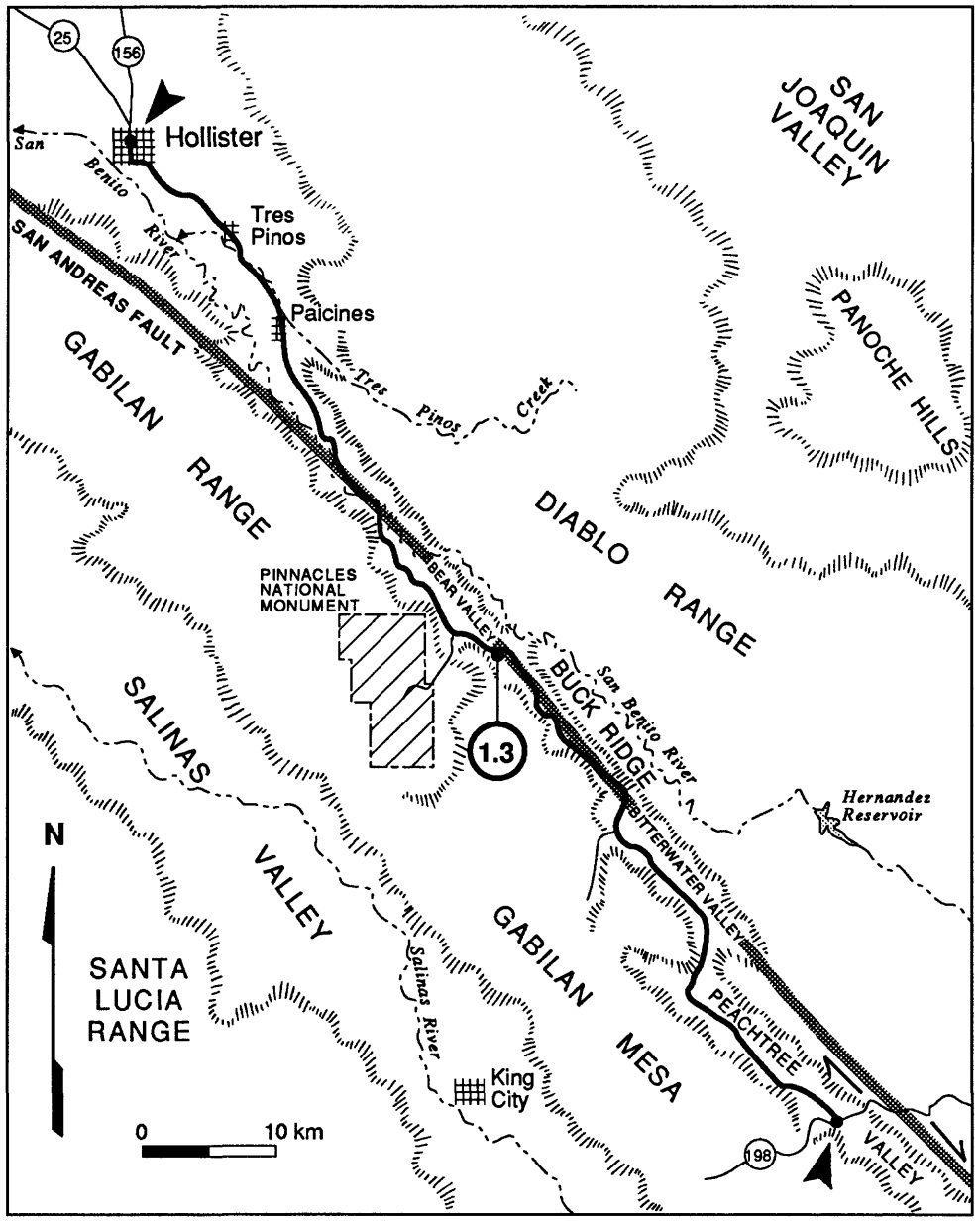

Figure 1-13. Route map for Segment 1C, Hollister to Peachtree Valley.

Route Narrative (continued)--Proceed to the intersection of Third Street and San Benito Street (California Highway 25) and note the odometer reading. Turn right onto San Benito Street and drive south on California Highway 25 toward the town of Tres Pinos.

Terraces of Tres Pinos Creek and the San Benito River

About 7 miles south of Hollister we pass through the town of Tres Pinos and begin following the course of Tres Pinos Creek, a tributary of the San Benito River, for several miles. Both of these rivers have a well-developed sequence of fluvial terraces that are visible at numerous places along the route. Dohrenwend (1977) has identified six terrace levels along these drainages. The three lowest terraces, at about 6 m, 15 m, and 25 m above stream level can be correlated throughout the drainage basin on the basis of distinctive soil profiles. The three higher terraces, which typically range from 45 to 85 m above present stream level and are believed to be several hundred thousand years old, lack diagnostic soil characteristics and cannot be correlated throughout the drainage basin. Dohrenwend (1977) concluded that longitudinal profiles of 20,000- to 50,000-year-old terraces (the three lowest) showed no evidence of warping parallel to the trace of the San Andreas fault. However, he found that terraces are more abundant on the northeast side of the valleys, indicating progressive migration of the rivers to the southwest, which he attributes to regional southwestward tilt of the San Benito River basin during at least the past several hundred thousand years.

Route Narrative (continued)--At Mile 12, pass through town of Paicines. *Note the sign "Next Services 65 Miles."* Just beyond Stone Canyon Ranch at Mile 19, a hillside trench on the right marks the trace of the San Andreas fault. To the southeast, at 10 o'clock, there are exposures of dark gray and pale brown rocks of the San Benito and Etchegoin Formations in the fault zone.

At Mile 25 the route passes through Bear Valley. The San Andreas fault lies on the east side of the near low ridge at 9 o'clock. About 2 miles past the junction with California Highway 146 (to Pinnacles National Monument), pull off at the roadcut at the crest of the hill.

Stop 1.3--Pinnacles Overlook, Bear Valley-San Benito Area

Looking to the west you can see the jagged skyline of the Pinnacles. These are part of an early Miocene (23.5 Ma) sequence of flow-banded rhyolite, rhyolite breccia and tuff, and andesite, all of which overlie granitic basement rocks. Matthews (1976) correlated these rocks with a nearly identical sequence known as the Neenach volcanics that are exposed 315 km to the southeast on the east side of the San Andreas fault on the basis of stratigraphic, chemical, and petrographic characteristics. Nilsen (1984) documented a similar amount of offset of correlative Eocene rocks overlying distinctive gabbroic basement at two sites on opposite sides of the San Andreas fault zone. Thus, there appears to have been no significant strike-slip displacement on the San Andreas fault from Eocene to Miocene time. The average rate of slip since early Miocene has been about 14 mm/yr based on the correlation of the Pinnacles and Neenach volcanics. Sims (1989) studied the spatial relationships of blocks of crystalline basement rocks and Tertiary sedimentary and volcanic rocks adjacent to the San Andreas fault in the Parkfield area and inferred a history of increasing rate of slip since Miocene time. The most recent stage, which he proposes began about 5 Ma, has an average rate of slip of 33 mm/yr and is comparable to Holocene slip rates and current geodetic rates of 27-34 mm/yr.

To the east, a linear trench and ridge in the foreground mark the trace of the San Andreas fault, which crosses the road a few hundred meters to the southeast. The Paicines fault lies on the opposite side of the ridge in the middle distance.

Route Narrative (continued)--Proceed southeast on California Highway 25. At Mile 40 cross through a small ridge at a roadcut. Note the excellent geomorphic expression of the fault zone about 100 m to the right of the road in this area. Continue 0.4 mile downhill to the junction with Coalinga Road, which is straight ahead at the sharp right turn. Stay on California Highway 25 through the sharp right turn and continue into Bitterwater Valley.

Enter the northwest end of Peachtree Valley at Mile 51 and intersect California Highway 198 at Mile 62. Turn left onto California Highway 198 (marked "Coalinga 38 miles").

Pleistocene Drainage from San Joaquin Valley

The present outlet for drainage from the San Joaquin Valley is northeast of San Francisco, but it has had different outlets through time as the geometry of drainages crossing the San Andreas fault were modified in response to accumulating slip on the fault. The outlet for drainage from the San Joaquin Valley during late Pliocene and most of the Pleistocene was at Bitterwater Valley, on the east side of the Temblor Range about 90 km southeast of here (see fig. 2-1). A series of corresponding underfit drainages west of the fault, which have been displaced northerly by slip on the San Andreas fault, are preserved between Peachtree Valley and southern Cholame Valley. Late Pliocene drainage through Bitterwater Valley crossed the San Andreas fault and flowed into the Salinas River by way of Pancho Rico Creek (fig. 1-14) about 2.5 Ma (Sims and Hamilton, 1989). The San Joaquin drainage was captured by Indian Valley about 2 Ma and then by Cholame Creek about 0.7 Ma as slip on the San Andreas fault lengthened the drainage path. About 25 ka, with Cholame Creek near its present position, the connection with Bitterwater Valley was broken, and a lake present in the previously closed Cholame Valley was emptied.

Segment 1D--Peachtree Valley to Parkfield (42 Miles)

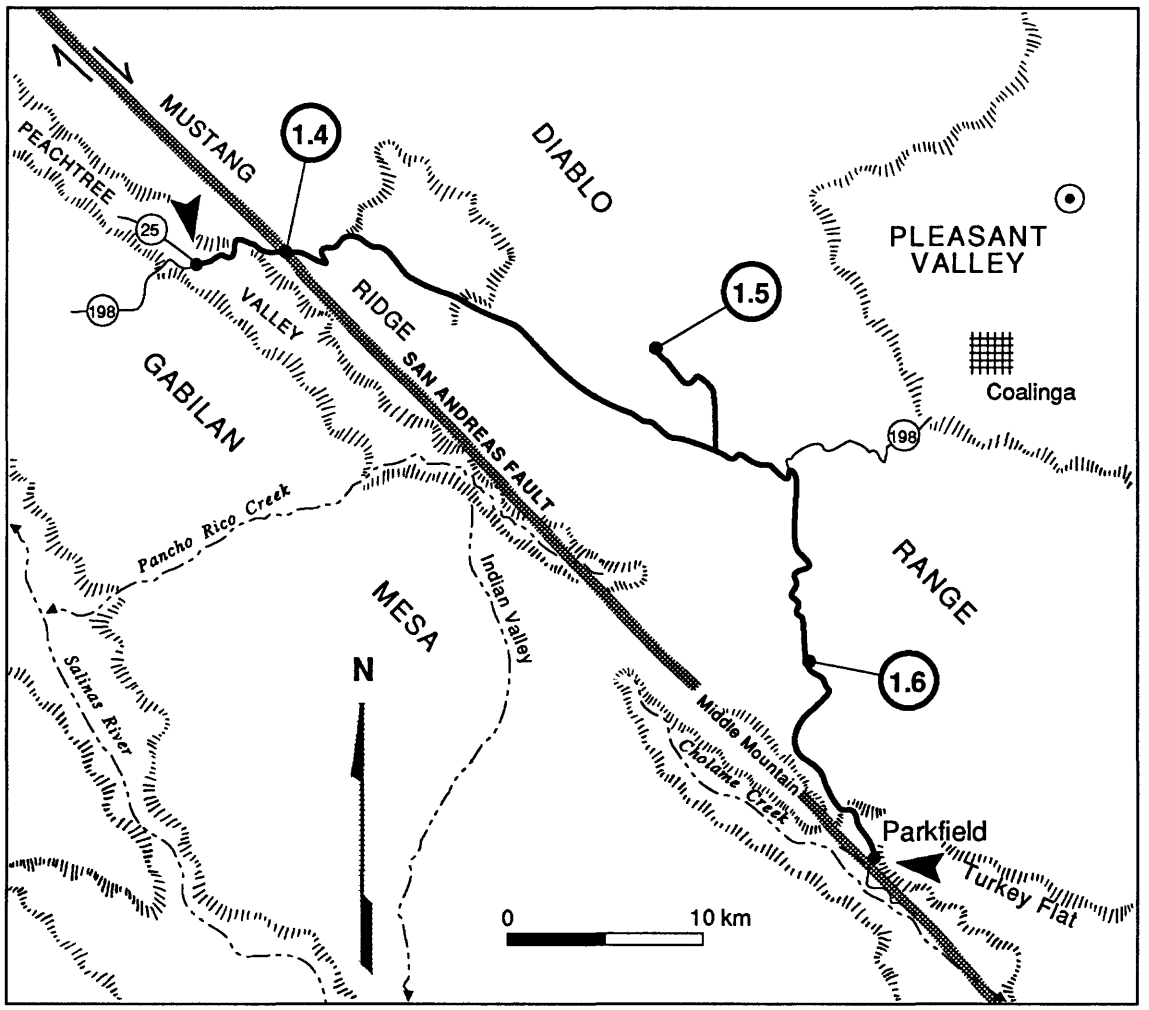

Figure 1-14. Route map for Segment 1D, Peachtree Valley to Parkfield.

Route Narrative--From the junction of Highways 25 and 198 in Peachtree Valley, drive about 4 miles east on Highway 198 to the crest of the grade on the southwest side of Mustang Ridge, pass through a roadcut, and park at a turnout at the gate on the north (left) side of highway for *Stop 1.4*.

Stop 1.4--San Andreas Fault at Mustang Ridge

Mustang Ridge is the result of vertical movement associated with two faults, subparallel to the San Andreas fault, which bound the ridge. Franciscan rocks underlying the ridge have been thrust over Miocene to Pliocene rocks on the northeast side of the fault and Pliocene rocks on the southwest side, forming in effect, a thin elongate extrusion (Rymer, 1981; 1982). The instability of the ridge, reflected by numerous landslides on its flanks, some up to 1 km wide, is probably due in part to the recency of the uplift (M.R. Rymer, 1989, written commun.).

Note the conspicuous modern sag pond along the trace of the San Andreas fault, which lies at the base of the linear ridge on the south side of the highway. We will walk north along the trace of the fault to see geomorphic details of the fault zone.

From the gate, walk about 250 m northwest along the ridge on the northeast side of a prominent linear gully to the first large tree. The tree is at the head of a shallow trench on the ridge crest where the linear gully makes a right step. The tree is split and offset in a right-lateral sense. Several hundred meters northwest of the tree you can see black mud deposits of another sag pond along the trend of the linear gully. From the vicinity of the tree, and extending along the side of the gully to the northwest, a distinctive side-hill bench lies midway up the slope from the bottom of the gully. This bench is, in part, marked by a concentration of burrows of ground squirrels and likely marks the currently active trace of the San Andreas fault.

Route Narrative (continued)--Continue to the southeast on Highway 198 for 17 miles to the turnoff to Coalinga Mineral Springs County Park. Turn left and drive 5 miles to the park at the end of the road. The road from the main highway to the park passes through a section of Etchegoin Formation (Tertiary marine sandstone and siltstone) dipping steeply to the south for about 1.5 miles and then enters the unconformably underlying section of Panoche Formation (Cretaceous marine sandstone, micaceous shale, and conglomerate) dipping more gently to the northeast (Dibblee, 1980). Locally the unconformable contact is the Curry Mountain fault (fig. 1-15).

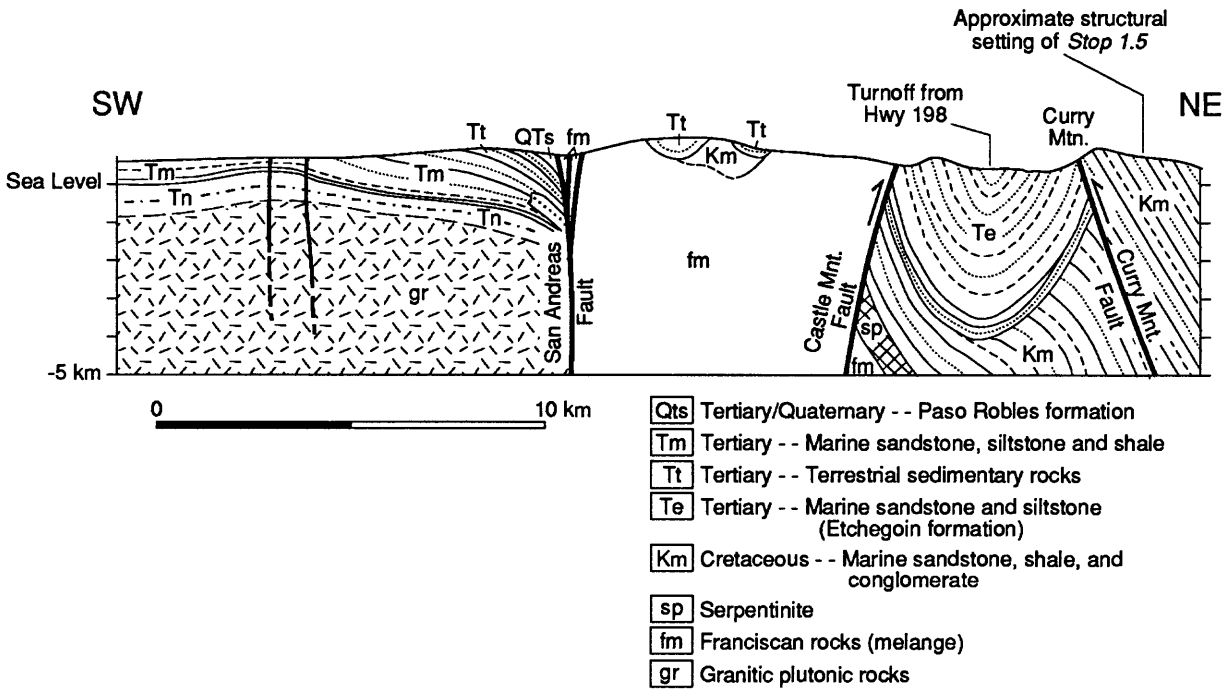

Figure 1-15. Cross section in the vicinity of *Stop 1.5* (modified from Dibblee, 1980).

Stop 1.5--Coalinga Mineral Springs County Park (Lunch Stop)

Route Narrative (continued)--Return to Highway 198, turn left, and continue to the southeast 2.5 miles to the Y intersection with the Parkfield Grade road. Note the odometer reading, and turn right onto the road marked "Parkfield Grade--Parkfield 19 miles." The road ahead includes 10 miles of fairly steep, crooked, but

well-graded road. Pavement ends at Mile 6. Continue to southeast to *Stop 1.6* at the topographic divide at Mile 12.

Stop 1.6--Cholame Valley Overlook

The skyline hills to the southwest are the Cholame Hills which flank Cholame Valley. Middle Mountain, in the foreground, is believed to be the area where the next Parkfield earthquake will initiate (Poley and others, 1987). The hypocenter of the 1966 Parkfield earthquake was about 10 km below Middle Mountain on the San Andreas fault, which trends along the slope on this side of the mountain. The Parkfield earthquake sequences and the experiment to predict the next earthquake along this section of the San Andreas fault will be discussed in more detail at the next stop.

Route Narrative (continued)--Proceed down the Parkfield Grade and cross Little Cholame Creek at Mile 16, which marks the end of the gravel section of the road. Continue on to Parkfield at Mile 21.

Segment 1E--Parkfield to Paso Robles (40 Miles)

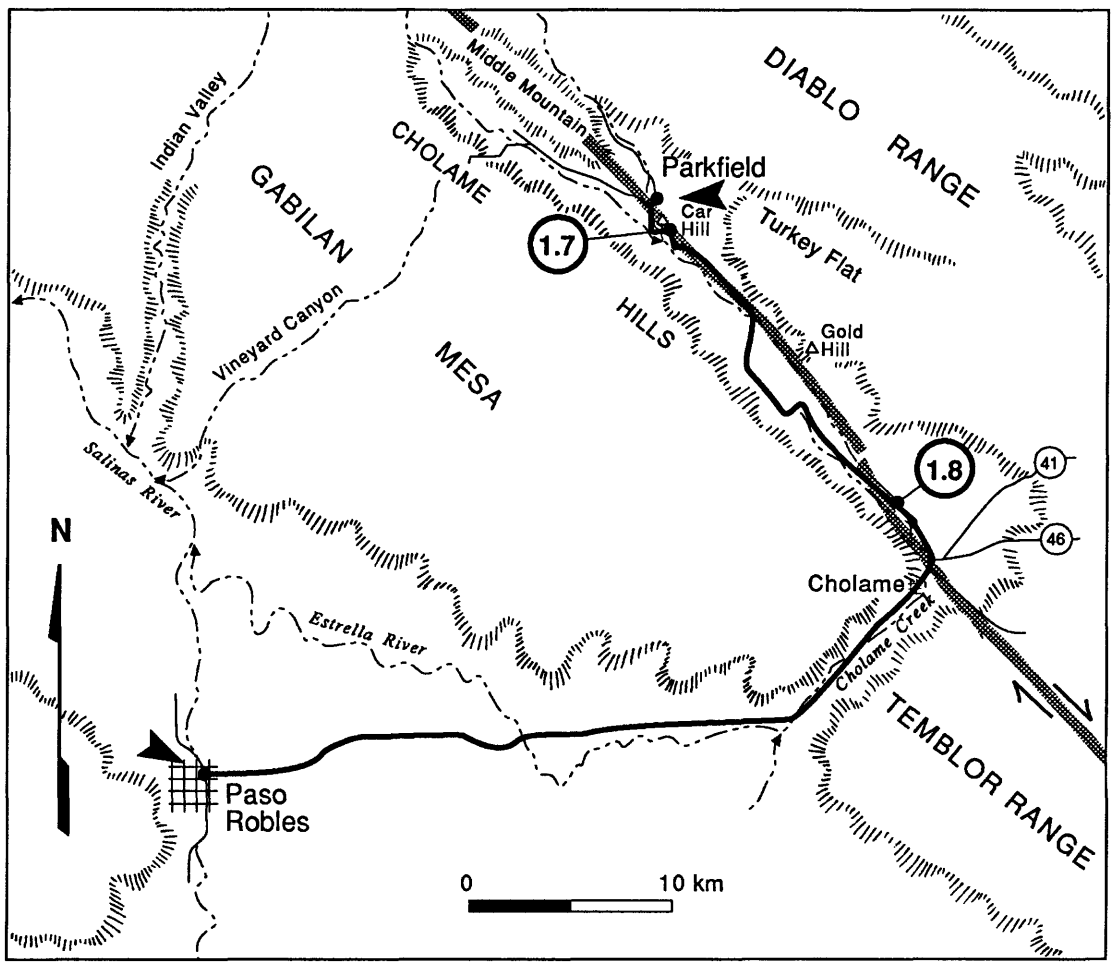

Figure 1-16. Route map for Segment 1E, Parkfield to Paso Robles.

Route Narrative--Head south through Parkfield, cross a bridge over Little Cholame Creek and intersect Cholame Valley Road. The bridge, built in 1932, has been deformed by slip on the San Andreas fault both from creep and earthquakes in 1934 and 1966 (Yerkes and Castle *in* Brown and others, 1967). Turn left on Cholame Valley Road and drive southeast for 1.1 miles to Taylor Valley Ranch on the left. *Stop 1.7* is several hundred meters to the north. The site is on private property and prior arrangements must be made for access.

Stop 1.7--Parkfield Earthquake-Prediction Site at Car Hill

The Parkfield segment (Working Group on California Earthquake Probabilities, 1988) of the San Andreas fault is the part of a 180-km-long interval characterized by continuous or quasi-continuous creep (figs. 1-6 and 1-17). Northwest of the 30-km-long Parkfield segment, the fault is characterized by creep at rates of up to 34 mm/yr, frequent earthquakes of magnitude less than 4, and an absence of historic earthquakes having magnitudes of 6 or greater. The 55-km-long segment of the fault southeast of the Parkfield segment (the Cholame segment), by contrast, is characterized by a lack of aseismic slip, a low level of microearthquakes, and a historic and geologic record of large (M > 7) earthquakes. The Parkfield section has characteristics intermediate between the adjoining sections. Since 1857, five magnitude 6 earthquakes have occurred on the Parkfield segment, and creep on the fault tends to occur in discrete events of a few millimeters in a period of a few hours (Bakun and Lindh, 1985; Schulz and others, 1982).

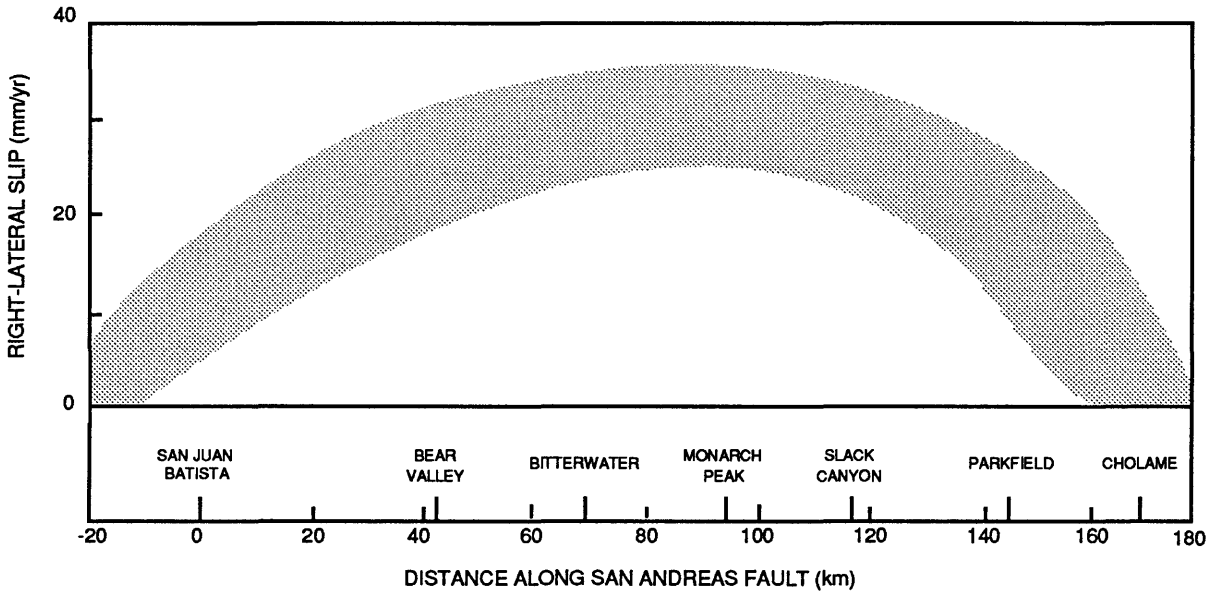

Figure 1-17. Generalized variation in slip rate along the creeping section of the San Andreas fault from San Juan Bautista to Cholame (modified from Lisowski and Prescott, 1981). Pattern indicates variability in data.

Irwin and Barnes (1975) noted that the occurrence of creep and frequent small earthquakes along the San Andreas and related faults is associated with the fault's juxtaposition against the Great Valley sequence (fig. 1-5); that is where serpentinite and ophiolite at the base of the Great Valley sequence intersect the fault. Infrequent large earthquakes and an absence of creep is, in contrast, associated with segments of the fault where the Great Valley sequence is absent. They suggested that the highly plastic serpentinite may allow creep and prevent stick-slip type faulting. In addition they suggested that where confined by the overlying, low perme-

ability Great Valley sequence, high pore pressures from mineral-rich water resulting from metamorphism of Franciscan rocks may migrate to the more permeable rocks of the fault zone and allow creep.

Numerous details of the five earthquakes which occurred on the Parkfield section since 1857 led to selection of the area as the site of a major earthquake-prediction experiment. One of the main factors is the surprisingly regular occurrence of the earthquakes (the mean interval between the events is 21.9 ± 3.1 years). In addition, the magnitudes of the earthquakes, location of main-shock epicenters, fault-plane solutions, direction of propagation of the rupture, foreshock and aftershock patterns, and pattern of surface rupture were all nearly identical for the 1934 and 1966 events and are consistent with what is known about earlier events (Bakun and Lindh, 1985).

Route Narrative (continued)--Leave the Car Hill site and return to Cholame Valley Road. Turn left, note the odometer reading and continue to the southeast. At Mile 2.4 the road follows a shutter ridge (on the right) that is associated with 700 m of right-lateral offset of the stream which flows along the base of the ridge. The open area at the southeast end of the ridge is underlain by sediment ponded against the shutter ridge.

At Mile 4.7, just before a broad sweeping curve leading to a bridge across Cholame Creek, note a lone cottonwood tree on the left. There, an irrigation pipe that crosses the San Andreas fault trace was reportedly broken 9 hours before the 1966 earthquake, indicating possible preearthquake deformation along the fault (Yerkes and Castle *in* Brown and others, 1967). About 1.5 miles from here, the road crosses to the southwest side of Cholame Valley where it turns parallel to the valley. After making the turn, look across the valley to Gold Hill, a prominent hill at the edge of Cholame Valley flanked on either side by conspicuous side valleys.

Gold Hill

Gold Hill is underlain by a sliver of a distinctive 150-Ma quartz-bearing hornblende gabbro that is sandwiched between strands of the San Andreas fault. The site provides further important evidence for large lateral displacement on the San Andreas fault. Ross (1970) correlated the rocks at Gold Hill with virtually identical rocks of the same age (about 150 Ma) within the fault zone at a site near San Juan Bautista, about 170 km to the northwest, and argued that both were originally part of the same terrane. The rocks at both localities may have been part of a similar suite of related rocks at another site in the San Emigdio Mountains along the east side of the San Andreas fault zone and just north of the Garlock fault, about 150 km southeast of Gold Hill. The total slip indicated by these offset rocks is 320 km, essentially the same as that determined for the offset Miocene Neenach volcanics.

Route Narrative (continued)--Drive to the southeast about 3 miles to a sharp left turn (to northeast) and in about 1.5 miles the road makes a sharp right turn to the southeast. In 1.5 miles the route crosses the Monterey-San Luis Obispo County line at a left bend in the road.

Cholame Valley "Pull-apart Basin"

As we cross the county line, you will see the active trace of the San Andreas fault to the left, near the base of the hills on the northeast side of the valley. From near this point, the fault crosses to the southwest side of the valley about 2 miles southeast of the county line. The fault here is associated with a pull-apart basin (Aydin and Nur, 1982). Surface faulting from the 1966 Parkfield earthquake was virtually continuous along the fault northwest and southeast of the point where the fault crosses the valley. Despite a careful search, no surface faulting from the 1966 earthquake was found along the part of the fault trace that crosses the valley (Brown and others, 1967). However, Eaton and others' (1970) map and cross-sectional view of epicenters of the 1966 Parkfield earthquake show that the fault plane is continuous at depth and steeply dipping (figs. 1-18 and

1-19), but they note that there is a sharp southwest swing in the trend of epicenters at depths of 5 to 10 km near where the surface trace of the fault crosses the highway (15-km mark on fig. 1-18).

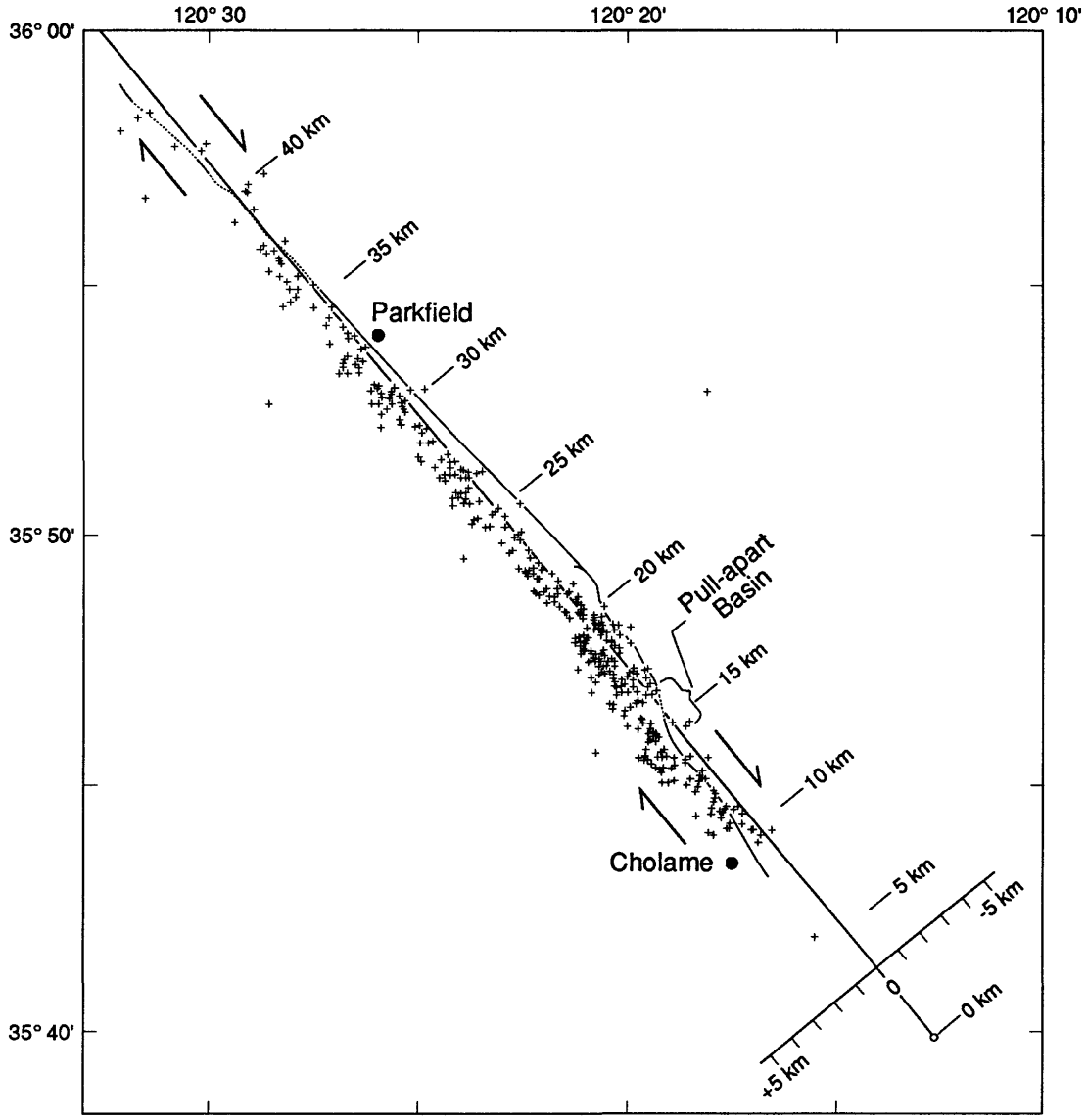

Figure 1-18. Epicenters of aftershocks of the 1966 Parkfield-Cholame earthquake (modified from Eaton and others, 1970). The heavy solid and dashed curved lines show the trace of associated surface faulting. The northwest trending line extending from the coordinates at the lower right is the surface trace of a reference plane fitted by linear regression to the aftershock hypocenters.

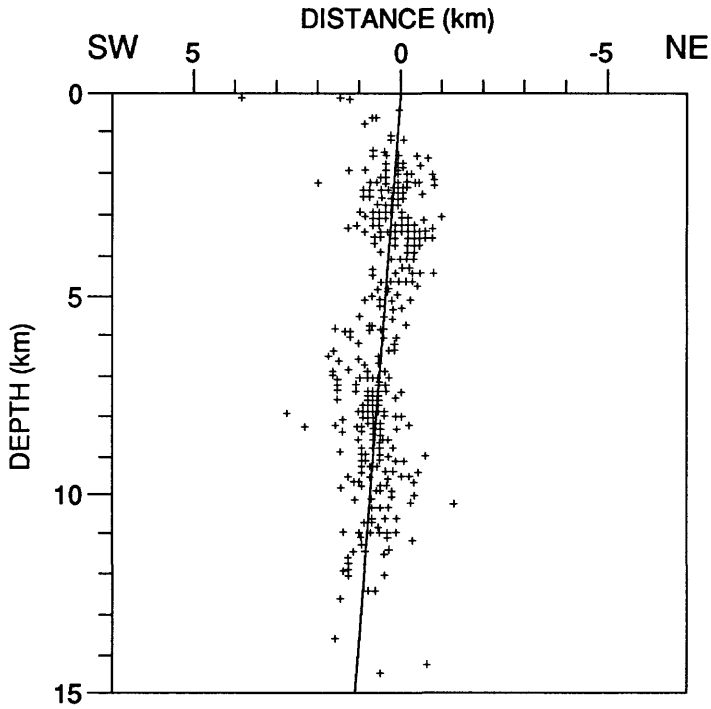

Figure 1-19. Hypocenters of aftershocks shown in figure 1-18 projected onto a vertical plane perpendicular to the surface trace of the reference plane described for figure 1-18 (modified from Eaton and others, 1970). The trace of the reference plane is shown by the heavy line.

Shedlock and others (1989) collected high-resolution seismic data along a northeasterly line that traversed the southern end of Cholame Valley, roughly along the fence that crosses the highway at *Stop 1.8*, and at several other locations in Cholame Valley. The profile (fig. 1-20), which extends northeast of the fault, shows a series of laterally continuous reflectors, presumably sediments, which generally dip towards the fault and are truncated beneath the presently active trace. The reflectors are broken and offset in the subsurface northeast of the fault, possibly along step faults associated with development of a basin adjacent to the active trace of the fault. The profile indicates that the prominent, active trace on the southwest side of the valley represents a major structural discontinuity and does not represent a new, recently activated trace. Note the very thick basin fill (>500 m) adjacent to the fault.

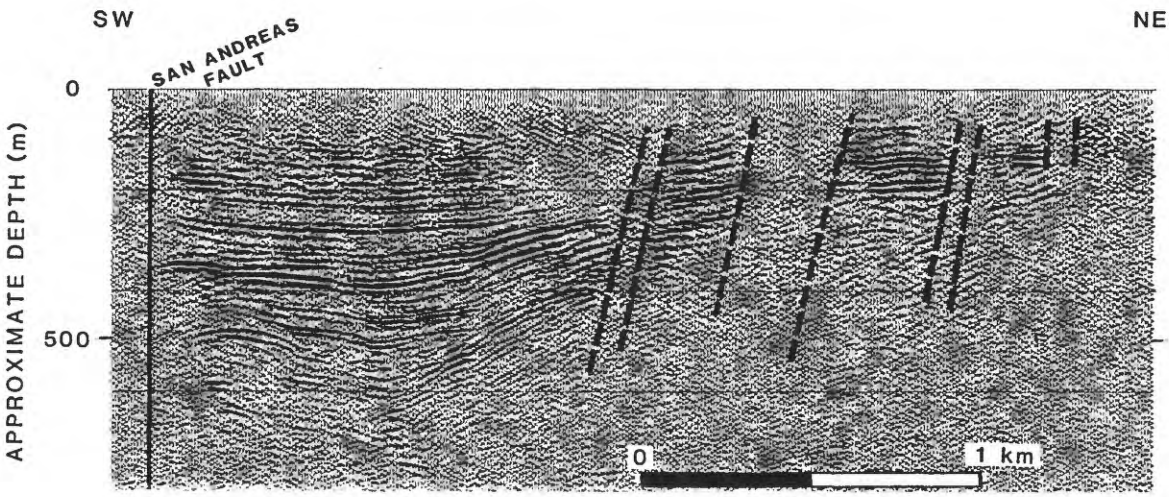

Figure 1-20. High-resolution seismic reflection profile across southern Cholame Valley at *Stop 1.8* (from Shedlock and others, 1989). Heavy dashed lines are approximate boundaries of inferred faulted zones.

Stop 1.8--Cholame Valley Fault-Creep Site

Measurements made soon after the 1966 Parkfield earthquake showed that the northeast-trending fence at this site had been offset 64 cm since it was built in 1908, including about 18 cm during the 1966 earthquake (Wallace and Roth *in* Brown and others, 1967) and presumably similar amounts of slip from earthquakes in 1922 and 1934. The 64 cm of slip yields a 58-yr slip rate of 11 mm/yr. Creep at this site between 1966 and 1979 was determined from an alinement-array survey to be 4 mm/yr (Burford and Harsh, 1980).

Several trenches dug by Sims (1987) adjacent to the fault where it crosses the alluvial fan south of the fence exposed a distinctive sedimentary unit that has been offset right laterally about 47 m. That offset and a date of 1,772 yr B.P. for detrital charcoal from the unit gave an average slip rate at the site of 26 mm/yr (Sims, 1987). This is similar to the slip rate of 34 mm/yr for the past 13,000 years at Wallace Creek about 70 km to the southeast (Sieh and Jahns, 1984) but more than double the 58-yr slip rate determined from the offset fence. Large-slip earthquakes prior to 1908 may have produced slip at this site that would explain the difference between the 58- and 1,772-yr slip rates. For example, Sieh and Jahns (1984) suggest that several meters of slip occurred along this part of the San Andreas fault during the 1857 Fort Tejon earthquake, which, when added to the post-1908 displacement record, would give a slip rate similar to the slip rate at this site reported by Sims (1987). Slip on nearby faults that show geomorphic evidence of Holocene right-lateral slip, such as the nearby White Canyon fault which is parallel to the San Andreas fault and several kilometers to the southwest, may also account for some of the slip deficit at this site (Sims and others, 1988).

Route Narrative (continued)--Note the odometer reading and continue south on Cholame Valley Road. About 0.5 mile to the south, fault scarps on the west (right) side of valley are conspicuous when shadowed by the late afternoon sun. At Mile 2 the road intersects California Highway 41/46. Turn right onto Highway 41/46 and proceed west, through Cholame (about 1 mile) and on to Paso Robles (25 miles).

DAY 2--PASO ROBLES TO PALMDALE, CALIFORNIA

Summary

Today we proceed south along the San Andreas fault with stops at classic sites that show the geomorphic expression of strike-slip faulting on the Carrizo Plain. Several of the stops provide an opportunity to look at geomorphic details along the fault trace that have been combined with careful stratigraphic studies to develop a late Holocene history of faulting. Most of the route is within the zone of surface faulting from the 1857 Fort Tejon earthquake, and geomorphic evidence of the young displacement is well preserved at many of the stops.

Segment 2A--Paso Robles to the Northern Carrizo Plain (61 miles)

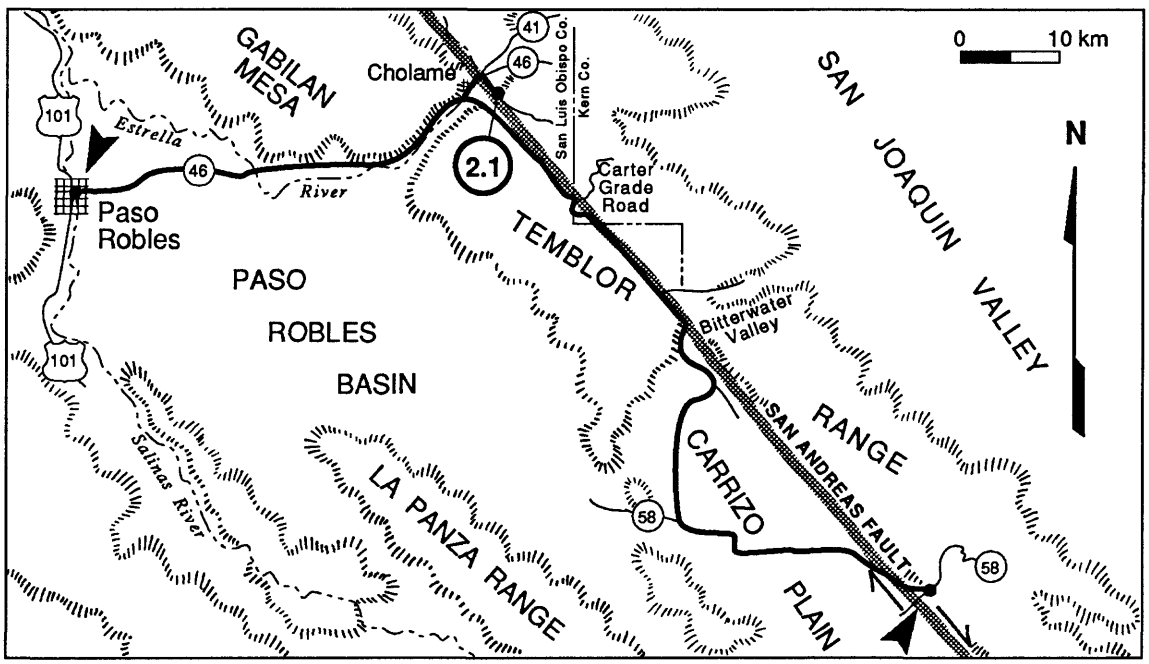

Figure 2-1. Route map for Segment 2A, Paso Robles to northern Carrizo Plain.

Route Narrative--We will retrace the last part of yesterday's route and return to the southernmost part of Cholame Valley. Leave Paso Robles from the intersection of California Highway 46 and U.S. Highway 101 and drive 24 miles east on California Highway 46 to Cholame. Continue east past Cholame for 0.8 mile and cross the bridge over Cholame Creek. Turn right on Cholame Valley Road (paved) just after the bridge and drive 1.1 miles to the intersection with a dirt road on the left. Park here for *Stop 2.1*.

Stop 2.1--Southern Cholame Valley

Youthful, small gullies and stream channels offset by the San Andreas fault are well preserved here and illustrate some of the complications involved in using geomorphology to determine late Holocene and historic slip rates.

The stop is within the northern part of the surface faulting produced by the 1857 Fort Tejon earthquake, at the southern limit of surface faulting from the 1966 Parkfield-Cholame earthquake, and near the southern limit of the creeping section of the San Andreas fault. The 55-km-long section of the fault from Cholame southeast to the northern Carrizo Plain has been defined as the Cholame segment by the Working Group on California Earthquake Probabilities (1988); it represents a zone of transition between large amounts of slip that occurred in 1857 along the Carrizo segment to the southeast and relatively small amounts of slip that occurred along the Parkfield segment to the northwest. Uncertainties in relations among fault creep, the amount of slip associated with the 1857 earthquake, and the fraction of accumulated strain released in earthquakes in this region strongly affect estimates of the likelihood of seismic rupture on the Cholame segment of the San Andreas fault in the next few decades. The Working Group has assigned a 30-year probability of 0.3 to this segment, but assign a low reliability to the value because of the uncertainties in the data.

Historical accounts of the great 1857 earthquake cited by Sieh (1978a) indicate that surface faulting extended at least as far north as Cholame Valley and possibly as far as 80 km northwest of Cholame, to the southern end of Bitterwater Valley. As part of a study of fault slip associated with that earthquake, Sieh (1978b) measured a number of offset gullies along the Cholame segment of the San Andreas fault. He reported offsets ranging between 1 and 9 m, and assumed that the smaller offsets are probably associated with the 1857 earthquake and that larger offsets are the cumulative result of the 1857 earthquake and other earlier earthquakes. He favored an average slip of about 3.5 m for this segment of the fault, but noted that pre-1857 earthquakes could have contributed to the measured total slip at some sites, such as the gully at this field-trip stop.

Lienkaemper (1987) independently repeated the measurement of offset gullies in the same 30-km-long section of the San Andreas fault (including the gully at this stop) and concluded that the 4 most reliable measurements yield values of 5-7 m. He argues that Sieh's (1978b) measurements of 3-4 m for slip from the 1857 earthquake in this area could be 2-3 m greater, depending on assumptions made about amounts of post-1857 erosion. Both authors agree that there is about 6-7 m of offset of the gully at this stop. The 1966 Parkfield-Cholame earthquake offset the gully at this stop about 3 cm (Brown and others, 1967).

This stop is at the approximate southern limit of the creeping section of the San Andreas fault (fig 1-6). Neither an alinement array nor a 29-year-old fence several kilometers to the southeast of this stop show evidence of slip according to Burford and Harsh (1980). However, their alinement array several kilometers north of here (*Stop 1.8*) yielded a slip rate of 4 mm/yr.

Route Narrative (continued)--Return to California Highway 46 and turn left toward Paso Robles. Note the odometer reading at Cholame, and continue west for 1.2 miles to the intersection of California Highway 46 and Palo Prieto Canyon Road. Turn left onto Palo Prieto Canyon Road, cross another bridge at Cholame Creek, and proceed south into the Temblor Range. The San Andreas fault forms a prominent slot along the axis of this range, which separates Cholame Valley from the Carrizo Plain.

At Mile 7.4 the road enters the northwest end of the prominent linear valley of Palo Prieto Pass (also known as Choice Valley). Continue for about 2.5 miles to a conspicuous left turn in the road at Mile 9.8. Immediately after the turn, the trace of the San Andreas fault lies midway up the slope of the hills at 10 to 1 o'clock, parallel to the valley. About 0.5 mile further, the highway intersects the Carter Grade Road at the San Luis Obispo-Kern County line.

In about 2 miles, at Mile 12.3, the road makes another conspicuous left bend to the east and continues straight for 0.25 mile toward the hill at the east edge of the valley at 12 o'clock. A trace of the San Andreas fault lies at the base of the hill about 50 m east of the road. For about the next mile a southwest-facing scarp along the fault trace parallels the road about 50 m to the east.

At Mile 16.5 the highway passes a ranch (on left). A southwest-facing fault scarp trends along the eastern edge of the ranch buildings. Note the closed depression about 500 m long on left side of the road about a mile southeast of the ranch. The trace of the fault is marked by a southwest-facing scarp along the opposite (northeast) side of the depression.

In 0.5 mile there is a Y intersection at the head of Bitterwater Valley to the east. Take the RIGHT fork. The fault continues across the head of Bitterwater Valley, the late Pliocene and Pleistocene drainage from the San Joaquin Valley inferred by Sims and Hamilton (1989), and along the southwest side of the Temblor Range to the south. In 1.9 miles, at a right bend, the road diverges from the trace of the fault. The field-trip route intersects the fault again in the Carrizo Plain. Continue nearly 15 miles on the paved road to its intersection with California Highway 58 in the Carrizo Plain at Mile 32.

Segment 2B--Northern Carrizo Plain to Maricopa (43 miles)

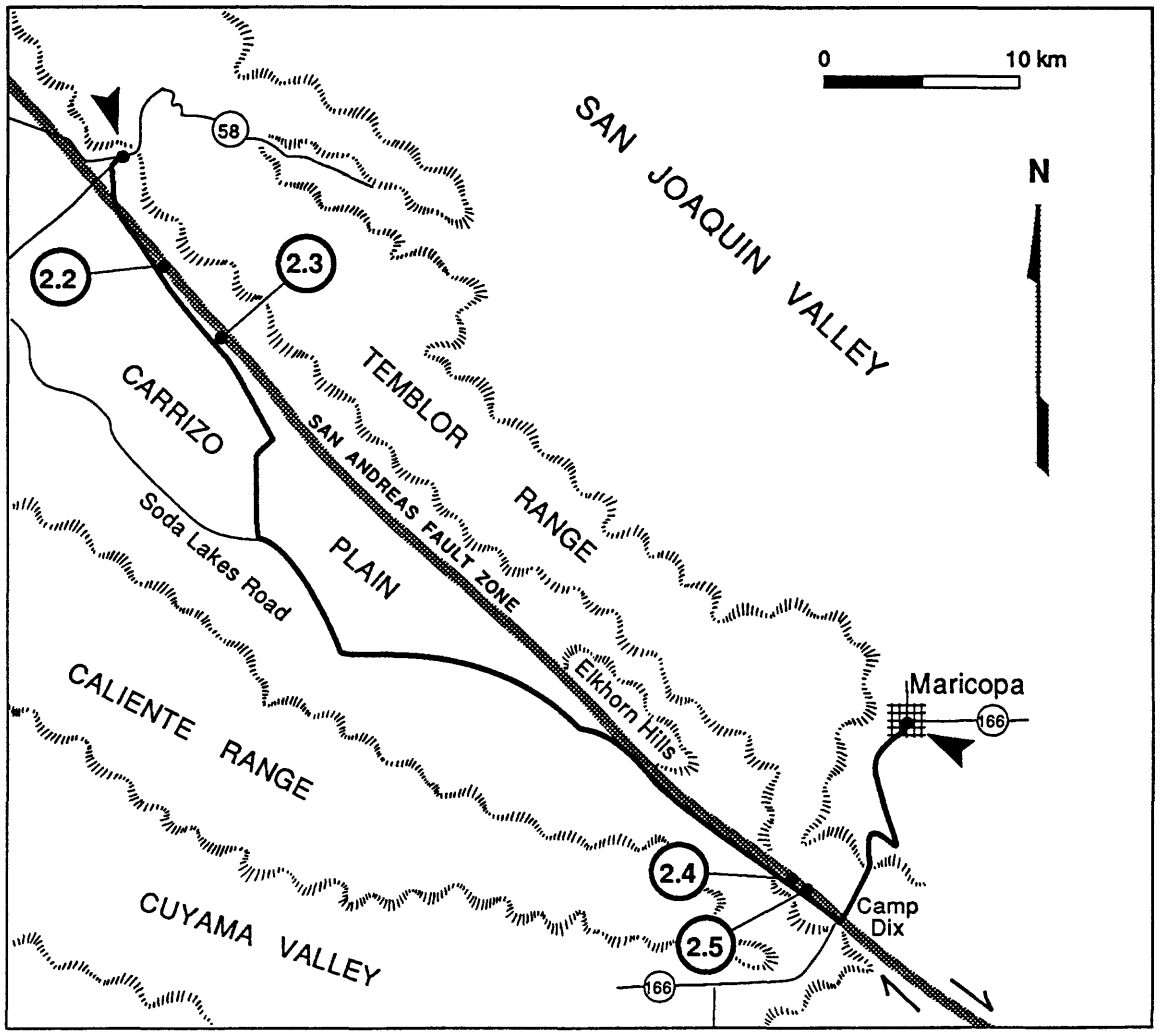

Figure 2-2. Route map for Segment 2B, northern Carrizo Plain to Maricopa.

About 3 miles after turning onto the highway you pass the ARCO Photovoltaic Solar Power Production Plant, and, 6 miles farther, 7 Mile Road intersects the highway at the mouth of San Diego Creek at the base of the Temblor Range. Note the odometer reading again and turn right onto 7 Mile Road.

Route Narrative--Drive 0.2 mile to the southwest, past the gas station, and turn left (south) onto Elkhorn Road (gravel). Continue on the gravel road 3.7 miles to *Stop 2.2* at Wallace Creek. *Do not attempt to drive on this road during or soon after wet weather; it is likely to be impassible.*

Stop 2.2--Offset Stream Channels, Wallace Creek

A variety of geomorphic features associated with strike-slip faults are particularly well expressed at this classic site. From the stop at Wallace Creek (locality A on fig. 2-3) southeast along the fault for about 2.5 km

(locality B), there are spectacular examples of offset and beheaded stream channels, shutter ridges, and sag ponds (fig. 2-4). The description of the features in this area is a brief summary of some of the major points in a detailed field guide to the site by Sieh and Wallace (1987). We will walk along the San Andreas fault, traversing the area shown in fig. 2-3.

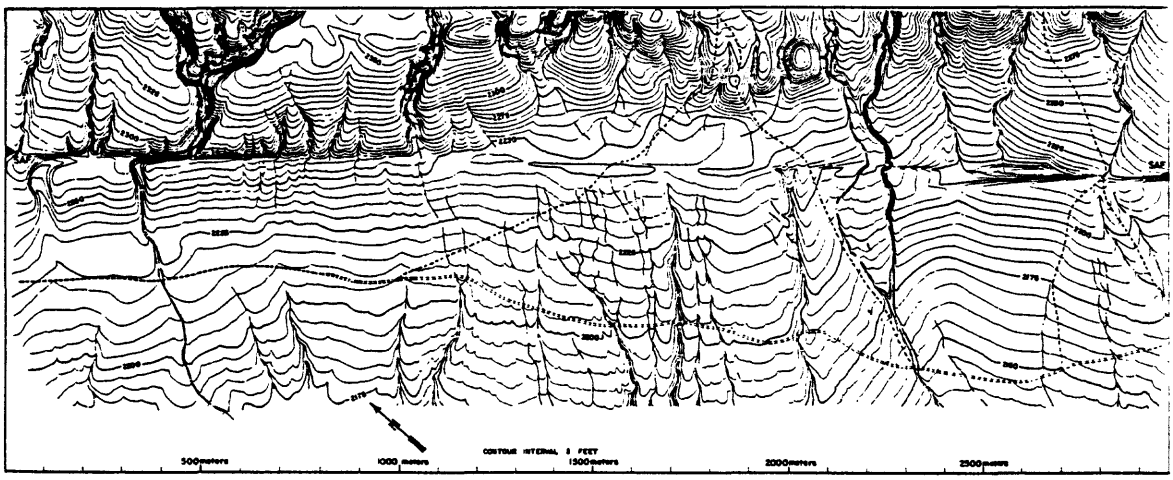

Figure 2-3. Topographic map along the San Andreas fault in the vicinity of Wallace Creek (from Sieh and Wallace, 1987). Field-trip *Stop 2.2.*

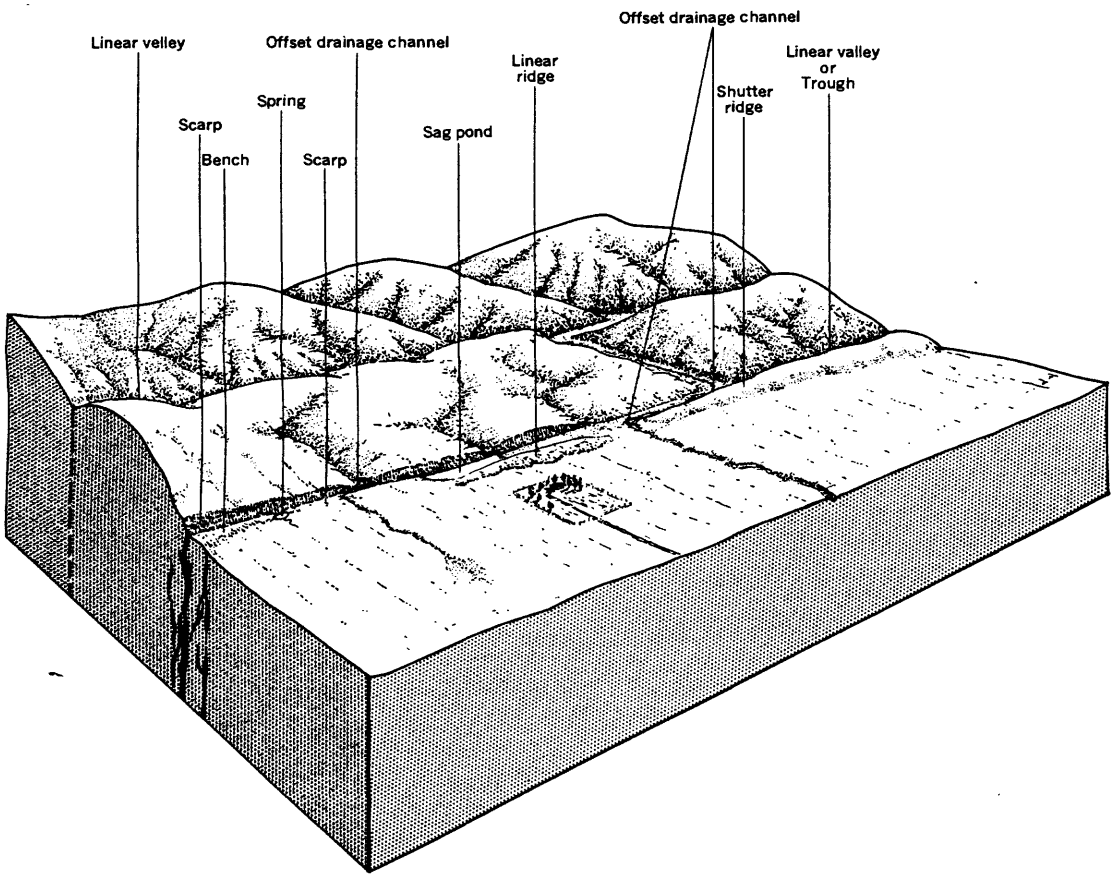

Figure 2-4. Block diagram showing landforms produced along recently active strike-slip faults, such as the San Andreas (from Vedder and Wallace, 1970).

Detailed study of Wallace Creek (fig. 2-3) by Sieh and Jahns (1984) has shown an average slip rate at this site of 34 mm/yr for at least the past 13,000 years. During that time, the channel of Wallace Creek upstream from the fault has essentially maintained its channel while the downstream section has abandoned its channel and cut a new channel several times. The oldest abandoned channel of Wallace Creek (at the -10-m mark, just beyond the edge of fig. 2-3) is offset 475 m relative to the upstream channel. A second abandoned channel, active between 11,000 and 3,700 years ago is located at the 100-m mark of figure 2-3. The part of that channel which followed the fault was partly filled by alluvium 3,700 years ago, producing a terrace 7 m above the present channel floor near the fault. The sedimentation in the channel caused cutting of the present channel across the fault. Displacement subsequent to 3,700 years ago along the fault has resulted in the 130-m offset of the present channel.

Southeast of Wallace Creek, horizontal offset of the convex surface of an alluvial fan between the 960- and 1,100-m marks has produced scarps facing in alternate directions along the fault trace. The scarp on the northwestern (downhill) part of the fan faces uphill and the scarp on the southeastern part of the fan faces downhill.

Continue along the fault about a kilometer to the southeast to a large shutter ridge located between 1,100- and 1,900-m marks on figure 2-3. Shutter ridges are topographic highs that have been displaced across drainages along strike-slip faults (Buwalda, 1936). The abrupt change in stream gradient behind shutter ridges commonly results in a conspicuous accumulation of sediment, particularly where the shutter ridge has formed a closed depression, such as at this site.

Walk to the southeast about another kilometer to the area between the 2,350- and 2,700-m marks on figure 2-3. A right-stepping echelon offset of the fault trace in that interval has produced a depression. A severe storm in February 1978 produced a pond about 3.5 m deep in the depression. Drainage of the water into fractures along the fault planes eroded near-surface sediment along the walls of the fractures, and slumping and collapse into the resulting voids produced pits as much as 3 m in depth and length along the fault traces. This process has been described in detail by Clark (1972) from study of similar features that formed following a historic earthquake in southern California.

Route Narrative (continued)--Return to the vehicles and drive southeast 2.8 miles to an east-west road junction. Turn left and drive east about 0.2 mile to intersect the fault trace at *Stop 2.3*.

Stop 2.3--1857 Earthquake Geomorphic Features, Panorama Hills.

Small geomorphic features produced by the 1857 earthquake are preserved from here to the southeast for about a kilometer (Sieh, 1978b). At his site 31, a shallow (40-cm-deep) gully about 80 m southeast of here, he measured 9.1 m of offset caused by the 1857 earthquake. Figure 2-5, taken from Sieh's article, is a plane-table map at the offset stream. Walk in a southeasterly direction for about 1 km to look at various geomorphic features produced by the 1857 earthquake.

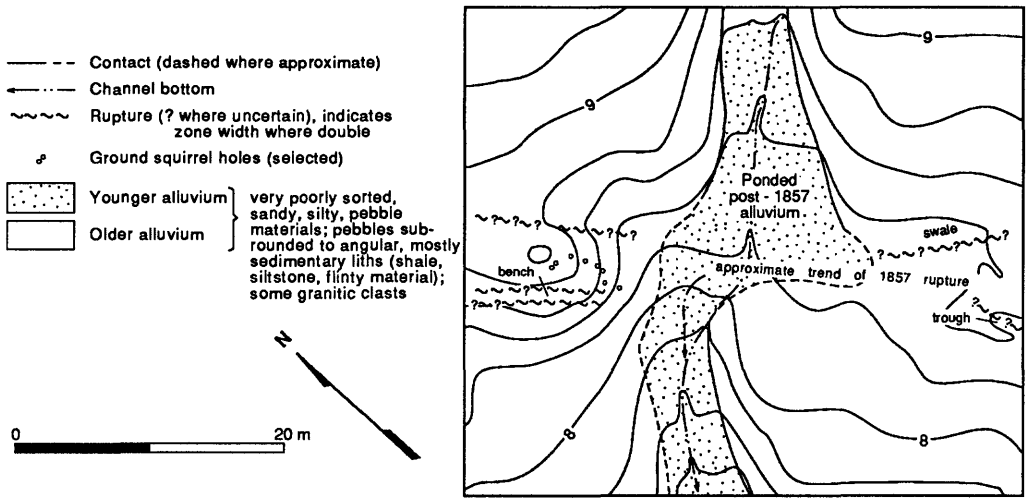

Figure 2-5. Plane table map (modified from Sieh, 1978b) of offset channel at *Stop 2.3* along San Andreas fault at Carrizo Plain (site 31 of Sieh, 1978b).

Route Narrative (continued)--Return 0.2 mile to the main road, drive southeast 3 miles to a prominent road junction, turn right, drive about 0.8 mile southwest, turn left at a junction, drive about 2.5 miles and turn left (south) on Soda Lake Road (paved). Drive southeast for 22.4 miles to *Stop 2.4*. Walk to the site about 30 m northeast of the road.

Stop 2.4--Offset Gullies, Southern Carrizo Plain

Several small alluvial fans at the foot of the slope have been offset from their source gullies about 6.5 m (fig. 2-6). Younger, active fans at the mouths of the gullies are slowly burying the older, offset fans. The gullies are at sites 82, 83, and 84 of Sieh (1978b) who argued that the lack of intermediate-age alluvial fans between those offset 6.5 m (pre-1857 fans) and the currently active fans indicates that the displacement occurred in a single event or multiple events within one or two decades at most and is most likely the result of the 1857 earthquake.

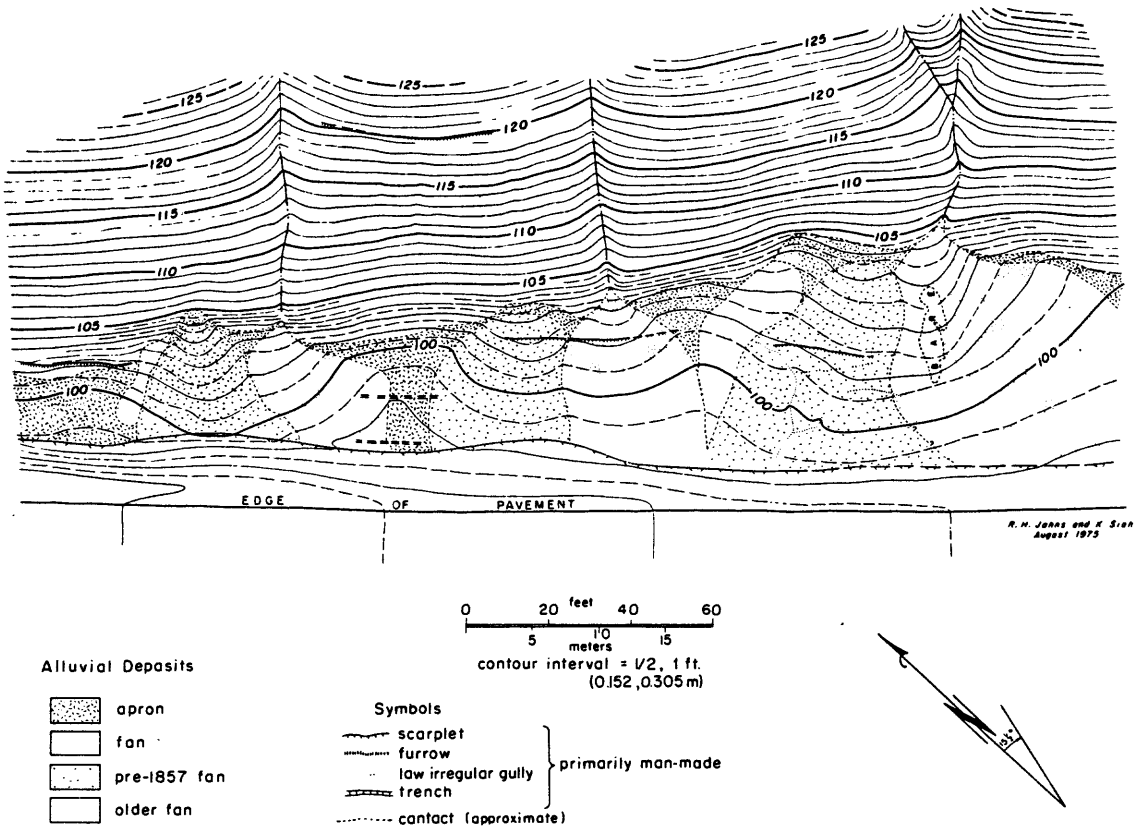

Figure 2-6. Map of offset alluvial fans (modified from Sieh, 1978b) at *Stop 2.4* along San Andreas fault at southern Carrizo Plain (sites 82, 83, and 84 of Sieh, 1978b).

Route Narrative (continued)--Continue southeast along Soda Lakes Road (or walk) for about 0.6 mile to *Stop 2.5* at a prominent salt-encrusted sag pond. The pond lies along a linear trench in the fault zone having a prominent scarp on the east side.

Stop 2.5--Sag Pond, Southern Carrizo Plain

This is the area of sites 86, 87, and 88 of Sieh (1978b) where he measured 3.9- to 7.4-m offset of gullies in the face of the scarp and associated beheaded gullies incised into the fan at the foot of the scarp. He suggests that the offset of 3.9 m may be small due to additional movement on a parallel fault, which has a very fresh scarplet about 340 m to the southwest across the road, and by movement on a possible fault strand buried by sag-pond sediment.

Route Narrative (continued)--Drive 1.1 miles southeast to the junction of Soda Lakes Road and California Highway 166 at Camp Dix. Turn left onto Highway 166 and drive northeasterly to Maricopa (6.4 miles). The road crosses the fault trace about 150 m east of the intersection.

Segment 2C--Maricopa to Palmdale (100 miles)

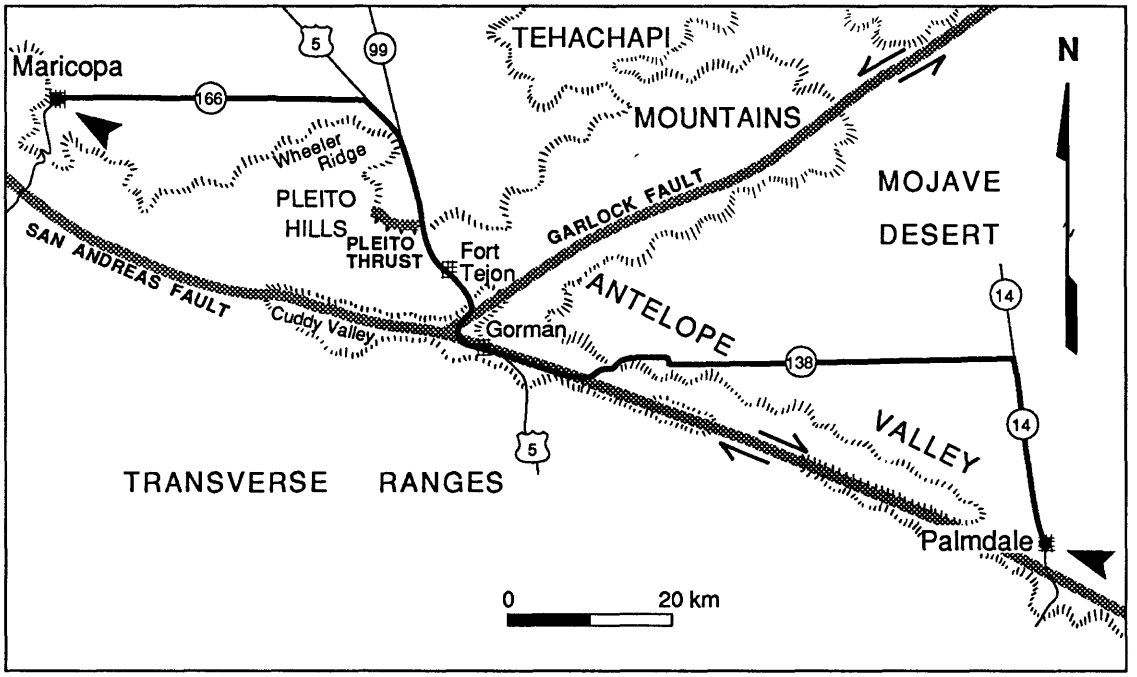

Figure 2-7. Route map for Segment 2C, Maricopa to Palmdale.

Route Narrative--Note the odometer reading in Maricopa and go east on California Highway 166. At the junction of Highways 166 and 33 (Mile 2.4), continue right on Highway 166. Ahead lie the Tehachapi Mountains, a southwest projecting spur at the southern end of the Sierra Nevada. The northwest base of the Tehachapi Mountains (at 11 o'clock) is bounded by the southeast-dipping White Wolf thrust fault. The fault trends southwest from the range front to Wheeler Ridge, which is the east-trending ridge at 1-2 o'clock. Surface ruptures formed along this fault at the base of the Tehachapi Mountains during the 1952 Arvin-Tehachapi earthquake (Buwalda and Saint-Amand, 1955) but did not extend across the valley to the epicentral area, which was located beneath Wheeler Ridge. At Mile 19.6, Highway 166 crosses the California Aqueduct, and at Mile 24 you reach the junction of Highway 166 and Interstate 5. Note the odometer reading again and turn right onto I-5, southbound.

Wheeler Ridge, to the right, is an east-west-trending anticlinal spur of the Pleito Hills. Sands and gravels of the Pleistocene Tulare Formation, which are being mined near the east end of the ridge, are folded by the deformation that is largely responsible for the topographic expression of the ridge (Sharp, 1976). Deformation of Holocene alluvial surfaces at the east end of the ridge suggest an uplift rate of about 1.4 mm/yr (Zepeda and others, 1986). Wheeler Ridge, which overlies the epicenter of the 1952 Arvin-Tehachapi earthquake, was uplifted coseismically 70 cm during the earthquake (Stein and Thatcher, 1981) without accompanying surface faulting.

The mountains ahead are the Transverse Ranges, which consist of a series of nearly east-west trending ranges and valleys that are oblique to the generally northwest trending topography of California. Namson and Davis (1988) interpret the Transverse Ranges to be an active fold and thrust belt that has had an average

convergence rate of 18-26 mm/yr since the belt began to form about 2-3 Ma (late Pliocene time). Deformation here on the north flank of the Transverse Ranges is associated with the Pleito thrust system, which is rooted at depth in a common detachment fault (Namson and Davis, 1988). Folds, such as the Wheeler Ridge anticline, are interpreted to have formed as fault-bend or fault-propagation folds (Suppe, 1985) over south-dipping splays of thrust faults that do not reach the surface. Davis and Lagoe (1987) have suggested that the 1952 Arvin-Tehachapi earthquake occurred on one of these buried thrusts rather than on the White Wolf fault, the commonly cited source for that earthquake. The occurrence of earthquakes on buried faults associated with overlying young folds is becoming recognized as a widespread geological process and as an important factor in the evaluation of seismic hazards (Stein and Yeats, 1989). They cite the 1983 Coalinga, California, earthquake (fig. 1-14) as another recent example of slip on a buried fault that produced uplift of an overlying anticline.

At Mile 8, as you approach the Pleito Hills at 12 o'clock, small scarps along the Pleito thrust are visible at the base of the range on the west (right) side of the highway. At Mile 15, I-5 passes the exit to Fort Tejon State Historical Park. About 2 miles past the Fort Tejon exit, we enter Castac Valley, and, just after the broad bend to the right at Lebec, I-5 crosses the Garlock fault. The fault trends up the valley (east) at 7 o'clock, across Castac Lake. At Mile 19 the route passes the junction of the Garlock and San Andreas faults in Cuddy Canyon at 2 o'clock.

Turn off I-5 onto California Highway 138 about 4 miles ahead near Gorman, and follow the trace of the San Andreas fault for about 6 miles to the road junction just beyond Quail Lake. Displacements along the fault from the 1857 earthquake were about 6 m in this area (Sieh, 1978b). Stay left on Highway 138 at the junction and continue east 34 miles to the junction with California Highway 14. Turn right at Highway 14 and drive south through Lancaster (6 miles) to Palmdale (8 miles).

DAY 3--PALMDALE TO MAMMOTH LAKES, CALIFORNIA

Summary

Today we turn northeastward to follow the central part of the left-lateral Garlock fault and then northward along the eastern front of the Sierra Nevada at the western margin of the Basin and Range, where faults show right-slip and normal movement. The first three stops are along the Garlock fault. Later in the day, three stops are scheduled to evaluate the mode of surface displacement resulting from the 1872 Owens Valley earthquake, including a site where slip is predominantly right oblique and a site where dip slip has offset a 300-ka cinder cone. Then, we continue north along the frontal fault zone of the Sierra Nevada. After our last stop along the Owens Valley fault zone, we ascend Sherwin Summit and descend into the Long Valley caldera and make a brief stop to view some of its features.

Garlock Fault

The Garlock fault extends more than 250 km east-northeast from the San Andreas fault near Gorman to the Death Valley fault zone and marks the boundary between the Mojave Desert block on the south and the Sierra Nevada and Basin and Range provinces on the north (fig. 3-1). There has probably been about 64 km of horizontal slip on the fault since 9 Ma (Carter, 1987), based on offset of a late Mesozoic dike swarm (Smith, 1962). The lack of a similar, large offset where the Garlock intersects the San Andreas and Death Valley faults has been modelled in several ways. For example, Hill and Dibblee (1953) suggested that the Garlock and the Big Pine fault, west of the San Andreas, were originally continuous, and that the Garlock, Big Pine, and San Andreas faults are conjugate shears in a regional pattern of east-west extension and north-south shortening. Davis and Burchfiel (1973) interpreted the Garlock fault as an intracontinental transform fault separating the region extended by late Cenozoic Basin-and-Range faulting north of the fault from the relatively undeformed Mojave Desert block to the south (fig. 3-1). In this model, westward movement (extension) of the northern block is partly responsible for the westward bend in the San Andreas fault where it intersects the Garlock fault.

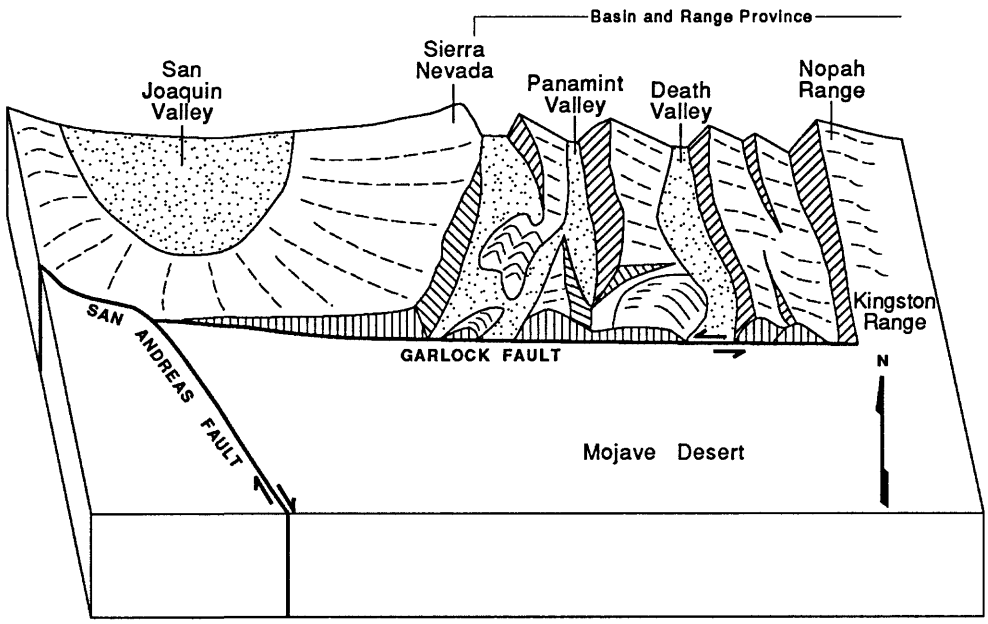

Figure 3-1. Schematic diagram of the Garlock fault as an intracontinental transform fault accommodating the Basin-and-Range extension north of the fault relative to the unfaulted Mojave Desert block to the south (modified from Davis and Burchfiel, 1973).

The Garlock fault displays many of the geomorphic characteristics of the San Andreas fault, although it has a conspicuously lower slip rate. Matching offset alluvial deposits south of the fault with source areas having distinctive lithologies north of the fault, in the El Paso Mountains (discussed further at *Stop 3.2*), indicates an average rate of slip of 7 mm/yr since about 9 Ma (latest Miocene) (Carter, 1987). Data on Holocene deformation from sites along the fault as summarized by Astiz and Allen (1983) indicates an average latest Pleistocene and Holocene slip rate of 7 mm/yr and a recurrence interval of 1,000±500 years for large earthquakes.

The fault is divided into two contrasting sections by a left-stepping echelon offset of its trace midway along the fault at Koehn Lake (*Stop 3.1*). The two sections differ in geomorphic expression, levels of historic seismicity, and evidence of aseismic slip. In general, the western section is characterized by relatively poor geomorphic expression of the fault zone (Clark, 1973), by a low but persistent level of seismicity (Astiz and Allen, 1983), and by local evidence of aseismic slip (Louie and others, 1985). In contrast, the eastern section is characterized by good geomorphic expression of the fault zone (with local preservation of evidence of very youthful movement), by a near absence of historic earthquakes, and by lack of evidence for aseismic slip.

Segment 3A--Palmdale to Garlock (69 miles)

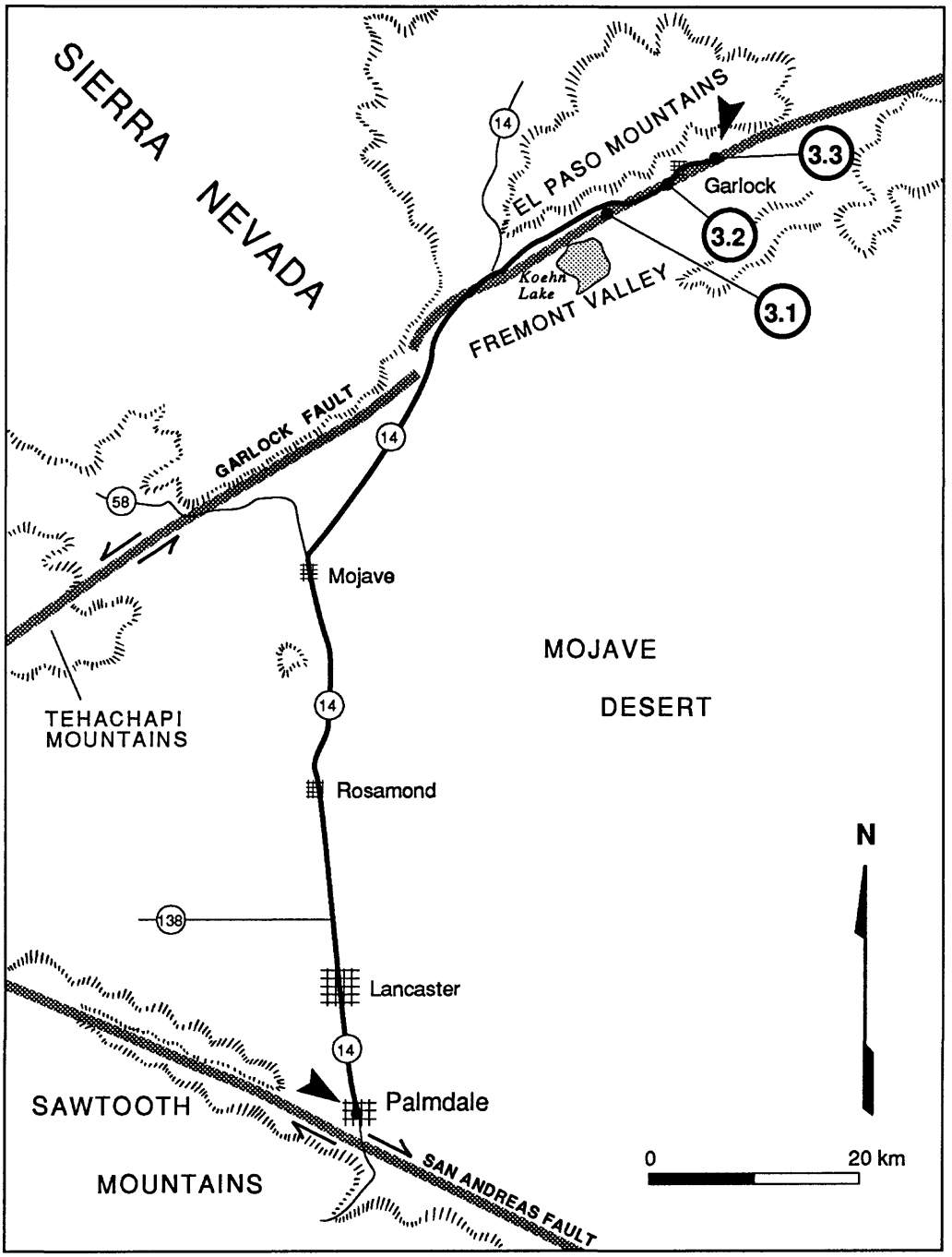

Figure 3-2. Route map for Segment 3A, Palmdale to Garlock.

Route Narrative--Leave Palmdale and drive north on California Highway 14 through Lancaster (Mile 8) and Rosamond (Mile 18). Continue north through Mojave and note the odometer reading at the intersection of

California Highways 14 and 58, about 1 mile north of Mojave. Bear right (northeast) on California Highway 14. To the northwest of the intersection there is a large complex of windmills used to generate electric power. The mountains at the head of the alluvial fans to the left (north) of the highway are the southern end of the Sierra Nevada, which is truncated abruptly by the Garlock fault at the foot of the range.

At Mile 13.5 the highway passes over the crest of a hill and at 2 o'clock you get a good view of Fremont Valley and Koehn Lake. Fremont Valley occupies a pull-apart basin at a left step in the Garlock fault (Clark, 1973; Aydin and Nur, 1982), in a setting analogous to that at the stepover along the San Andreas fault at the southern end of Cholame Valley (*Stop 1.8*). On the basis of gravity data, Mabey (1960) estimated that more than 3 km of Cenozoic sediment underlies part of Fremont Valley; the valley has the steepest gravity gradient in the western Mojave Desert (fig. 3-3).

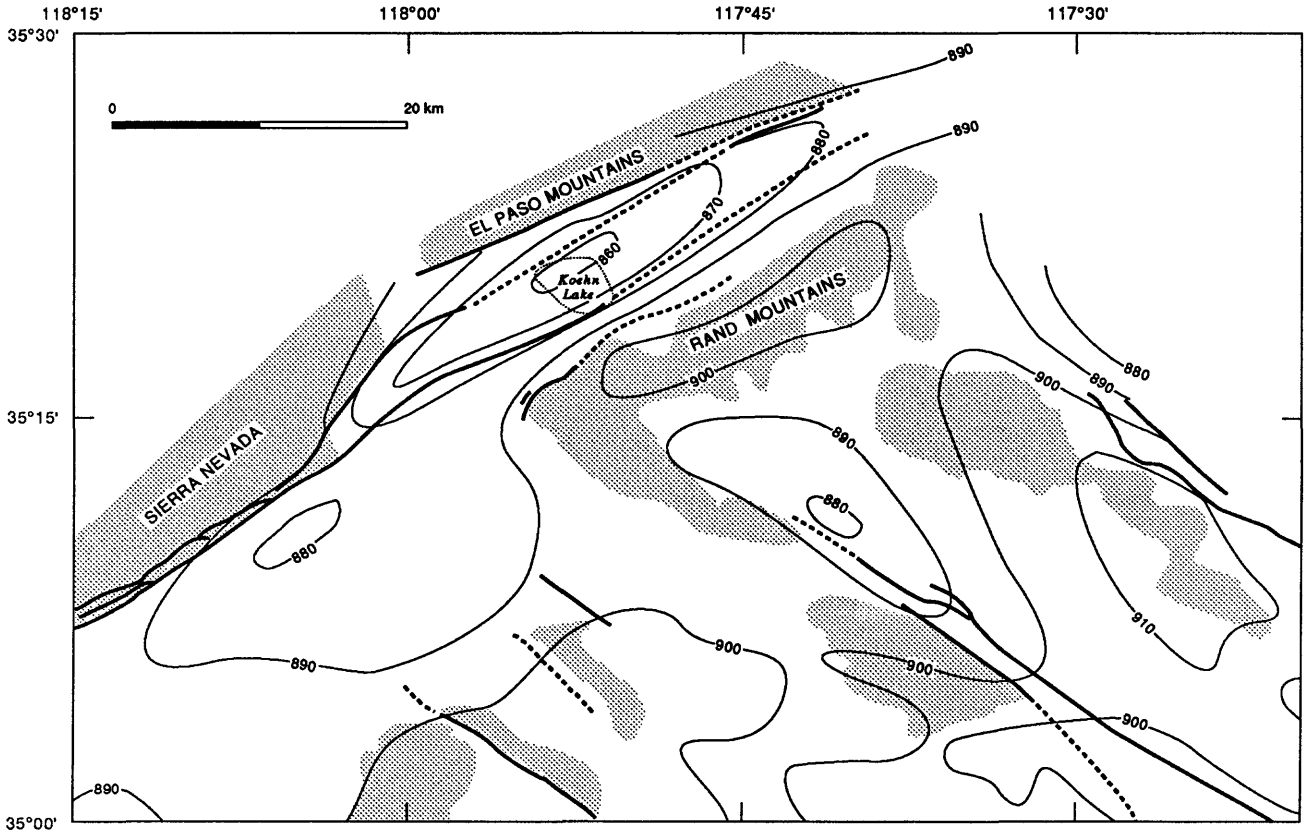

Figure 3-3. Gravity map along the central Garlock fault (from Mabey, 1960).

Fissuring and vertical displacement along- and on-trend with Holocene scarps of the Garlock fault have been observed in Fremont Valley near, and to the southwest of, Koehn Lake (Pampeyan and others, 1988). This modern ground failure, first noted in 1971, is restricted to a part of the valley in which large quantities of ground water have been withdrawn for irrigation. Based on analysis of data from ground-water levels in wells and geodetic monitoring of the ground surface, Pampeyan and others (1988) concluded that the faulting is a result of compaction of aquifers and not the result of tectonic activity.

At Mile 16, and for about the next 4 miles as the highway swings close to the mountain front, low scarps (several meters high) mark the trace of the Garlock fault on the alluvial fans on the left (north) side of

the highway. Continue on Highway 14 to the Randsburg-Johannesburg Road intersection on the right at Mile 20.2, turn right onto Randsburg-Johannesburg Road. The road forks after turning off Highway 14; take the left fork and note the odometer reading. In about 8 miles, as the highway crests a gentle hill to the east, there is a good view of a lacustrine bar of late Pleistocene Fremont Lake which trends across the east end of present-day Koehn Lake. At Mile 8.3 from Highway 14 turn onto a dirt road on the right. Follow the road for 0.4 mile southeast along the gravel pit excavated into the lake bar to the railroad tracks and park. *Stop 3.1* is at a site where the bar is offset by the Garlock fault.

Stop 3.1--Garlock Fault at Koehn Lake

Walk 400 m to the southeast along the lake bar to intersect the Garlock fault, which has offset the bar about 80 m left laterally and 7 m down to the north (Clark and Lajoie, 1974; Carter, 1987). A ^{14}C age of 11,360 years on tufa deposited on the bar suggests an average latest Pleistocene and Holocene slip rate of 7 mm/yr (Clark and Lajoie, 1974). They suggest that movement has continued well into the Holocene because the younger playa surface to the west is also offset down to the north, but by a smaller amount.

West of the bar the fault trace is marked by an elongate string of low mounds 1-2 m high. The low mound of dirt about 300 m west of fault-bar intersection marks the location of a trench excavated across the fault (Burke, 1979) and provides a convenient reference for locating the general strike of the fault. The trench exposed sediment deposited during the last deep-lake cycle in Fremont Valley and younger (Holocene) fluvial sediment. Burke (1979) reported a ^{14}C age of 14,200 years on fossils from the older lake beds, which he associated with the last highstand of the lake. Sediment exposed in the trench is deformed into an anticline within the fault zone. Burke (1979) interpreted the relations between buried faults and unconformities in the trench as evidence of at least nine episodes of fault activity in the past 14,200 years. This level of repeated faulting suggests a recurrence interval of less than 1,500 years.

Route Narrative (continued)--Return to the Randsburg-Johannesburg Road and turn right (east). At Mile 2.7 the highway intersects a dirt road (Mesquite Canyon Road) on the left and then passes to the south of low hills of highly dissected and tilted Pleistocene rocks that are unconformably overlain by coarse alluvial fan gravels (Dibblee, 1952). The gravels contain clasts of the Mesquite Schist, a distinctive quartz-sericite-albite schist which nearly always contains porphyroblasts of chlorite, albite, or chloritoid (Carter, 1987).

The fault crosses the highway near the western end of the low hills, its location locally marked by springs and by a prominent scarp farther east. The highway forks in about a mile, just as it bends to the right. Take the left fork and continue 0.8 miles to the Garlock historic site monument. A dirt road on the north side of highway about 100 m west of the historic monument leads to a flat area suitable for parking about 200 m to the west for *Stop 3.2*.

Stop 3.2--Mesquite Fan at Garlock

Walk to the shutter ridge about 150 m to the south of the parking area for an overview of strike-slip features along the Garlock fault and of grabens on the Mesquite fan. Walk about 1 km northwest along the road from the area where the cars are parked to study the evidence for recurrent movement on the normal faults that offset the Mesquite alluvial fan surfaces north of the Garlock fault (fig. 3-4). Note clasts of the distinctive Mesquite Schist in the gravel along the road. The schist only crops out in a small area near Mesquite Canyon, and any alluvial deposits south of the Garlock fault which contain clasts of this schist must have been originally deposited in the vicinity of Mesquite Canyon. Clasts of this schist are found in deposits as old as latest Miocene on the south side of the fault and as far as about 47 km to the east, giving a long-term slip rate of 7 mm/yr (Carter, 1987).

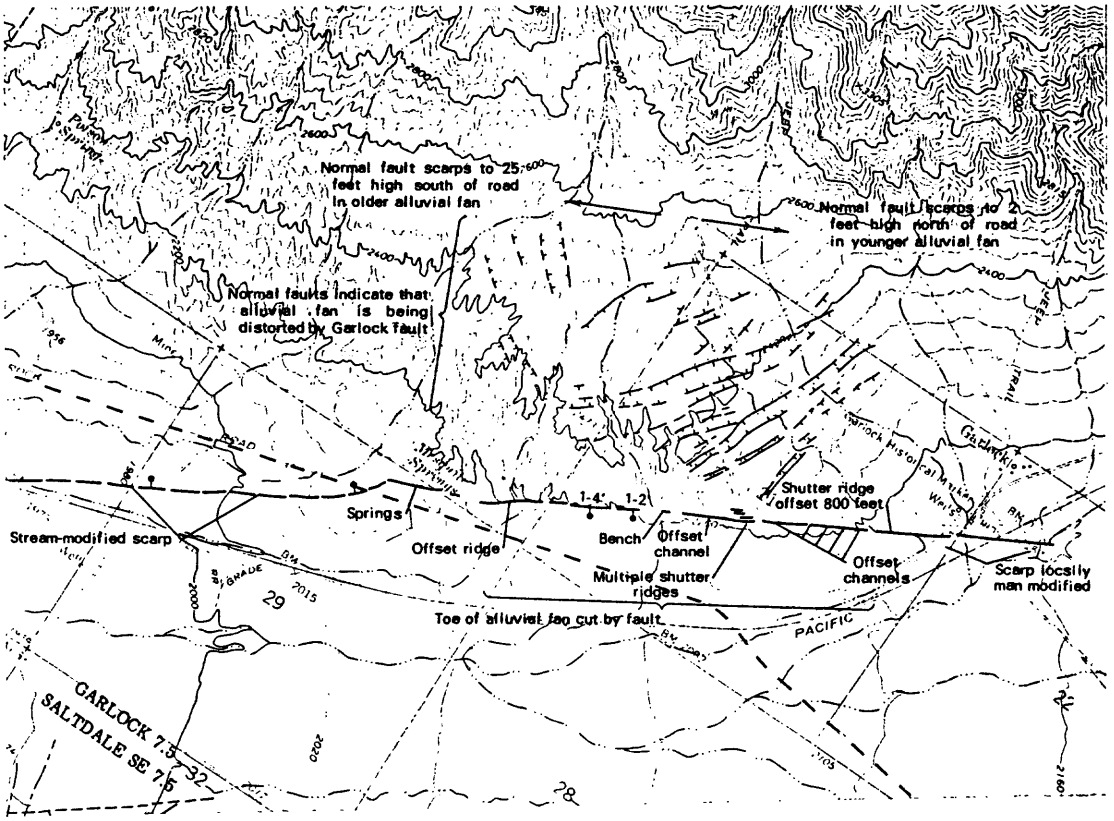

Figure 3-4. Map of faults and fault-related features along the Garlock fault at Mesquite Fan (from Clark, 1973).

Route Narrative (continued)--Return to the Randsburg-Johannesburg Road and drive 2.7 miles easterly to a closed depression along the Garlock fault at lower Goler Wash.

Stop 3.3--Goler Depression

This conspicuous depression has been formed by about 800 m of offset of the curving east bank of Goler Gulch along the Garlock fault. Subsequent deposition of alluvium from the wash has blocked the western end forming a closed depression (Carter, 1987). About 1 km to the east of this depression, a large graben is present along the north side of the Garlock fault and the south side of the El Paso fault along the southern foot of the El Paso Mountains. The fault scarp east of the graben exposes terrace gravels which underlie surficial gravels deposited by Goler Wash. The terrace gravels, which contain abundant clasts of Mesquite Schist, now lie 11 km east of the area in which they were deposited near the mouth of Mesquite Canyon (Carter, 1987).

Route Narrative (continued)--Return to Highway 14 (15.5 miles west of *Stop 3.3*) and turn right, toward Bishop. Mining in the El Paso Mountains, northwest of the route, and the Rand Mountains, southeast of the route (fig. 3-2), began with a 1849 placer discovery by two German immigrants. Presumably John Goller and Wolfgang Tauber left Death Valley on foot. Enroute to Los Angeles, they found signs of placer gold somewhere in the El Paso Mountains. Although Goller returned frequently to the area, he never found the site of the original discovery; however, his obvious interest brought other prospectors into the area. Mining districts on the northeast side of the Rand Mountains produced more than $35 million between 1895 and 1924

from gold and silver, and, in later years, tungsten was mined until the mid-1950's (Sharp, 1976). The ore bodies were emplaced in the country rock during Miocene volcanic activity.

Mining in the El Paso Mountains is evidenced by numerous placer mines and several abandoned camps; in the 1890's, a single nugget worth nearly $2,000 was found near Red Rock Canyon (see fig. 3-5). Gold worth about $2.5 million was mined from this area (Leadabrand, 1966). The most notable effort, however, is the 600-m-long tunnel extending from the interior of the range (in Copper Basin) to near Saltdale. William H. (Burro) Schmidt began excavating this tunnel in the early 1900's by to shorten the distance of hauling his ore to the smelter (Leadabrand, 1966;). His single-minded preoccupation with the tunnel did not end until its completion in 1938, when he was 68; after which, he sold his holdings and the tunnel.

SEGMENT 3B--INTERSECTION OF RANDSBURG ROAD AND CALIFORNIA HIGHWAY 14 TO OLANCHA (70 MILES)

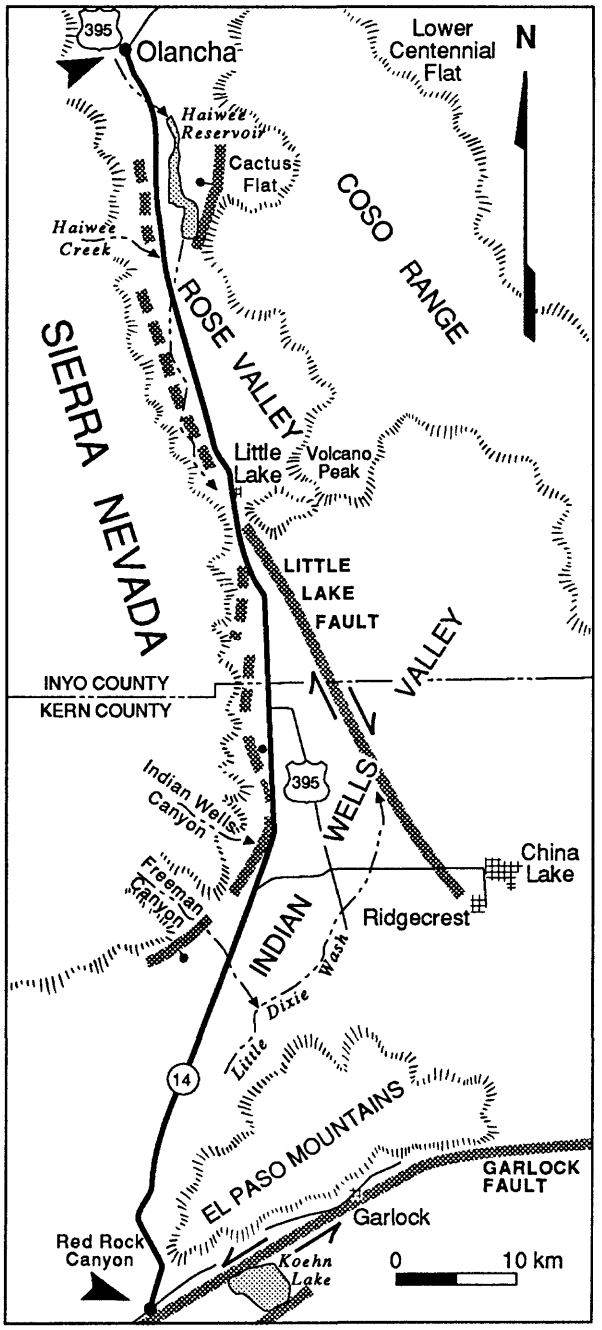

Figure 3-5. Route map for Segment 3B, Garlock to Olancha.

Route Narrative--The route enters the El Paso Mountains, at Red Rock Canyon (fig. 3-5), in about 2 miles; at Mile 3.8 there is a scenic turn off. The lower part of the canyon is a steep-walled gorge cut through pre-Tertiary crystalline rocks; however, the upper part of the canyon forms a broad amphitheater cut through Pliocene Ricardo Formation, a nearly 2,000-m-thick sequence of terrestrial sand, silt, clay, and gravel. The particularly colorful basal part of the Ricardo has a large component of volcanic debris. The formation contains a diverse assemblage of vertebrates and abundant petrified wood (Sharp, 1976). This assemblage indicates an open forest and grassland environment; precipitation may have been about three times what is is today.

As the route emerges from Red Rock Canyon, the southern end of the Sierra Nevada comes into view. Here, the mountains are less rugged than they are to the north, primarily because exposures to the north have been freshened by extensive glaciation. Ahead is Indian Wells Valley, which contained one of the smallest Pleistocene lakes (occupying approximately 155 m^2) of the Owens River system (Smith and Street-Perrott, 1983); this system of lakes was linked in a chainlike array from Mono Basin (300 km to the northwest) to Death Valley (120 km to the east). The large military installation seen on the southeast side of the valley, at China Lake, was established during World War II as a Naval weapons-testing site; it is still in use today.

Faulting along the southeastern part of the Sierra Nevada is complex, consisting of predominantly dip-slip faulting along the range front (on the Sierra Nevada frontal fault zone) and oblique faulting having a large component of right-lateral offset on faults several kilometers east of the range front. Although these faults coexist spatially, their late Quaternary histories often differ

markedly. Two fault zones in Indian Wells Valley, the normal Sierra Nevada frontal fault zone and the right-lateral Little Lake fault (fig. 3-5), demonstrate this complexity. The 30-km-long Little Lake fault extends from Ridgecrest to south of Little Lake; at its northern end, the fault nears the Sierra Nevada frontal fault zone but the two probably do not merge (Roquemore, 1988). Earthquakes having magnitudes greater than 5.0 have occurred every 20 years for the past 60 years, and trenching studies suggest that prehistoric earthquakes as large as magnitude 7 have occurred. Late Quaternary slip rates may be in excess of 1 mm/yr.

The Sierra Nevada

The Sierra Nevada is a 600-km-long, asymmetrical, west-tilted mountain block composed primarily of Mesozoic granite of the Sierra Nevada batholith, older metamorphic rocks, and isolated patches of Tertiary sediments and Tertiary and Quaternary volcanics (Jahns, 1954). The eastern front of the Sierra Nevada is marked by a system of north-trending, high-angle, echelon right-oblique and normal faults. The echelon pattern is particularly notable along the northern part of the fault zone (from near Mammoth Lakes north) where the individual faults step rangeward, from south to north, and bound small discontinuous basins. Faulting near the southern end of the range is generally characterized by both oblique and dip slip; however, farther north Quaternary displacement is primarily dip slip. The Sierra Nevada frontal fault zone marks the transitional boundary between extension accommodated by normal faulting in the Basin and Range province and strike-slip deformation on the San Andreas (fig. 3-1). In the southern Sierra Nevada, least-principal horizontal stress directions are approximately NW-SE; the directions change to WNW-ESE to E-W at the northern end of the range (Zoback and Zoback, 1980). They suggest that the coexistence of strike-slip and normal faulting near the eastern flank of the southern Sierra Nevada indicates that vertical and greatest-principal horizontal stresses are approximately equal and the trend of faults and local variation in relative stress magnitude may determine the sense of displacement.

The Sierra Nevada became a major topographic barrier to eastward storm tracks after the end of the Pliocene, with about 2 km of uplift occurring during the Quaternary. Evidence indicating the initiation of the most recent phase of uplift in this area is based on Tertiary (1) paleobotanical distributions, (2) inferred paleoclimatic conditions, and (3) distribution and texture of stream deposits (Axelrod, 1962). Deposits at elevations of approximately 1,500-2,700 m contain Miocene floras similar to modern floras found at elevations less than 600 m; likewise, deposits at elevations of 2,700-3,000 m contain fossils of Miocene deciduous hardwood forests similar to modern forests found at 900 m. The hardwood forests probably occupied the summit region of this area.

Paleoclimatic evidence also suggests this area had low relief during the Tertiary. Based on the similarity of fossil Tertiary floras throughout the area, rainfall was essentially identical on opposite sides of the modern Sierra Nevada. In addition, the Tertiary flora population does not show the wide zonation expected in areas of extreme relief; therefore, high gradients for temperature or rainfall were not present during the Miocene and Pliocene in this region.

The lateral extent of basalt flows and Tertiary river deposits preserved high in the Sierra Nevada and the texture of the latter also suggest low topography and subdued relief when they were deposited (Axelrod, 1962). The extent and texture of Miocene river deposits indicate they were probably deposited in wide channels (about 1,500 m wide) by streams with considerably lower gradients than modern Sierran streams. These Miocene sediments, found at elevations of 2,100 m, are similar in texture to Quaternary sediments in the low foothills of the Sierra Nevada, which have low gradients. The texture of the Tertiary deposits (typically sand and silty clay) suggests that post-Pliocene tilting has steepened their gradients to nearly that of present-day mountain

streams. In addition, Pliocene basalts extend across large areas of the Sierra Nevada, even across the present-day range crest, indicating the divides were not present in the Pliocene.

Even though the modern Sierra Nevada is primarily the product of renewed tectonism beginning in the early Quaternary, faulting occurred throughout much of the Tertiary in this area. As many as six episodes of faulting separated by extended periods of erosion (and thus tectonic inactivity) are indicated. The considerable thickening of post-Miocene strata and intervening unconformities in the basin fill of the San Joaquin Valley (west of the Sierra Nevada) suggests periods of tilting separated by relative tectonic quiescence (Hoots and others, 1954). Even though the landforms that we see today are young, tectonism has molded this region for a much longer time period.

Route Narrative (continued)--Beyond the Inyo-Kern County line, the Coso Mountains (to the northeast) contain many volcanic cones that are apparent from the highway. Beyond Little Lake, on the right (east) side of the road (fig. 3-5), are jointed volcanic flows; Pleistocene Owens River carved a gorge in these rocks during glacial times. Flow through this gorge probably ceased 2,000-3,500 years ago (Gale, 1914) when the level of Owens Lake (in the next basin to the north) dropped below the level of its outlet. About midway along the length of Rose Valley, on the west side of the highway, is a linear embankment known as Portuguese Bench, which is a fault scarp on the alluvium flanking the Sierra Nevada (Sharp, 1976).

Glacial Chronology of the Sierra Nevada

The Quaternary record in and near the Sierra Nevada is characterized by episodes of volcanism and glaciation as well as range-front normal faulting. Because of the interrelation of these different processes, there is an abundance of geologic literature on the Quaternary geology of this area; however, the times of faulting along the eastern flank of the Sierra Nevada are often constrained only by the assumed age of the deposits that are displaced. Therefore, because the most widespread alluvium was deposited during the glacial maxima, a discussion of glacial chronology is given here.

In the past 120 years, the understanding of the glacial history of the Sierra Nevada has advanced from Whitney's (1865) concept of glacial modification of the Sierra Nevada to a general acceptance of a Quaternary glacial stratigraphy. In his pioneering work, Russell (1889) recognized three glacial advances separated by recession of the glaciers, but it was not until 1931, when Blackwelder defined four Pleistocene glacial stages (table 3-1), that these recessions were recognized as representing interglacial periods. The nomenclature of Blackwelder has remained relatively intact, undergoing minor revisions by Sharp and Birman (1963), Birman (1964), and Curry (1966, 1971). Although correlation problems still exist, the ages of some of these deposits have been bracketed by K-Ar and ^{39}Ar-^{40}Ar dating of interlayered volcanic rocks.

Table 3-1. Generally accepted glacial stratigraphy of the eastern Sierra Nevada.

GLACIAL STAGE	SIERRA GLACIATION TERMS	AGE[1]	REFERENCE
Neoglacial	Matthes	present to 700 yr	Birman (1964)
	Recess Peak	2,000 to 2,600 yr	Birman (1964)
	Hilgard	9,000 to 10,500 yr	Birman (1964)
Wisconsin	Tioga	about 20,000 yr	Blackwelder (1931)
	Tenaya	about 45,000 yr	Sharp and Birman (1963)
	Tahoe	60,000 to 75,000 yr	Blackwelder (1931)
Illinoian	Mono Basin	about 130,000 yr	Sharp and Birman (1963)
	Casa Diablo	about 400,000 yr	Curry (1966, 1971)
Kansan	Sherwin	>710,000 yr[2]	Blackwelder (1931)
Nebraskan	McGee	>2.6 Ma[3]	Blackwelder (1931)
	Deadman Pass	2.7 to 3.1 Ma[4]	Curry (1966, 1971)

[1]Ages from Curry, 1971, except where noted
[2]Dalrymple and others, 1965; commonly accepted age of Bishop Tuff is 740,000 yr (Izett and others, 1988)
[3]Dalrymple, 1963
[4]Curry, 1966

Most correlation of glacial deposits within a specific area with deposits at their type localities has been made on the basis of relative-age characteristics of the till, on moraine morphology, and on degree of soil development. However, recent advancement of Quaternary dating methods may aid in developing a regional correlation based on the absolute age of the deposits. Wisconsin and Illinoian glacial till have been dated by different methods at two separate sites along the Sierra Nevada.

Dorn and others (1987) dated rock varnish on boulders of Pleistocene till at Pine Creek (our route will pass near this site); these dated samples were assigned to Sierra Nevada glacial stages based on the mapping and stratigraphic correlation of Bateman (1965). The ages for these deposits (table 3-2) represent minimum ages for each deposit; however, Dorn and others believe that the interval of time between depositing the sediments and initiation of varnish accretion may be only a few years to a couple of decades based on modern varnish formation. The ^{14}C ages for the Tioga moraines are from three distinct ages of moraines, and therefore, retreat from the maximum glacial extent occurred at or before 19 ka. Tenaya moraines are not preserved at this site. The cation-ratio dates of the Tahoe moraines indicate an equivalence to marine oxygen-isotope stage 6 (Shackleton and Opdyke, 1973). The oldest moraines at Pine Creek were mapped as "old Tahoe" by Bateman (1965); however, their ages, determined by cation-ratio dating, indicate that the moraines may correlate with the Mono Basin glaciation (Dorn and others, 1987), as shown in table 3-2.

Table 3-2. Comparison of ^{36}Cl, cation-ratio, and ^{14}C age determinations of Sierra Nevada glacial tills.

[Ages for ^{36}Cl dating method from F.M. Phillips, oral commun., 1988; ages for ^{14}C and cation-ratio dating of rock varnish from Dorn and others, 1987]

SIERRA GLACIATION	^{14}C AGE (yr B.P.)	CATION-RATIO AGE (yr B.P.)	^{36}Cl AGE (yr)
Tioga	13,200-19,000	.....	22,000
Tenaya	.....	.....	70,000-90,000(?)
Tahoe	.....	143,000-156,000	90,000 and 180,000
Mono Basin (Old Tahoe)	.....	182,000-187,000	200,000 or 370,000

Phillips and others (1988) dated till (table 3-2) near Sawmill Canyon and Bloody Canyon (near Mono Lake) using ^{36}Cl dating method and the assigned glacial correlation and mapping of Sharp and Birman (1963). This relatively new method of dating relies on the time-dependent accumulation of ^{36}Cl in boulders that are exposed to cosmogenic rays. Fresh rock derived from the cirque walls is transported by the glacier and deposited in moraines. When these rocks are at the surface, they are exposed to cosmogenic rays and ^{36}Cl begins to accumulate. The ratio of isotopic chlorine (^{36}Cl) to normal chlorine (^{35}Cl) increases with the age of the deposit, and age can be determined based on the time-dependent accumulation of isotopic chlorine.

Although there is some discrepancy in ages of similar-age deposits between these two methods (table 3-2), a rather crude agreement does exist. If concordant ages are correct, at least in a broad sense, these deposits can be correlated with the marine oxygen-isotope record (Shackleton and Opdyke, 1973). The Tioga glaciation probably correlates with oxygen-isotope stage 2, the Tenaya possibly with stage 4, and the Tahoe prob-ably correlates with stage 6 (Dorn and others, 1987). However, the discordant ages of the two Tahoe deposits studied by Phillips and others (1988) suggest that this correlation is still problematic (table 3-2).

Segment 3C--Olancha to Bishop (82 Miles)

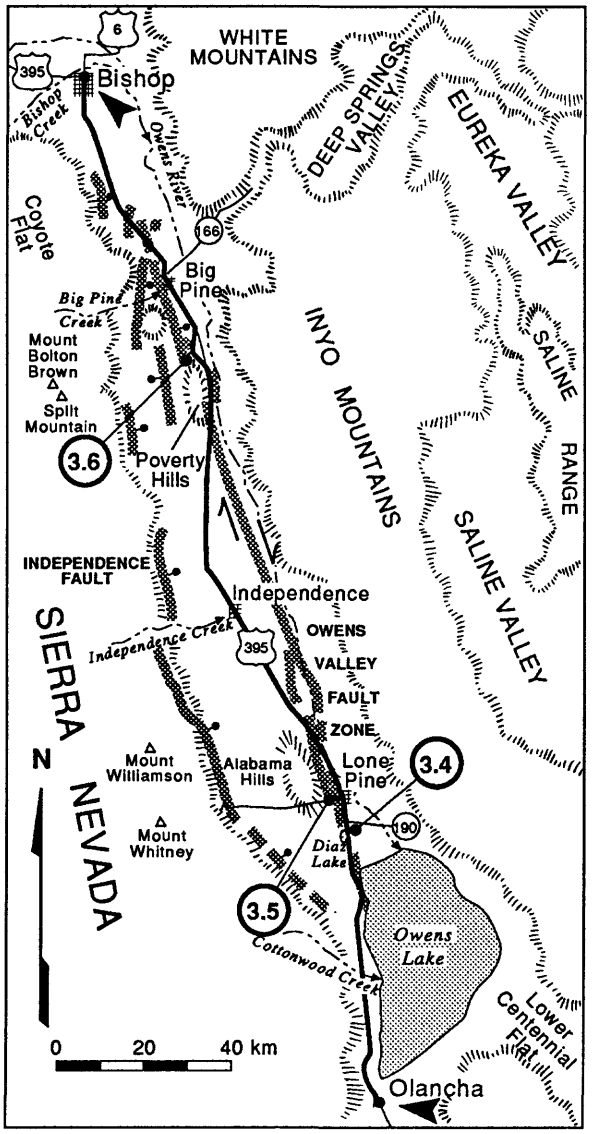

Figure 3-6. Route map for Segment 3C, Olancha to Bishop.

Route Narrative--The Sierra Nevada along this segment of the trip is more rugged than it is to the south because of the effects of glaciation and higher rates of uplift. Most of the high valleys were occupied by glaciers during the Pleistocene, and the remnants of some still persist today. Southwest of Big Pine, glaciers on Mount Bolton Brown and Split Mountain (fig. 3-6) and Palisade Glacier, further west, are the southernmost active glaciers in the United States and extend down to an elevation of about 3,400 m (Hill, 1975). Active tectonism also has played an important role in maintaining the youthful appearance of the landscape. The total throw across the Sierra Nevada frontal fault zone (including the basinward Owens Valley fault zone) is approximately 5.5 km (McCaffrey and Hollett, 1988).

The Inyo Mountains, composed primarily of Paleozoic sedimentary rocks, are on the east side of Owens Valley along this segment of the route. They are probably bounded on the west by a steeply dipping fault, across which the total throw is about 4 km; maximum depth to basement in the valley is probably 1.8 km (Pakiser and Kane, 1965). Scarps are preserved only locally on this fault.

This segment of the trip parallels the 100-km-long Owens Valley fault zone, which ruptured during a major earthquake in the early morning hours of March 26, 1872 (Irelan, 1888a). This earthquake is generally regarded as one of the largest historic earthquakes in the Western United States (excluding Alaska) having an estimated magnitude of 8.0-8.3 (Oakeshott and others, 1972); however, a magnitude of 7.5-7.7 is more probable if a strike-slip mechanism is considered (Beanland and Clark, in press). Ground shaking was felt throughout the West but was greatest near Lone Pine, where nearly 10 percent of the population was killed. This area was sparsely inhabited at the time of the earthquake, Lone Pine had only 250-300 people; however, 52 out of the 59 buildings in the town were partially or wholly destroyed during the earthquake (Oakeshott and others, 1972).

The entire length of the Owens Valley fault zone, from Owens Lake to north of Big Pine (Whitney, 1872), ruptured in 1872 (fig. 3-7). Slip, in general, was predominantly right lateral; the historic surface ruptures followed preexisting

scarps and mimicked pre-1872 displacements (Beanland and Clark, in press). Although the vertical component of slip has been well documented, it is clearly subordinate to horizontal slip and is locally absent. The overall strike of the fault zone is N. 20° E.; however, individual strands within the fault zone vary in strike, to which the magnitude of vertical to horizontal slip is closely related. The presence of tectonic depressions, ridges, and the predominance of left-stepping scarps all strongly suggest right-lateral movement on this fault zone. The average displacement was 6 m horizontal and about 1 m vertical (Lubetkin and Clark, 1988). The largest displacement values, both of which were measured at *Stop 3.5*, are 10 m of horizontal slip and 4.4 m of vertical slip. Owens Valley fault zone has a late Quaternary horizontal slip rate of about 1-2 mm/yr (the vertical slip rate is about 0.2-0.4 mm/yr), and a recurrence interval for large-magnitude earthquakes of about 5,000-10,000 years (Lubetkin and Clark, 1988). The total horizontal displacement on the Owens Valley fault zone is on the order of 20 km based on the correlation of the Independence dike swarm and two Cretaceous plutons (Beanland and Clark, in press).

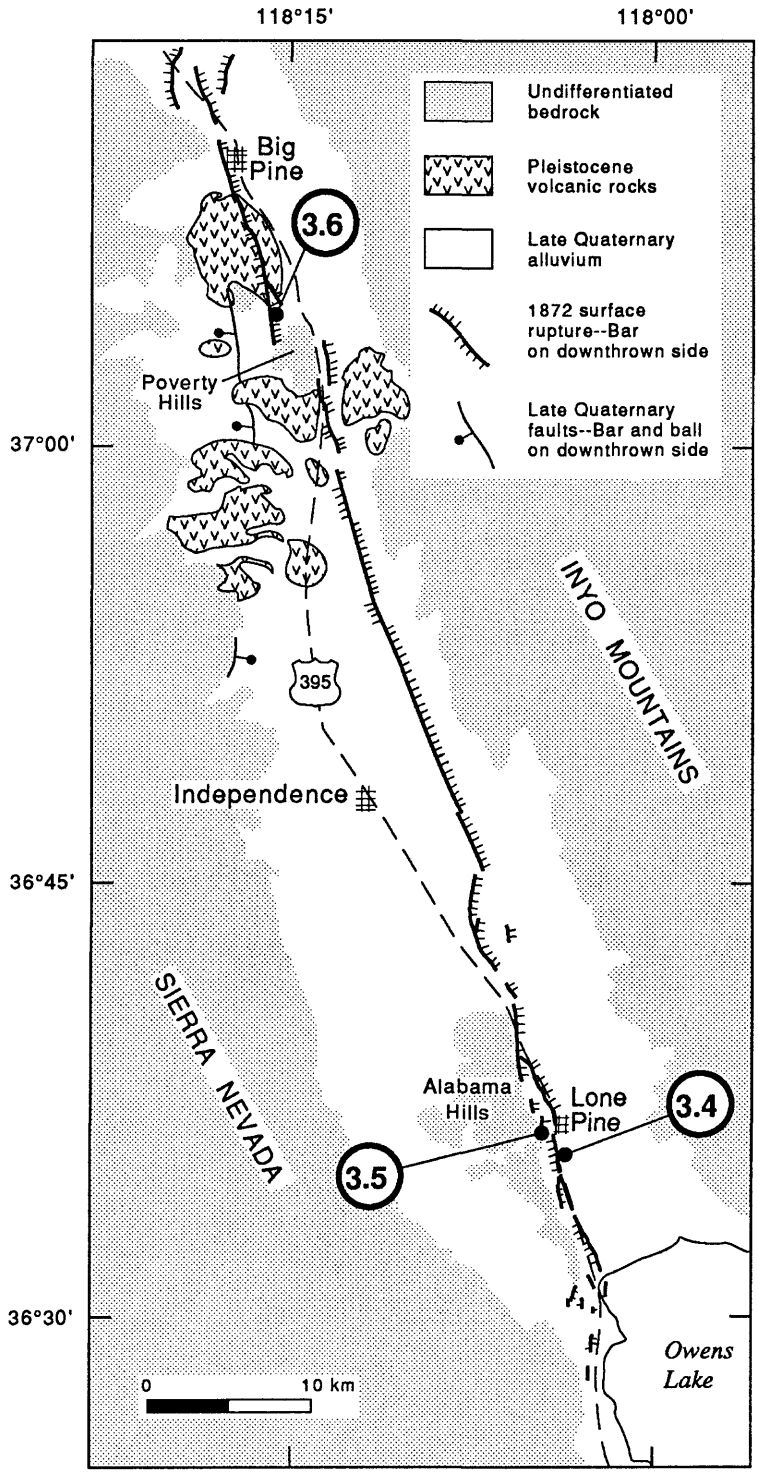

Figure 3-7. Generalized map of surface rupture from 1872 Owens Valley earthquake (modified from Beanland and Clark, in press).

Owens Lake, which is dry most or all of the year, was the site of a large Pleistocene lake of the Owens River system. During the Pleistocene, the lake covered about 500 km^2 and was as much as 70 m deep (Sharp,

1976). Late Pleistocene shorelines are evident in many locations around the lake. The lake drained through its outlet on the south until about 2,000 years ago; at which time, lake level dropped below the outlet. Prior to 1913, when the Los Angeles Aqueduct was constructed to divert water from this area to Los Angeles, the historic lake was about half the size of the Pleistocene lake and was about 10 m deep. Owens Lake now only contains water during exceptionally wet years when river flow exceeds the capacity of the Los Angeles aqueduct.

The dry lake bed is mantled by alkali crusts that contain sodium chloride, carbonate, sulfate, and minor amounts of borates, nitrates, potassium, and lithium (Saint-Amand and others, 1987). These salts form where the water table is less than 3 m below the surface. The chemistry of the crust varies diurnally and is temperature and precipitation dependent. The hardness of the surface depends on the chemistry of the crust; because of this, dust storms are common in the winter months. The absence of salines in the upper 280 m of sediment in the central part of Owens Lake indicates that the lake had not been completely desiccated for several hundred thousand years prior to the turn of the century, and the salines present near the surface represent that which accumulated since Owens Valley became a closed basin about 2,000 years ago (Smith and Street-Perrott, 1983).

The small basin occupied by the playa of Owens Lake is bounded by two subparallel faults. The one on the west, an extension of the Owens Valley fault zone, ruptured in 1872; here, displacements are primarily down to the west and right lateral (Beanland and Clark, in press). The strand to the east has apparent left-lateral displacement (Saint-Amand and others, 1987). This fault may not have moved during the 1872 earthquake, but its total strike-slip offset may be 8 km. This value is based on correlation of a cemented, well-sorted, and folded conglomerate (of unknown source) on the northwest shore of the lake with similar sediment on top of the Coso Range to the southeast (Saint-Amand and others, 1987). This correlation is tentative and based on appearance of the conglomerates; both occur in rather anomalous locations, probably the result of fault transport.

The following excerpt (Sarah Beanland, 1989, written commun.) describes some of the characteristics of 1872 faulting from here at Owens Lake to *Stop 3.4*, 12 miles to the north.

> "The southern end of the 1872 Owens Valley fault rupture terminated in Owens Lake, south of Point Bartlett [at the northwest end of the lake]. At Point Bartlett there is no definite 1872 trace, but a zone of fault lineaments can be seen in the playa surface. . . . Deformed strata [east of the highway] represent bulging between two strands of the fault zone, in a left-stepping relationship, consistent with right-lateral strike-slip movement.
> "On the northern side of Point Bartlett the southernmost positively identified 1872 surface rupture crosses the playa surface. Although primarily a vegetation and groundwater contrast, in places a west facing scarp of 0.5-1.0 m is present. To the north the trace becomes obscure, but a west-facing warp occurs across the youngest set of beach ridges at the northwest corner of the lake. Here the youngest beach ridge has a vertical offset of 0.3 m (1872), while the older ones are vertically offset 2.2 m. Although indicating progressive offset, it is uncertain why there is such a large difference in offset as the older beach ridges of this set are considered to have a maximum age of only 2,000 years (Beanland and Clark, in press; Carver, 1970). The difference may suggest that individual events have produced varied displacements at this site.
> "The west-facing 1872 (and older) Owens Lake scarps contrast with the overall structural sense of displacement of Owens Lake, which is obviously down relative to the Sierra Nevada. The dominance of strike-slip movement, however, at least in Holocene time, explains the presence of changes in upthrown side, several of which occur between Owens Lake and Diaz Lake [see fig. 3-6]. Much of the vertical separation of the lake basin and the range is on the nearby parallel, normal, Independence fault [local name for this part of the Sierra Nevada frontal fault zone]."

Route Narrative (continued)--Proceed north on U.S. Highway 395 to *Stop 3.4* at the Lone Pine Visitors Center, which is on the right (east) side of the highway at the south end of Lone Pine, 21.8 miles north of Olancha.

Stop 3.4--Lone Pine Visitors Center (Lunch Stop)

The Lone Pine Visitors Center has picnic tables, water, and restrooms and provides an excellent view of Mount Whitney (elev. 4,418 m), the highest mountain in the continental United States From this stop to about 10 km north of Lone Pine, the highway parallels the eastern flank of the Alabama Hills (fig. 3-6). The southern part of these low hills are composed of Mesozoic plutonic rock, the northern half is composed of early Mesozoic metavolcanic rocks intruded by the same plutonic rocks (Smith, 1989).

Route Narrative (continued)--Return to U.S. Highway 395 and proceed north into Lone Pine. Turn left onto Whitney Portal Road (2.2 miles beyond visitors center) and drive 0.8 mile to parking lot on right for *Stop 3.5*. At this stop we will visit a site that is used for an on-going study of scarp-degradation rates and processes. Please do not climb on any of the scarps, dislodge any boulders, or modify the site in any way.

Stop 3.5--Lone Pine Fault

The Lone Pine fault (Lubetkin, 1980) is a secondary strand of the Owens Valley fault zone. At this stop, we will walk about 700 m north of the road to see abundant evidence of right-lateral slip. Even though the presence of large scarps gives the impression of overwhelming dip-slip displacement, the average ratio of horizontal to vertical slip on the Lone Pine fault is about 6:1 (Lubetkin and Clark, 1988). The predominantly east-facing scarps on alluvial fans composed of late Pleistocene glacial outwash and Holocene alluvium (fig. 3-8) are the result of two or more surface-faulting events (fig. 3-9), as evidenced by bevelled scarps and progressively larger offset on older alluvium.

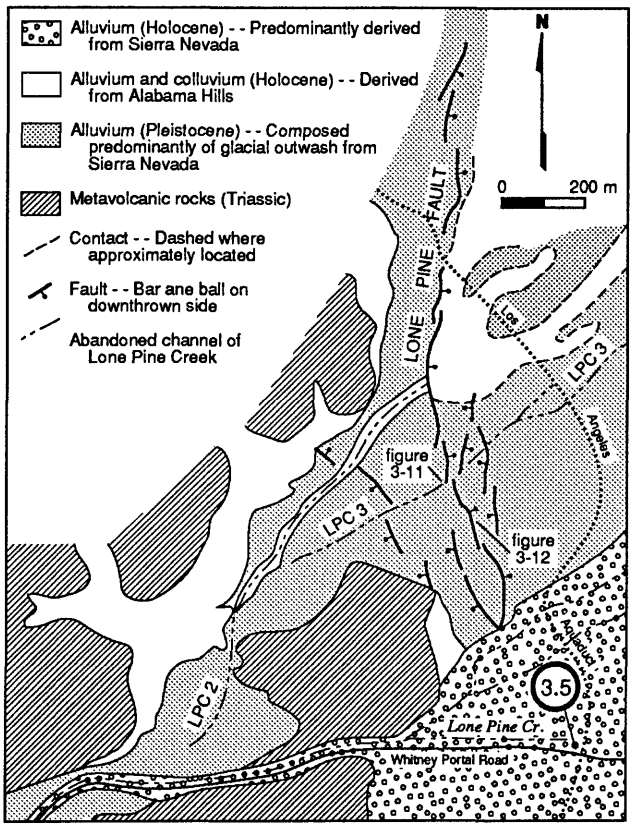

Figure 3-8. Generalized geologic map of Lone Pine fault north of Whitney Portal Road (modified from Lubetkin and Clark, 1988) showing locations of figures 3-11 and 3-12. LPC2 and LPC3 are older courses of Lone Pine Creek.

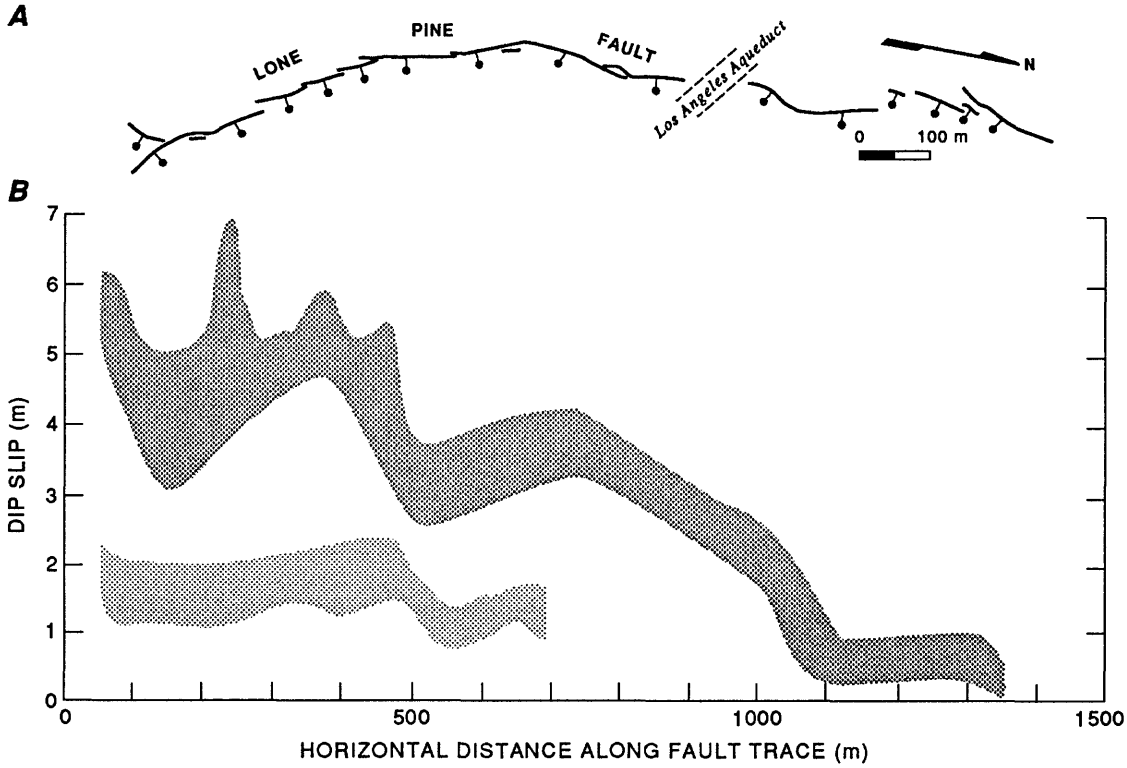

Figure 3-9. ***A***, Map of scarps on Lone Pine fault, bar and ball on downthrown side. ***B***, Estimated dip slip on Lone Pine fault; light stipple represents amount of 1872 displacement only, dark stipple represents total dip slip (modified from Lubetkin and Clark, 1988). Width of pattern indicates variability in data.

In addition to the pronounced bevels on the scarps, which indicate multiple movements on the fault, we will see two notable features at this stop: (1) offset stream channels, and (2) a weathered boulder on the upthrown block of the fault (locations on fig. 3-8). The former illustrates the horizontal component of displacement and the latter the vertical component. This stop is a good example of geologic evidence that supports the concept of characteristic earthquakes (Schwartz and Coppersmith, 1984; 1986). The characteristic-earthquake model defines a condition where the distribution of slip on a fault is repeated in successive events (fig. 3-10). Therefore, single-event displacements at any location along the fault are equal to displacements of successive events, but cumulative slip rates at different locations along the fault may vary.

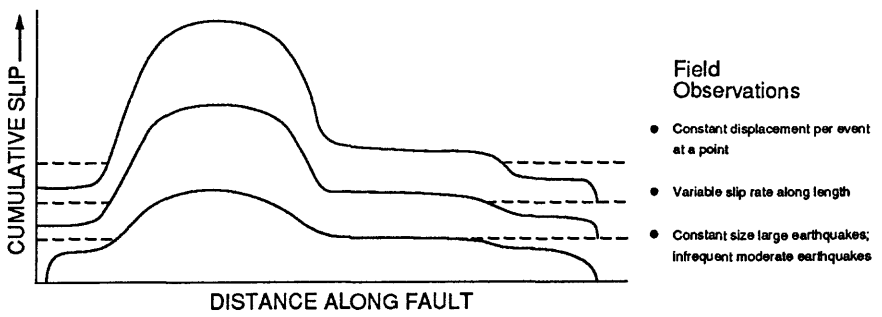

Figure 3-10. Schematic diagram showing distribution of displacement associated with large-magnitude earthquakes along strike of a fault that demonstrate the characteristic-earthquake model (modified from Schwartz and Coppersmith, 1984). Dashed lines represent overlapping slip from earthquakes on adjacent parts of the fault.

An abandoned channel of Lone Pine Creek (LPC3, fig. 3-8) is about 700 m north of the parking area. Figure 3-11 shows progressively larger amounts of offset of the stream-channel deposits and older fan crest, which illustrates how this strand of the fault has been reactivated through several seismic cycles. The intermediate terrace demonstrates that, at a given site, recurrent faulting not only can reactivate near-surface structures but can also produce similar styles and amounts of slip. For example, the 1872 surface faulting resulted in 6 m of horizontal slip and 2 m of vertical slip (equivalent to the single-event offset of the incised channel); the entire scarp on the intermediate terrace indicates a total displacement of between 8 and 12 m of vertical slip and about 4 m of horizontal slip (Beanland and Clark, in press). Therefore, the total scarp is probably the result of two similarly scaled surface-faulting events. Displacement of the fan crest records a third event (two Holocene events and the 1872 event) by the same line of reasoning. The deposit is offset about 14 m horizontally and 6-6.5 m vertically. Although the amount of horizontal displacement is not proportionally larger than that of the two-event scarp, the amount of vertical displacement is three times that of the 1872 displacement and nearly half as much again as the two-event scarp.

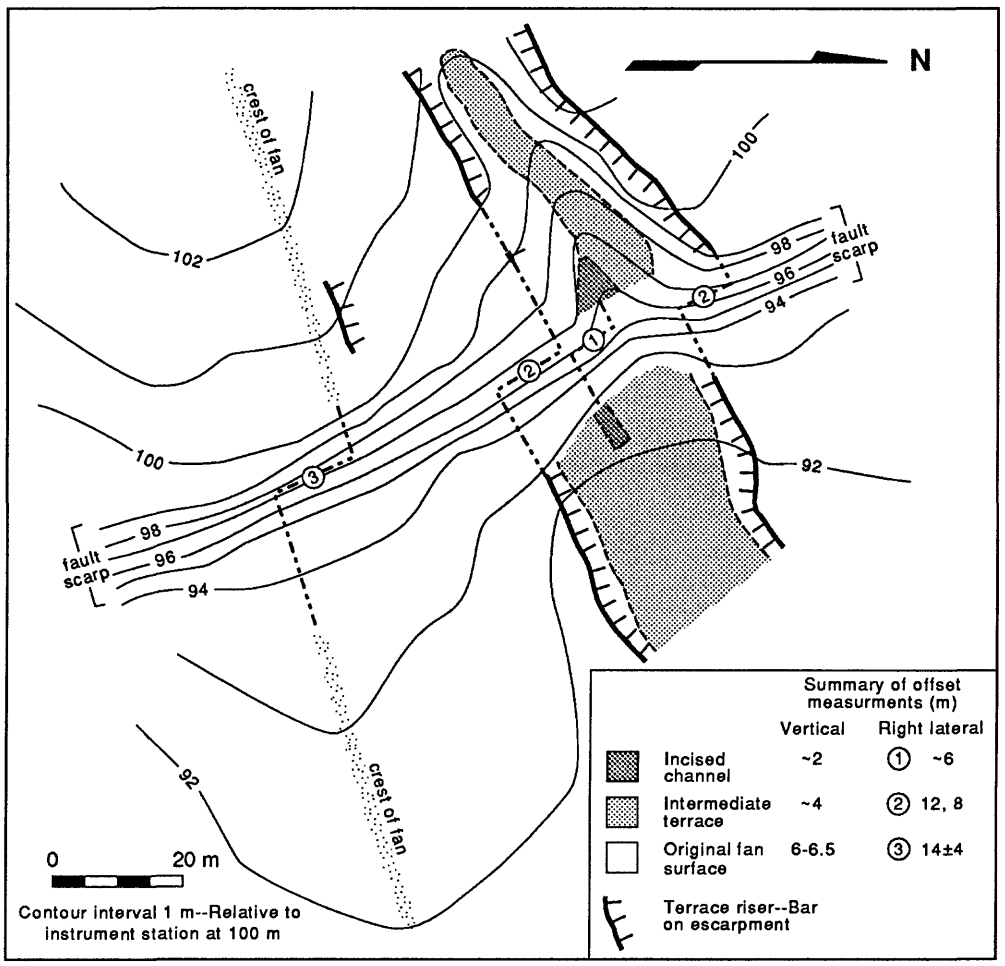

Figure 3-11. Map of stream channels and fan crest showing relative amounts of offset by displacement on the Lone Pine fault (modified from Beanland and Clark, in press). Abandoned stream channel is LC3 on figure 3-8. Dash-dot line shows correlation of geomorphic features across the fault.

About 100 m southwest of the offset terraces (fig. 3-8), is a boulder that has been exhumed approximately 2.5 m (fig. 3-12*A*) by scarp degradation following three faulting events as evidenced by difference in weathering of its surface and rings of desert varnish on the surface of the boulder (Lubetkin and Clark, 1988). When this boulder was deposited, the ground surface was at line A, which exposed only the uppermost part of the boulder to surficial-weathering processes (fig. 3-12*B*). Sometime after the boulder and surrounding fan material were deposited, faulting occurred. Subsequent degradation of the scarp exposed the surface of the boulder between weathering lines A and B. As the surface became more stable and degradation rates decreased, a ring of desert varnish began to form on the fresh surface of the boulder at the new ground surface (fig. 3-12*C*). Then another displacement occurred, which eventually exposed a fresh surface between B and C, and the cycle repeated resulting in the formation of another desert-varnish ring at the new ground surface (fig. 3-12*D*). Then, once again, displacement occurred in 1872 exposing fresh rock between C and the present ground surface (fig. 3-12*E*).

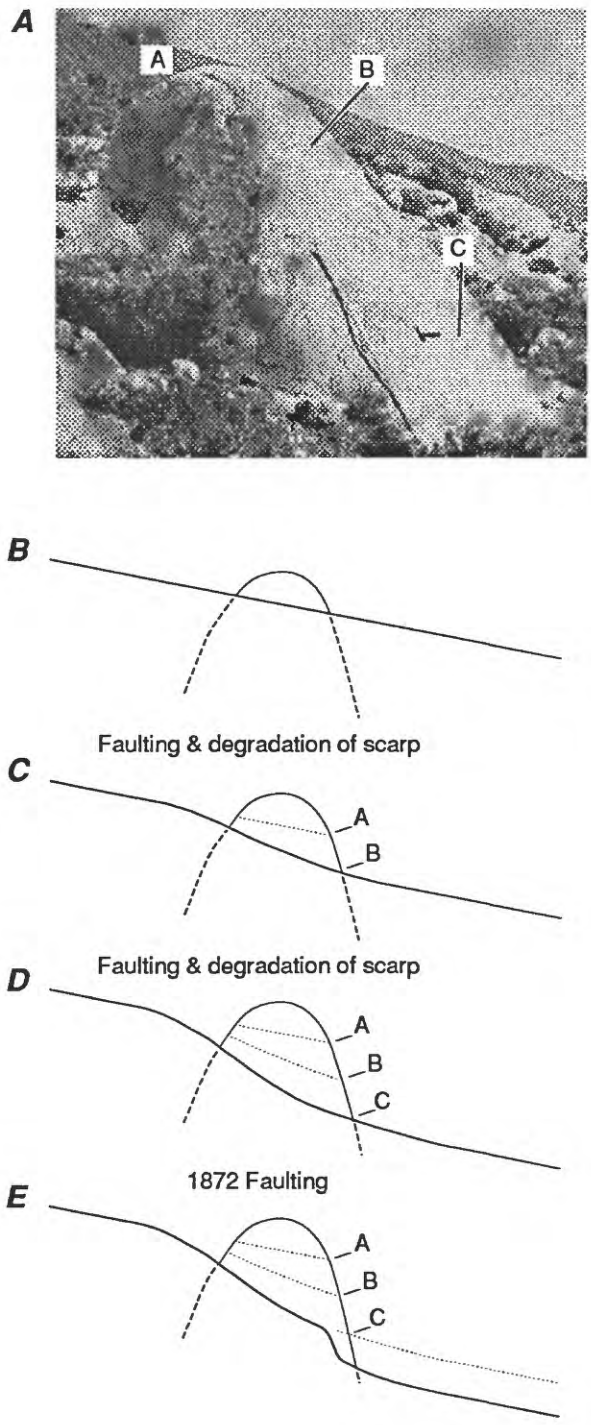

Figure 3-12. ***A***, Photograph of boulder on scarp of Lone Pine fault (from Lubetkin and Clark, 1988); location of site shown on figure 3-8. Zones of differential weathering (indicated by A, B, and C) are described in text. Rod is 1.5 m long; view is to north. ***B***, Schematic diagram of relation of pre-faulting surface and boulder, ***C***, relation of surface and boulder after first faulting event and subsequent degradation of the scarp, ***D***, relation of surface and boulder after second faulting event and subsequent degradation of the scarp, and ***E***, relation of surface and boulder after 1872 faulting event.

Route Narrative (continued)--After leaving *Stop 3.5*, return to U.S. Highway 395 and turn left (north). Before entering Lone Pine from the west, you can get a good view of the spatial relations of the Lone Pine fault and the remainder of the Owens Valley fault zone, which extends along the west side of town (fig. 3-7). Just before entering town, the route crosses a down-to-the-west scarp; it is here that W.D. Johnson measured 4.9 m of right-lateral offset of the original Whitney Portal Road during his field studies in 1907 (Bateman, 1961).

At the north end of Lone Pine, on the left (west) side of U.S. Highway 395, is one of two grave sites of the victims of the Owens Valley earthquake; here, 16 people were buried. The scarp on the west side of the road had vertical displacements of about 1.5 m in 1872; the total scarp height is about 3 m. The scarp appears more degraded than those at *Stop 3.5*; the rapid degradation is probably due to the fine-grained, poorly consolidated nature of this sediment. About 30 m south of the grave site, the east-facing scarp becomes a west-facing scarp, another example that typifies the strike-slip nature of the fault zone.

At the north end of the Alabama Hills (fig. 3-7), 4.5 miles north of Lone Pine, the route crosses the main trace of the Owens Valley fault zone. For the next 32 miles the fault trace is in the valley, to the east of the highway. From just south of the town of Independence (15 miles north of Lone Pine) to the Poverty Hills (a distance of about 20 miles), the Owens Valley fault zone is remarkably straight (fig. 3-7). The vertical sense of displacement is generally east side down, but locally the sense reverses. Along this part of the fault, 10,000-year-old lake deposits are displaced by three events according to Beanland and Clark (in press).

About 5 miles beyond the north end of the Alabama Hills on the left (west) side of the highway is the site of Manzanar. This was the first of several camps used during World War II for the tragic internment of as many as 10,000 Japanese-Americans.

North of Manzanar, the route enters the Big Pine volcanic field, which extends north to Big Pine; the field includes at least 40 vents that erupted predominantly olivine-bearing basalts (Smith, 1989). The vents may be on or near normal faults, which have been active throughout much of the Quaternary. North of Big Pine, there is an obvious absence of cones and flows.

The Independence fault flanks the eastern Sierra Nevada front in this area. Regardless of its proximity to the Owens Valley fault zone, the Independence fault is primarily dip slip and has a Holocene history that may not coincide with that of the Owens Valley fault zone (Beanland and Clark, in press). Holocene slip rate of about 0.1 mm/yr is suggested for the Independence fault (Clark and others, 1984), or about one-tenth that of the Owens Valley fault zone.

About 17 miles north of Independence, near the northern end of the Poverty Hills, which consist of Cretaceous granodiorite and older marble (Bateman, 1965), scarps of the Owens Valley fault zone make a 2-km-wide echelon left step (Beanland and Clark, in press). From here north, the trace of the 1872 and older ruptures are on the west side of the field-trip route. *Stop 3.6* is at scarps 2.5 km north of this echelon step.

Near the northern end of Poverty Hills, at Mile 33.6 turn left (west) on Fish Springs Hatchery Road and proceed through the intersection with Tinemaha Road (Mile 34.1). At Mile 36.3, Fish Hatchery Road crosses a small gully. Turn left (west) 0.3 miles beyond the gully onto a dirt road at north end of a fenced area containing bales of hay. Continue west for 0.1 mile, following the fence line. At the northwest corner of the fence line, continue going straight through a road intersection. In 0.1 mile, continue straight through another \intersection, then bear left at a Y intersection, and drive under a power line. Follow the main road for 0.4 mile and park at end of road for *Stop 3.6*. From here we will walk along the north side of the cinder cone to its faulted west edge.

Stop 3.6--Fish Springs Fault

At this stop, we will see a middle Pleistocene cinder cone as well as fans deposited during the Wisconsin Tahoe and Tioga glaciations, all of which are displaced by the Fish Springs fault (fig. 3-13). Fish Springs fault, a strand of the Owens Valley fault zone, extends about 5 km north from the northwest end of the Poverty Hills. Movement on this fault is primarily dip slip, down to the east, unlike the predominantly strike-slip movement apparent to the south; however, the main strand of the Owens Valley fault zone is inferred to lie east of this site and be predominantly strike slip (Sarah Beanland, written commun., 1989). Another strand of the Owens Valley fault zone, the Red Hills fault, is west of this site; however, there is no evidence to suggest that this down-to-the-west fault moved during the 1872 earthquake.

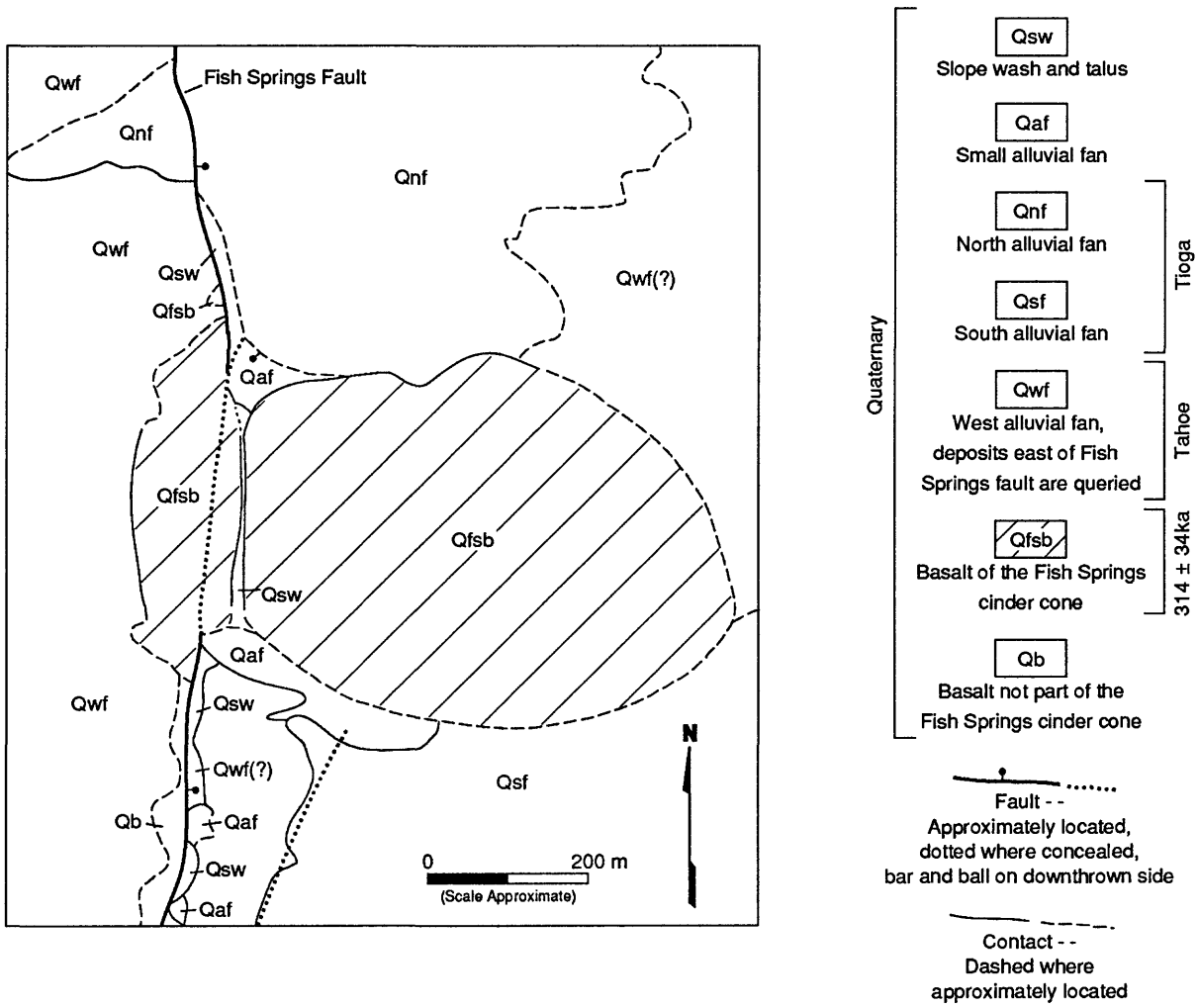

Figure 3-13. Geologic map of Fish Springs fault, cinder cone, and surrounding area (modified from Martel and others, 1987).

This site, like the Lone Pine stop (*Stop 3.5*), illustrates recurrent movement of a single strand of a fault. The cinder cone at this site is the oldest Quaternary feature that is both well dated and displaced by the Owens

Valley fault zone. The cinder cone was deposited 314±36 ka, based on ^{39}Ar-^{40}Ar dating method, and is offset 78±6 m vertically (table 3-3). Progressively smaller scarps are present on younger alluvial deposits. The wide range in age of faulted deposits provides the opportunity to evaluate slip rates through time. The age of Tahoe glaciation is not well constrained (see discussion in Glacial Chronology of the Sierra Nevada); therefore, Martel and others (1987) used slip rates from the cinder cone (0.25 mm/yr) to estimate an age of 124±19 ka for the west fan (Qwf, assumed to be Tahoe equivalent in this area). If the west fan is in fact equivalent to marine oxygen-isotope stage 6, then the slip rate at this site has not changed considerably during the late Quaternary; however, if the west fan correlates to stage 4, the slip rate has varied considerably from 0.19 to 0.44 mm/yr in the late Pleistocene (fig. 3-14).

Table 3-3. Slip rates based on offset features on the Fish Springs fault from Martel and others (1987).

FEATURE (unit on fig. 3-13)	VERTICAL DISPLACEMENT (m)	AGE (ka)	SLIP RATE (mm/yr)
Tioga fan (Qnf, Qsf)	3.3±0.3 m	10.6-26	0.10-0.26
Tahoe fan (Qwf)	31±3 m	124±19[1]	0.25±0.03
cinder cone (Qfsb)	78±6 m	314±36	0.25±0.03

[1]The rate of displacement of the cinder cone was used to estimate the age of the Tahoe surface.

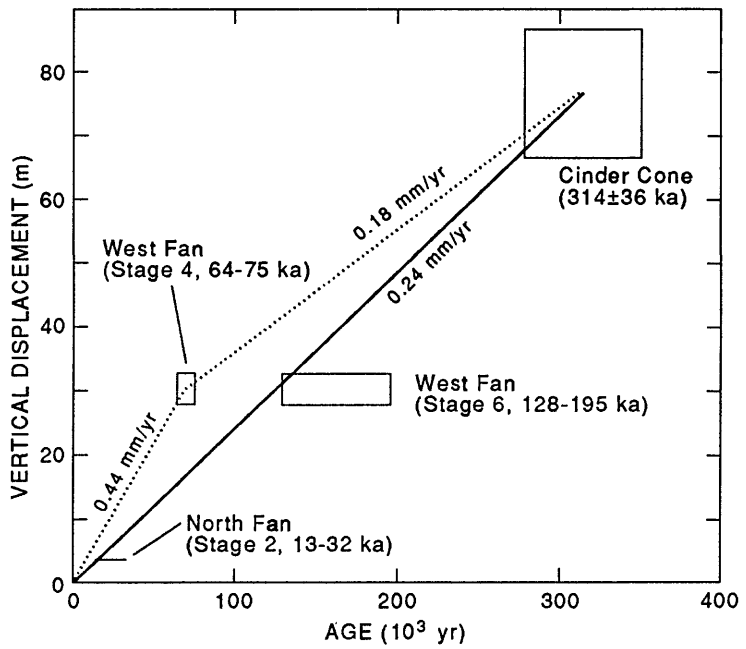

Figure 3-14. Late Quaternary displacement history of Fish Springs fault (modified from Martel and others, 1987). Solid line depicts displacement rate if west fan (Qwf) is marine oxygen-isotope stage 6 equivalent, dotted line depicts variable rates if west fan is equivalent to marine oxygen-isotope stage 4.

Other interesting features at this site is the morphology of the fault scarps on materials of different ages and lithology and evidence of movement on this fault in 1872. The 1872 displacement on the Fish Springs fault is evident as the small offset across young channel floors and as the steep facet of the main scarp through the cinder cone. Although the 1872 vertical offsets are similar to those at *Stop 3.5*, the scarps are more degraded here.

Route Narrative (continued)--Return to Fish Springs Hatchery Road, turn left (northeast) and proceed 1.5 miles to U.S. Highway 395; turn left (northwest) onto the highway. Near Bishop (about 20 miles north of *Stop 3.6*), the flank of the Sierra Nevada steps westward nearly 15 km. At the north end of Owens Valley, vertical displacement along the range front apparently is accommodated by warping rather than faulting. Coyote Flat (fig. 3-6), west of U.S. Highway 395 and southwest of Bishop, is a flat erosional surface of probable middle to late Pliocene age on Cretaceous granodiorite. Coyote Warp is the broad monoclinal warp that dips gently east from Coyote Flat into Owens Valley and north toward Bishop (Bateman, 1965). Geophysical data indicates that this warped surface extends under Owens Valley and terminates at the fault on the west side of the White Mountains to the east (Pakiser and Kane, 1965). Proceed to Bishop on U.S. Highway 395.

Segment 3D--Bishop to Mammoth Lakes (35 Miles)

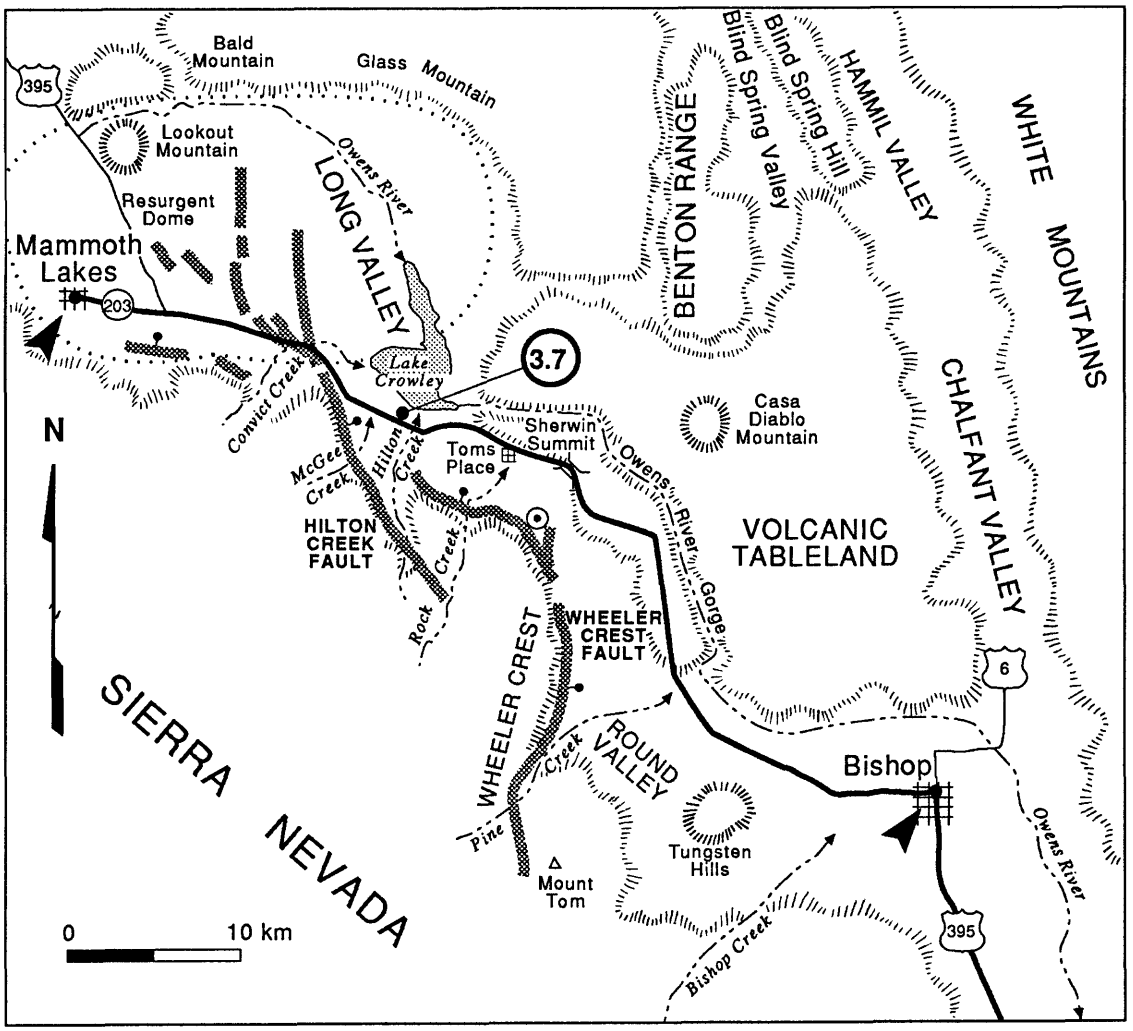

Figure 3-15. Route map of Segment 3D, Bishop to Mammoth Lakes. Bulls-eye is location of magnitude 5.7 earthquake occurring in 1978. Dotted oval around Mammoth Lakes is boundary of Long Valley caldera (Bailey and others, 1976).

Route Narrative--Proceed through Bishop on U.S. Highway 395. Note odometer reading at intersection of U.S. Highways 395 and 6. As we leave Bishop, look southwest of the highway; the low, rocky terrain is

the Tungsten Hills (fig. 3-15). They are named for the deposits of tungsten-bearing sheelite that were found here in 1913 (Knopf, 1918; Bateman, 1965). These deposits, along with others near Pine Creek (13 miles to the west), comprise one of the richest tungsten reserves in the United States and have also yielded large amounts of molybdenum. Both minerals form contact deposits with the Cretaceous Tungsten Hills Quartz Monzonite (Bateman, 1965). Beyond the Tungsten Hills on the skyline is Mount Tom (elev. 4,161 m), named for Thomas Clark, a resident of the area, who made the first ascent of the peak in the 1860's. Note the rock glaciers high up in the canyons.

North of U.S. Highway 395 and beyond the Owens River, the Volcanic Tableland comes into view. The tableland is composed entirely of middle Pleistocene Bishop Tuff (Bateman, 1965) and represents the largest remnant of this regionally extensive deposit. The steep escarpment on the south side of the tableland is probably not fault controlled but instead is an erosional scarp of the Owens River. About 6 miles northwest of Bishop, you will see small, isolated outcrops of Bishop Tuff on either side of the highway, evidence of the erosional retreat of the escarpment. Although this is the first exposure of the tuff we have seen, it extends at least as far south as Big Pine in the subsurface (Lipshie, 1976). Ash from these eruptions are found throughout the Western United States (Izett and others, 1988) and often provide important stratigraphic markers.

The Bishop Tuff originated as a series of *nuees ardentes* from caldera eruptions in Long Valley (Gilbert, 1938), 30 km to the north, approximately 740,000 years ago (Izett and others, 1988). Although the duration of emplacement has not been constrained by conventional dating methods, consistent magnetization directions suggest it probably did not encompass more than several centuries (Dalrymple and others, 1965). On the basis of an absence of significant reworking between cooling units, absence of a second air-fall ash unit, and evidence that the tuff cooled as a single unit, the tuff was possibly emplaced over an interval of as little as a few hours or days (Lipshie, 1976).

The Bishop Tuff is a rhyolitic ignimbrite consisting of a basal nonwelded air-fall ash bed, overlain by a true welded tuff (Bateman, 1965), and capped by a sillar tuff (that is, a tuff indurated by recrystallization due to escaping gases). In general, fresh exposures of the tuff are pink but may be brown where oxidized and may have a white zone of pedogenic calcium carbonate at the top. Carbonate may also be concentrated along vertical fractures. The unit is typically 120-150 m thick in this area (Gilbert, 1938), but locally is more than 1,000 m thick in Long Valley caldera (Bailey and others, 1976). The volume of magma extruded during the deposition of the Bishop Tuff is estimated to have been 600 km^3.

Looking west from the base of the Sherwin Grade, the faulted moraines at the mouth of Pine Creek are apparent, especially in late-afternoon light. These moraines were dated utilizing the ^{14}C and cation-ratio methods on desert varnish (Dorn and others, 1987) discussed previously. At the mouth of Pine Creek, the most distal Tioga moraines are displaced 12-14 m suggesting an average slip rate of about 1 mm/yr (Clark and others, 1984).

One of the world's largest-producing tungsten mines is farther up Pine Creek valley. The Pine Creek mine has been in production since 1918, and in the first 35 years of operation it produced 10,575 tons of tungsten trioxide (Bateman, 1965). The ore formed by the interaction of calcium-rich sedimentary or metamorphic rocks with hot fluids from plutonic magmas.

Approximately 8 miles northwest of Bishop, we start the 10-mile-long climb up Sherwin Grade, named for James Sherwin who began ranching north of here in 1859. He built a toll road (just west of the present U.S. Highway 395) in the 1870's during a brief episode of gold mining at Mammoth Lakes. This road linked Mammoth Lakes and Bishop, and for years, U.S. Highway 395 followed the route of the original toll road. Sherwin Grade is on the tilted constructional surface of the Bishop Tuff. Near the base of the grade you can see small (<25-m-high) conical mounds on either side of the road. These resistant mounds are ancient fumaroles (steam vents); the high temperatures of escaping gasses recrystallized and hardened the tuff around the vent

(Sharp, 1976). Subsequent erosion preferentially removed 15-60 m of the surrounding less indurated tuff, and the more indurated mounds now stand in relief.

Big Pumice Cut, a large roadcut on the right (east) side of the highway about 1 mile beyond Sherwin Summit (elev. 2,133 m) was excavated in 1957 during the construction of U.S. Highway 395; this exposure finally laid to rest the controversy of the relative ages of the Sherwin Till and the Bishop Tuff, which had raged for decades. As we pass the road cut, notice the bouldery till (Sherwin) at the bottom of the cut and the overlying tuff (fig. 3-16). The type locality of the Sherwin Till is about 10 km northeast of this cut, near Rock Creek (Blackwelder, 1931); however, Blackwelder probably believed the Sherwin was younger than the Bishop Tuff. Sharp's (1968) study of the relation of the till and the tuff in this area established that Sherwin is older than Bishop Tuff and the till in this exposure is in fact Sherwin. Therefore, the Sherwin glaciation probably correlates with the Kansan glacial stage of the midcontinent (table 3-1). Note also in the cut, the nearly vertical clastic dikes of gravel that extend from the surface down into the till. Wahrhaftig and others (1965) contend that the dike-filling gravels are derived from Tahoe or older glacial outwash that filled fissures in the tuff.

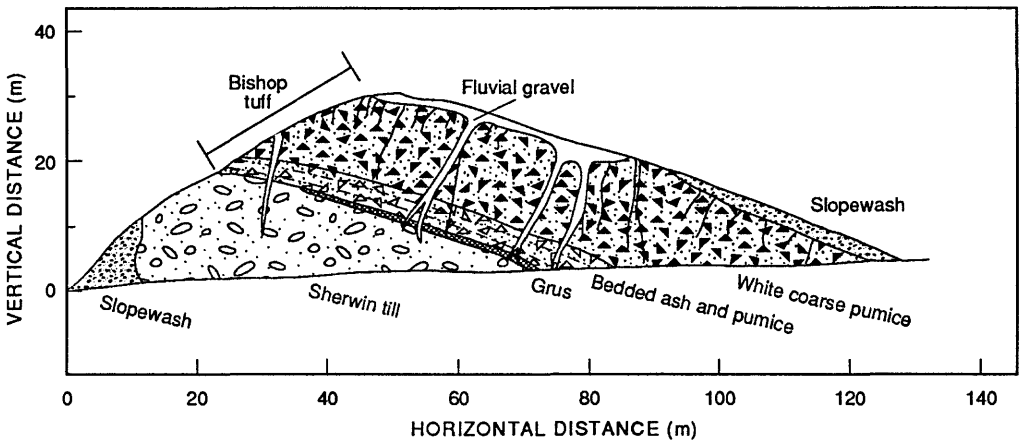

Figure 3-16. Sketch of exposure at Big Pumice Cut on U.S. Highway 395 (from Sharp, 1968) showing stratigraphic relation between Sherwin till and Bishop Tuff. Subparallel gravelly clastic dikes that extend from surface into Sherwin till are discussed in text.

Bishop Tuff can be seen to the north of the highway dipping northeast into the Long Valley caldera about 1 mile north of Tom's Place (fig. 3-15). These dips suggest post-eruption rotation of the southern wall of the caldera. Proceed about 4 miles past Tom's Place to *Stop 3.7*, the scenic overlook on the right side of the highway.

Stop 3.7--Overlook of Long Valley Caldera

This stop affords a beautiful view of the Long Valley caldera and the spectacular front of the Sierra Nevada. We are about 6 km southeast of the southern margin of the Long Valley caldera. Even though the southeast rim of the caldera is poorly defined topographically, the northeast rim (about 25 km away) is clearly visible from here.

Pre-caldera volcanism, eventually culminating in the formation of the Long Valley caldera, began 3.2 Ma and was derived primarily from mantle sources (Bailey, 1987). Later differentiation of the magmatic source rocks resulted in the formation of the silicic, shallow Long Valley magma chamber. Looking north, you can see Glass Mountain, a ridge that forms the northern margin of the caldera (fig. 3-15). The ridge is 1,200 m

above the floor of Long Valley. The rocks of Glass Mountain, which represent the earliest eruptions from the Long Valley magma chamber (Bailey, 1987), were erupted between 2.1 and 0.8 Ma (Metz and Mahood, 1985).

The Long Valley area was changed dramatically 740,000 years ago with the violent eruption of the Bishop Tuff that resulted in the formation of the Long Valley caldera. After the eruption of the tuff, the roof of the partially emptied magma chamber collapsed to form an oval-shaped depression (Bailey, 1987). Possibly as much a 3 km of surface subsidence occurred after the eruption of the Bishop Tuff, and as much as 1,400 m of Bishop Tuff is present in the caldera beneath the younger materials. Only a third of the total amount of collapse is apparent in the present-day topography.

After the collapse of the caldera, localized rhyolite eruptions formed a resurgent dome complex. Lookout Mountain (northwest of here) represents one of these post-collapse rhyolite domes. This resurgent phase may have lasted about 50,000 years and was completed by 500,000 years ago. Another phase of rhyolitic emplacement occurred between 100,000 and 500,000 years ago; these younger rhyolites were emplaced along the ring fractures of the caldera (Bailey, 1987). Volcanism then shifted to the eruption of rhyodacite flows from at least 10 vents that are near the southwest edge of the caldera. Mammoth Mountain (southwest of Mammoth Lakes) is composed entirely of 50,000- to 180,000-year-old rhyolite flows.

In the late Pleistocene, volcanism changed to a mixed assemblage of basalt and andesite flows. We will pass by some of these basalts, which are interbedded with glacial till, as we near Mammoth Lakes. Bailey and others (1976) have suggested that these basalts are from a source other than that of the magma chamber, and that the mafic and silicic magmas may not interact significantly. The most recent phase of volcanism is Holocene, which we will view at Inyo Craters later in this trip (*Stop 5.1*).

To the west are the spectacular moraines of Hilton Creek and McGee Creek. The moraines at Hilton Creek (directly west of here) were deposited by a glacier that only extended to the edge of the hanging valley where it dumped till down the steep mountain face and created a pile of boulders and finer sediment. In contrast are the large (over 200-m-high) lateral moraines near McGee Creek (just north of Hilton Creek). Fault scarps on these moraines are obvious from this vantage point; we will stop at the Hilton Creek fault to see displaced McGee Creek moraines later in this trip (*Stop 4.1*).

Although Crowley Lake to the east is artificial, Long Valley Lake (Mayo, 1934) covered much of the eastern end of the caldera in the Pleistocene following the subsidence of the caldera about 600,000 years ago (Bailey, 1987). The lake was about 60 m deep and covered more than 200 km^2. Emplacement of the resurgent dome raised the level of Long Valley Lake sometime in the past 100,000 years, which resulted in overtopping of its sill on the southwest rim and caused gradual downcutting, resulting in the spectacular Owens Valley Gorge southeast of here.

Tilted lake shorelines are well preserved on the east wall of the Long Valley caldera. These highstand shorelines are at an elevation of 2,200 m near the southeastern end of Lake Crowley and an elevation of 2,400 m at the north side of the caldera (Bailey and others, 1976). The terraces are both warped and locally faulted; deformation is probably due to the combined effect of magma emplacement and tectonic deformation.

Route Narrative (continued)--Reenter U.S. Highway 395 and continue northbound about 9 miles; exit onto California Highway 203 (to Mammoth Lakes). Proceed west 2.6 miles to Mammoth Lakes.

DAY 4--MAMMOTH LAKES LOOP

Summary

This part of the field trip emphasizes the spatial and possible tectonic relations between volcanism in the Long Valley caldera and large-magnitude earthquakes on the Sierra Nevada frontal fault zone. Range-front faulting on the Hilton Creek fault, a part of the Sierra Nevada frontal fault zone, has resulted in about 20 m of surface offset in the past 20,000 years (amount is typical of other fault offsets along the Sierra Nevada). The Hilton Creek fault extends north into the caldera and bifurcates into several splays, each of which have more subdued scarps. Minor movement occurred on the Hilton Creek fault in 1980 following a swarm of earthquakes ($M \geq 6$), which were related to dike intrusion in the caldera.

Recent Seismic Activity in Long Valley Caldera

Long Valley caldera and the surrounding area has one of the highest rates of seismicity at magnitudes of 5-6 in California in the past 150 years (Hill and others, 1985). Some scientists not only believe that seismicity is associated with intrusion of magma in this area, but that large-magnitude earthquakes on the range-front faults may be responsible for triggering major volcanic eruptions. In 1978, a magnitude-5.7 shock occurred between Mammoth Lakes and Bishop near the Wheeler Crest fault (fig. 3-15) and was followed by a swarm of earthquakes (Ryall and Ryall, 1980). In May 1980, four earthquakes having magnitudes greater than 6 occurred within 48 hours (Cramer and Toppozada, 1980), south of Mammoth Lakes.

The resurgent dome in the caldera began to rapidly inflate in 1979 (Savage and Clark, 1982); inflation continues today but at a slower rate. A resurvey of a 1975 first-order level line showed a maximum elevation change of 25 cm between 1975 and 1980 near Casa Diablo Hot Springs (Savage and Clark, 1982). Between 1982 and 1987, a maximum of 1.2 cm of uplift occurred (Savage, 1988). Deformation has proceeded at a constant, albeit slow, rate since 1984, but the rate between 1983 and 1984 was twice that of present. In addition, moderate earthquakes have persisted in the south margin of the caldera (fig. 4-1). This seismicity is thought to be the result of stress induced from the injection of magma, because the swarms have tended to become shallower with time (Miller and others, 1982). The U.S. Geological Survey initially issued an earthquake hazards watch on May 27, 1980, because of the high rate of seismicity; subsequently, a notice of potential volcanic hazard was issued on May 17, 1982, in response to the apparent emplacement of magma (Bailey, 1983).

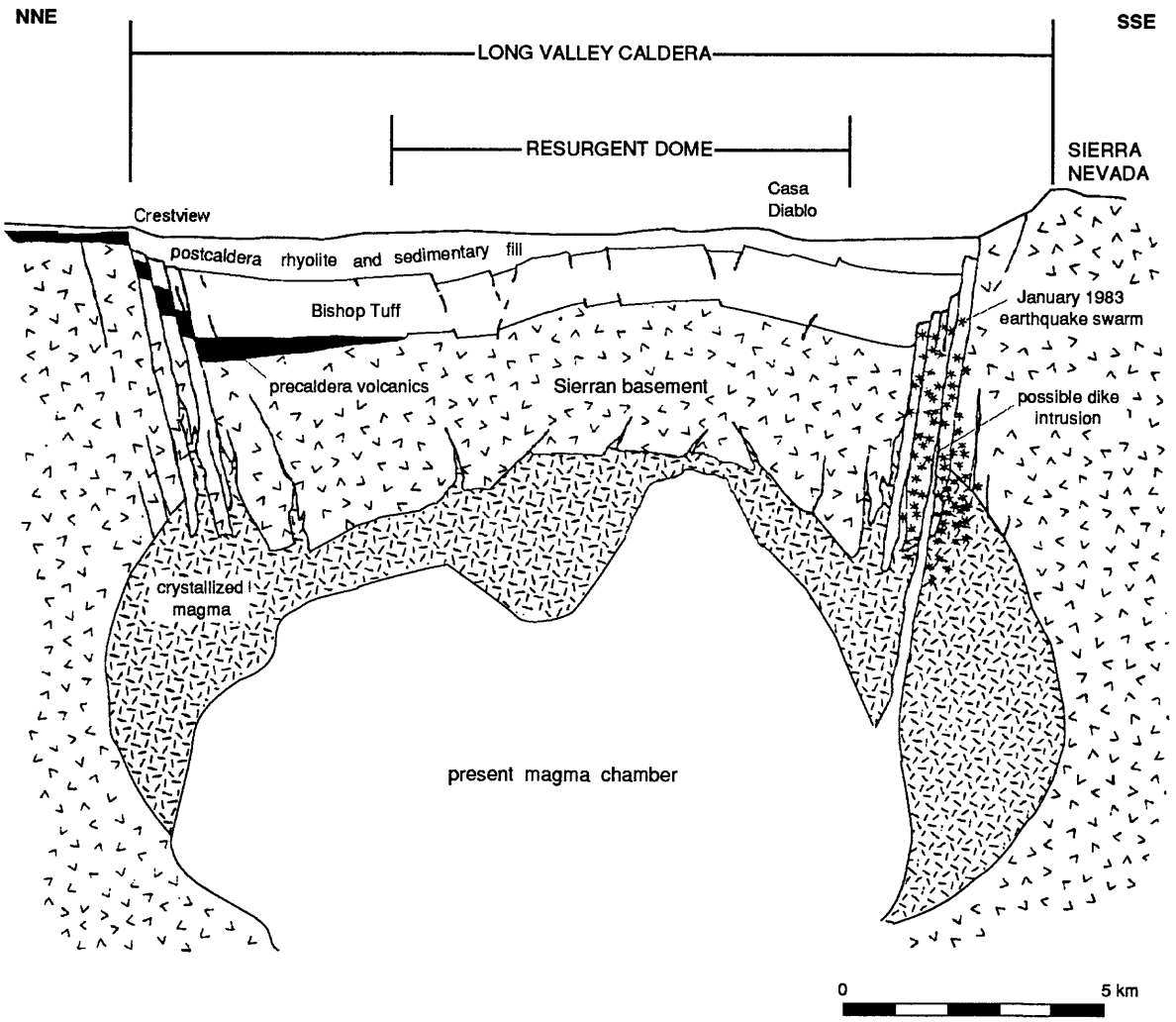

Figure 4-1. Schematic of subsurface structure in Long Valley caldera showing hypocentral zone for January 1983 earthquake swarm and possible associated dike intrusion (from Hill and others, 1985).

The 1980 swarm of magnitude-6 earthquakes formed new small, discontinuous scarps on preexisting scarps over a distance of about 20 km on the Hilton Creek fault (Taylor and Bryant, 1980). However, surface rupture did not extend along the entire length of previously recognized scarps. The largest scarp resulted from 27 cm of vertical offset across the Hilton Creek fault approximately 1.7 km north of *Stop 4.1* (see fig. 4-2).

As previously mentioned, some geologic evidence suggests that volcanic eruptions in this area are triggered by large-magnitude earthquakes. The timing of prehistoric pyroclastic and phreatic explosions of the Inyo and Mono Craters to the north (*Stops 5.1* and *5.2*, respectively) were closely associated with five seismic events. The distribution of earthquake-induced sandblow deposits suggest surface-wave magnitudes exceeding 6 (Sieh and Bursik, 1986). These seismic events are thought to have occurred on the Sierra Nevada frontal fault zone. The thickness of the dike near North and South Inyo Craters (*Stop 5.1*), as determined in drill holes, is an order of magnitude smaller than expected by models of surface deformation (Eichelberger and others, 1988), which suggests that the surface deformation is not entirely due to volcanism. Instead, a major earthquake on the Hartley Springs fault (local name for that part of the Sierra Nevada frontal fault zone) may have triggered

the eruptions. Similarly, Metz and Mahood (1985) suggest that the eruption of the Bishop Tuff was tectonically triggered. The chemistry of the tuff indicates that the degree of differentiation in the magma chamber should have precluded such explosive behavior. The Bishop Tuff was erupted from a vent probably located at the intersection of the caldera wall and an echelon part of the Sierra Nevada frontal fault zone (Hildreth and Mahood, 1984). Because of these spatial and apparent temporal associations, large-magnitude earthquakes on the range-front faults in this area can be associated with a multitude of hazards, including volcanism.

Segment 4--Mammoth Lakes Loop (36 Miles)

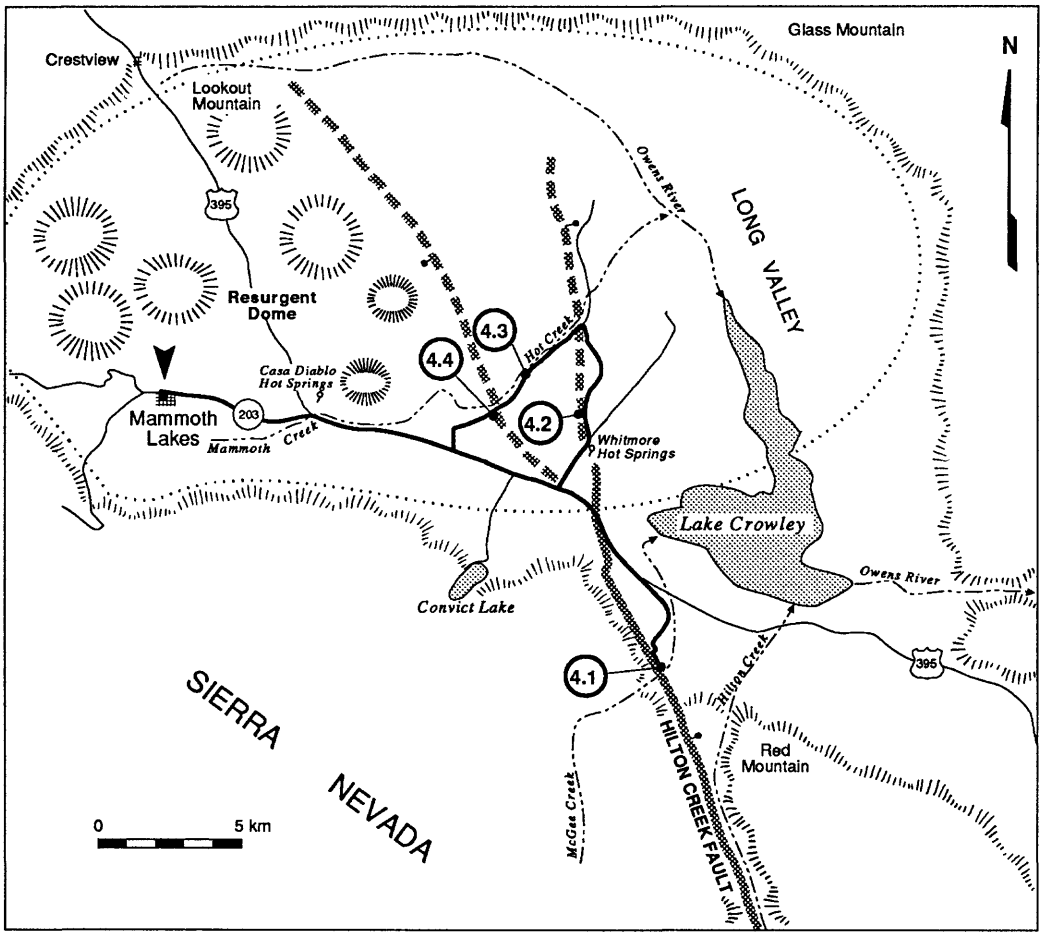

Figure 4-2. Route map for Segment 4, Mammoth Lakes Loop, California.

Route Narrative--Intersection of Old Mammoth Road and California Highway 203. Drive east on California Highway 203 to U.S Highway 395, turn right (south) on Highway 395.

Mammoth Lakes is in the Mammoth embayment, the large east-facing scallop in the Sierra Nevada caused by the Long Valley caldera. Within the embayment, the timing of the most recent surface-faulting events differs on each of the echelon strands of the range-front fault zone. Evidence for surface faulting along the southern edge of the embayment is poorly preserved. At Convict Creek (7 miles southeast of Mammoth

Lakes), scarps are preserved only on the westernmost of the lateral moraines (fig. 4-3). Although the age of the moraines is subject to a variety of interpretations, the faulted moraine may be the oldest Tioga moraine preserved at that site (Sharp, 1969; Lipshie, 1976). On the east side of Convict Creek is a 300-m-high Tahoe lateral moraine; however, the moraine does not extend over the fault. This deposit is actually the left-lateral moraine; during Tahoe time the Convict Creek glacier had a more easterly course than the Tioga glacier, which had a northeast course. Thus, when the Tioga glacier reached the mouth of the canyon, it removed much of the Tahoe till at the range front.

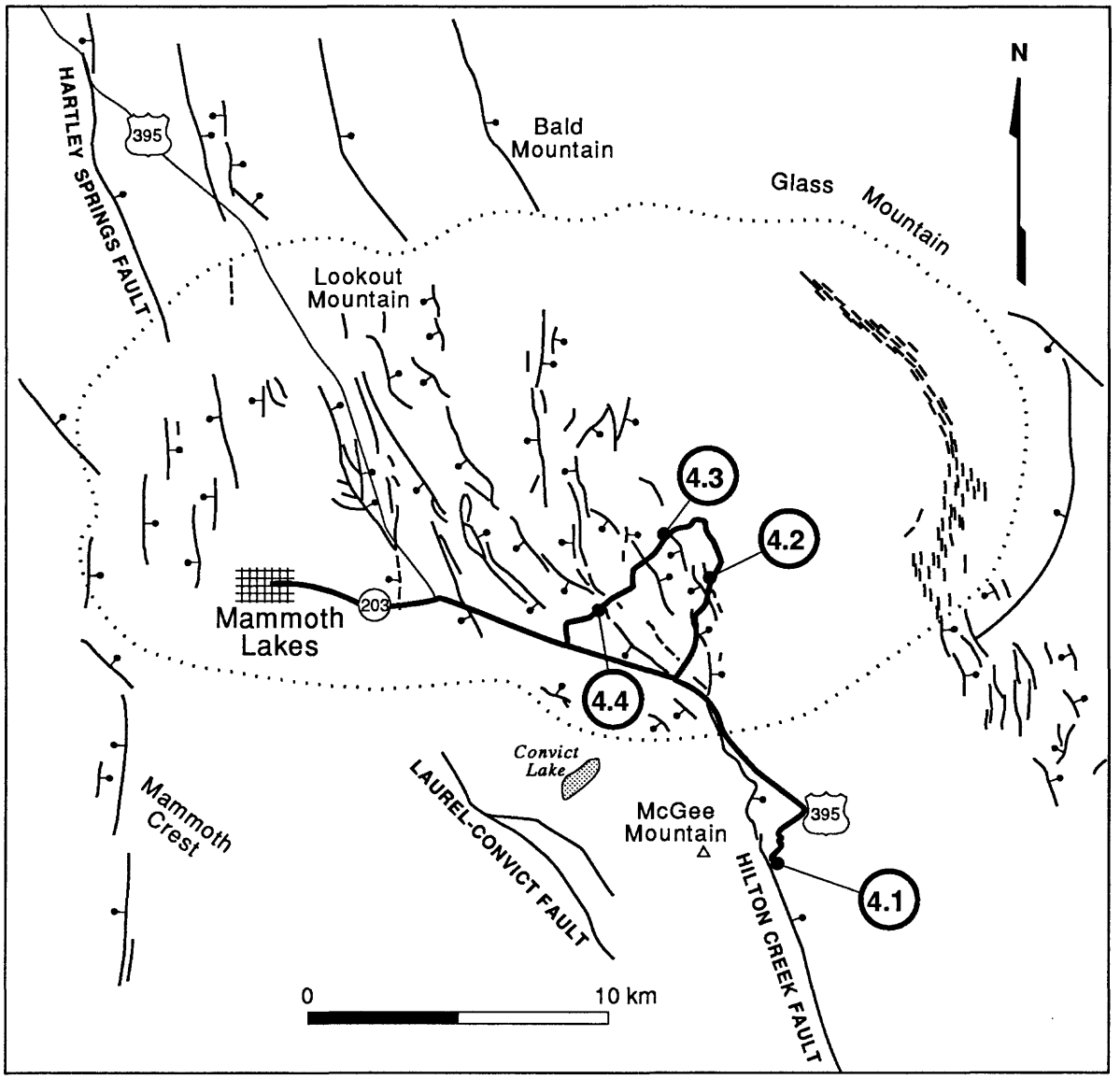

Figure 4-3. Map of Long Valley caldera and associated faults. Bar and ball is on downthrown side of faults; dotted line defines the topographic boundary of the caldera. Route for Segment 4 shown by heavy line.

Just beyond the Tahoe lateral moraine at Convict Creek, the road makes a broad curve to the right (southwest) and descends the scarp on the Hilton Creek fault. The scarp, which is at the base of the range front, is the product of repeated late Quaternary movement. Based on the position of glacial tills in this area,

Putnam (1960) suggested there has been 900 m of vertical offset between the McGee (early Pleistocene) and Sherwin (<740 ka) glaciations and an additional 300 m between Sherwin and Tahoe. Recent studies suggest that vertical displacement between Tahoe and Tioga glaciations is approximately 130 m (Clark and Gillespie, 1981) and post-Tioga displacements are about 26 m (Margaret Berry, University of Colorado, 1989, oral commun.). Thus, there has been approximately 1350 m of displacement during the Quaternary.

At Mile 11.4 turn right (west) onto McGee Creek road. After the route leaves U.S. Highway 395, the road circles around the end of the Tahoe moraine from McGee Creek canyon (fig. 4-4). At the first sharp turn in the road, we climb onto the crest of the Tahoe lateral moraine and then the crests of three Tioga lateral moraines. Proceed to McGee Creek Campground (Mile 15.3). Turn into campground and park at the west end for *Stop 4.1*.

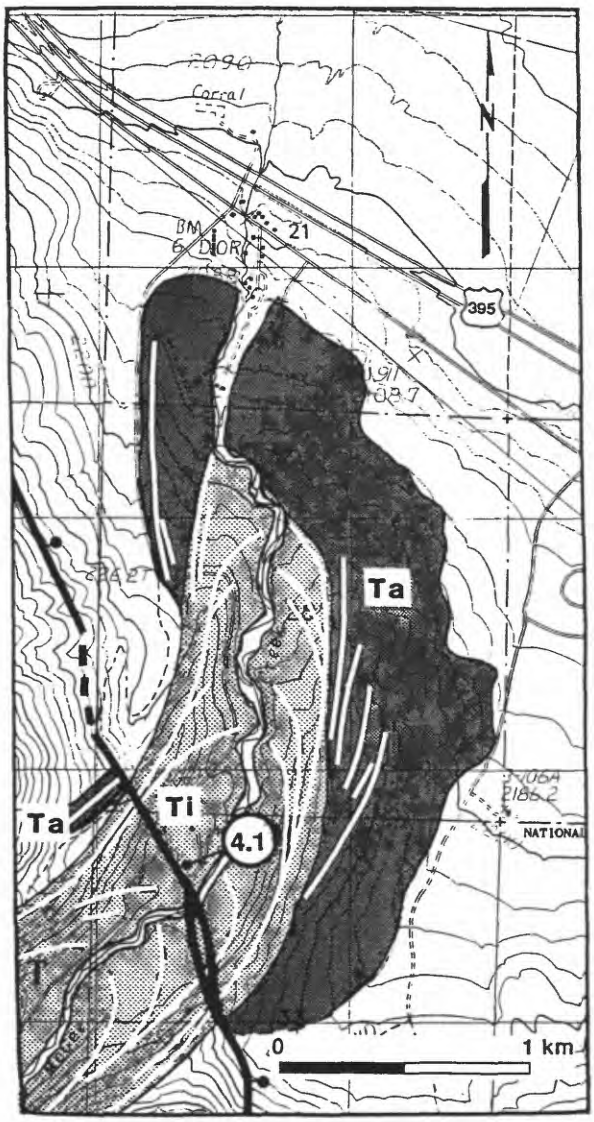

Figure 4-4. Map of glacial deposits and Hilton Creek fault at McGee Creek (from Margaret Berry, 1989, written commun.). Dark stippled unit is Tahoe (Ta), light stippled unit is Tioga (Ti), white lines within these deposits are the location of moraine crests. Hilton Creek fault is shown by heavy line with bar and ball on downthrown side, dashed where inferred.

Stop 4.1--Hilton Creek Fault at McGee Creek

The following discussion of the Hilton Creek fault is based on studies of Margaret Berry (1989, oral commun.). The 25-km-long Hilton Creek fault trends northwest from within the Sierra Nevada block into the Long Valley caldera (fig. 4-3). At McGee Creek, fault scarps are found on Tioga and younger deposits; the older Tahoe deposits extend across the fault but they do not straddle the fault (fig. 4-4).

The amount of surface offset of the two, paired Tioga lateral moraines is variable; however, all of the scarps here are the result of multiple displacements. On the north side of McGee Creek, the outer Tioga is displaced 26 m; no data are available for the inner Tioga moraine. The offset of the valley floor is 17 m. To the south of McGee Creek, the Tioga moraines are offset about 14 m, which is distributed across at least two strands of the fault (fig. 4-4).

Berry excavated a trench at the base of the Hilton Creek scarp in the McGee Creek Campground (fig. 4-5); although she was not permitted to trench across the trace of the fault, stratigraphic relations suggest that at least two major faulting events occurred in the past 22 ka. The stratigraphy exposed by the trench includes a basal till unit (Tioga) overlain by colluvium derived from the fault scarp. A prominent stone line within the colluvium (particularly noticeable between meters 12-20 and in southwest wall of trench, fig. 4-5) is thought to be a stratigraphic marker separating deposits of two major faulting events at this site. The stone line probably does not represent a climatic event, as similar stone lines are not present in colluvium deposited on flanks of moraines.

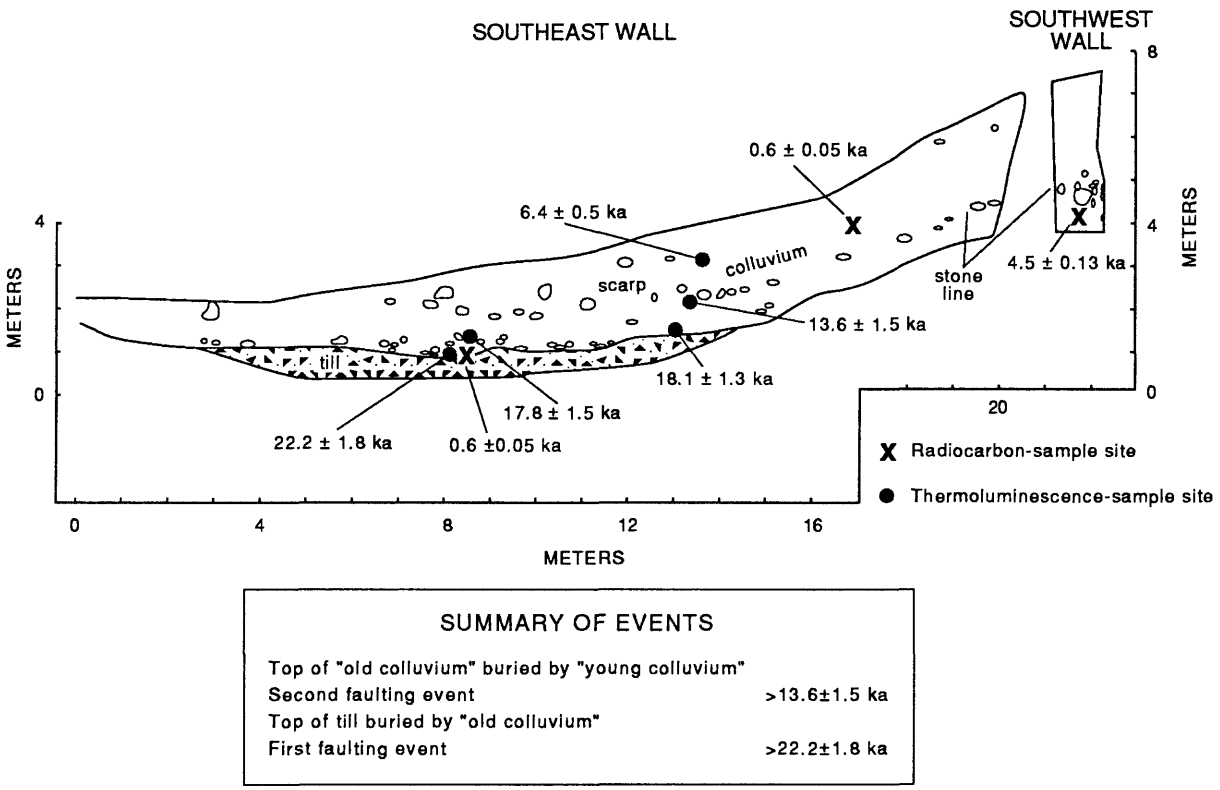

Figure 4-5. Log of southeast and southwest wall of trench across lower part of Hilton Creek fault scarp at McGee Creek Campground and inferred timing of faulting events (from Margaret Berry, 1989, written commun.).

Both thermoluminescence- and radiocarbon-dating techniques were used to evaluate the age of the various parts of the colluvial package and, thereby, bracket the times of faulting. Berry found large discrepancies in the ages of materials sampled from approximately the same stratigraphic position, but dated by different methods. For example, the two samples that have radiocarbon ages of 0.6 ka are now thought to be tree roots because of their discordance with other dated materials at the same stratigraphic position. In general, the thermoluminescence dates show the proper stratigraphic succession and, thus, are believed to be reliable age estimates. As such, they indicate that the top of the till was buried by colluvium about 22 ka. Colluviation continued and the top of the lower colluvial wedge was buried, first by the stones derived from the free face and then by finer colluvium, beginning about 13 ka.

Route Narrative (continued)--Retrace route to U.S. Highway 395 and turn left (northwest). Proceed on highway for 3.2 miles (Mile 19.2), turn right (east) onto Benton Crossing/Owens River Road. Proceed past Whitmore Hot Springs and bear left at Y intersection (Mile 22.4) onto U.S. Forest Service Road 2S07. Proceed 1 mile to small parking area on right at unnamed hot springs for *Stop 4.2*.

Stop 4.2--Eastern Extension of Hilton Creek Fault in Long Valley Caldera

This site is about 3 km north of the bifurcation of the Hilton Creek fault and just inside the caldera wall. This strand of the fault trends almost due north, but it is poorly expressed at the surface. Small, somewhat discontinuous scarps characterize this part of the fault, and both east- and west-facing scarps are equally common on the hill to the west of the main road. The bedrock of the hill is moat rhyolites (Bailey and others, 1976) that are probably about 350,000 years old. The small size of the scarps suggest low slip rates on this part of the Hilton Creek fault. As is common near faults throughout the Long Valley caldera, a small spring is present near the base of the small fault scarp east of the road.

There was 2 cm or less of vertical displacement at this site following the 1980 swarm (Taylor and Bryant, 1980). About 1 cm of horizontal extension was evident at some locations prior to the swarm; after the 1980 swarm, the cracks opened an additional 8 cm.

Route Narrative (continued)--Return to Forest Service Road 2S07 and turn right (north); proceed 1.7 miles (Mile 21.6) to Forest Service Road 3S44 and turn left (southwest). Drive 1.1 miles (Mile 27.4) and park at Hot Creek for *Stop 4.3*.

Stop 4.3--Hot Creek Gorge

Hot Creek is the part of Mammoth Creek where numerous hot springs warm the stream water and provide a popular bathing spot. The wall rocks in the gorge are 280,000-year-old flows of Hot Creek rhyolite. The rhyolite was erupted from a vent south of here at the shoreline of late Pleistocene Long Valley Lake (Bailey, 1987). The rhyolite was deposited subaqueously here because this location was beneath the lake at the time of the eruption. Travertine is being deposited around the numerous active fumaroles lending a unique beauty to this spot.

These springs are located on an extension of the Hilton Creek fault. Because the recent seismicity within Long Valley caldera greatly influences the amounts and subsurface patterns of water flow, as well as water level in Hot Creek (Bailey, 1987), the location and vigor of boiling pools often change. The hot waters are from shallow aquifers (<700 m deep), but are probably heated by magma (Bailey, 1987). Numerous efforts to utilize this geothermal resource has been initiated recently, two of them are north of this site, one at Casa Diablo Hot Springs and the other north of *Stop 4.4*.

Route Narrative (continued)---From *Stop 4.3*, return to Forest Service Road 3S44 and turn right, proceed straight through the intersection at Mile 29.0. Park on the shoulder of the road, 0.2 mile beyond Hot Creek Ranch for *Stop 4.4*.

Stop 4.4--Western Extension of Hilton Creek Fault in Caldera

Drilling began in this area to develop the geothermal potential in 1959. Chance No. 1, one of the original geothermal well sites, is near the hot springs to the north, across the valley. The flow of the hot springs, which is marked by the plume of steam rising from the ground, fluctuates such that the level of the pool surrounding the springs rises and falls. The period of the pool fluctuations is 4-7 hours, and the typical rise of about 0.3 m represents approximately 350 liters of water (W.H. Diment and T.C. Urban, 1989, oral commun.). Water levels in the Chance No. 1 well are almost exactly out of phase with levels in the pool. The flow rate changes considerably in response to the local earthquakes; in 1980, and again in 1983, the pool completely drained.

South of the road, scarps on the western bifurcation of the Hilton Creek fault are predominantly down-to-the-west and trend northwest. The prehistoric scarp south of the road is continuous along the west flank of the hill and ends near where the route departed from U.S. Highway 395. Somewhat continuous cracks having maximum vertical displacement of about 1 cm formed on this scarp following the 1980 swarm (Taylor and Bryant, 1980).

Route Narrative (continued)---Proceed west to stop sign and turn left toward U.S. Highway 395. Turn north on highway and return to Mammoth Lakes.

DAY 5--MAMMOTH LAKES, CALIFORNIA, TO FALLON, NEVADA

Summary

The field trip proceeds north along the eastern Sierra Nevada front, stopping at sites of some of the youngest volcanism in the conterminous United States and at sites of Holocene surface faulting along the Sierra Nevada frontal fault zone. At Carson City, Nevada, the route diverges from the Sierra Nevada and proceeds northeast into the Basin and Range province. The final stop is at scarps along the 200-km-long, northeast-striking Carson lineament.

Segment 5A--Mammoth Lakes to Conway Summit (51 Miles)

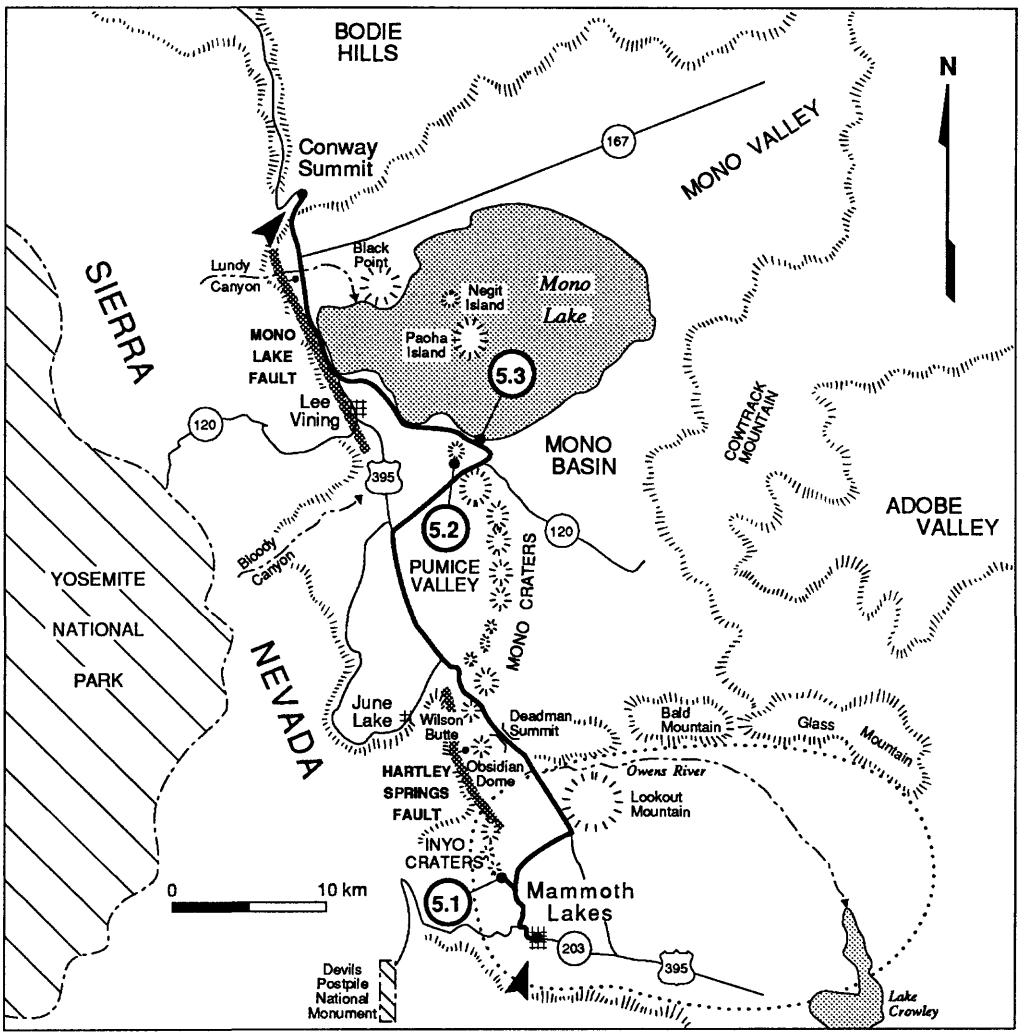

Figure 5-1. Route map for Segment 5A, Mammoth Lakes to Conway Summit, California.

Route Narrative--Note the odometer reading at intersection of Old Mammoth Road and California Highway 203 and proceed west on Highway 203 for 1.2 miles. At the traffic light turn right (north) on the road to Devils Postpile National Monument. At Mile 2.2 turn right (north) onto Scenic Loop Drive (Mammoth Scenic Road), and at Mile 4.8 turn left (west) onto Inyo Craters Road. Proceed 0.2 mile and turn right, after another 0.1 mile bear right at the Y intersection, then bear right again in another 0.5 mile. Follow Forest Service Road 3S27 to the parking lot at Inyo Craters for *Stop 5.1.*

The route from Mammoth Lakes to U.S. Highway 395 (fig. 5-1) skirts around the west and north sides of the resurgent dome in the Long Valley caldera. As we approach Inyo Craters from the south, numerous domes of the Inyo volcanic chain are on both sides of the road.

Inyo-Mono Volcanic Chain

Inyo and Mono Craters comprise a 30-km-long chain of late Quaternary volcanic craters and domes that extend from the northwest part of the Long Valley caldera to the north shore of Mono Lake (fig. 5-2). These extrusive vents represent some of the youngest volcanism in the conterminous United States (Hill and others, 1985). Eruptions within the chain have occurred at approximately 500-year intervals for the past 2,000-3,000 years; the most recent eruptions occurred at the ends of the chain. The recurrent eruption of the aligned centers are due to repeated injection of magma into preexisting zones of crustal weakness along the base of the Sierra Nevada.

The Inyo volcanic chain is a 10-km-long, linear group of chemically and physically heterogeneous domes and phreatic craters (Lajoie, 1968) extending from about 2 km south of North and South Inyo Craters (*Stop 5.1*) to Obsidian Dome (fig. 5-2). The pyroclastics from these vents are predominantly rhyolitic and rhyodacitic (Wood, 1977) and their chemistry probably reflects mixing of magma from the chamber beneath Long Valley caldera (rhyodacitic source) with magma from the chamber beneath Mono Craters (rhyolitic source) (Bailey and others, 1976).

It is apparent that the eruptive behavior of the Inyo chain differs across the caldera boundary. Inside the caldera, eruptions were primarily phreatic, produced only minor amounts of tephra, and accompanied by extensive surface faulting (Eichelberger and others, 1988). In contrast, eruptions from vents outside the caldera produced widespread tephra deposits and extensive faulting is not apparent. This contrasting eruptive behavior appears to be the result of the different geologic and hydrologic conditions across the caldera boundary. These conditions may be due either to the increased ground water circulation in the caldera, which aids cooling and rapid degassing of the magma, or to the inherent mechanical weakness of the rocks in the caldera, which allows them to deform easier and thereby impede the upward migration of the magma.

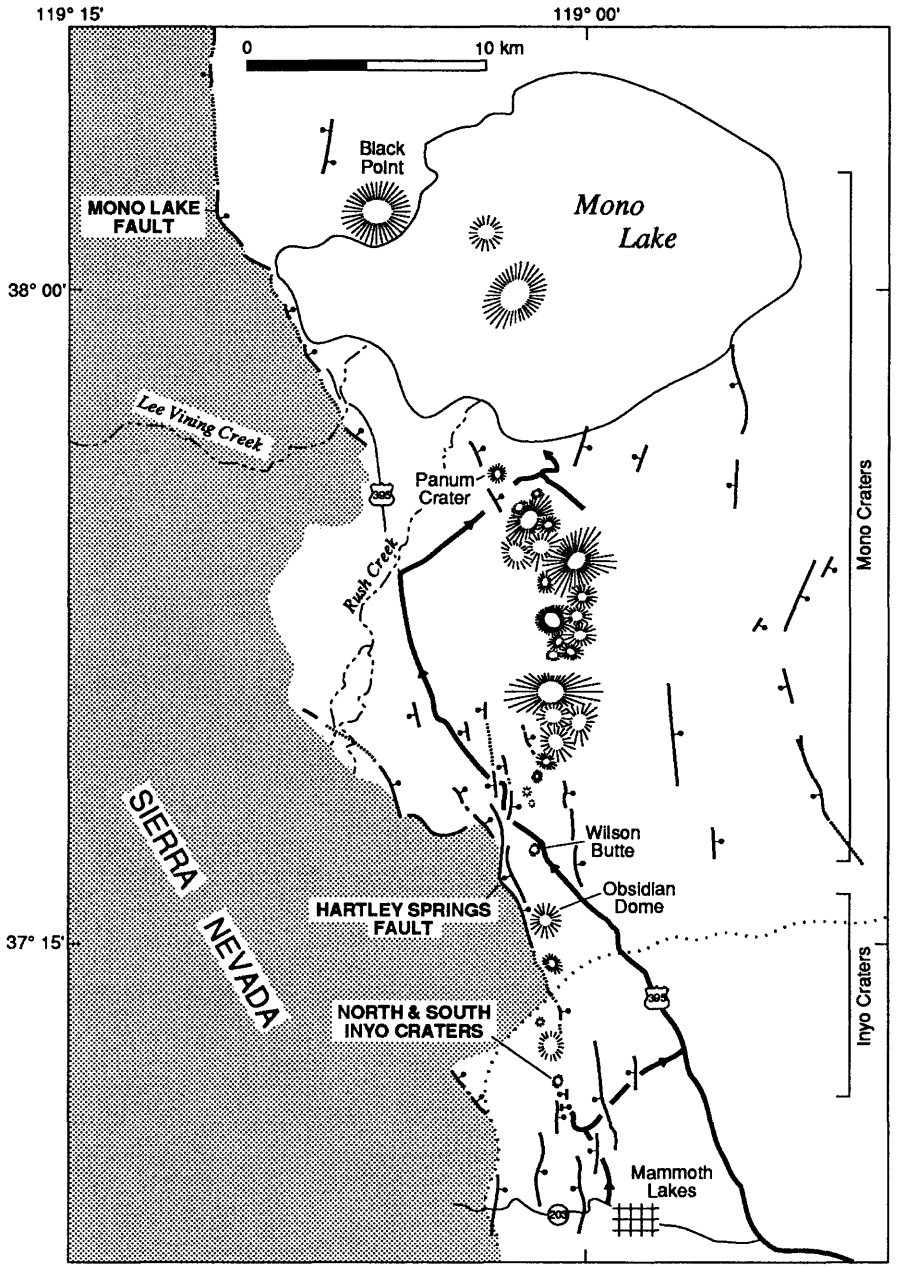

Figure 5-2. Map of Inyo-Mono volcanic chain and associated faults (modified from Sieh and Bursik, 1986; Mastin and Pollard, 1988) showing field-trip route (heavy line) from Mammoth Lakes to Mono Lake. Medium lines are faults, bar and ball on downthrown side; dotted lined is boundary of Long Valley caldera; Sierra Nevada is stippled.

Mono Craters is a 17-km-long arcuate chain of domes and flows (fig. 5-2) that extends from Black Point on the north to Wilson Butte on the south. The domes are late Holocene in age and are composed of chemically similar rhyolites (Carmichael, 1967); the older deposits in the chain, which are primarily rhyodacitic to dacitic, occur on the islands in Mono Lake and the Black Point basaltic tephra cone (Lajoie, 1968). The craters are coincident with an 18-km-diameter ring-fracture zone, across which Bishop Tuff is displaced 200 m down to the west (Bailey and others, 1976). The craters along with interbedded lacustrine sediments and rhyolitic ash-fall deposits record a period of active volcanism spanning at least the past 35,000 years (Lajoie, 1968).

The most recent eruptions of Mono Craters, which produced North Mono tephra and related lava, occurred between A.D. 1325 and 1365 and are nearly contemporaneous with the eruptions of Inyo Craters (Sieh and Bursik, 1986) to the south. North Mono tephra and related lava originated from at least ten vents, including Panum Crater (*Stop 5.2*) on the south margin of Mono Lake. This violent episode of volcanism probably lasted only a few months (Sieh and Bursik, 1986).

The time of the most recent eruptions of the Inyo and Mono Craters and their spatial coincidence with range-bounding faults have led many authors to suggest that the processes of faulting and volcanism are related, although the geologic record indicates differing histories for the two range-front faults west of craters. Stratigraphic relations clearly indicate that the most recent Mono eruptions are younger than the Inyo eruptions, but both eruptions appear to be temporally related to at least moderate-sized earthquakes (Sieh and Bursik, 1986). Sands on the floor of Mono Lake were liquified a total of five times during the most recent episode of volcanic activity; this suggests that at least moderate ($M_L \geq 5.5$) earthquakes were associated with the eruptions.

The northern part of the Inyo chain is parallel to and east of the Hartley Springs fault (fig. 5-2). The trends of the primarily north-striking volcanic chain and north-northwest-striking fault seem to intersect at or near the caldera boundary (Mastin and Pollard, 1988). There has been 1-2 m of late Pleistocene displacement on the fault in the past 13,000-20,000 years, which suggests an average slip rate of about 0.15 mm/yr (Clark and others, 1984), or a rate about one order of magnitude less than that of other parts of the Sierra Nevada frontal fault zone.

Mono Craters are not on the Sierra Nevada frontal fault, but instead are on the valley floor. Even though scarps are present within the chain, they may be the product of surface displacement in response to the evacuation of the magma chamber. Scarps are absent at the range front adjacent to most of the trend of the Mono Craters (fig. 5-2). Along this part of the Sierra Nevada front, which is embayed about 8 km west of Mono Craters, faulting does not appear to be the major mechanism for relieving strain in the past tens of thousands of years (Sieh and Bursik, 1986); instead, regional extension is probably accommodated by dike intrusion during periods between major earthquakes. Recent range-front faulting is only present along the northernmost end of the Mono chain on Mono Lake fault, which extends north from the south end of Mono Lake and offsets Tioga recessional moraines 22-25 m vertically at Lundy Canyon (Clark and others, 1984).

Stop 5.1--North and South Inyo Craters

North and South Inyo Craters are approximately 600 m northwest of the parking area (fig. 5-3). If you walk up the trail to the craters, note scarps parallel to the trail that are the easternmost expression of the asymmetric graben bounding the craters. If you walk up the road, note the ground fissures and scarps to the left (west) of the road, all of which are on the floor of the graben.

The pumice lying on the surface around Inyo Craters probably originated from a vent in the northern end of the Inyo chain, based on strontium content (Wood, 1977; Miller, 1985). The pumice was deposited at high temperatures, destroying much or all of the vegetation in the area, and thus, the forest surrounding these craters is younger than the tephra. In contrast, the phreatic eruption of North and South Inyo Craters resulted in low-temperature ejecta and did not destroy the forest. The forest here is nearly entirely composed of firs and Jeffrey pines, the oldest of which are about 400 years old (Huber and Rinehart, 1967). Miller (1985) believes the pumice deposits to be no more than about 600 year old and the lack of chemical alteration and absence of soil on this deposit also indicates a young age.

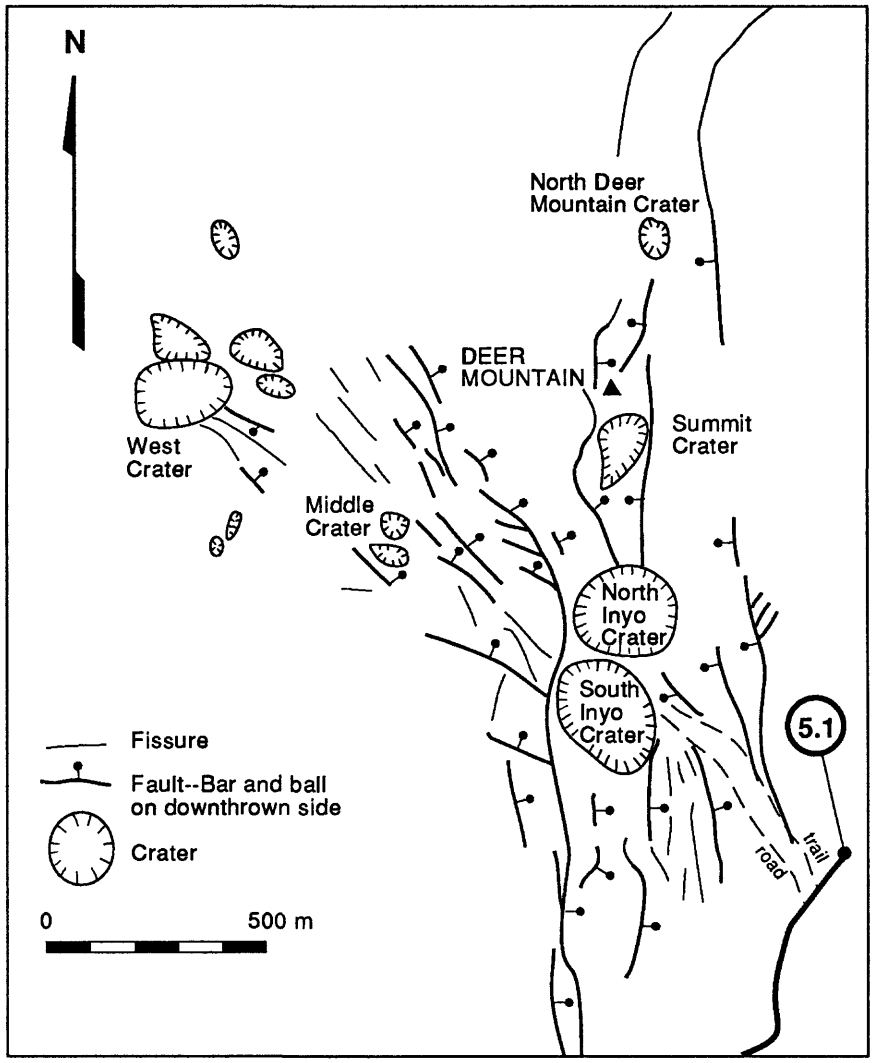

Figure 5-3. Map of part of Inyo volcanic chain near North and South Inyo Craters (*Stop 5.1)* and associated faults and fissures (from Mastin and Pollard, 1988).

During the most recent period of activity of Inyo Craters (650-550 years ago), at least four eruptions, each from different vents, deposited 0.17 km^3 of tephra (approximate volume of magma erupted), and 0.53 km^3 of magma was extruded as domes (Miller, 1985). The formation of South and North Inyo Craters, however, did not involve the eruption of magma. Instead, the craters are the result of phreatic explosions caused by rapid mixing of ground water and magma. The ejecta from these explosions is predominantly a heterogeneous mixture of fine-grained material and rock derived from the craters and is younger than the explosions that produced the tephra deposits in this area (Wood, 1977). The final stages of this episode of volcanism produced extensive rhyolite flows from some of the vents on the north end of the chain.

Both the trail and road lead to South Inyo Crater where the stratigraphy in the crater wall is better exposed than in North Inyo Crater (approximately 200 m to the north). Both craters are about 180 m in diameter; North Inyo Crater is about 30 m deep and South Inyo Crater is approximately twice as deep. Above the talus covering the lower slopes of South Inyo Crater is a prominent bench composed of late Pleistocene andesite flow (Huber and Rinehart, 1967). Above the bench is approximately 1.2 m of tephra from one of the northern vents in the Inyo chain (Wood, 1977); the upper 15 m of the crater wall is composed of locally derived, layered phreatic explosion debris. Wood (1977) radiocarbon dated the logs in the latter deposit and concluded that North and South Inyo Craters were formed between A.D. 1340 and 1460.

North and South Inyo Craters lie within a prominent 2.5-km-long, north-trending graben. The down-to-the-east, 15-m-high scarp that parallels the west edge of South Inyo Crater forms the west boundary of the up to 700-m-wide graben containing the craters (fig. 5-3). The scarp is geomorphically young and has maximum slope angles of as much as 30° (Mastin and Pollard, 1988). An east-facing scarp about 6 m high, which postdates the phreatic deposit, can be seen on the southern rim of South Inyo Crater.

Route Narrative (continued)--Return to Scenic Loop Drive, turn left (northeast), and proceed 3.1 miles to U.S. Highway 395. Turn left (north) onto U.S. Highway 395. Note the odometer reading at intersection of Scenic Loop Drive and U.S. Highway 395.

Between *Stops 5.1* and *5.2* we will travel north on U.S. Highway 395 parallel to the Inyo-Mono volcanic chain (fig. 5-1) and the Hartley Springs fault (fig. 5-2), the major range-bounding fault along this part of the Sierra Nevada. About 1 mile north of where the route joins U.S. Highway 395, the road descends into 1.5-km-wide ring-fracture zone that forms a graben at the northern edge of the Long Valley caldera. Note the thin basalt flow filling the graben. Ahead and to your right (north) is Lookout Mountain, an approximately 670,000-year-old obsidian plug dome (Bailey and others, 1976). Just beyond the rest area (at Mile 1.8), note the aligned flows on the left (southwest) side of the highway. These are the northernmost of the Inyo chain and are markedly different in appearance from the phreatic craters to the south.

As we approach Crestview, near the topographic rim of the caldera, roadcuts expose 3-Ma andesites overlain by glacial outwash and Bishop Tuff. Obsidian Dome (part of the Inyo chain), about 3 km northwest of Crestview, erupted between A.D. 1369 and 1433 according to Miller (1985), or prior to the eruption of the vent that produced the tephra deposits at Inyo Craters (*Stop 5.1*).

As we cross Deadman Summit (elev 2,451 m) and the topographic rim of the Long Valley caldera, Wilson Butte is straight ahead; this is the southernmost volcanic center of the Mono chain. Explosive activity occurred about 1,350-1,220 yr B.P. at Wilson Butte and preceded the emplacement of the rhyolite dome about 1,200 years ago (Miller, 1985). The highway flanks the east and northeast side of Wilson Butte.

Note the large explosion crater approximately 1.5 miles beyond Wilson Butte where the road makes a turn to the right (north). About 0.5 mile beyond the explosion crater, the road rounds the toe of a ridge, the south half of which is underlain by Bishop Tuff and the north half by Tahoe till. The road crosses another Tahoe moraine and then a large Tioga moraine before we reach the June Lake turnoff (Putnam, 1949). Tioga till covers the flat valley floor in the vicinity of the turnoff.

Aeolian Buttes to the right (northeast) of the June Lakes turnoff is composed almost entirely of Bishop Tuff. These buttes were named by Russell (1889) for their spectacular wind-erosion features. About 4 miles beyond June Lakes turnoff, the highway descends into Mono Basin, a triangular-shaped topographic depression. On your right (northwest) is the remainder of the Mono Craters and on your left are moraines deposited by glaciers of the Grant Lake area.

At Mile 15.1 turn right (northeast) on California Highway 120 (to Benton). Note odometer reading at intersection of U.S. Highway 395 and California Highway 120. As the route leaves U.S. Highway 395 and continues northeast to Panum Crater, note the general lack of trees and the rugged appearance of the part of Mono Craters straight ahead. The five domes and coulees and four tephra rings are the sources of the most recent volcanism in this chain. North Coulee (south of the road) represents over half of the total volume of the recent eruptions (Sieh and Bursik, 1986). Proceed 3.0 miles to turnoff to Panum Crater, turn left (northwest), and proceed 0.9 mile to parking area at the crater for *Stop 5.2*.

Stop 5.2--Panum Crater

Panum Crater is but one of the many Mono Craters that were named by Russell (1889). "Pan-um" is an Indian word that means lake. Russell noted that Panum Crater is younger than the Pleistocene lake that occupied this valley, and he suggested that the lake was at its highstand during the last major glaciation of this area; he was correct on both accounts. The Pleistocene lake was later named after this illustrious scientist.

Panum Crater and its domes are the products of the least explosive phase of the North Mono eruption . Based on historic accounts of similar eruptions and geologic evidence, Wood (1977) and Sieh and Bursik (1986) suggest that the entire eruptive phase of Panum Crater may have occurred within one month to a few years. The sequence of materials erupted from Panum Crater include an early massive breccia, a pyroclastic flow, a pyroclastic surge deposit from a violent explosion, and a block-and-ash flow deposit that is on the north and west side of the crater (fig. 5-4). The final two phases of this episode, however, yielded the most prominent features at this stop: the tephra ring surrounding the crater and the domes in the crater.

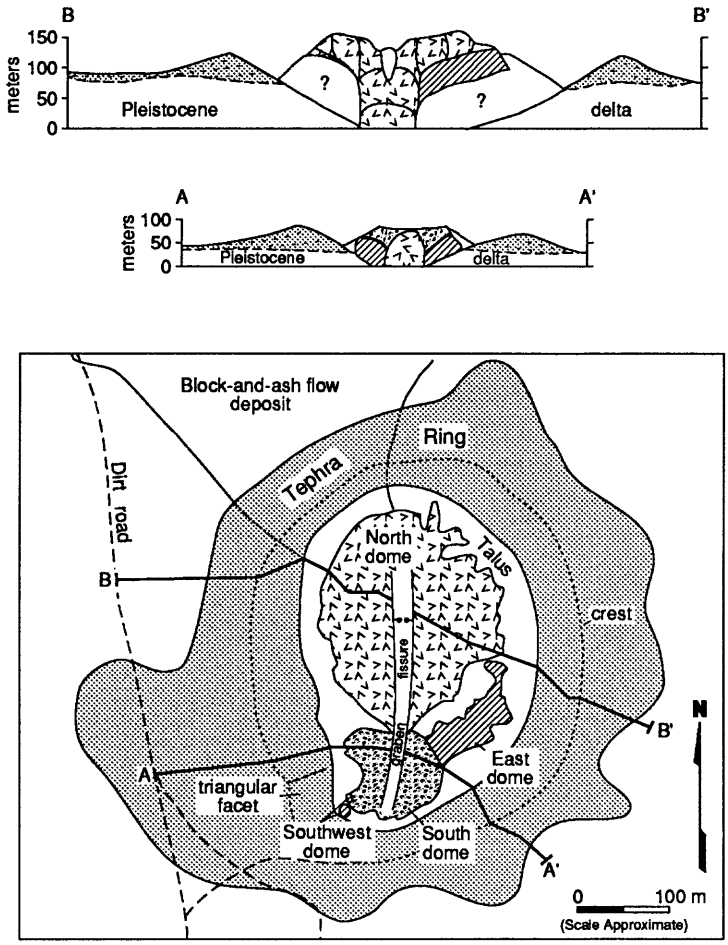

Figure 5-4. Generalized map and cross sections of Panum Crater and its domes (modified from Sieh and Bursik, 1986).

Panum Crater is characterized by an elliptical 70-m-high tephra ring of pumice ash, lapilli, and obsidian fragments, all of which only extend about 700 m from the crater. The crest of the ring is lowest on the north

and south primarily because of the north-south elongation of the vent; however, other factors also affected its morphology. The triangular facet on the south rim (fig. 5-4) is due to a late explosion that probably issued from the present location of South dome (Sieh and Bursik, 1986). The low crest on the north rim marks the northward flow path of the block-and-ash flow. Here, tephra mantles a preexisting notch, through which the block-and-ash flow exited Panum Crater.

Within the tephra ring are two domes and fragments of two smaller domes (fig. 5-4), all of which are structurally and texturally distinct (Sieh and Bursik, 1986). North dome, the youngest of the group, is composed of light-gray, flow-banded stony rhyolite that is surrounded by light-gray pumiceous rhyolite. The elliptical dome is bilaterally symmetrical about an elongate north-south graben. South dome consists of banded gray and black rhyolite and obsidian and also is symmetrical about the graben. The graben in south dome may be due to brittle extension associated with the extrusion of north dome. Southwest and east domes, only fragments of which are preserved, are the oldest of the group as evidenced by their limited surface expression. Southwest dome consists of white stony rhyolite and east dome of stony to pumiceous rhyolite.

From the crest of the tephra ring of Panum Crater, you can see older tuff rings on the southeast side of the crater. Also from this vantage looking to the southwest, you can see the unfaulted morainal complexes of Sawmill and Bloody Canyons and the high Lake Russell shoreline, which cuts across the Tahoe moraine at Lee Vining Creek canyon.

Route Narrative (continued)--Return to California Highway 120 and turn left (northeast). Turn left toward Tufa Reserve in 1.6 miles, proceed to parking lot on right in 0.9 mile. Park in lot for *Stop 5.3*.

Stop 5.3--Mono Lake and Tufa Reserve

Mono Lake is 24 km long east-west, 15 km wide north-south, approximately 50 m deep, and presently has no outlet. The present-day lake is a hypersaline remnant of a much larger fresh-water body known as Lake Russell (Putnam, 1949), the northernmost lake of the Pleistocene Owens River system (Smith and Street-Perrott, 1983). During the early part of the Tioga glaciation, the lake was about 275 m deep and emptied into Adobe Valley to the southeast across a high spillway; the sill was never dissected and as lake level dropped at the end of the Tioga glaciation, drainage of the basin ceased. Because of this, the present-day salinity of Mono Lake is nearly two times that of sea water (Scholl and Taft, 1964) and is highly alkaline, having a pH of 10.3 (Dunn, 1953).

The Mono Lake Tufa Reserve was established in 1982 and is jointly managed by the California Department of Parks and Recreation and the U.S. Forest Service to preserve the spectacular tufa formations and other natural features around Mono Lake. The tufa towers and domes are formed of nearly pure calcium carbonate deposited in a shallow subaqueous environment around fresh-water springs. Many of the tufa formations are hollow columns with axial channels through which spring water flows or has flowed. The largest towers are 7.5 m high and 15 m in diameter and all are probably less than 10,000 years old (Scholl and Taft, 1964). Even though these deposits were first described in detail by Russell (1889) over a hundred years ago, their origin still is controversial. Although the lake water has a very low concentration of calcium ion, its chemistry is highly complex; the spring waters, however, are relatively high in calcium. Dunn (1953) attributes the precipitation of calcium carbonate to differences in temperature and chemistry between the fresh spring water and the highly alkaline lake water; although, pH differences may also play a role. In contrast, Scholl and Taft (1964) believe that the presence of algae directly or indirectly causes the precipitation of the calcium carbonate; however, they do concede that precipitation would occur even if these organisms were absent. The relative importance of water chemistry and biological activity in the formation of these spectacular deposits remains unclear.

Since water diversion began in 1941, Mono Lake has fallen about 10 m and doubled in salinity. Water diverted from four of the seven streams that feed Mono Lake represents about 65 percent of the lake's potential annual water supply.

Route Narrative (continued)--Exit the parking lot and turn right (northwest) onto the dirt road. Note the odometer reading at the parking lot. Continue straight at intersection at Mile 0.5 (to Lee Vining) and also at intersection at Mile 2.1 (proceed toward fish hatchery at top of hill). Additional tufa deposits can be seen from the road as the route skirts the southern shore of Mono Lake. After passing the fish hatchery (on left, 2 miles beyond *Stop 5.3*), the road is built on a shoreline bench; note the other lower shorelines to the right (northeast) of the road. At Mile 3.9 turn right (north) at T intersection and drive toward the lake (not to Lee Vining); at Mile 7.4 turn right at T intersection and bear left at Y intersection at Mile 7.6. As the route returns to U.S. Highway 395, note the linear range front to the left (southwest). The Mono Lake fault extends north from here to Conway Summit. Proceed to U.S. Highway 395 and turn right (northwest) onto the highway. At the mouth of Lundy Canyon (near the north end of Mono Lake, fig. 5-2), you will be able to see fault scarps as much as 25 m high on a Tioga recessional moraine (10,000-15,000 years); the late Quaternary slip rate on this part of the Sierra Nevada frontal fault zone is 2.5 mm/yr (Clark and others, 1984). Follow U.S. Highway 395 to Conway Summit; the grade to the summit provides a spectacular view of Mono Basin. Roadcuts near Conway Summit (elev. 2,553 m) expose till of probable Sherwin age (Wahrhaftig and others, 1965).

Segment 5B--Conway Summit to Walker (47 Miles)

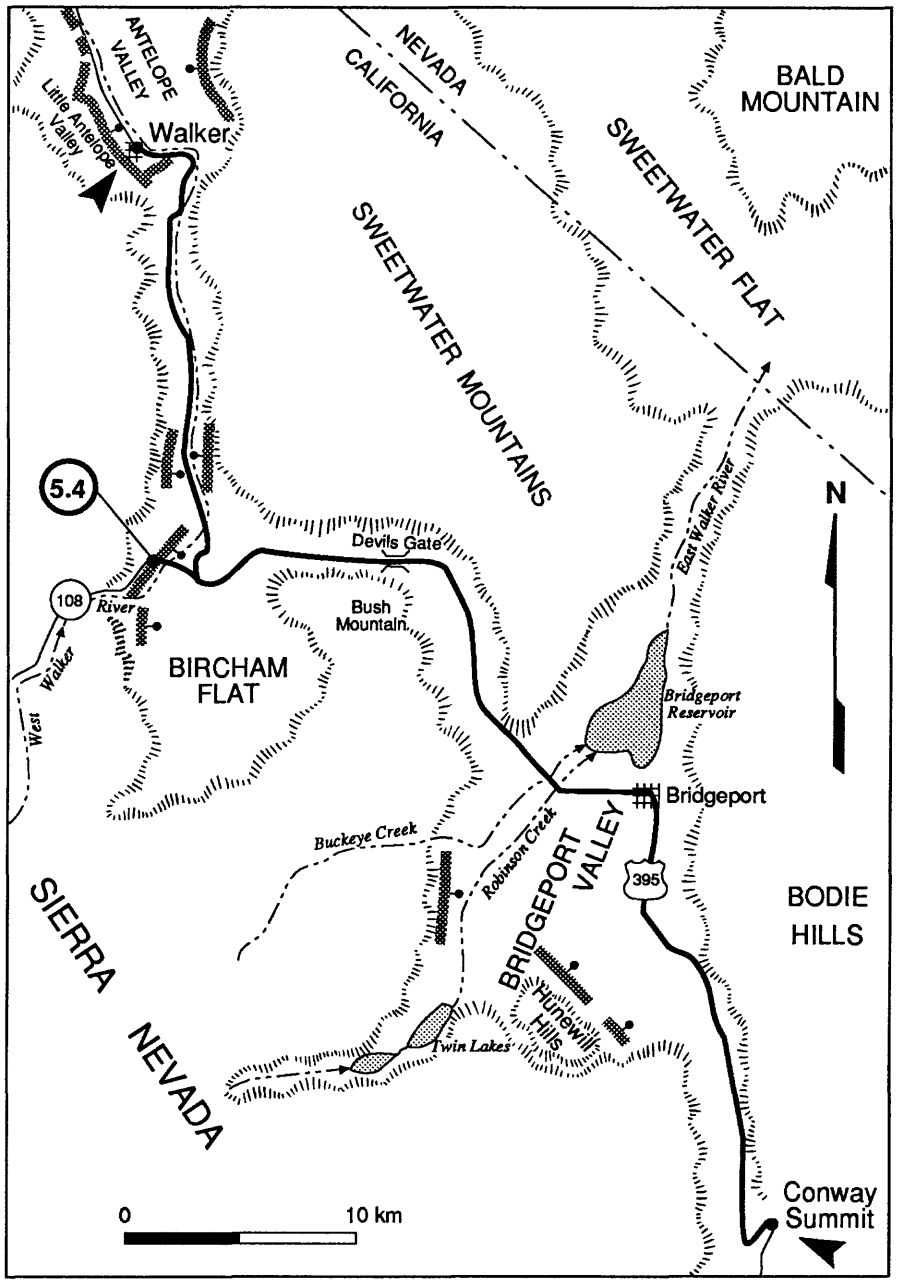

Figure 5-5. Route map for Segment 5B, Conway Summit to Walker.

Route Narrative--At Conway Summit, our route crosses into the Great Basin section (fig. 5-6) of the Basin and Range province (Harrill and others, 1988). Drainages originating within the the Great Basin do not flow to the ocean, but terminate in a number of separate closed drainage basins. Despite its internal drainage, the Great Basin is topographically high having an average elevation of more than 1,400 m. Continue north on U.S. Highway 395 for 29.8 miles beyond Conway Summit to Sonora Junction (California Highway 108).

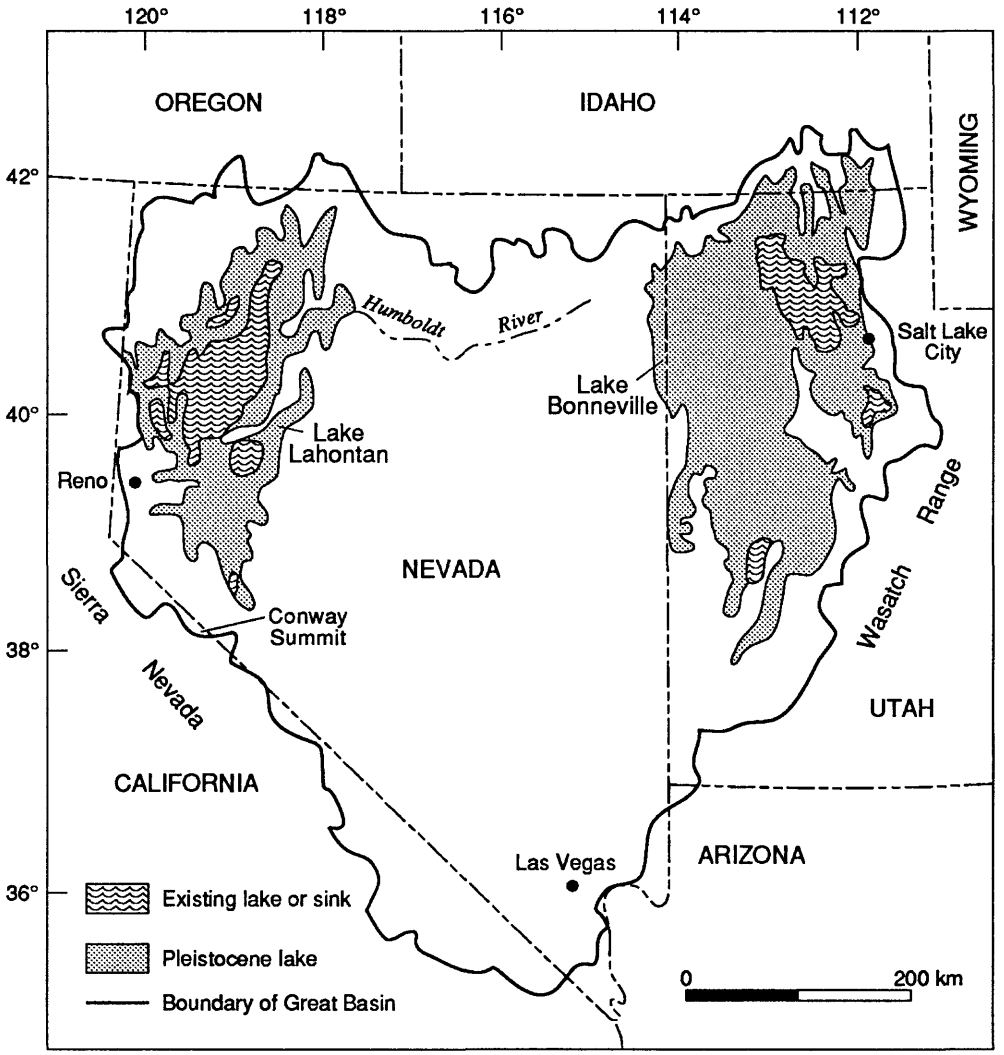

Figure 5-6. Map showing boundary of the Great Basin and the locations of the late Pleistocene lakes Lahontan and Bonneville (from Harrill and others, 1988).

The Sierra Nevada front loses its typical continuous prominent escarpment north of Conway Summit and is characterized by poorly defined, short, steep escarpments that bound deep alluvial basins alternating with nearly north-trending highlands (see fig. 1-1). Late Quaternary faulting is expressed as short scarps along the west edge of basins, each of which step westward from south to north. Many of these basins are formed in Tertiary calderas; however, all of the calderas are much smaller than those seen to the south.

The subdued topography of the Bodie Hills, on the right (east) side of U.S. Highway 395 just beyond Conway Summit, contrasts sharply with the rugged peaks of the Sierra Nevada to the west. The hills are underlain predominantly by Cenozoic volcanic rocks (Chesterman, 1968), some of which originated from two large calderas north and east of Conway Summit. The Bodie Mining District was organized in 1860 and thrived for a short period of time before it was nearly completely abandoned. In 1872, a second and larger strike of gold and silver was made, and once again Bodie flourished. Between 1877 and 1886, ore shipments exceeded $18 million, the value of which was equally divided between gold and silver (Irelan, 1888b).

Bridgeport Valley is an example of one of the previously mentioned small, fault-bounded basins. The scarps south of Buckeye Creek (fig. 5-5) are 3-5 m high on Tioga outwash and suggest a slip rate of 0.5 mm/yr (Clark and others, 1984). Faults also bound the northeast side of Hunewill Hills, the low hills southwest of the mouth of the canyon as we enter Bridgeport Valley. The Tahoe, Tenaya, and Tioga piedmont glaciers that

occupied the canyons of Buckeye, Robinson, and Green Creeks built two prominent moraines at the south end of Bridgeport Valley.

In Bridgeport, the highway turns west and about 4 miles beyond Bridgeport, the road ascends a valley of another north-trending mountainous area, the Sweetwater Mountains. At Devils Gate, the road crosses the drainage divide of the West Walker and the East Walker Rivers. From here we descend a narrow, flat-floored gorge cut in the granitic rocks of the Sweetwater Mountains. This gorge was probably cut during the Sherwin or Mono Basin glaciations.

At the mouth of the gorge, we enter into Bircham Flat. Turn left (northwest) at Sonora Junction, intersection of California Highway 108 and U.S. Highway 395, and proceed 1.5 miles to Sonora Junction Campground; park in the campground for *Stop 5.4*. Bircham Flat, like Bridgeport Valley, is a small, fault-bounded basin. Here, the Sierra Nevada front is offset some 15 km to the west with respect to that near Bridgeport; however, the style and magnitude of post-Tahoe displacement are equivalent (Clark, 1975). As the route leaves U.S. Highway 395, the terminal moraines of the West Walker River glacier, which extended about 36 km from its source in the Sierra Nevada, are to the right of the road. This was the largest glacier on the east side of the Sierra Nevada. The steep-sided hills west of Sonora Junction are underlain by till deposited by stagnant ice.

Stop 5.4--West Walker River Fault (Lunch Stop)

Scarps of the West Walker River fault can be followed southwest from the Sonora Bridge Campground turnoff. Near the road, scarps are on Tioga morainal debris (fig. 5-7) and are about 7 m high; 3 km farther to the south, scarps on eroded Tahoe till attain heights of 30 m. The most recent surface faulting on the West Walker River fault is Holocene (Hart and others, 1984) and appears to have a minor component of horizontal displacement (Clark, 1975). Clark and others (1984) estimate a late Quaternary slip rate of 0.6 mm/yr for this fault.

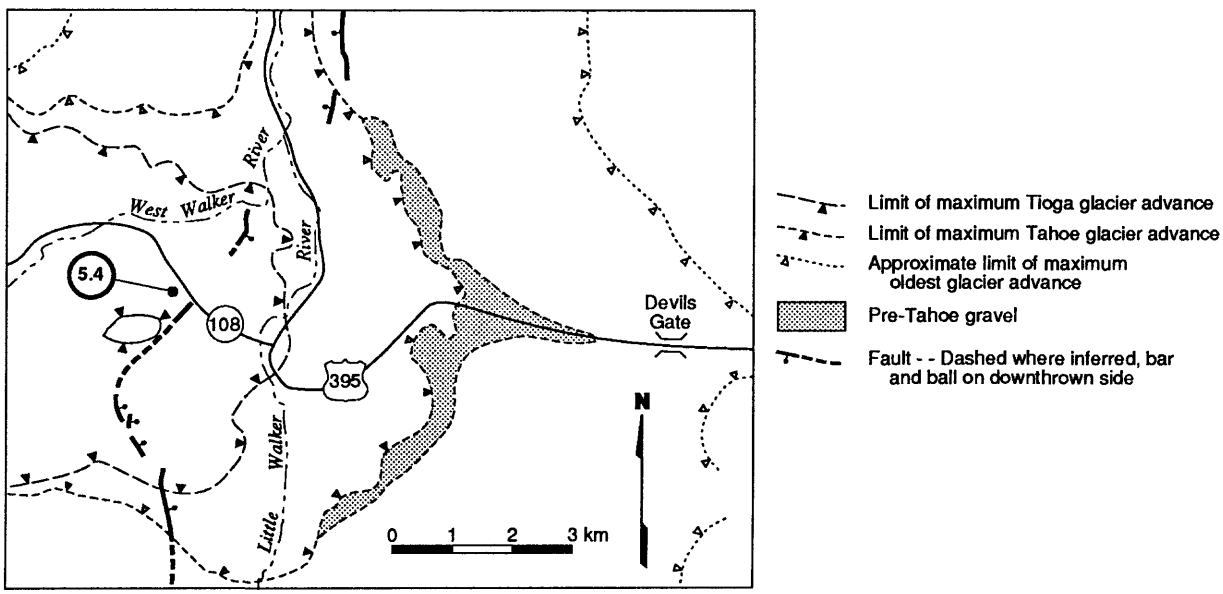

Figure 5-7. Map of scarps of the West Walker River fault, near Sonora Junction (from Clark, 1975).

The Eureka Valley Tuff was erupted about 9 Ma to form a caldera (Noble and others, 1974) that is now the topographic low Bircham Flat. Quaternary displacement on the West Walker River fault is more than 300 m, and like other faults along the Sierra Nevada front, this fault has had recurrent movement from the late Tertiary into the Holocene.

Route Narrative (continued)--Return to U.S. Highway 395 and turn left (north). The West Walker River fault crosses U.S. Highway 395 near the bridge over the West Walker River. To the north, scarps on Tahoe till indicate down-to-the-west displacement (fig. 5-7). At this point, we leave Bircham Flat and enter the deep gorge of the West Walker River, which separates the Sweetwater Mountains to the east from the Sierra Nevada to the west.

Segment 5C--Walker to Carson City (55 Miles)

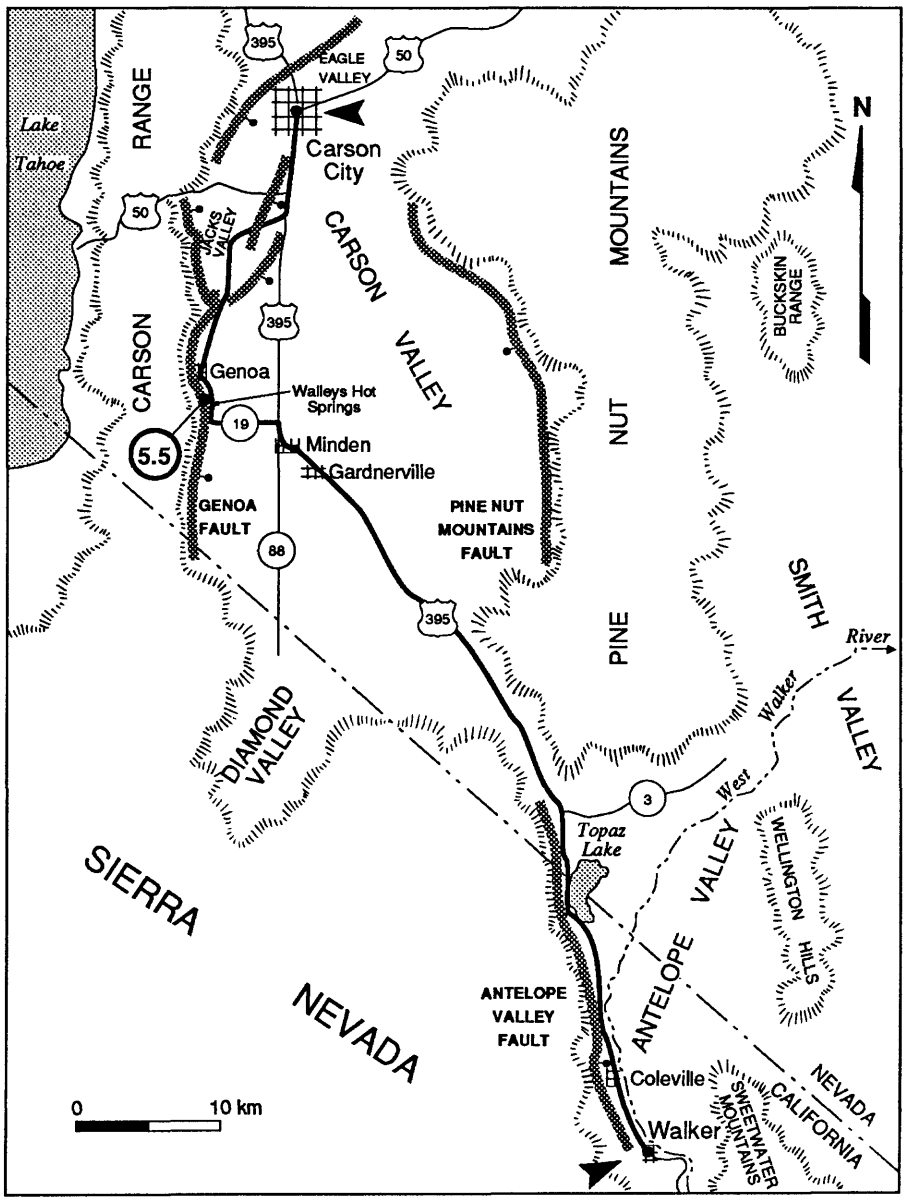

Figure 5-8. Route map for Segment 5C, Walker, California, to Carson City, Nevada.

Route Narrative--As we emerge from the West Walker River gorge, we enter Antelope Valley (fig. 5-8), which is bounded on the west by the Antelope Valley fault. Although the fault has Holocene displacement (Hart and others, 1984), it does not have as much offset as those to the south; post-Sherwin vertical displacement is approximately 80 m (Clark, 1975).

Just beyond the California-Nevada state line, the road turns northwest and crosses the flank of another north-trending mountain range, the Pine Nut Mountains. To the north is the Carson Valley, a graben bounded on the east side by the Pine Nut Mountains fault and on the west by the 50-km-long Genoa fault. The most recent movement on the Pine Nut Mountains fault is late Pleistocene (Bell, 1984a); however, multiple displacements have occurred on the Genoa fault during the Holocene (Bell, 1984b). Scarp heights on the southern end of the Genoa fault where Tioga outwash is displaced 8-12 m suggest a slip rate of about 1 mm/yr (Carson Valley fault in Clark and others, 1984).

At the north end of Minden, bear right at Y intersection and stay on U.S. Highway 395. Turn left 0.7 mile beyond the Y intersection onto Nevada Highway 19 (marked "Kingsbury Grade and Lake Tahoe"). Continue west for 3 miles on Highway 19 and turn right (north) at T intersection onto Foothill Road. *Stop 5.5* is in the gravel pit on the left, 0.5 mile beyond Walley's Hot Springs Resort.

Scarps along the Genoa fault are clearly visible in late afternoon from where the route turns left (west) off of U.S. Highway 395 (north of Minden) and onto Nevada Highway 19. Lawson (1912) briefly visited the area around the turn of the century and his account provides some insight into the age of faulting in this area.

> "The scarps appeared to me to be so fresh and so little degraded that I considered it possible that the displacement which caused them might have occurred within the memory of man. To settle this point I hunted up the oldest inhabitant, whom I found to be Mr. D. R. Hawkins, of Genoa, a very intelligent and well informed gentleman. He told me that he first came to Carson Valley in 1854 and that the scarps were then in apparently the same condition as they are today. The displacement of which they are the evidence occurred, therefore, more than fifty-eight years ago.. . .
> "Another notable feature of the physiography is the abruptness with which the flat floor of Carson Valley abuts upon the base of the steep mountain slope. This is most marked at Walley's Hot Springs. The lowest part of the valley floor is close to the base of the mountain and recalls the way in which Mono Lake hugs the great fault scarp on its west side without any intervening alluvial embankment or beach. The Carson River flows northerly at the base of the mountain and is distributed through an extensive marsh, the waters of which are in places so close to the rocky slope that one may stand upon the latter and throw a stone into them with ease. It is evident from this fact that the relations of mountain and valley are abnormal, and that the abnormality is due to recent depression of the valley floor; since under normal conditions and stability of level, the erosional waste from the mountain front would have long since crowded the stream away from the mountain base, and the lowest part of the valley would be located some miles to the east."

The morphology of the scarps near Walleys Hot Springs, as described in his paper, demonstrate the recency of faulting:

> "Opposite the shallow wide gullies which flute the mountain slope, the alluvium has the arched profile characteristic of steep fans, and where the fault cuts through these the scarp is most effectively displayed as a steep slope (36°) between two flat slopes (3° to 7°). In general the height of the scarp measured vertically is from thirty to forty feet [9-12 m]; but locally its height may be greatly diminished by the accumulation of debris at its base."

South of Walleys Hot Springs, the Genoa fault strikes N. 83° E. following an embayment in the range front; striations on the 68° south-dipping fault plane indicate left-oblique motion (Lawson, 1912). At *Stop 5.5*, we will see that the northwest-striking fault plane has nearly vertical striations on bedrock. Between these two sites, the strike of the fault changes 73°. In his discussion of the consequences of simultaneous fault rupture on these two parts of the fault, Lawson (1912) states:

> "Considering now the faults of both segments E and F [north-striking and east-striking part to the fault respectively] it seems probable from the fact that both scarps are equally fresh and equally little degraded that

the displacement which caused them was simultaneous on both segments. If this be so then one of three things must have happened: either, first, the two blocks of ground moved in a common direction which is determined by the line of intersection of the two fault planes; or, second, if the line of movement were less steeply inclined than this line of intersection the two blocks would be jammed together with the formation of a ridge of crushed rock; or, third, if the line of movement were more steeply inclined, the two blocks would be torn apart and a void would be formed over the hip of the footwall formed by the two intersecting fault planes. On the assumption that the displacement was simultaneous the evidence of the direction of movement indicates that the last of these three possibilities must have been realized. Such a sundering of the two blocks under divergent displacement would doubtless cause a sink hole or depression at the surface due to collapse; but if such a depression exists it is concealed by the marsh."

Gravity data generally confirm Lawson's perceptive speculations; the depth to bedrock in the valley near this intersection is approximately 1,300 m (fig. 5-9); in contrast, depth to bedrock elsewhere along the fault is generally less than 300 m (Maurer, 1985).

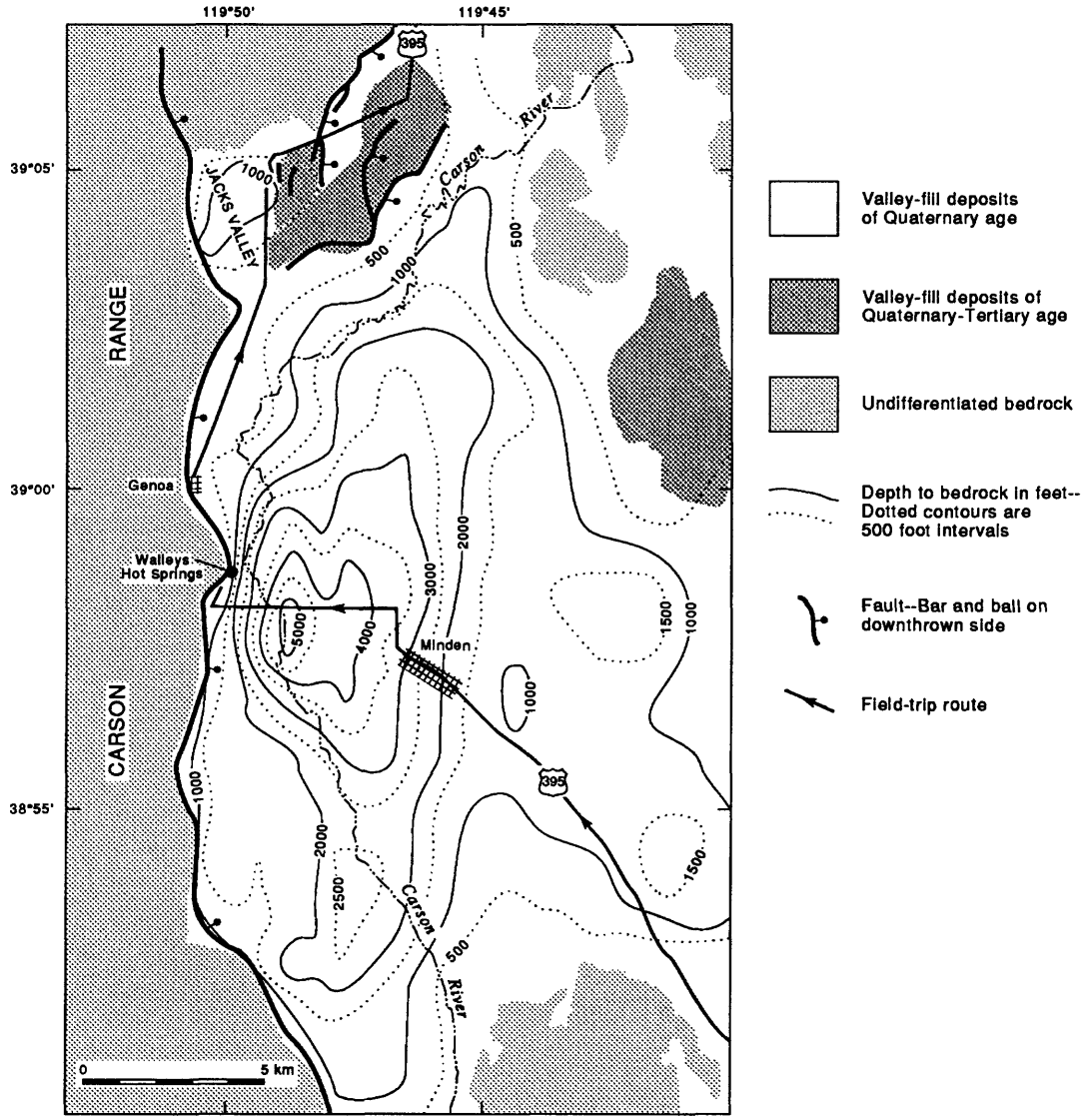

Figure 5-9. Generalized map of Sierra Nevada frontal fault zone, including the Genoa fault, and depth to basement (in feet) in adjacent Carson Valley (modified from Maurer, 1985).

Stop 5.5--Genoa Fault

At the time this field guide was prepared, there were two quarries at this site. The larger of the two quarries is owned by the State of Nevada and is entered from the main road; however, the smaller is owned by a private company and has the best exposures. The only remaining remnant of the faulted gravels is on the north side of the small quarry. These nearly horizontal, bedded, well-sorted gravels are both fractured and faulted. Even though the gravels are clearly horizontal, tilting of the downthrown block is suggested by the position of the Carson River on the extreme west side of the valley (fig. 5-9).

The exposed bedrock fault plane has both striations and small remnants of gouge on its surface. Here, the bedrock is a metavolcanic. The single scarp south of the quarry exemplifies a unique aspect of this fault. With the exception of the northern end of the Genoa fault, movement on this part of the Sierra Nevada frontal fault zone is accommodated along a single strand and only minor, local antithetic faults are present (fig. 5-9).

Route Narrative (continued)--Leave the parking area and turn left (north) on Foothill Road. Proceed north through the town of Genoa, staying on the road to Carson City. As we head north, the route parallels the Genoa fault. The part of the fault behind the town of Genoa is expressed primarily as scarps on bedrock; however, the few scarps formed on alluvium are about the same size and are morphologically similar to those on alluvium to the south. About 3 miles north of Genoa, the Sierra Nevada frontal fault bifurcates. The route passes over the valleyward strand and roughly parallels the rangeward strand (fig. 5-8) and then enters Jacks Valley, a small fault-bounded basin. Large scarps are present on the rangeward strand of the fault at the mouth of the first canyon north of the prominent bend in the range front.

Lawson (1912) speculated that the scarps on the north of the bend were separate and distinct from those south of the bend (possibly meaning two segments). Data from trenching and scarp-morphology studies neither confirm or refute his interpretation but suggest that both parts of the fault have ruptured at least twice in the past 4,000 years (Pease, 1979a, 1979b). Scarps on both parts of the Genoa fault have steep slope angles (>33°) with respect to surface offset (7-13 m) and have bevels indicating multiple movements. The Genoa fault extends north from the edge of Jacks Valley into the bedrock of the Carson Range (Pease, 1980). The primary range-front fault is on the east side of the low hills 3-4 km to the right (east) of the route (fig. 5-9), on the strand of the Sierra Nevada frontal fault zone that we crossed before we entered Jacks Valley.

Jacks Valley is formed by the differential movement of the diverging strands of the range-front fault. Although faulting on the west side of Jacks Valley is along a relatively simple, single surface trace, faulting on the east side of the valley is complex. North-trending scarps extend from the west side of the low hills, which are composed of Quaternary and Tertiary pediment gravels (Pease, 1980), on the right side of the road to near the Carson River (fig. 5-9).

Beyond Jacks Valley Ranch, the route rounds the northern part of the hills and descends a large alluvial fan; at the east side of the hills, the road crosses a 1-m-high scarp. To the north of the road, this scarp is as much as 8 m high. Data from a trench located immediately south of the road (studies by R.C. Pease) suggest that the 1-m-high scarp is the result of one faulting event with a maximum age of 7,140±400 years (Bell, 1984b).

Approximately 5 miles beyond Jacks Valley Ranch, the route intersects U.S. Highway 395. Turn left (north) onto highway and proceed into Carson City. After the route rejoins U.S. Highway 395, we enter Eagle Valley, a structural basin bounded by predominantly down-to-the west faults along the Pine Nut Mountains and echelon strands of the Sierra Nevada frontal fault zone on the west, which trend northeast through Carson City and merge with the Carson lineament north of the city. Holocene fault scarps are present in many locations in Carson City.

Stay on U.S. Highway 395 in Carson City. Note the odometer reading at intersection of U.S. Highways 395 and 50 East, 3.3 miles beyond the intersection of U.S. Highway 395 and 50 West.

Segment 5D--Carson City to Fallon (65 Miles)

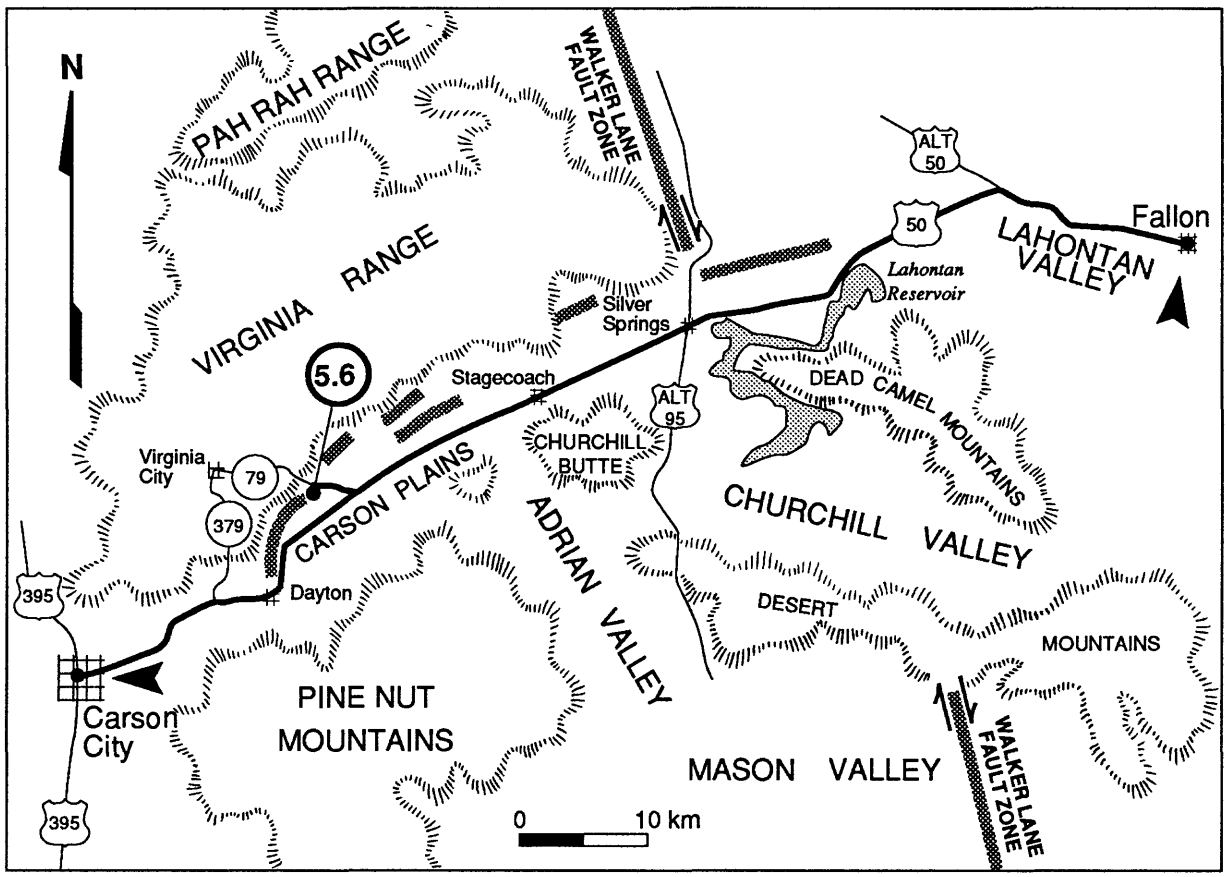

Figure 5-10. Route map for Segment 5D, Carson City to Fallon.

Route Narrative--Turn right (east) on U.S. Highway 50 and proceed through Carson City. This segment of the trip parallels the western part of the 200-km-long Carson lineament (Slemmons and others, 1979). The lineament is primarily expressed as a northeast-trending topographic depression bounded on the north by discontinuous fault scarps that flank the southern edge of the Virginia Range (fig. 5-10). After leaving Dayton, 11 miles east of Carson City, note the scarps at mobile home park on the left of the highway; these scarps are part of the surficial expression of the Carson lineament. The route for the next 10 miles crosses the Carson Plains.

Much of this area was occupied by Lake Lahontan (Russell, 1885) during the late Pleistocene (Morrison, 1964); thus, many pluvial features will be evident along this part of the trip. The lake, which covered a large part of western Nevada (fig. 5-6), had reached an intermediate level in the Lahontan Basin by at least 24 ka. It rose to its highest level by 13,820 years ago, and by 12,070 yr B.P. the lake level had abruptly declined by about 100 m. The timing and general character of its last rise and abrupt decline is very similar to that of Lake

Bonneville on the eastern side of the Great Basin (Thompson and others, 1986). Shoreline features of both lakes provide useful markers and morphometric datums for timing of faulting.

At Mile 16.9 turn left (north) onto Sixmile Canyon Road. Bear left at Y intersection in 1.6 miles (stay on Sixmile Canyon Road). Park on left side of road at Mile 19.2, just beyond fault scarp, for *Stop 5.6*. Walk along scarps south of the road to the south side of creek.

Stop 5.6--Sixmile Canyon Scarps

There is little surface expression of the Carson lineament and no evidence of Holocene displacements (Bell, 1989, oral commun.). This is one of the few locations where scarps of the Carson lineament are on alluvium. The scarp on the high terrace south of the mouth of Sixmile Canyon is 6-7 m high. Although this site has not been rigorously investigated thus far, faulting is thought be pre-Holocene, based on alluvial-fan and soil chronologies (Bell, 1984b). Displacements represented by these scarps are thought to be normal. Even though late Quaternary scarps are present, this area is characterized by low levels of historic seismicity (see fig. 3 in Bell, 1984b).

Entrenchment of the stream issuing from Sixmile Canyon allows an opportunity to observe the degree of soil development on the high terrace. The pre-Lahontan gravels, which make up this terrace, have remained subaerially exposed since they were deposited because this site is above the highstand of Lake Lahontan This soil has a well-developed carbonate-rich B horizon that is at least 1 m thick, the bottom of which extends below the surface of the Holocene flood plain.

Route Narrative (continued)--Return to U.S. Highway 50 and turn left (northeast). Note odometer reading at intersection of Sixmile Canyon Road and U.S. Highway 50. Beyond Stagecoach (fig. 5-9), at Mile 31 the road climbs onto a pre-Lahontan fan; watch for well-developed soils in roadcuts. This fan is displaced by numerous northeast- and east-northeast-trending faults that are older than the Lahontan shorelines (Bell, 1984b). To the south is Churchill Butte, which is composed of Mesozoic metasedimentary and granitic rocks capped by Tertiary andesites and basalts.

Near Silver Springs, the projections of the Carson lineament and Walker Lane fault zone intersect (fig. 5-11). East northeast-trending lineaments and scarps on pre-Lahontan fans around the Virginia Hills align with those we saw at *Stop 5.6*, and are also considered part of the Carson lineament. However, no evidence of northwest-trending Walker Lane faults are apparent in the area around Silver Springs. The inference is that the Carson lineament truncates structures in the Walker Lane; however, a more complex relation may exist (Bell, 1984b).

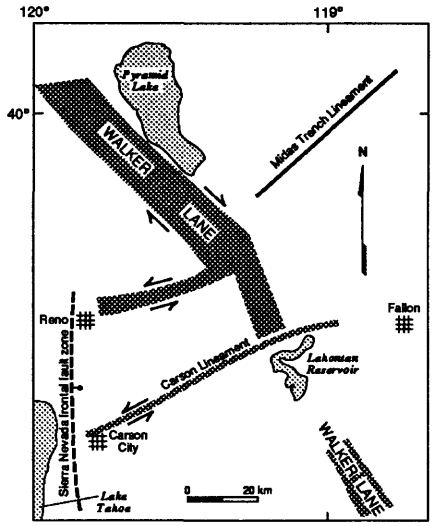

Figure 5-11. Map showing relation of Carson lineament and Walker Lane fault zone and nearby northeast-trending structures (modified from Sanders and Slemmons, 1979).

Lahontan Reservoir and Dam comes into view about 7 miles beyond Silver Springs. The U.S. Bureau of Reclamation built the dam in 1915 to store Carson River water for irrigation. The shorelines of Pleistocene Lake Lahontan are seen beyond the reservoir, on the flanks of the Dead Camel Mountains.

About 2 miles beyond the entrance to Lahontan Dam, the road descends a terrace consisting primarily of Sehoo formation (Morrison, 1964), which records the most recent deep-lake cycle (roughly equivalent to Tioga glaciation and Lake Bonneville deep-lake cycle). Part of this formation can also be seen in the gravel pit to the right (northwest) of the highway. In another 3 miles, the route ascends Swingle Bench, which also is underlain by deep-lake cycle sediments.

Continue northeast on U.S. Highway 50 to intersection with U.S. Alternate Highway 50, turn right (southeast) and proceed 9 miles to Fallon.

DAY 6--FALLON TO WINNEMUCCA, NEVADA

Summary

Today's field-trip route continues through the Great Basin to the eastern California-central Nevada seismic belt, a zone of large historic earthquakes and surface faulting that extends northward from Owens Valley to north-central Nevada. Stops focus on the surface ruptures produced by large earthquakes in 1915 and 1954 and on some of the evidence for prehistoric faulting in the same area.

The Basin and Range

The topography of the Basin and Range province is characterized by alternating linear mountain ranges and intervening basins, which are formed by widespread high-angle normal block faulting. This characteristic structural style was initiated about 10 Ma (late Miocene time), and it overprinted an earlier phase of extensional deformation characterized by highly tilted strata and low-angle normal faults that began at least 30 Ma (Eaton, 1982; Zoback and others, 1981).

In the Great Basin section of the Basin and Range province, ranges are flanked by broad piedmont slopes of coalescing alluvial fans. Many of the high-angle normal faults have been active in Quaternary time, and continuing activity on many of these faults has produced scarps on the alluvial fans near the foot of the ranges. By contrast, to the south, in the Mojave Desert section of the Basin and Range, tectonic activity largely ceased 10 Ma (Eaton, 1979), and the mountains are smaller and with less relief. Broad pediments flank many of the ranges, and the range-bounding faults commonly lie a considerable distance basinward from the topographic foot of the ranges and are buried beneath alluvium.

The Cenozoic evolution of the Basin and Range province, like that of the Coast Ranges and Sierra Nevada of California that were described earlier, is closely linked to the history of plate interactions to the west. During the late Mesozoic, convergence of the Farallon and North American plates about normal to the arc-trench system at the western margin of North America resulted in folding, thrusting, and uplift in the western interior as much as 1500 km east of the trench. The rate of convergence between the plates slowed in middle Paleogene time, and the dip of the subducting slab steepened, resulting in the early phase of extension in the Basin and Range, which was accompanied by voluminous silicic magmatism (Eaton, 1982; Hamilton, 1988; Zoback and others, 1981). About 10 Ma, increased coupling between the North American and Pacific plates led to a 45° clockwise rotation in the least principal stress orientation from WSW-ENE to WNW-ESE. This also marks the beginning of the second, more recent, period of extensional faulting, which produced most of the present topography in the Great Basin (Zoback and others, 1981).

Central Nevada Seismic Belt

A 750-km-long zone of nearly continuous historic surface faulting and diffuse historic seismicity (fig. 6-1) extends from near Ventura, California, to Winnemucca in north-central Nevada (Ryall and others, 1966). The portion of this zone in Nevada, variously referred to as the central Nevada seismic belt (Wallace, 1984a) and the Nevada seismic zone (Doser, 1988), is the most seismically active area in the Basin and Range. Five major historic earthquakes ranging between M_S = 6.9 and 8.0, each of which produced surface faulting (Rogers

and others, 1989), have occurred in the Nevada seismic zone and its extension to the south in eastern California. These major events are the 1872 (Owens Valley), 1915 (Pleasant Valley), 1932 (Cedar Mountain), and 1954 (Dixie Valley and Fairview Peak) earthquakes.

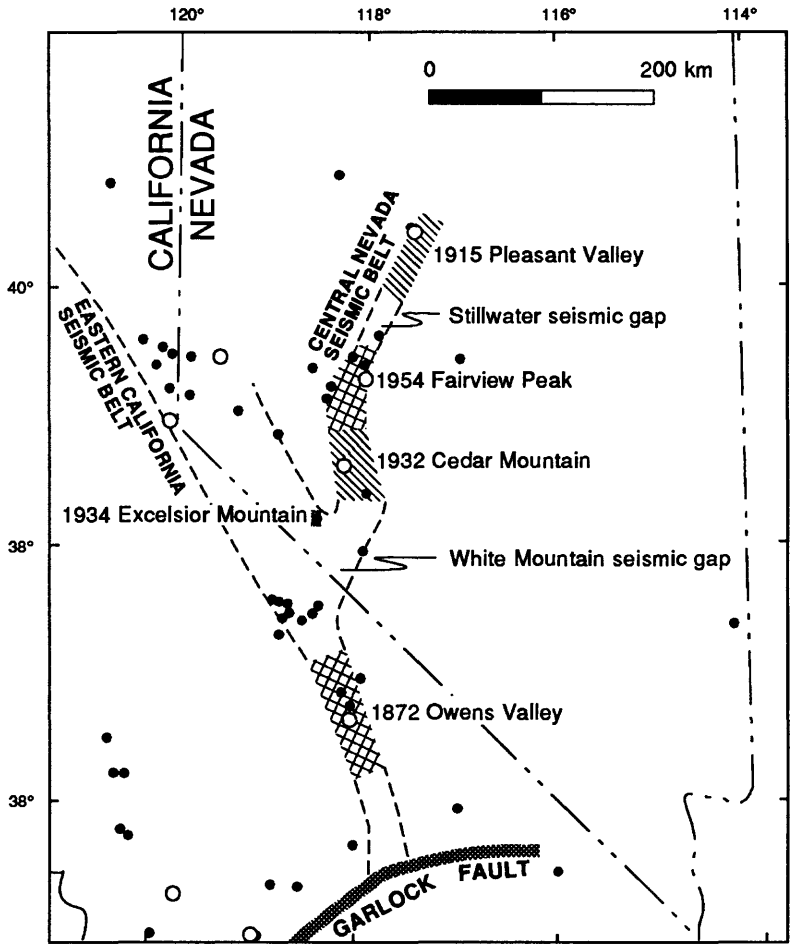

Figure 6-1. Map showing locations of earthquakes having magnitudes of 6.0-7.0 (solid circles) and 7.0 or greater (white circles) in Nevada and adjacent regions for the period 1852-1986 (from Rogers and others, 1989). Rupture zones of historic earthquakes in the central Nevada seismic belt (Wallace, 1984a) are shown by the shaded north-trending zone, dashed lines define parts of the central Nevada and eastern California seismic belts that have not ruptured during historic time.

The relatively frequent occurrence of large historical earthquakes on major zones of surface faulting in the central Nevada seismic belt is not typical of its long-term behavior as reflected by the Holocene geologic record. Wallace (1984a) believes that the youngest comparable prehistoric scarps in the zone are probably thousands of years old, and he notes that the large earthquakes that have occurred in the zone since 1872 appear to represent a temporal cluster of events that was preceded by at least hundreds of years of quiescence prior to 1872. Pearthree and Demsey (1987) estimate that the recurrence interval for large surface-faulting earthquakes in a 30,000 km^2 area in central Nevada, which includes the Nevada seismic zone, has been about 500 years during the past 7,000 years. There are two major gaps in historic surface faulting in the zone: the 40-km-long Stillwater seismic gap in north-central Nevada and the 150-km-long White Mountain seismic gap north of Owens Valley. These may be the locus of future large-scale surface faulting (Wallace, 1978).

Segment 6A--Fallon to Dixie Valley Road (39 miles)

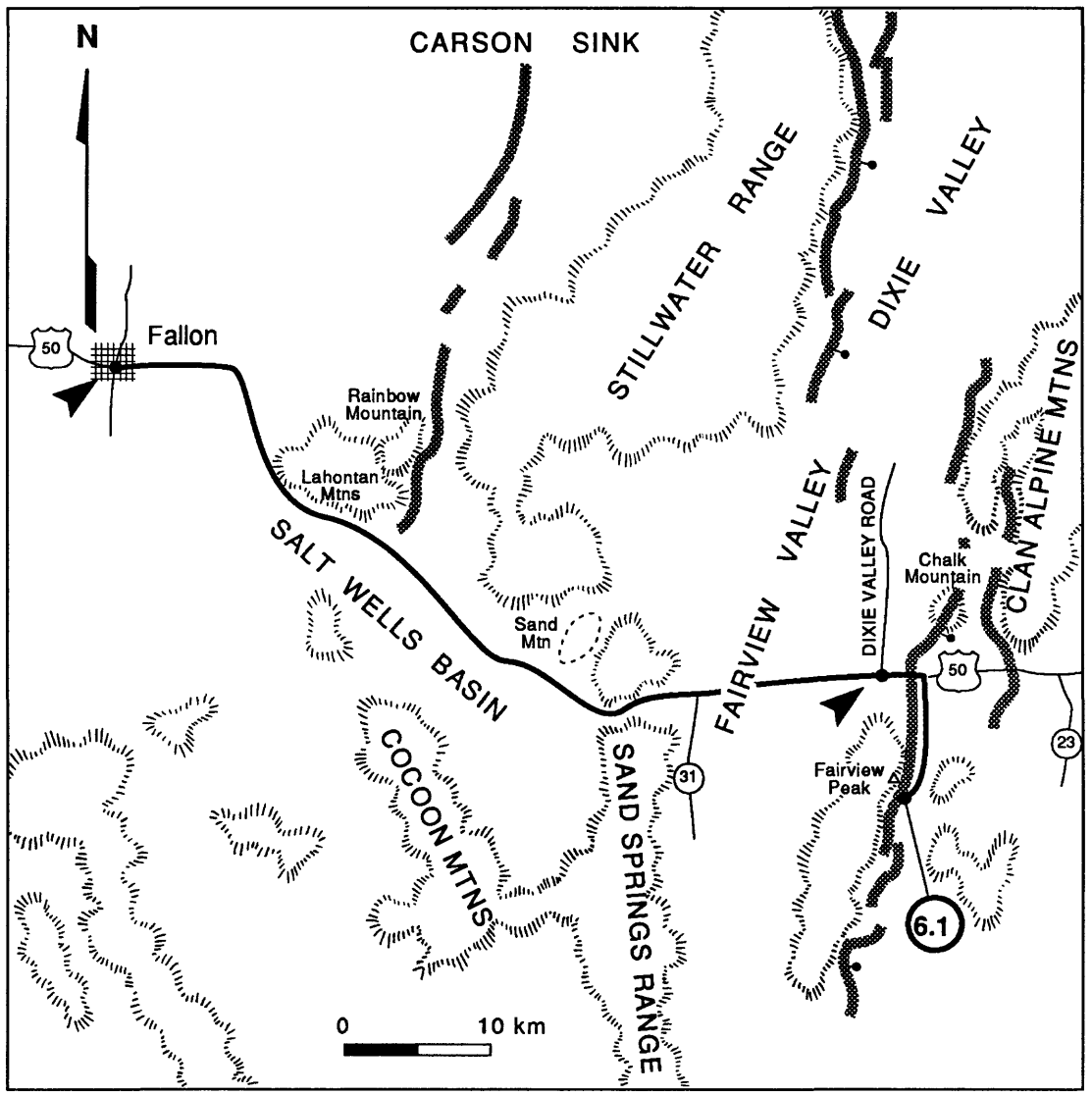

Figure 6-2. Route map for Segment 6A, Fallon to Dixie Valley Road/U.S. Highway 50.

Route Narrative--Leave from the intersection of U.S. Highway 50 and Main Street in Fallon. Note the odometer reading and drive east on U.S. Highway 50. Note: *No gas or services are available along today's field-trip route. Be sure to take plenty of gas and drinking water.*

About 5.5 miles east of Fallon, shorelines of late-Pleistocene Lake Lahontan are conspicuous on the flanks of the Lahontan Mountains at 10-11 o'clock. The highway skirts the southern end of the Lahontan Mountains about 12 miles east of Fallon and crosses the broad mud flats of Salt Wells Basin. At Mile 16, the highway intersects the approximate southern end of the Rainbow Mountain earthquake fault zone, which trends northerly along the eastern base of Rainbow Mountain at about 8 o'clock. The earthquake that produced 15 km of surface ruptures along this zone in July 1954 (event A of fig. 6-3), was the first of a sequence of four surface-faulting events that struck this region in that year. A second earthquake in August 1954 (event B, fig.

6-3) extended the Rainbow Mountain zone of faulting 20 km to the north (Tocher, 1956). The surface ruptures from these earthquakes showed only dip-slip displacement, but focal mechanisms and waveform modeling of seismograms by Doser (1986) indicate that predominantly right-lateral strike-slip displacement was associated with these events. Two additional earthquakes that produced surface faulting during the 1954 sequence occurred to the east in the Dixie Valley-Fairview Peak area and are described in the following section.

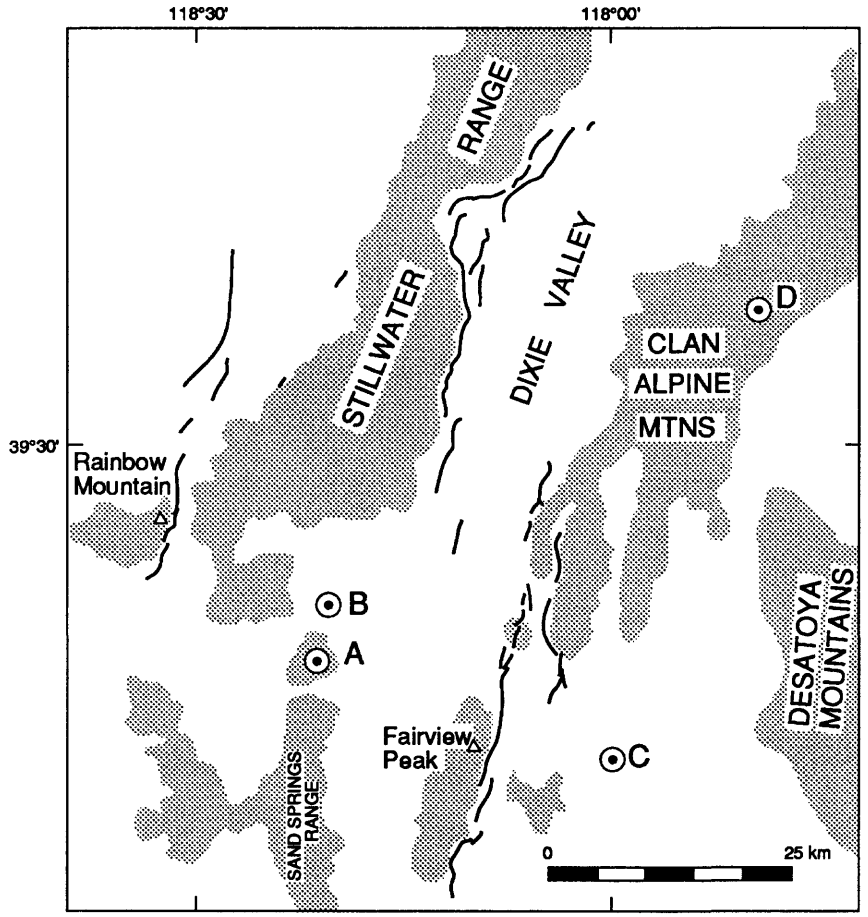

Figure 6-3. Epicenters and surface faulting from the 1954 series of earthquakes in the Rainbow Mountain-Dixie Valley-Fairview Peak region (from Doser, 1986).

At Mile 22.6, there is room to pull off on the side of the highway to photograph Sand Mountain, the large sand-dune complex at 10 o'clock.

Cross the divide in the Sand Springs Range at Mile 29 and descend into Fairview Valley. The Stillwater Range is at 9 o'clock, Dixie Valley is at 10:30 o'clock, and Fairview Peak, with radio towers on top, is at 1 o'clock.

Dixie Valley-Fairview Peak Earthquakes of 1954

Two large earthquakes occurred in this area on December 16, 1954. The first earthquake, M = 7.1, nucleated about 15 km ENE of Fairview Peak at a depth of 15 km. The second earthquake, M = 6.8, occurred 4 minutes later about 60 km NNE of the first shock on the east side of Dixie Valley at a depth of 12 km (Doser, 1986). Extensive surface faulting was associated with both earthquakes; the combined zone of rupture is about 102 km long (dePolo and others, 1989). Measurements of displacements along surface ruptures produced by

the Fairview Peak earthquake (event C, fig. 6-3) showed right-lateral oblique slip, with as much as 3.7 m right-lateral separation and 3.1 m dip separation on surface ruptures near the southern end of the fault zone (Slemmons, 1957). An analysis of geodetic data of the region by Savage and Hastie (1969) indicated that the fault slip associated with the earthquake was 2.9 m right-lateral separation and 2.3 m vertical separation. Doser's (1986) body-wave modeling for the Fairview Peak earthquake gave a focal mechanism of a fault which strikes 355°, dips 60° E., and had a slip vector that raked 20° S. with a right-lateral sense of motion. These three different lines of evidence for the deformation produced by the Fairview Peak earthquake consistently indicate that it was the result of right-lateral oblique slip. Doser's (1986) focal mechanism for the Dixie Valley earthquake (event D, fig. 6-3), by contrast, indicates a normal fault that strikes 350°, dips 50° E., and had a vertical slip vector (90° ±20°).

Route Narrative (continued)--Proceed 10 miles to the east (to Mile 39.1), pass the junction of Dixie Valley Road (to the north) and U.S. Highway 50; to see the 1954 earthquake fault scarps along Fairview Peak we will continue east on U.S. Highway 50 for 1.6 miles. Before the bottom of the grade, turn right (south) on a gravel road marked "Earthquake Faults 6 miles." *This is a good gravel road but is likely to be impassable if the road is wet.*

At 0.7 mile south of U.S. Highway 50, small scarps from the 1954 earthquake are visible at 3 o'clock, several hundred meters west of the road. At Mile 5.0, turn right onto a dirt road that follows a drainage. Take the right fork in the road after 0.3 mile and continue to a parking area in an additional 0.5 mile.

Stop 6.1--Fairview Peak Earthquake Fault Scarps

The parking area is within a few meters of spectacular fault scarps associated with the first of the two large earthquakes that struck this region on December 16, 1954. Walk south from the parking area along the scarp for about 1 km to see a variety of well-expressed fault-scarp features. Most of the scarp in this area is still preserved as a free face. Several hundred meters to the south of the parking area there is a particularly well-defined right-lateral oblique offset of a sharp-crested ridge. Slemmons and Bell (1987) have measured 2.1 m vertical separation and 3.4 m horizontal separation of tree roots at this site.

Route Narrative (continued)--Return, to U.S. Highway 50, turn left and retrace the route west to the Dixie Valley Road junction. Turn right on Dixie Valley Road and drive north.

Segment 6B--U.S. Highway 50 to Northern Dixie Valley (53 miles)

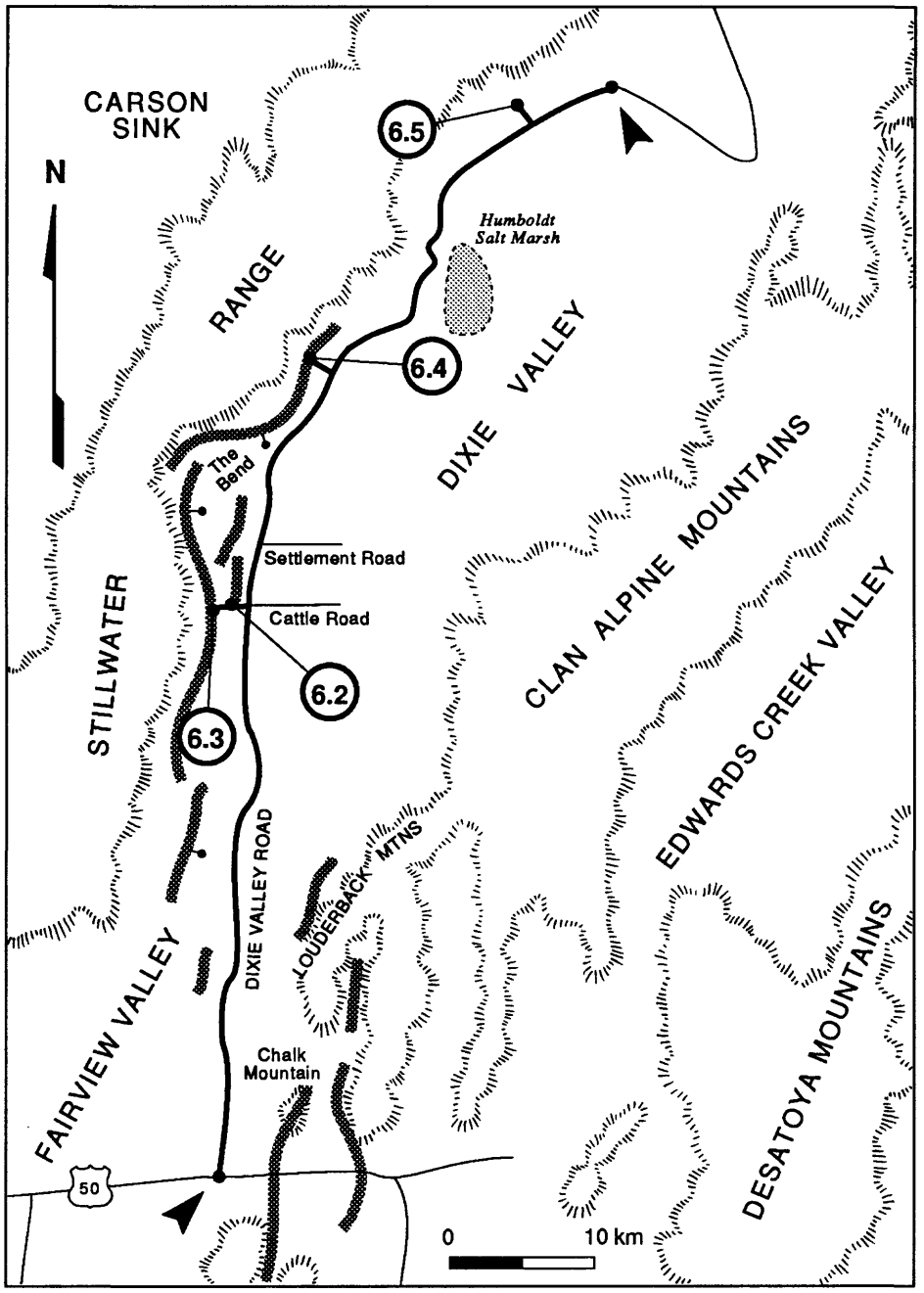

Figure 6-4. Route map for Segment 6B, Dixie Valley Road/U.S. Highway 50 to northern Dixie Valley.

Route Narrative (continued)--The road ahead is paved for about 26 miles, the remainder is gravel. Gas is not available.

Note the odometer reading at the junction. At Mile 2.6, the highway passes the road to Wonder, an abandoned mining town, on the right. As much as 0.6 m of normal dip-slip displacement occurred near

Wonder during the December 1954 earthquakes along a fault that lies primarily in Tertiary(?) bedrock of the range block to the northeast. Historical accounts compiled by Slemmons and others (1959) indicate that as much as 19 km of historical surface faulting had previously occurred on this fault, probably in 1903.

As the road climbs onto a rise at Mile 16, note the fault scarp that appears as a white line in the morning sun along the base of the Stillwater Range to the west, at 10-11 o'clock. (There are good locations for photographs of the scarp in the next several miles.) This is the primary surface rupture for the second large earthquake of December 16, 1954.

Continue north to the junction of Dixie Valley Road and Cattle Road (to right) at Mile 23.7. Turn left off the highway onto a dirt road to west. The dirt road is rough and clearance for passenger cars is marginal. Vehicles with catalytic converters may be a fire hazard during the dry season. If there is any question of a problem with driving the dirt road, the sites to the west can be easily reached on foot. Drive 0.6 mile west to *Stop 6.2* at a trench across a 2.5-m-high fault scarp that crosses the road. The trench is about 50 m north of the road.

Stop 6.2--Piedmont Fault Scarps, Willow Canyon Area

Dixie Valley is an asymmetric graben that has its largest fault displacements on the west side of the valley. The structure beneath the valley fill (fig. 6-5) is more complex than evident from surface geologic relations (Stewart, 1971). Here we will see Bell and Katzer's (1987) trenches which are excavated across a prehistoric piedmont fault scarp about 2.5 m high at their locality 4. Displacement along this fault during the 1954 earthquakes produced a fresh scarp about 30 cm high. Wallace and Whitney (1984) noted that almost all evidence of pre-1954 Holocene faulting is restricted to piedmont scarps several kilometers east of the range front, such as at this site. They also noted that there is virtually no evidence of Holocene or pre-Holocene faulting in alluvium and colluvium along the trace of the main range-front scarp that broke in 1954, suggesting that no faulting had occurred there for at least 10,000 years. Although the piedmont faults are not conspicuous physiographic features, the primary structural relief of the range is the result of displacement on them (Bell and Katzer, 1987) as shown on figure 6-6.

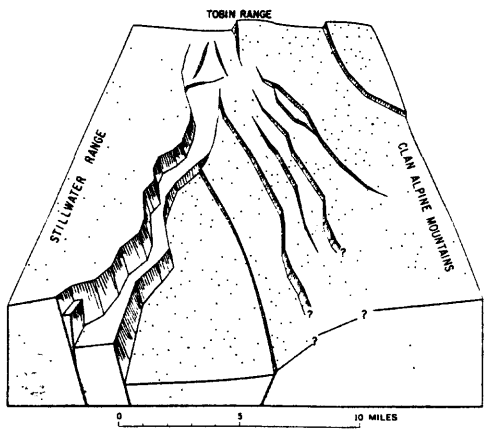

Figure 6-5. Generalized block diagram of the bedrock surface of central and northern Dixie Valley (from Stewart, 1971). Alluvium removed and eroded bedrock restored.

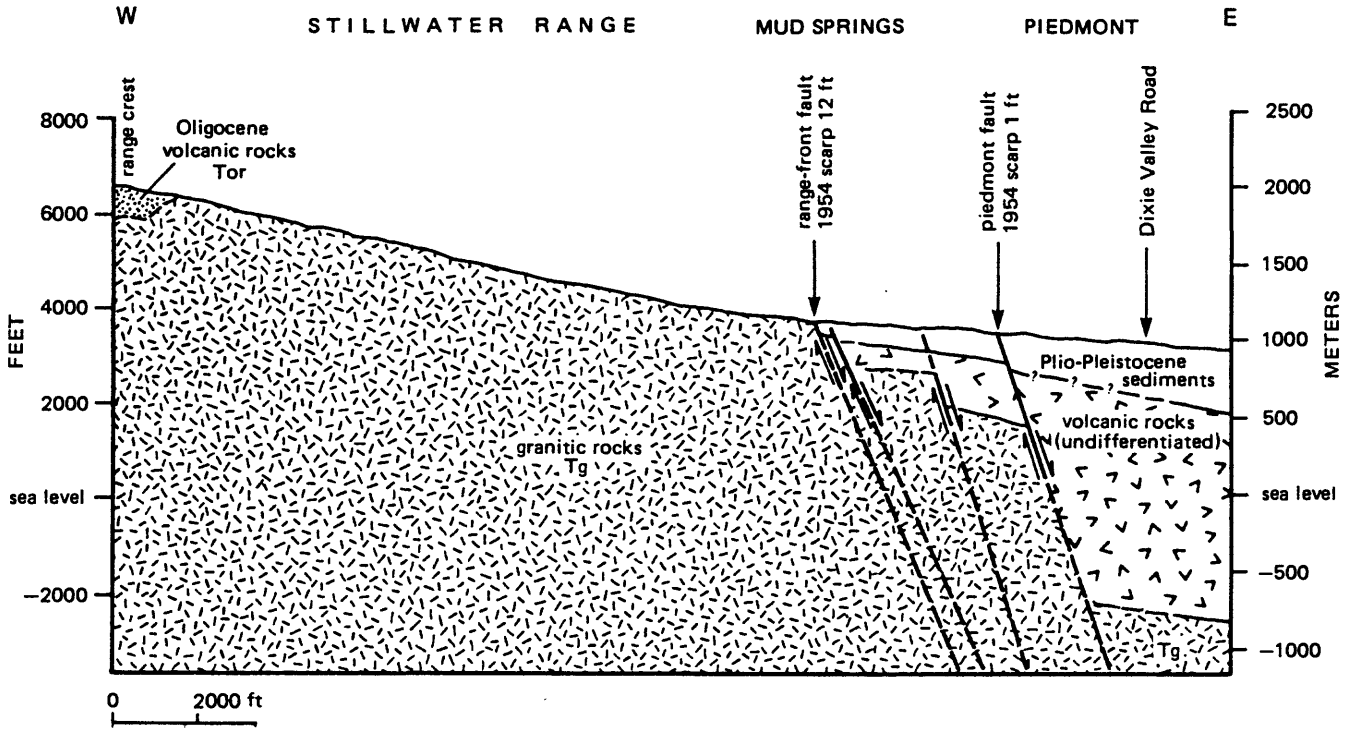

Figure 6-6. Cross section across the Stillwater Range and western part of Dixie Valley in the vicinity of Willow Canyon at *Stops 6.2* and *6.3* (from Bell and Katzer, 1987).

The trench exposes faulted, poorly stratified coarse sand having scattered pebbles, cobbles, and boulders as much as 20 cm in diameter. Clasts in the unit are predominantly granitic and commonly are decomposed (Bell and Katzer, 1987; plate 2). Adjacent to the fault on the east is a wedge of fault scarp colluvium derived from deposits upslope from the fault. The colluvium overlies a 1- to 2-cm-thick bed of eolian silt which Bell and Katzer (1987) interpret as the top of the prefaulting fan surface.

Route Narrative (continued)--Drive 0.7 mile further west on the dirt road to the prominent fault scarp near the foot of the Stillwater Range for *Stop 6.3*.

Stop 6.3--1954 Fault Scarp, Willow Canyon Area, Dixie Valley

The southern end of surface faulting along the base of the Stillwater Range is about 5.5 km south of here. Slemmons (1957) reported scarp heights of about 3.7 m and vertical displacements of about 2.1 m along this part of the range. In general, displacements were everywhere dip slip except for an area on the north side of Coyote Canyon, 2.5 km south of here, where he measured a 2-m component of left-lateral displacement; the vertical component of displacement at that site is about 3 m (Bell and others, 1984).

This stop provides an opportunity to compare the morphology of the fault scarp and the character of the zone of faulting with that at *Stop 6.1* at the Fairview Peak scarp. Note that where the scarp is formed on generally fine-grained alluvium derived from decomposed granitic rock, such as at this site, most of the free face has been lost.

This range-front scarp marks a major discontinuity in the ground-water flow. At IXL Canyon about 3 km north of here (fig. 6-7), the ground-water table is offset 30 m from the mountain block to the alluvium of

the piedmont at the range-front fault. Drill holes on opposite sides of the piedmont fault to the east, such as at *Stop 6.2*, show that the water table is not offset across that fault (Bell and Katzer, 1987).

Zones (1957) reported dramatic changes in the flow of Mud Springs near this site as a result of the 1954 earthquake. Prior to the earthquake, the spring provided enough water to support a small area of grass, shrubs, and a few trees. Surface flow of the spring prior to the earthquake was less than 1 gallon per minute (gpm). In January 1955, a month after the earthquake, surface flow from the spring area was 220 gpm at a temperature of 24°C. The water partially filled a graben 6 m wide and 1.5 m deep (which had formed along the surface rupture associated with the earthquake), overflowed, and flowed down the fan. The flow continued at a high rate until at least June 1955 when it was measured at 180 gpm. By June 1956, the surface flow had decreased to 16 gpm. Bell and Katzer (1987) report that surface flow stopped entirely by the summer of 1956, but had resumed by summer 1984 at a flow of 16-25 gpm.

Route Narrative (continued)--Return to Dixie Valley Road and continue north. Pass Settlement Road on the right, 2.6 miles beyond Cattle Road, at Mile 23.7. Pavement ends about 100 m beyond the intersection; the route is on gravel road for about the next 100 miles.

Gravel pits 0.2 and 0.5 mile north of Settlement Road and 500 m to the west mark the eastern edge of eroded remnants of beach gravel deposited during the last highstand of a late Pleistocene lake in Dixie Valley. Drilling data show the gravel to be at least 18 m thick (Bell and Katzer, 1987). Scattered remnants of this gravel are within about 1 km west of the road for about the next 3 miles. This lake was separated from nearby Lake Lahontan, but the highstands of the two lakes were generally contemporaneous. Radiocarbon dating of samples of calcareous tufa deposited near the highest shoreline of this lake yielded an age of about 11,600 yr B.P. (Thompson and Burke, 1973), which is similar to Thompson and others' (1986) age of >12,070 yr B.P. for the highstand of Lake Lahontan.

For the next several miles, scarps formed by liquefaction during the 1954 earthquakes are within a narrow zone adjacent to both sides of the road. West of the road, tectonic surface faulting associated with the 1954 earthquake broadens into a zone about 4 km wide (fig. 6-7).

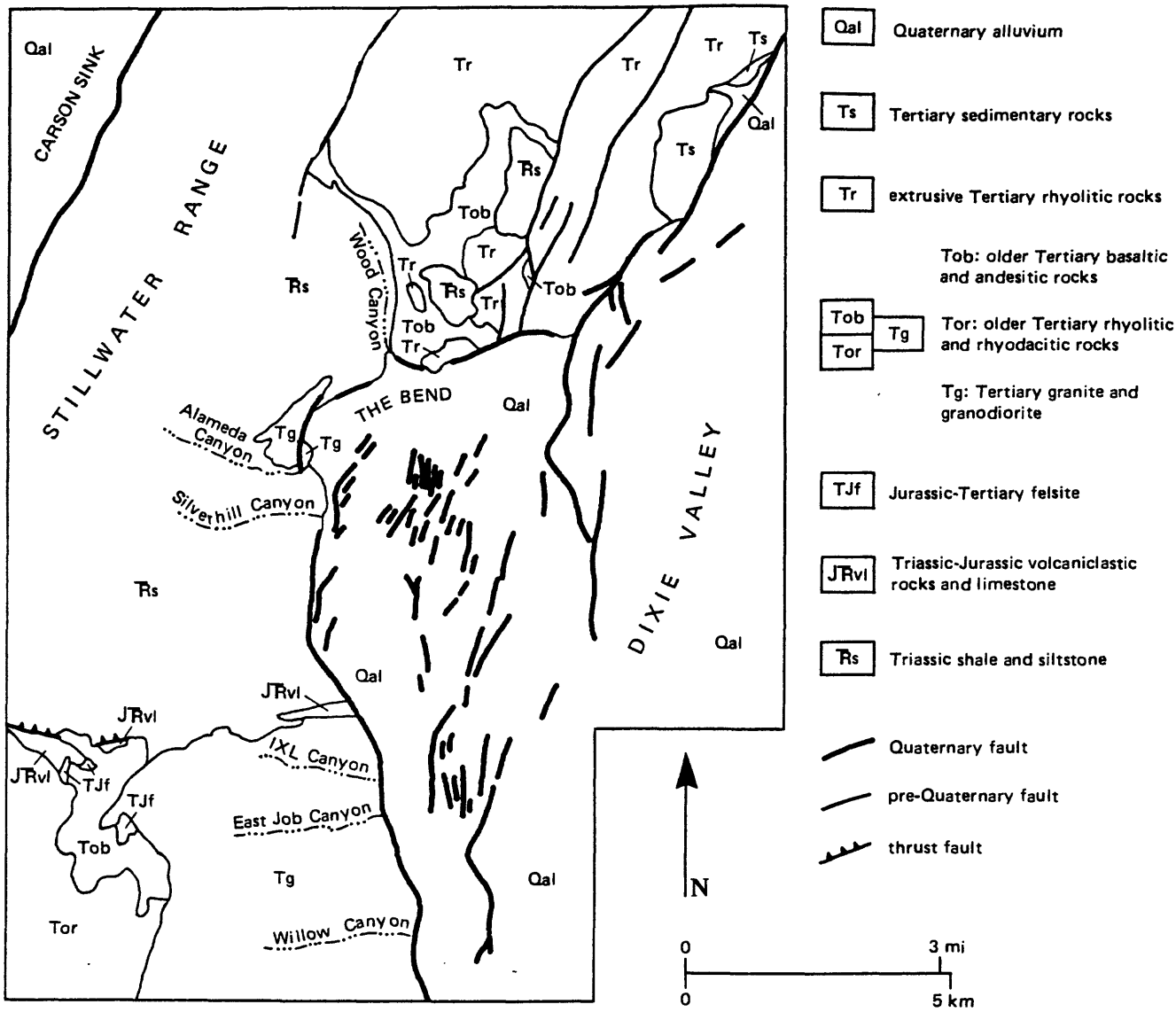

Figure 6-7. Generalized geologic map of the Stillwater Range and central Dixie Valley near The Bend (from Bell and Katzer, 1987).

At Mile 30, at the north end of the area known as The Bend, the highstand shoreline of the late Pleistocene lake in Dixie Valley is visible nearly 1 km west of the road where it is deposited on old alluvial fan gravels at an elevation of 1,086 m. Bell and Katzer (1987) estimated these fan gravels to be several hundred thousand years old.

At Mile 33.5, turn left on a side road to the west toward Cottonwood Canyon, and drive about 1 mile northwest to an east-facing fault scarp at *Stop 6.4*.

Stop 6.4--Faulted Sequence of Terrace Creek, Dixie Valley

Terraces and alluvial units developed along this drainage, informally known as Terrace Creek (Chadwick and others, 1984), provide a record of late Quaternary and Holocene tectonic and geologic events along this part

of the range front. The terraces are truncated on the east by a fault scarp that was reactivated during the 1954 Dixie Valley earthquake.

Figure 6-8 shows the alluvial-geomorphic units mapped at the site by Chadwick and others (1984). The four terraces (T1 to T4) show progressive development of a variety of soil and geomorphic characteristics that indicate significantly different ages for the terraces. Soil development, indicated by the characteristics of the B horizon, increases from cambic B horizons on terrace T1 to argillic B horizons with increasingly redder hues on the older, higher level terraces (T2 to T4). There is also a corresponding increase in the degree of development of soil carbonate on the older terraces. Terrace surfaces (T1 to T4) show a progressive increase in the degree of dissection and in the development of rock varnish and desert pavement on them. Alluvial-fan surfaces F1 and F2 are correlative geomorphic units to terraces T1 and T2.

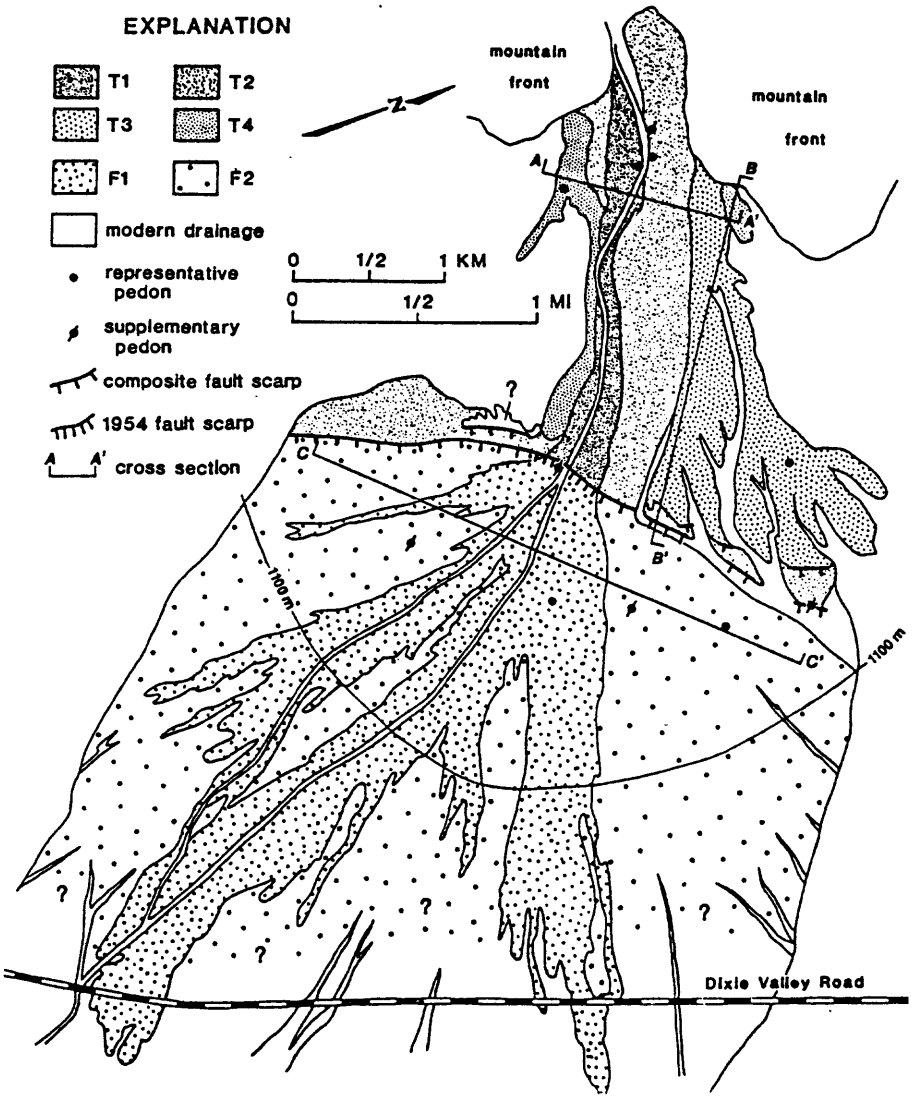

Figure 6-8. Surficial geologic map at *Stop 6.4* (from Chadwick and others, 1984).

Chadwick and others (1984) could not find evidence of the 12 ka shoreline on fans in this part of Dixie Valley. They interpret this as evidence that the fan (F2) was deposited after the lake receded. Based on the

degree of development of soils on the T2 and F2 surfaces, they suggest that these surfaces are early Holocene. Surfaces T2 and F2 are offset 2.0 m at the fault scarp; 0.75 m from 1954 and 1.25 m from one or more events since the early Holocene.

The soil on terrace T3 is substantially better developed than that on terrace T2, indicating that T3 is much older (Chadwick and others, 1984); Hecker (1985) estimates that T3 may be on the order of 100,000 years old. Terrace T4 is a highly dissected remnant of an originally continuous pediment cut on Tertiary sediment. Its age is not well defined; Chadwick and others (1984) only note that it is significantly older than T3.

Route Narrative (continued)--Return to Dixie Valley Road, turn left and continue to the north. In 2.4 miles you will pass the northern limit of surface faulting from the 1954 earthquake. This point marks the southern end of a 40-km-long gap in historic surface faulting (Stillwater seismic gap; Wallace and Whitney, 1984) between scarps formed in 1915 to the north and in 1954 to the south.

At Mile 39, note the prominent Holocene scarp along the base of the range at about 9 o'clock. The scarp continues to the north where it intersects a shoreline of the late Pleistocene lake in Dixie Valley, where Thompson and Burke (1973) inferred 9 m of vertical offset of the 12,000-year-old highstand shoreline. Hecker (1985) infers that this scarp is the result of a single pre-1954 Holocene event that ruptured along this part of the range-front fault, and she estimates the age of the event as 2,600-3,200 years from fault-scarp modeling and sedimentation rates.

At Mile 41.8, at a broad westerly bend in the road, there is a good view of a scarp at the base of a hanging bedrock valley (wineglass valley). At Mile 46.6 note the prominent scarp along the foot of the range. Fonseca (1988) measured about 6.5 m of vertical offset along this scarp which has a maximum slope angle of 37° (fig. 6-9).

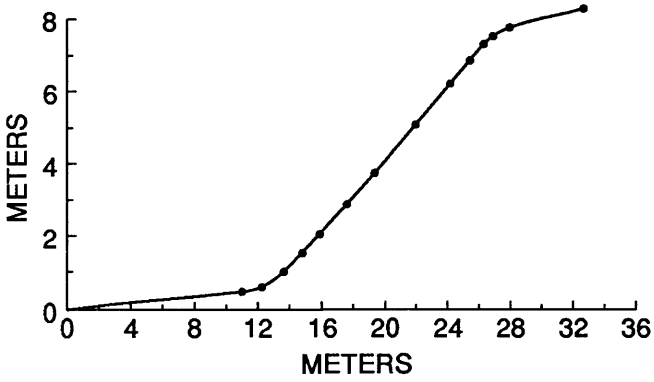

Figure 6-9. Profile of scarp in northern Dixie Valley (from Fonseca, 1988).

At Mile 49.2, at a broad westerly bend in the road, turn left onto a dirt road and drive 1 mile northwest to the foot of the Stillwater Range at *Stop 6.5*. If you drive on this road in the early afternoon, you can see bright reflections from slickensided fault surfaces just to the left of the road and near the base of the bedrock.

Stop 6.5--Bedrock Exposure of Range-Front Fault, Northern Dixie Valley

The surface of a range-front fault along the east side of the Stillwater Range is well exposed at this site. Geologic relations at this site and detailed study of the mineralogy and textures of the slickensided surface material by Power and Tullis (1989) indicate that the surfaces formed at depths of less than 2 km and temperatures less than 270°C. The footwall rocks are metamorphosed Jurassic gabbroic rocks that have been enriched in silica near fracture surfaces by deposition from hydrothermal fluids circulating within the fault zone. The slickensided material, which is 98 percent quartz, is composed of grains .01-1 μm in diameter and contains scattered

particles of iron oxides and kaolinite. Because quartz and kaolinite react to form pyrophylite at temperatures of 270°C, Power and Tullis (1989) infer that the slickensides formed below that temperature.

Route Narrative (continued)--Return to Dixie Valley Road, turn left, and drive to the northeast. As the Dixie Valley Road turns toward the range note the youthful fault scarp at 12 o'clock. Holocene surface offset across the scarp is about 3 m (Fonseca, 1988). Enter the Boyer Ranch area, now the site of a geothermal energy plant, at the end of Segment 6B.

About 10 km north of this point, at the crest of the Stillwater Range, there is a 1.6-km-long west-facing scarp as much as 1.8 m high. It formed in 1915 as a result of the Pleasant Valley earthquake and also moved in 1954, but Wallace (1984b) questions whether the scarp is directly related to tectonic faulting. The scarp is near the eastern edge of the 1-km-high, 30° slope of the east face of the Stillwater Range and may be the result of gravitational spreading of the range. Such structures have been termed "sackungen" (Wallace, 1984b; Zischinsky, 1969) and are generally regarded as aseismic in origin.

Segment 6C--Northern Dixie Valley to Winnemucca (93 miles)

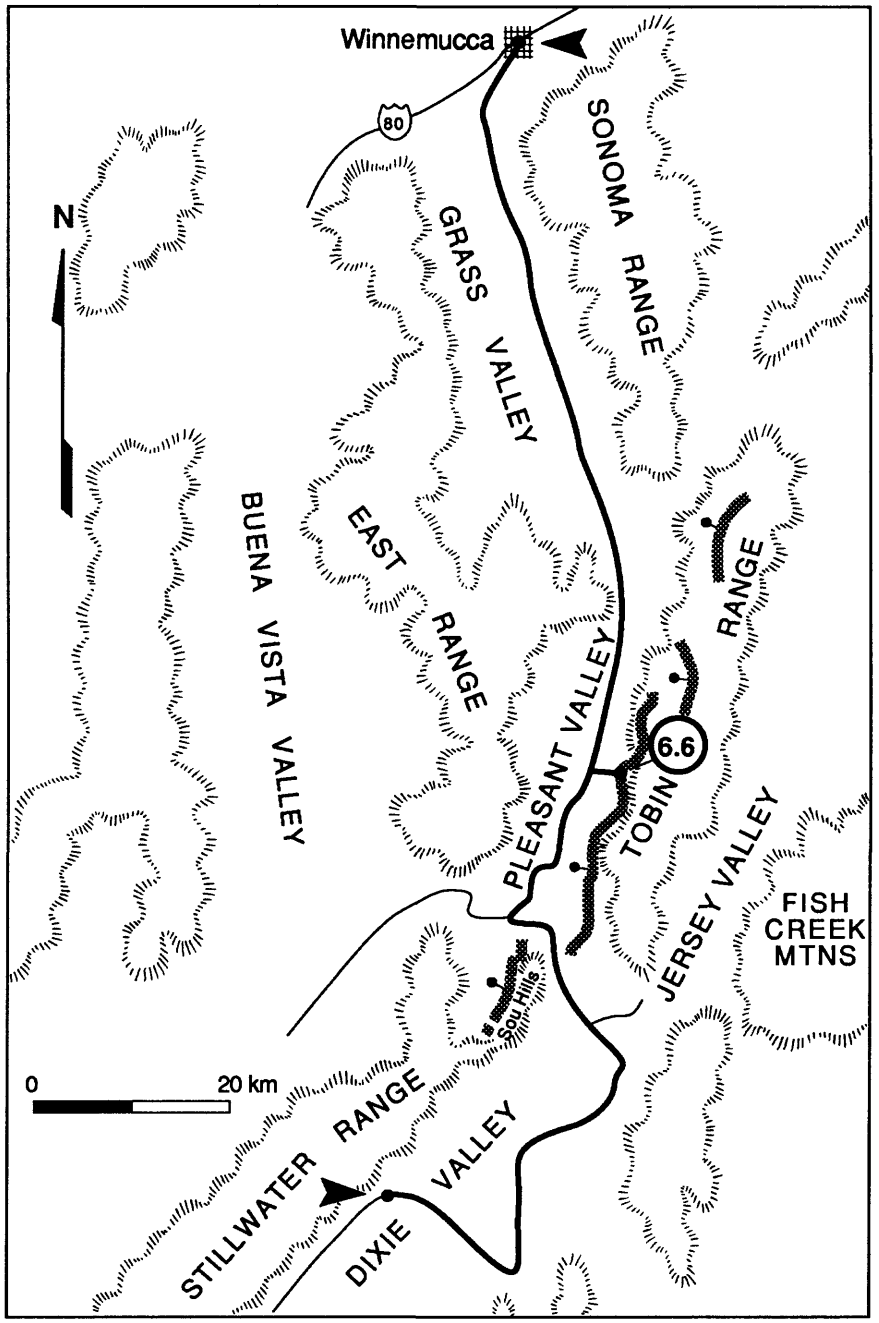

Figure 6-10. Route map for Segment 6C, northern Dixie Valley to Winnemucca.

Sou Hills

From northern Dixie Valley, the route crosses the bedrock divide known as the Sou Hills, which joins the Stillwater Range to the southwest and the Tobin Range to the northeast. The Sou Hills are along a north-

west-trending zone that separates a regional domain of eastward-tilted range blocks on the north from a domain of westward-tilted and horst-like range blocks on the south (Stewart, 1980; Wallace and Whitney, 1984; Thenhaus and Barnhard, 1989). Both the total late Cenozoic displacement on range-bounding faults and relative uplift rates of the Stillwater and Tobin Ranges appear to decrease in the vicinity of the Sou Hills (Fonseca, 1988). These structural characteristics and the age and patterns of historic and prehistoric fault scarps in the area led her to conclude that the Sou Hills has been a barrier to through going propagation of fault ruptures during the late Cenozoic.

1915 Pleasant Valley Earthquake

North of the Sou Hills, the route trends north to Winnemucca along Pleasant Valley on the west side of the Tobin Range and along Grass Valley on the west side of the Sonoma Range. A major earthquake and associated foreshocks and aftershocks in 1915 in Pleasant Valley produced four echelon zones of normal surface faulting (fig. 6-11), named, from south to north, the Sou Hills, Pearce, Tobin, and China Mountain scarps by Wallace (1984b). The ruptures totaled 59 km in length and had an average displacement of 2 m (fig. 6-12) and a maximum displacement of 5.8 m (Wallace, 1984b). Evidence of prehistoric surface faulting commonly is expressed as one or more bevels above the steeper 1915 scarp. Ages for these older scarps are not well determined, but, based on comparison of the scarps to wave-cut cliffs of Lake Lahontan, Wallace (1984b) estimates that at least one large displacement event occurred along the Pearce scarp (fig. 6-11) within the past 12,000 yr B.P.

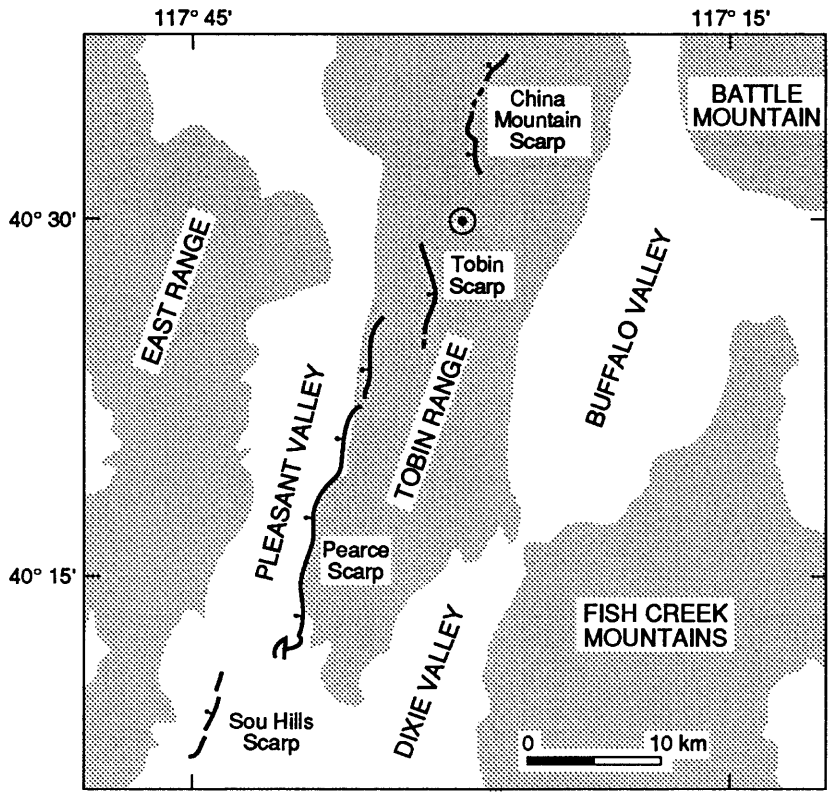

Figure 6-11. Principal zones of surface faulting from the 1915 Pleasant Valley earthquake (from Wallace, 1984b).

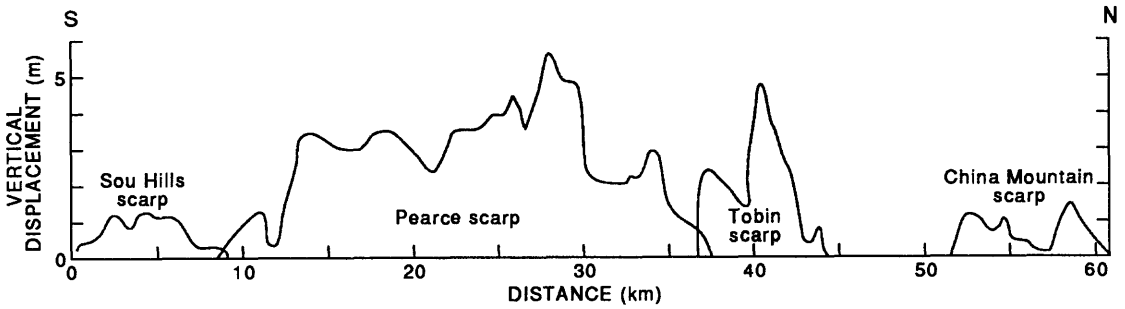

Figure 6-12. Displacement on the four main zones of surface faulting from the 1915 Pleasant Valley earthquake (from Wallace, 1984b).

Route Narrative (continued)--Turn right (east) from the Dixie Valley Road at the geothermal plant (Boyer Ranch) and drive east and north across Dixie Valley to intersect the Jersey Valley Road at the southwest end of the Tobin Range (about 30 miles).

Note the odometer reading at the junction marked Brinkerhoff Seed Farm/Lovelock/Jersey Valley. The hills at 10 o'clock are the Sou Hills. A fault scarp at the western foot of the Sou Hills (Sou Hills scarp) is the most southerly of the four echelon scarps produced by the 1915 Pleasant Valley earthquake. At Mile 4.4, pass the turnoff to the Paris Ranch on the right. At Mile 5.7 the road crosses the northern part of the west-facing Sou Hills scarp, where 1915 vertical displacement is about 40 cm. Continue to the northwest and at Mile 6.6 make a sharp right turn at a Y intersection and drive northeast.

From this point, there is a good view across Pleasant Valley of the prominent scarps along the foot of the Tobin Range at 11 to 1 o'clock. This is the Pierce scarp, the second of the four echelon scarps from the 1915 earthquake. It will be in view to the east for about the next 18 miles and offers a good opportunity to note details of the surface rupture pattern. Note, for example at Mile 16.5, the arcuate pattern of the scarp as it climbs high on the hillside and the shattered zone of colluvium downslope from the scarp.

At Mile 17.6, turn right (east) onto the road to Golconda Canyon and drive 1.2 miles to the fault scarp at the mouth of the canyon at *Stop 6.6*.

Stop 6.6--1915 Pleasant Valley Earthquake Fault Scarp, Golconda Canyon

Walk about 100 m south of the road to an erosion-monitoring network installed by R.E. Wallace in 1979 to determine the rate of degradation of the fault scarp. His observations show that the crest of the scarp retreats as much as 10 cm/yr (R.E. Wallace, 1983, written commun.). The near-vertical scarp at the end of the fence shows virtually no modification, whereas the crest of the scarp 16-30 m to the south has retreated 6 m in 68 years (9 cm/yr).

There is evidence of prior surface-faulting events at many locations along the Pearce scarp. About 500 m north of Golconda Canyon, there is a compound scarp that shows morphologic evidence of at least three surface-faulting events (Wallace, 1984b). There, the 1915 rupture is at the base of the scarp and two bevels (sloping 23° and 18°) on the upper part of the scarp represent older movements. A fence at the same site, which trends N. 60° E., is offset 2 m in a right-lateral sense. Displacement across the scarps is predominantly dip slip, although locally an oblique-slip component has been observed. Wallace (1984b) determined a regional extension direction of N. 60° W. from displacement indicators along the 1915 scarps. Features, such as this fence line, that do not trend parallel to the dip direction, will be laterally offset along their trend, even though the displacement at the site is primarily dip slip.

Route Narrative (continued)--Return to main road, note the odometer reading, and continue north. At Mile 11.5, a northeast-trending prehistoric fault scarp crosses road. The north end of the Tobin scarp, the third

echelon break from the 1915 earthquake is at the base of the Tobin Range at about 3:30 o'clock. The China Mountain scarp, the fourth echelon break, lies at about 2 o'clock at the far end of the Tobin Range.

To the north for about the next 20 miles, prehistoric scarps are intermittently visible east of the road on the piedmont and along the western foot of the Sonoma Range. Wallace (1979) estimated these scarps are about 12,000 years old. At Mile 19.6 the road passes Leach Hot Springs, at the southwest end of a northeast-trending fault scarp.

At the road junction at Mile 37.5, stay on Grass Valley Road and continue into Winnemucca at Mile 45.

DAY 7--WINNEMUCCA, NEVADA, TO SALT LAKE CITY, UTAH

Summary

The final day of the field trip traverses the remainder of the Great Basin, ending at its eastern margin at the Wasatch fault zone, which marks the boundary between the Basin and Range province and the Middle Rocky Mountains and Colorado Plateaus provinces. Most of the route provides a roadside view of the physiography and geography of the region, but two field stops will be made along the Wasatch fault to compare Holocene faulting there with similar features seen earlier in the trip.

Paleozoic Orogenic Belts of Central Nevada

During Paleozoic time, two major tectonic belts developed in Nevada, presumably due to collisions between active island arcs to the west and the passive continental margin to the east (Dickinson, 1981). The route traverses these orogenic belts, both of which are major tectonic elements of the Great Basin. Excellent exposures of the types of folds and thrusts and stratigraphic relations characterizing these periods of deformation are present in the Sonoma Range about 21 km south of Winnemucca, east of the Grass Valley Road (see Segment 6C). These features are described in a field guide by Stahl (1987).

The older of these two belts, which is referred to as the Roberts Mountains allochthon, is a north-trending belt of rocks extending across central Nevada that were deformed during the early Mississippian Antler Orogeny. The belt is composed of eugeosynclinal rocks that were thrust eastward over adjacent cratonic miogeosynclinal rocks, mainly along the Roberts Mountains thrust. The allochthon is bounded on the west by lower Mesozoic rocks and by upper Paleozoic rocks of the younger of the two belts, the Golconda allochthon. Rocks of the Golconda allochthon were emplaced during the Permo-Triassic Sonoma Orogeny along the Golconda thrust (Nilsen and Stewart, 1980; Silberling and Roberts, 1962).

Segment 7A--Winnemucca to Elko, Nevada (125 miles)

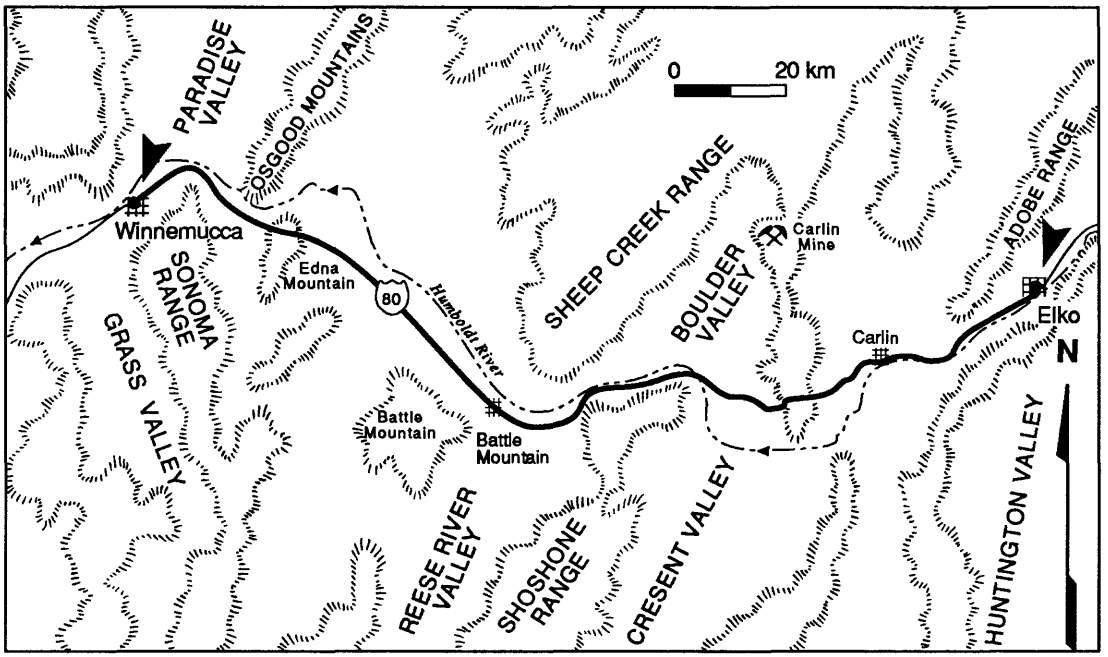

Figure 7-1. Route map for Segment 7A, Winnemucca to Elko, Nevada.

Route Narrative--Note the odometer reading and leave Winnemucca on Interstate Highway 80, eastbound. About 15 miles east of Winnemucca pass Golconda Hot Spring to the left (north). About 4 miles east of the Hot Spring exit, the highway climbs across Cambrian phyllitic shales on the west flank of Edna Mountain. In about 0.5 mile, after a broad bend to the right, the road crosses the trace of the Golconda thrust, along which brown calcareous quartzite of Permian age on the west has been thrust over interbedded black chert and gray limestone of Permo-Pennsylvanian age on the east (Erickson and Marsh, 1974). We pass by a rest area at Golconda Summit 1.2 miles beyond the fault.

Along this segment, the highway generally follows the course of the Humboldt River, which, as the only natural arterial across the Great Basin, was followed by thousands of emigrants moving to the Pacific Coast between 1841 and 1870. At Mile 57, about 2 miles beyond the town of Battle Mountain, note the steep interval at the foot of the Shoshone Range front at 2:30 o'clock. This is part of a series of scarps (fig. 7-2) in northern Reese River Valley (south of I-80) and in Boulder Valley (north of I-80) that Wallace (1979, 1984a) believes are less than about 2,000 years old. Only a part of the range-front fault along the west side of the Shoshone Range broke during this period; Wallace (1984a) believes that the youngest scarps along the southern part of the range are possibly more than 12,000 years old. These type of spatial relations reflect characteristics of late Quaternary faulting seen in many parts of the Great Basin--large surface-faulting events only break a fraction of the total length of a range front, and the interval between events on the same range may be many tens of thousands of years.

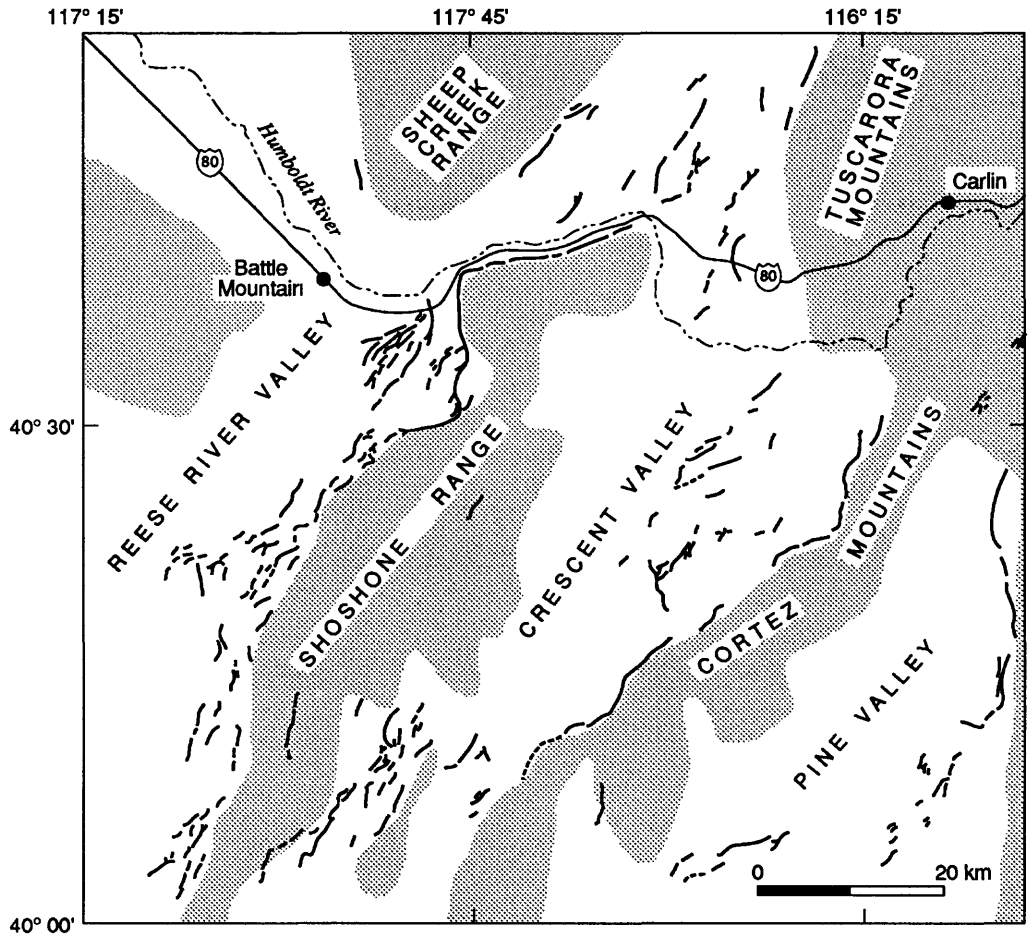

Figure 7-2. Fault scarps in northern Reese River Valley and adjacent areas (from Wallace, 1979).

Temporal Distribution of Late Quaternary Faulting in Central Nevada

Yesterday's field-trip route and today's as far east as about Elko, Nevada, are within a part of the Great Basin that is characterized by a relatively dense pattern of faults of late Quaternary age (fig. 7-3) and includes the belt of historic surface faulting of the central Nevada seismic zone. The recurrence interval for major faulting events on individual faults within much of the Great Basin appears to be thousands of years, and for some faults the interval may be more than 10,000 years (Wallace, 1984a). He points out that surface faulting events have not been uniformly distributed in space or time in the Great Basin, but appear to occur both as clusters in elongate belts (such as the central Nevada seismic zone) or in somewhat equidimensional zones, as well as sporadic events on individual range fronts (such as just noted for the Shoshone Range).

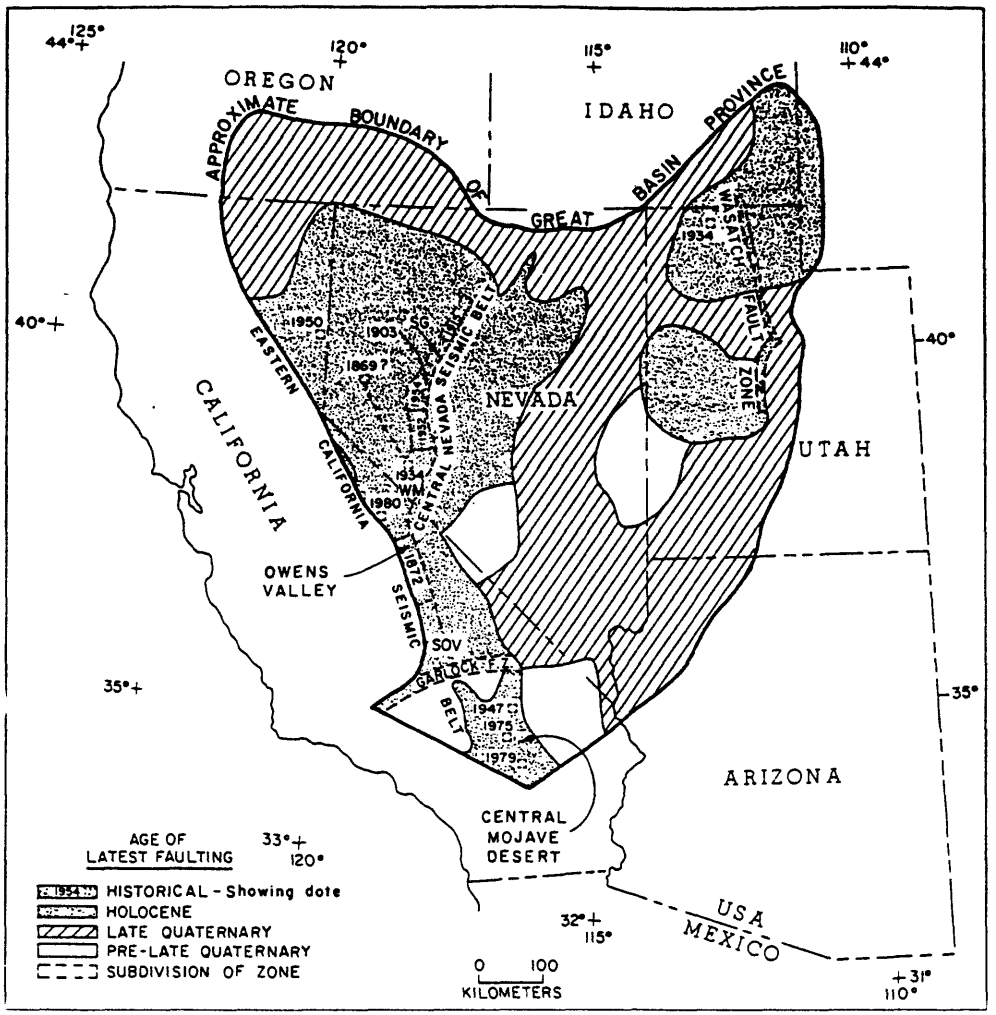

Figure 7-3. Distribution of late Quaternary faulting in the Great Basin (from Wallace, 1984a).

Compilation of mapped fault scarps throughout the Great Basin and assignment of approximate ages to the scarps on the basis of geologic and geomorphic relations provides a means of estimating regional averages for the long-term average frequency of occurrence of large surface-faulting earthquakes. The distribution and ages of fault scarps in the Great Basin indicates that 0.7 to 3.4 $M_s \geq 7$ events occur every 10,000 years in areas of 10,000 km^2. Comparison of the rates of historical seismicity extrapolated to the magnitude range 7-7.7 yields a generally good agreement with rates determined from the regional late Quaternary geologic record. There are large discrepancies, however, when historical seismic activity and the late Quaternary record of activity of individual faults are compared (Bucknam and Algermissen, 1984).

Route Narrative (continued)--At Mile 105, the highway passes Carlin, well-known for the gold deposit being mined about 35 km northwest of the town. The Carlin district contains one of the largest known hydrothermal disseminated-replacement gold deposits in North America. From the beginning of production in 1965, through 1976, the mine produced about 2 million troy ounces of gold. Distinctive associations of gold-pyrite-silica with extremely fine-grained ore minerals have come to be generally known as "Carlin-type" deposits (Radtke, 1985). Continue east for 17 miles to Elko, Nevada.

Segment 7B--Elko, Nevada, to Salt Lake City, Utah (227 miles)

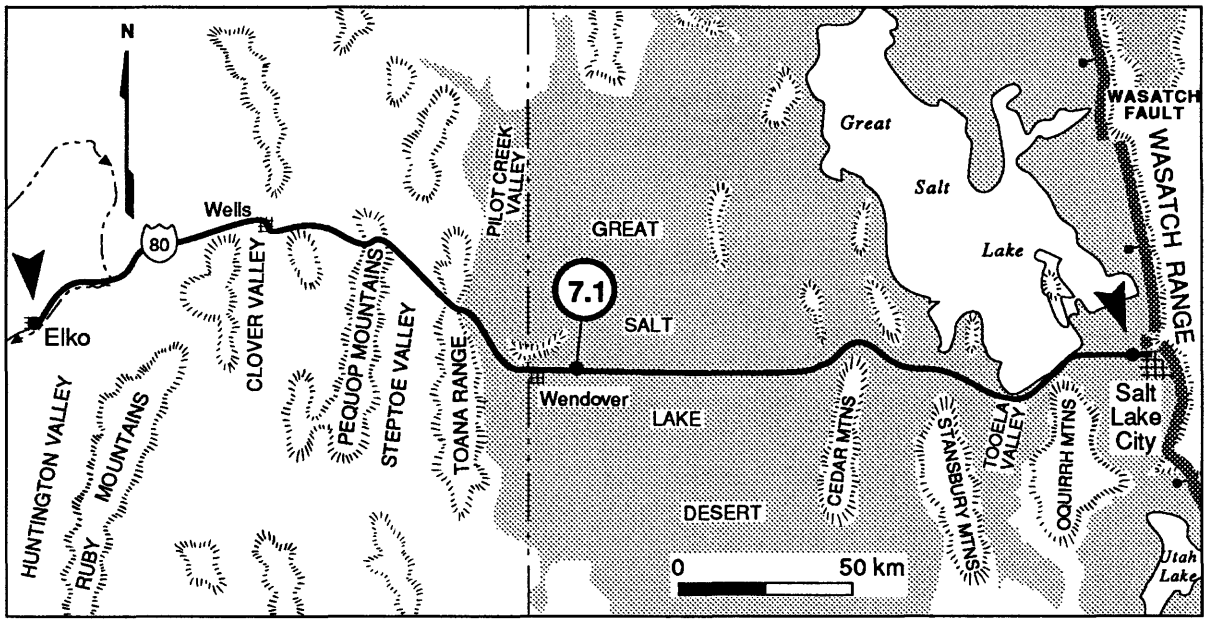

Figure 7-4. Route map for Segment 7B, Elko, Nevada, to Salt Lake City, Utah. Shaded area shows area covered at highstand of late Pleistocene Lake Bonneville.

Route Narrative--Note the odometer reading at Elko, and continue east from Elko on Interstate 80, through Wells, Nevada (51 miles), and over Silver Zone Pass (91 miles). From the pass the road drops down into Pilot Creek Valley, which is at the approximate western limit of late Pleistocene Lake Bonneville, the eastern Great Basin equivalent of Lake Lahontan. Well-expressed shorelines, formed between the Bonneville and Provo levels of Lake Bonneville, are visible less than a kilometer from the highway at 3 o'clock. At Mile 105, as the road climbs up the grade, note the etched shorelines on the hillside at 10 o'clock. Small alluvial fans have been deposited locally over shore platforms; their volume gives a good idea of the rates of erosion and deposition in the 14,000 years since the shorelines were abandoned.

Lake Bonneville

Lake Bonneville was the most recent and largest of a series of lakes that intermittently covered parts of northwest Utah in middle and late Pleistocene time. Lake Bonneville reached its highest level (1,380 m in Pilot Creek Valley) about 16,000 yr B.P. and formed the Bonneville shoreline during the next 1,500 years (Scott and others, 1983). Catastrophic downcutting at the lake's outlet in Idaho caused a sudden drop in lake level of about 100 m, where it stabilized to form the Provo shoreline. The lake remained at this level for about 300 years, cutting a locally conspicuous shoreline (Currey and Burr, 1988), and then dropped below the level of its outlet. By 11,000 yr B.P. the lake was near the present level (Scott and others, 1983). It briefly rose to a maximum depth of 40 m at the Gilbert shoreline about 10,500 yr B.P. and shortly after dropped again to near its present level by 10,300 yr B.P. (Currey and others, 1983). Subsequent Holocene fluctuations of lake level have been below the level of the Gilbert shoreline.

The lake's prominent, well-preserved shorelines provide a reference frame for measuring subsequent crustal deformation. As much as 60 m of isostatic rebound has been measured in the central part of the lake basin where the lake had been more than 300 m deep when it stood at the Bonneville shoreline (Gilbert, 1890;

Crittenden, 1963; Currey and others, 1983). Great Salt Lake to the east is the Holocene saline remnant of Lake Bonneville.

Scarp Morphology Calibration

The morphology of fault scarps provides a useful means of estimating the ages of scarps over wide regions of the Great Basin and consequently the ages of the events that produced them. There are a number of quantitative methods to estimate the age of fault scarps, from the empirical method of Bucknam and Anderson (1979) to a variety of diffusion-equation models of slope transport (Nash, 1980; Colman and Watson, 1983; Hanks and others, 1984; Hanks and Andrews, 1989). To derive a quantitative estimate of the age of a scarp, all of these methods require some sort of calibration against scarps of known age (Machette, 1989). So far, the primary calibration has been against morphologic data derived from profiles of lacustrine shoreline scarps where they are cut on poorly consolidated upper Pleistocene alluvial-fan gravels. Scarps of the Bonneville shoreline, well displayed in several locations along the field-trip route, form a well-defined curve on scarp-height--slope-angle plots (fig. 7-5*B*). Similar data collected from the approximately 2,000-year-old fault scarp along the eastern foot of the Fish Springs Range 100 km to the south of *Stop 7.1* provide additional control for late Holocene morphologic data (Bucknam, Crone, and Machette, unpub. data, 1989).

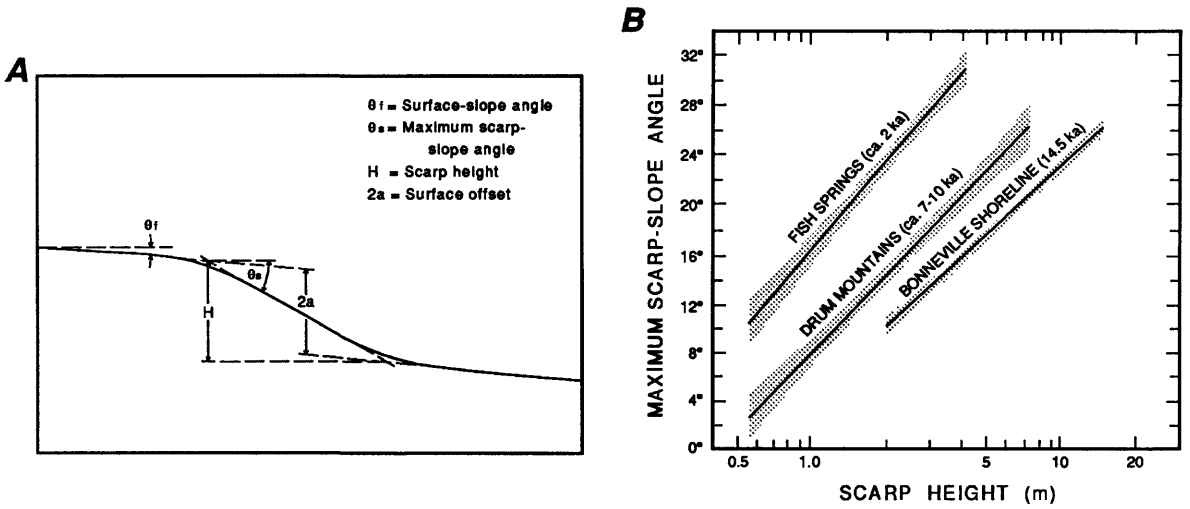

Figure 7-5. ***A***, Profile of a scarp showing definition of terms and measurements (from Machette, 1989). ***B***, Scarp measurements derived from profiles across the Lake Bonneville shoreline scarp and Drum Mountains fault scarp (data from Bucknam and Anderson, 1979) and the Fish Springs Range fault scarp in west central Utah (Bucknam, Crone, and Machette, unpub. data, 1989).

Route Narrative (continued)--Enter Wendover at Mile 110 and cross into Utah. Continue east on Interstate 80. Danger Cave State Historical Monument, on the left several miles east of Wendover, has been an important site in studies of the chronology of Lake Bonneville. Archaeological and radiocarbon age studies at the cave show that the lake has not risen above the 1,314-m level in the past 11,500 years (Jennings, 1957). For comparison, historic fluctuations of the Great Salt Lake have been between 1278 and 1284 m. About 9 miles east of Wendover, exit right to *Stop 7.1* at Rest Area for an overlook of the Bonneville Salt Flats.

Stop 7.1--Bonneville Salt Flats

An observation tower here provides an overlook of the Bonneville Salt Flats which lie at the western side of the Great Salt Lake Desert. The flats are a drainage sump for much of the surrounding desert basin and

represent the residue from the complete desiccation of the western part of Lake Bonneville. The location of the salt flats at the western edge of the Great Salt Lake Desert has been explained as resulting from cycles of solution and deposition of a westward tilting salt pan originally deposited near the center of the desert. The surface of the desert was upwarped and tilted by isostatic compensation following desiccation of the western part of Lake Bonneville (Gilbert, 1890; Eardley, 1962; Bingham, 1980).

The salt crust is as much as 1.2 m thick and is typically underlain by a layer of calcium sulfate (gypsum?) about 0.6 m or less thick. A few meters of soft, silty, plastic clay with interlayered sand and gravel beds underlies the sulfate layer. South of Interstate 80, the salt crust is overlain by up to 40 cm of loose gypsum-rich Holocene sand (Bingham, 1980). A high-speed racetrack on the north side of the interstate has been used for numerous attempts to set land speed records.

Route Narrative (continued)--Note the odometer reading and return to I-80 eastbound. At Mile 37 the highway climbs above the salt flats to cross around the north end of the Cedar Mountains ahead. At about Mile 52, at the north end of the Cedar Mountains, the south end of the Great Salt Lake is visible about 40 km to the east.

Great Salt Lake

Great Salt Lake, which has a maximum depth of only about 10 m, lies near the bottom of the closed basin formerly occupied by Lake Bonneville. About two-thirds of the inflow to the lake is from the surface flow of three major rivers, the Bear, Weber, and Jordan (Arnow, 1980). Nearly all of the remaining inflow is from precipitation, which averages about 385 mm/yr at Salt Lake City International Airport (National Oceanic and Atmospheric Administration, 1982). Inflow of water to the lake is very closely balanced by outflow, which is almost entirely by evaporation. Historical fluctuations in the level of Great Salt Lake have ranged over about 6 m and are closely linked to major variations in regional precipitation (Currey and others, 1984). Beginning in 1982, 5 years of above-normal precipitation in northern Utah led to a 3.4-m rise in the level of the lake, causing millions of dollars of damage as a result of flooding along the shore of the lake (Mabey, 1987).

The concentration of dissolved solids in the lake is strongly influenced by lake elevation and thus lake volume. The lake contains about 28 weight percent dissolved solids at an water surface elevation of 1279 m, making it one of the most saline lakes in the world (Sturm, 1980). Ocean water, by comparison, contains 3.5 weight percent dissolved solids. Salts, primarily sodium chloride, but including magnesium and potassium are commercially extracted from the lake water by evaporation in enclosed ponds, some of which are adjacent to Interstate 80 between Wendover and Salt Lake City. Brines derived from the salt crust and underlying calcareous sediments of the Bonneville Salt Flats are also utilized. The salts are marketed primarily for industrial use (Bingham, 1980).

Route Narrative (continued)--Pass the north end of the Stansbury Mountains at Mile 68 and enter the north end of Tooele Valley. The highway skirts the south side of the Great Salt Lake in Tooele Valley. The levels of both the highway and adjacent railroad were raised several meters during the wet years of 1982-1987 to prevent inundation by the rising level of Great Salt Lake.

Stockton Bar, a 3-km-long late Pleistocene lake bar is at the head of Tooele Valley to the right (south). The massive bar, which locally is more than 300 m wide at the crest, formed a barrier in a Lake Bonneville strait between Tooele Valley and Rush Valley to the south. Many important details of the history of Lake Bonneville are recorded in the deposits of the bar (Burr and Currey, 1988).

The range immediately ahead is the Oquirrh Mountains. Kennecott's open-pit copper mine at Bingham Canyon is located on the east side of the range. A zone of prominent 3- to 11-m-high fault scarps lies at the foot of the northern end of the range, but locally trend away from the range front and into Tooele Valley to the

south. Scarp morphology data and crosscutting relations with the Provo shoreline of Lake Bonneville indicate an age of between 9 and 13.5 ka for the scarps (Barnhard, 1988).

Cross the north end of the Oquirrh Mountains at Mile 93, pass the smelter at Magna, and continue east toward the Wasatch Range. Although the most conspicuous surface faulting in this area lies along the foot of the range, Holocene scarps with as much as 7 m of vertical displacement (down to the east) are present in the valley floor about 10 km west of the Wasatch fault (Keaton and others, 1987). Continue east, pass the south side of Salt Lake City International Airport, and prepare to merge with Interstate Highway 215 northbound for Segment 7C.

Wasatch Fault Zone

The Wasatch fault zone is a major intraplate normal fault marking the boundary between three structural and physiographic provinces: the Basin and Range on the west and the Middle Rocky Mountains and Colorado Plateaus on the east. The fault zone also lies within the Intermountain Seismic Belt, a zone of diffuse seismicity that also generally follows the boundary between the Basin and Range and the Middle Rocky Mountains-Colorado Plateaus provinces. The provincial boundary has been a zone of weakness since Precambrian time and may have formed first as a rift associated with a late Proterozoic passive margin (Stewart, 1972). It generally follows the zone of east-vergent Cretaceous thrusting and folding of the Sevier orogenic belt (Heller and others, 1986; Zoback, 1987). Smith and Bruhn (1984) noted that several parts of the fault are located above Sevier thrust fault ramps, and they interpreted seismic-reflection profiles as indicating that the fault may be listric, flattening at depth and merging with a reactivated thrust fault. Zoback (1987) suggested that the location of the thrust ramps may be controlled by normal-fault zones associated with Precambrian rifting.

The Wasatch fault zone is a prominent physiographic feature with as much as 2 km of local topographic relief from the crest of the Wasatch Mountains on the east to the coalescing alluvial fan apron at the base of the range on the west. Steep triangular facets characterize the lower part of the erosionally modified bedrock scarp along the mountain front, especially at their type locality near Spanish Fork, Utah (Davis, 1903). Late Quaternary displacement along the fault has produced prominent west-facing scarps as much as 60 m high on the middle Pleistocene alluvial fans at the base of the range. Alluvial surfaces are tilted back toward the fault over zones nearly 400 m wide, and grabens formed by antithetic faulting are common along the fault.

The fault trends nearly north-south for approximately 340 km in north-central Utah and is divided into at least 10 segments (fig. 7-6) ranging between 11 km and 70 km in length (Machette and others, 1989), which appear to control the locations of discontinuous late Pleistocene and Holocene surface faulting. Gravity data indicate that the thickness of low-density sediments in valleys along the Wasatch fault is commonly more than 1,000 m and locally more than 3,000 m (Mabey, 1987). Where exposed at the surface, the fault plane on bedrock dips 45°-70° to the west but typically 70°-90° in alluvium. Despite a vigorous program of research, the dip of the fault in the subsurface has not been clearly defined. Although seismic-reflection data indicate the presence of low-angle and listric faults in the subsurface, seismological data from small to moderate earthquakes within the Intermountain Seismic Belt in central Utah indicate that seismic slip is associated with faults with dips greater than 30°; the mean dip is 57° (Arabasz and Julander, 1986).

Although the Wasatch fault is within the Intermountain Seismic Belt and it displays abundant evidence of Holocene surface faulting, there has not been a major earthquake along the fault since the region was settled in 1847; precise epicentral locations (fig. 7-7) and historical data suggest the fault between Brigham City and Nephi has been virtually aseismic since at least 1955 (Arabasz and others, 1980). Nearly the entire fault is marked by prominent late Pleistocene and Holocene fault scarps on alluvium having typically 2 m or more of offset, thus providing a clear and comprehensive record of paleoseismicity. Such scarps have been associated with historical earthquakes of magnitude greater than 7 elsewhere in the Great Basin.

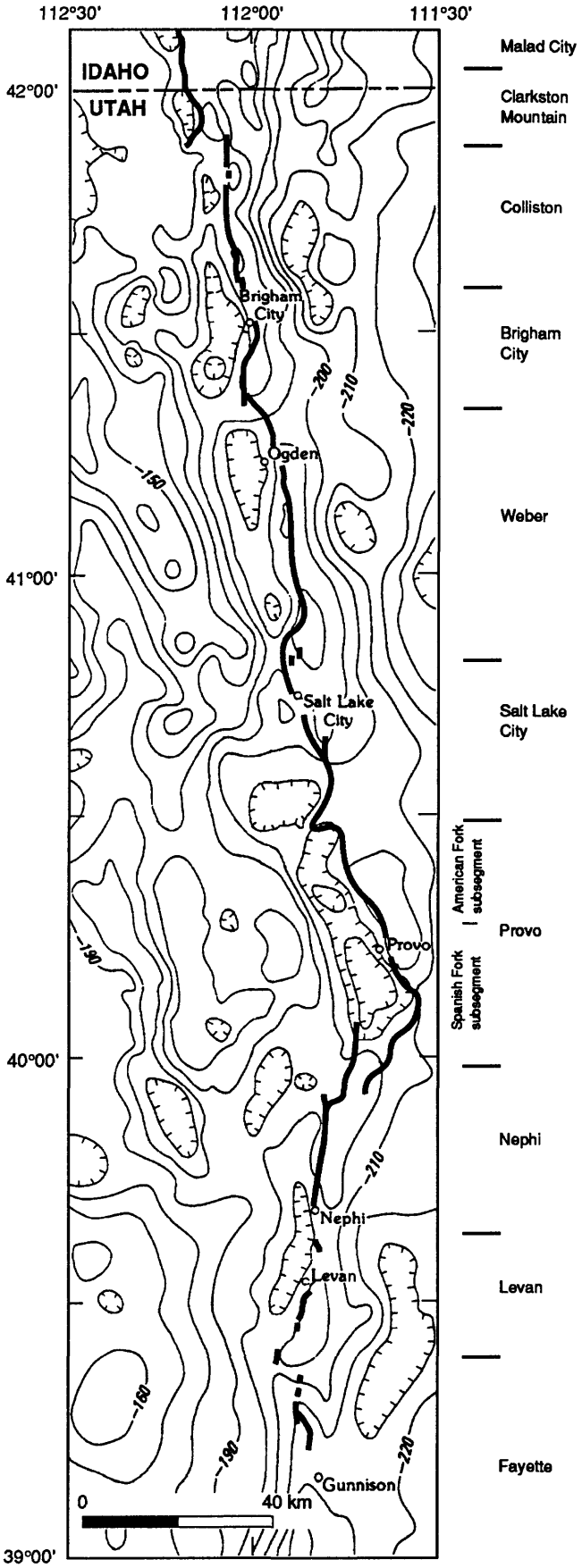

Figure 7-6. Bouguer gravity map of Wasatch front. Trace of late Quaternary fault scarps along the Wasatch fault shown by heavy line. Segment boundaries from Machette and others (1989). Gravity contours simplified by Wheeler and Krystinik (1988) from Zoback (1983).

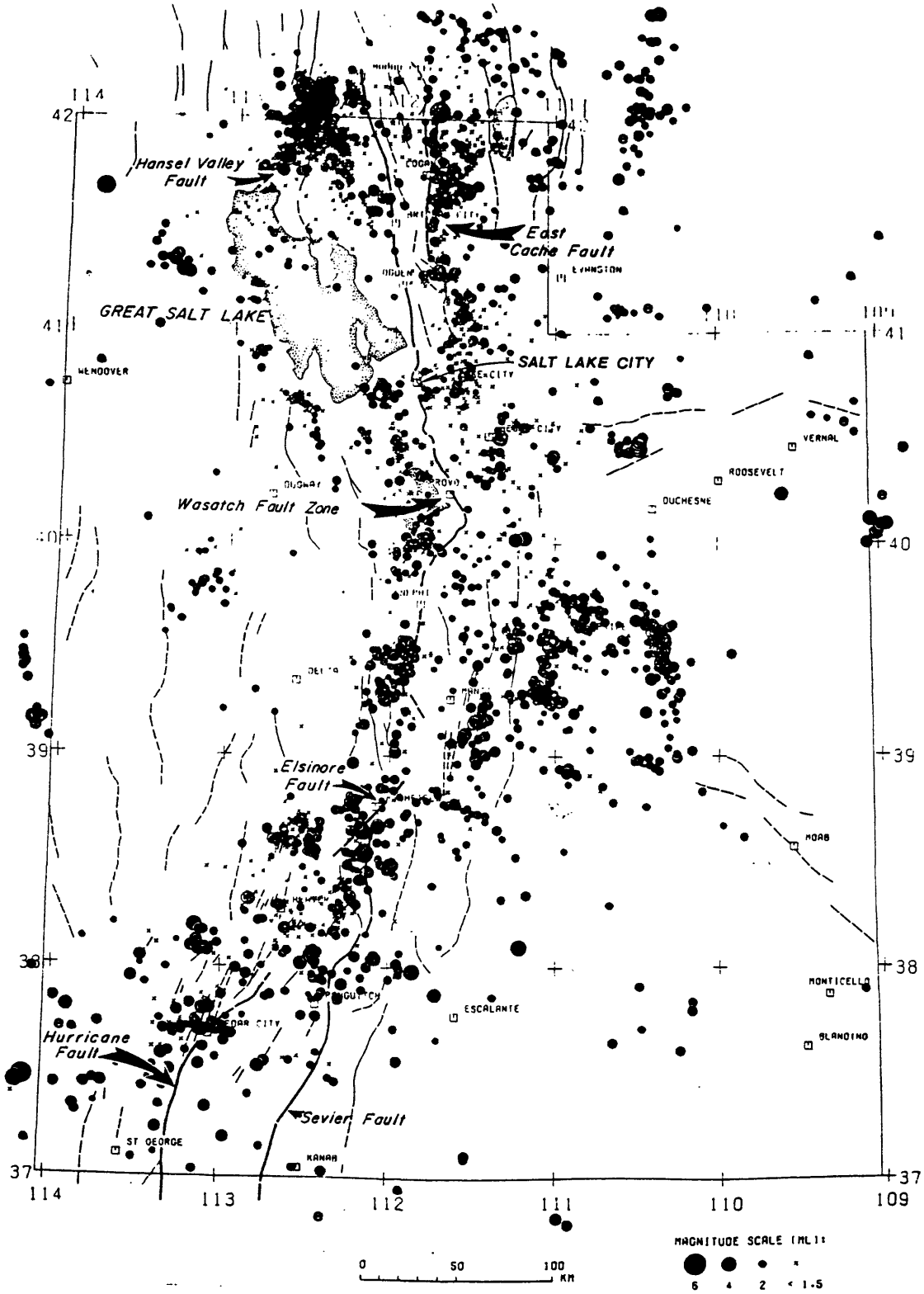

Figure 7-7. Map of earthquake epicenters in Utah, 1962-1978 (from Smith and Arabasz, 1979).

The slip rate along the fault has been variable in space and time, with the ends of the fault less active than the central part. Fission-track dating of apatite and fluid inclusions from uplifted basement rocks in the

footwall indicate a long-term uplift rate for the central part of the range of 0.4 to 0.7 mm/yr for the last 10-18 Ma (Naeser and others, 1980; Parry and Bruhn, 1986).

This is the region where many early ideas on the earthquake cycle were developed, initially through G.K. Gilbert's studies of the youthful fault scarps along the Wasatch fault zone in the late 1800's. Some of these ideas foretold Reid's elastic-rebound theory, which developed from studies of the 1906 San Francisco earthquake. In 1883, Gilbert published an article in the *Salt Lake Tribune* (newspaper) in which he discussed his concept of the earthquake cycle, which was based on his geologic studies of the region. He recognized that ranges in the Great Basin formed by a series of small, incremental uplifts that he believed were the result of the slow accumulation of tectonic strain that was subsequently released by earthquakes. He gave a practical application of his ideas by suggesting that a major earthquake was likely in the Salt Lake City area. It was a bold suggestion, because Salt Lake City had not experienced a large historical earthquake at the time (nor has it in the more than 100 years since his forecast). Gilbert (1883) wrote:

> "The subterranean upthrust is continuous and slow . . . but there is a great friction to overcome, the friction along the surface of fracture between the rising and stationary parts of the crust . . . The upthrust produces a local strain in the crust, involving a certain amount of compression and distortion, and this strain increases until it is sufficient to overcome the starting friction along the fractured surface. Suddenly, and almost instantaneously, there is an amount of motion sufficient to relieve the strain, and this is followed by a long period of quiet, during which the strain is gradually reimposed."

He argued that the presence of fault scarps along the base of the Wasatch Range were evidence of active uplift, and referring to an portion of the Wasatch where he noted that fault scarps were conspicuously absent, he wrote:

> ". . . the rational explanation of their absence is that a very long time has elapsed since their last renewal. In this period the earth strain has been slowly increasing, and some day it will overcome the friction, lift the mountains a few feet, and re-enact on a more fearful scale the catastrophe of [the 1872] Owens Valley [earthquake].
> "It is useless to ask when this disaster will occur. Our occupation of the country has been too brief for us to learn how fast the Wasatch grows; and, indeed, it is only by such disasters that we can learn. By the time experience has taught us this, Salt Lake City will have been shaken down .. . ."

Extensive study of the Wasatch fault since the late 1970's allows a somewhat more optimistic outlook on the hope for gaining an understanding the earthquake hazards posed by the fault to Salt Lake City and the Wasatch Front region in general. Geologic mapping and trenching of the fault at key sites make the Wasatch fault probably the most intensively studied normal-slip fault in the world (Machette and Scott, 1988). These studies have specifically addressed Gilbert's concern about learning ". . . how fast the Wasatch grows . . ." by developing a detailed chronology of Holocene movement on the fault zone.

It was recognized early in these modern studies (and implicitly in Gilbert's work) that surface faulting does not occur along the entire length of the fault in a single large earthquake, but is restricted to discrete *segments* whose location may be controlled by geometric and structural characteristics of the fault zone. Swan and others (1980) and Schwartz and Coppersmith (1984) suggested that the Wasatch fault is composed of six such major segments. Based on detailed surficial mapping along the entire 340-km-long fault zone, Machette and others (1989) have suggested that the fault zone is composed of 10 segments (fig. 7-6), with five active segments along the central part of the fault averaging about 50 km in length, with slip rates of 1-2 mm/yr, and recurrence intervals on each segment averaging about 2,000 years. The five less active distal segments average 20 km in length, with slip rates of less than 0.5 mm/yr, and recurrence intervals on each segment average 10,000 years or more. They have calculated a composite average recurrence interval of about 415 years for major earthquakes

(magnitude greater than 7) on the entire fault zone during the past 6,000 years but note that there is evidence of significant fluctuations in that rate (fig. 7-8). Between about 400 and 1,500 years ago, there was one major event every 220 years. They liken this temporal clustering to the clustering of historical events along the central Nevada seismic belt discussed under Day 6 of this field guide.

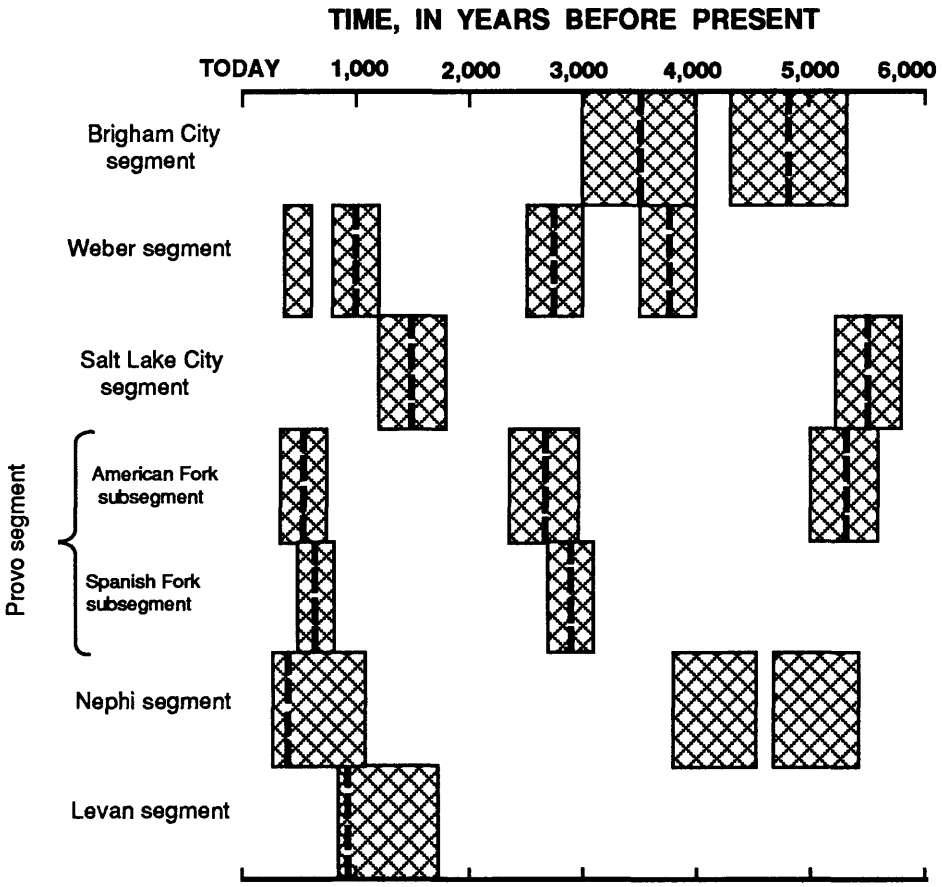

Figure 7-8. Timing of movement on segments of the Wasatch fault zone during the past 6,000 years (from Machette and others, 1989). Heavy-dashed lines indicate best estimates of times of faulting and cross-hachure pattern indicates likely limits for faulting as determined from radiocarbon dates and thermoluminescence age estimates. Although the American Fork and Spanish Fork subsegments are shown separately, they appear to be parts of a single segment as proposed by Schwartz and Coppersmith (1984).

Segment 7C--Wasatch Fault-Salt Lake City Loop (36 miles)

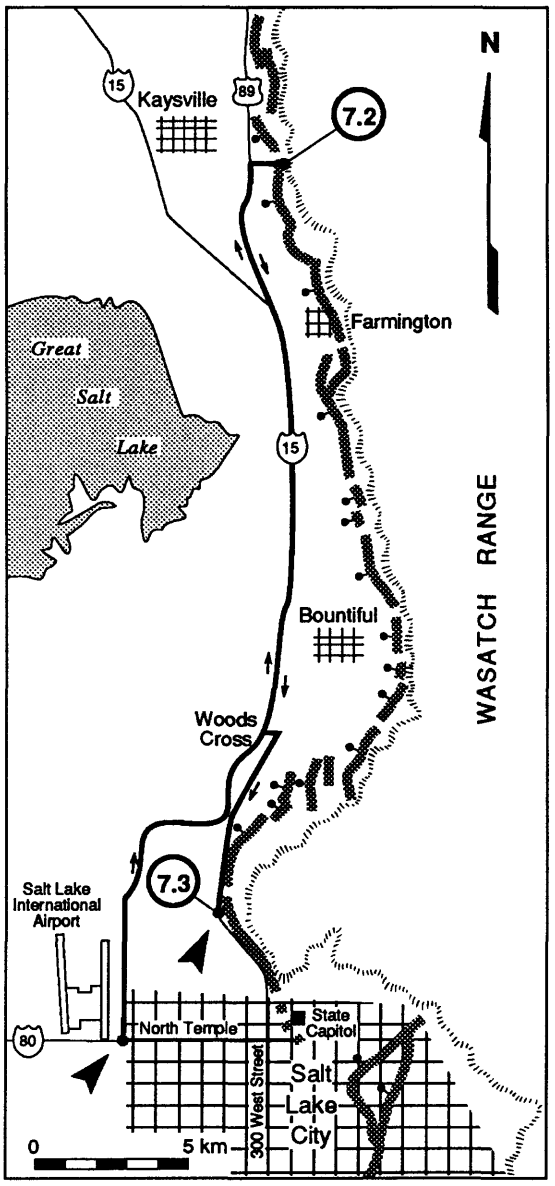

Figure 7-9. Route map for Segment 7C, Wasatch Fault-Salt Lake City Loop.

Route Narrative--Note the odometer reading at the junction of I-80 and I-215 and drive north on I-215. Merge with I-15 northbound at Mile 5, and follow I-15 north past the Bountiful and Farmington exits. Tectonic backtilting of the downdropped fault block in the vicinity of the Farmington exit has moved the eastern shore of the lake close to the foot of the range, similar to the spatial relation of the Carson River and the foot of the range at *Stop 5.5* near Genoa, Nevada. Leave I-15, 1.2 miles north of the Farmington exit at the junction with U.S. Highway 89N (Mile 16), note the odometer reading, and drive north on Highway 89N. The area north of the junction is a large lateral spread (landslide) that is younger than the 10.3 ka Gilbert shoreline of Lake Bonneville (Van Horn, 1975).

At Mile 2.1 pass intersection with Utah Highway 273. Continue north to Mile 4.2, intersect Mountain Road on the right (east) and turn right toward Kaysville (Fruit Heights) and *Stop 7.2*.

Stop 7.2--Wasatch Fault at Kaysville

Seven trenches were dug across the southern end of the closed depression in the graben at this site by Swan and others (1980) to characterize the Holocene history of movements along this section (Weber segment) of the Wasatch fault. The site lies below both the Bonneville and Provo shorelines, and lacustrine sediment of Lake Bonneville are exposed in the fault scarp and gullies. Faulted post-Provo level alluvial-fan deposits unconformably overlie lake sediment. The primary fault scarp, which is as much as 22 m high, faces west and forms the east side of a narrow graben (fig. 7-10). East-facing antithetic scarps up to 2.5 m high bound the west side of the graben. The net throw is about 10-11 m, or about 50 percent of the scarp height.

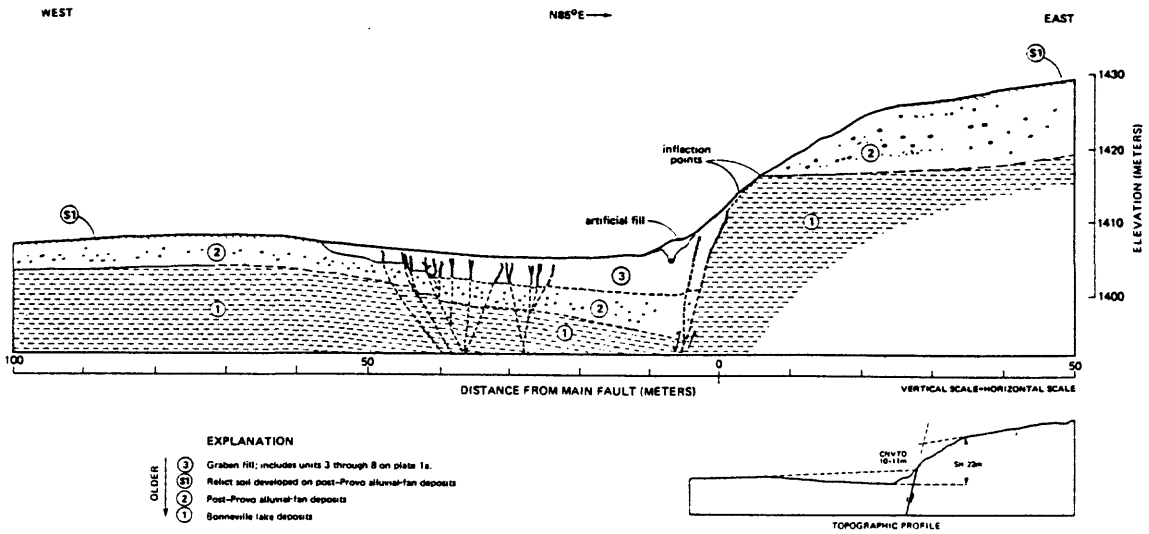

Figure 7-10. Cross section and profile of fault scarp and graben at *Stop 7.2*, near Kaysville, Utah (from Swan and others, 1980). Tilting of the hanging wall toward the fault and formation of a graben make the apparent displacement about twice the net tectonic displacement across the zone.

From stratigraphic relations exposed in the trenches, Swan and others (1980) infer that the vertical displacement at this site (10-11 m) is the result of at least three surface-faulting events, and the two most recent events occurred in the past 1,580 years. At a site on the northern part of the Weber segment, Nelson (1988) has found evidence for at least three, and possibly four, surface-faulting events in the past 5,500 years.

Route Narrative (continued)--Return to Highway 89N and drive south 6.3 miles. Merge with I-15, note the odometer reading, and continue south toward Salt Lake City. Watch for the lateral spread on the west side of the highway. Leave I-15 at the Woods Cross exit at Mile 8.6, turn left and proceed east on 2600 South for 0.4 mile. Turn right (south) onto U.S. Highway 89. In 3.4 miles Highway 89 passes under I-15 and for the next 2 miles coincides with Beck Street. Continue 1.3 miles south of the I-15 underpass on Beck Street to the large gravel pit of Monroc Rock Products at Jones Canyon on the left. The pit has revealed spectacular bedrock exposures of the planar striated fault surface of the footwall of the Warm Springs fault. The Warm Springs fault is the northernmost of three echelon breaks (Warm Springs, East Bench, main Wasatch fault zone) comprising the Salt Lake City segment of the Wasatch fault zone (Machette and others, 1989).

Stop 7.3--Warm Springs Fault at Jones Canyon, North Salt Lake City

Comments for this stop are summarized from a discussion by Scott (1988). Gravel quarrying has exposed Paleozoic bedrock of the footwall of the Warm Springs fault but has also removed geomorphic and stratigraphic evidence of the late Holocene history of slip on the fault that was available to G.K. Gilbert when he briefly studied the site in 1890. Here, at Jones Canyon, Gilbert traced the bedrock scarp into piedmont scarps formed on post-Lake Bonneville alluvial fans from which he determined 14 m of throw on the fault. Gilbert (1890) noted:

> "The portion of the alluvial cone that lies above the fault scarp is channeled by the stream, and a study of the system of terraces bordering this channel shows that the total displacement of 30 feet was produced by at least three independent movements, the measures of the parts being 15 feet, 5 feet, and 10 feet."

Evidence that would help date these events has been removed, but studies at a site just south of Salt Lake City (Dry Creek) have found evidence for two events there, which occurred 5,500 and 1,500 years ago (Machette and others, 1989). It remains to be determined if events can be correlated among the echelon faults comprising the Salt Lake City segment.

The field trip ends here, but additional travel to nearby sites using a recent field-trip guidebook edited by Machette (1988) will give a broader perspective on the history of faulting and neotectonics of this well-studied area.

REFERENCES CITED

Allen, C.R., 1981, The modern San Andreas fault, *in* Ernst, W.G., ed., The geotectonic development of California (Rubey volume 1): Englewood Cliffs, New Jersey, Prentice-Hall, p. 511-534.

Arabasz, W., and Julander, D., 1986, Geometry of seismically active faults and crustal deformation within the Basin and Range-Colorado Plateau transition in Utah: Geological Society of America Special Paper 208, p. 43-74.

Arabasz, W.J., Smith, R.B., and Richins, W.D., 1980, Earthquake studies along the Wasatch front, Utah--Network monitoring, seismicity, and seismic hazards: Seismological Society of America Bulletin, v. 70, p. 1479-1499.

Arnow, T., 1980, Water budget and water-surface fluctuations of the Great Salt Lake, *in* Gwynn, J.W., ed., Great Salt Lake--A scientific, historical and economic overview: Utah Geological and Mineral Survey Bulletin 116, p. 255-263.

Astiz, L., and Allen, C.R., 1983, Seismicity of the Garlock fault, California: Seismological Society of America Bulletin, v. 73, p. 1721-1734.

Atwater, T., 1970, Implications of plate tectonics for the Cenozoic tectonic evolution of western North America: Geological Society of America Bulletin, v. 81, p. 3513-3536.

Aydin, A., and Nur, A., 1982, Evolution of pull-apart basins and their scale independence: Tectonics, v. 1, p. 91-105.

Axelrod, D.I., 1962, Post-Pliocene uplift of the Sierra Nevada, California: Geological Society of America Bulletin, v. 73, p. 183-198.

Bailey, E.H., Irwin, W.P., and Jones, D.L., 1964, Franciscan and related rocks, and their significance in the geology of western California: California Division of Mines and Geology Bulletin 183, 177 p.

Bailey, R.A., 1983, Mammoth Lakes earthquakes and ground uplift--Precursors to possible volcanic activity?: U.S. Geological Survey Earthquake Information Bulletin, v. 15, p. 88-101.

_____1987, Long Valley caldera, eastern California, *in* Hill, M.L., ed., Cordilleran Section of the Geological Society of America, Decade of North American Geology Centennial Field Guide, v. 1: Boulder, Colorado, Geological Society of America, p. 163-168.

Bailey, R.A., Dalrymple, G.B., and Lanphere, M.A., 1976, Volcanism, structure, and geochronology of Long Valley caldera, Mono County, California: Journal of Geophysical Research, v. 81, p. 725-744.

Bakun, W.H., and Lindh, A.G., 1985, The Parkfield, California, earthquake prediction experiment: Science, v. 229, p. 619-624.

Barnhard, T.P., 1988, Fault scarp studies of the Oquirrh Mountains, Utah, *in* Machette, M.N., ed., In the footsteps of G.K. Gilbert--Lake Bonneville and neotectonics of the eastern Basin and Range province, guidebook for field trip twelve: Utah Geological and Mineral Survey Miscellaneous Publication 88-1, p. 52-54.

Bateman, P.C., 1961, Willard D. Johnson and the strike-slip component of fault movement in the Owens Valley, California, earthquake of 1872: Seismological Society of America Bulletin, v. 51, p. 483-493.

_____1965, Geology and tungsten mineralization of the Bishop District California: U.S. Geological Survey Professional Paper 470, 208 p., 11 pl.

Batson, R.M., Edwards, K., and Eliason, E.M., 1975, Computer-generated shaded-relief images: U.S. Geological Survey Journal of Research, v. 3, p. 401-408.

Beanland, S., and Clark, M., in press, The Owens Valley fault zone, eastern California, and surface rupture associated with the 1872 earthquake: U.S. Geological Survey Bulletin.

Bell, J.W., 1984a, Quaternary fault map of Nevada--Reno sheet: Nevada Bureau of Mines and Geology Map 79, 1 sheet, scale 1:250,000.

_____1984b, Guidebook for selected Nevada earthquake areas (field trip 18), *in* Lintz, Joseph, Jr., ed., Western geological excursions, prepared for 1984 Annual Meetings for the Geological Society of America, v. 4: Reno, Nevada, University of Nevada, Mackay School of Mines, p. 387-472.

Bell, J.W., and Katzer, Terry, 1987, Surficial geology, hydrology, and Quaternary tectonics of the IXL Canyon area, Nevada, as related to the 1954 Dixie Valley earthquake: Nevada Bureau of Mines and Geology Bulletin 102, 52 p.

Bell, J.W., Slemmons, D.B., and Wallace, R.E., 1984, Roadlog, Reno to Dixie Valley-Fairview peak earthquake areas, Guidebook for selected Nevada earthquake areas (field trip 18), *in* Lintz, Joseph, Jr., ed., Western geological excursions, prepared for 1984 Annual Meetings for the Geological Society of America, v. 4: Reno, Nevada, University of Nevada, Mackay School of Mines, p. 425-472.

Bingham, C.P., 1980, Solar production of potash from the brines of the Bonneville Salt Flats, *in* Gwynn, J.W., ed., Great Salt Lake--A scientific, historical and economic overview: Utah Geological and Mineral Survey Bulletin 116, p. 229-242.

Birman, J.H., 1964, Glacial geology across the crest of the Sierra Nevada, California: Geological Society of America Special Paper 75, 80 p., 5 pl.

Blackwelder, Eliot, 1931, Pleistocene glaciation in the Sierra Nevada and Basin Ranges: Geological Society of America Bulletin, v. 42, p. 865-922.

Bonilla, M.G., Mark, R.K., and Lienkaemper, J.J., 1984, Statistical relations among earthquake magnitude, surface rupture length, and surface fault displacement: Seismological Society of America Bulletin, v. 74, p. 2379-2411.

Brabb, E.E., and Pampeyan, E.H., 1983, Geologic map of San Mateo County, California: U.S. Geological Survey Miscellaneous Geologic Investigations Series Map I-1257-A, scale 1:62,500.

Brown, R.D., Jr., Vedder, J.G., Wallace, R.E., Roth, E.F., Yerkes, R.F., Castle, R.O., Waananen, A.O., Page, R.W., and Eaton, J.P., 1967, The Parkfield-Cholame, California, earthquakes of June-August 1966--Surface geologic effects, water-resources aspects, and preliminary seismic data: U.S. Geological Survey Professional Paper 579, 66 p.

Bucknam, R.C., and Algermissen, S.T., 1984, A comparison of geologically determined rates of late Quaternary seismic activity and historic seismicity data in the Great Basin, Western United States, *in* A

collection of papers of International Symposium on Continental Seismicity and Earthquake Prediction (September 8-14, 1982), Beijing, China: Beijing, China, Seismological Press, p. 169-176.

Bucknam, R.C., and Anderson, R.E., 1979, Estimation of fault-scarp ages from a scarp-height--slope-angle relationship: Geology, v. 7, p. 11-14.

Burford, R.O., and Harsh, P.W., 1980, Slip on the San Andreas fault in central California from alinement array surveys: Seismological Society of America Bulletin, v. 70, p. 1233-1261.

Burr, T.N., and Currey, D.R., 1988, The Stockton bar, *in* Machette, M.N., ed., In the footsteps of G.K. Gilbert--Lake Bonneville and neotectonics of the eastern Basin and Range province, guidebook for field trip twelve: Utah Geological and Mineral Survey Miscellaneous Publication 88-1, p. 66-73.

Burke, D.E., 1979, Log of a trench in the Garlock fault zone, Fremont Valley, California: U.S. Geological Survey Miscellaneous Field Studies Map MF-1028.

Buwalda, J.P., 1936, Shutter ridges, characteristic physiographic features of active faults [abs.]: Geological Society of America Proceedings 1936, p. 307.

Buwalda, J.P., and Saint-Amand, P., 1955, Geological effects of the Arvin-Tehachapi earthquake, *in* Oakeshott, G.B., ed., Earthquakes in Kern County, California during 1952: California Division of Mines Bulletin 171, p. 41-56.

Carmichael, I.S., 1967, The iron-titanium oxides of salicic volcanic rocks and their associated ferromagnesian silicates: Contributions to Mineralogy and Petrology, v. 14, p. 31-64.

Carter, B.A., 1987, Quaternary fault-line features of the central Garlock fault, Kern County, California, in Hill, M., ed., Cordilleran Section of the Geological Society of America, Decade of North American Geology Centennial Field Guide, v. 1: Boulder, Colorado, Geological Society of America, p. 133-135.

Carver, G.A., 1970, Quaternary tectonism and surface faulting in the Owens Lake basin, California: Technical Report AT2, Mackay School of Mines, University if Nevada, Reno 103 p.

Chadwick, O.A., Hecker, S., and Fonseca J., 1984, A soils chronosequence at Terrace Creek--Studies of late Quaternary tectonism in Dixie Valley, Nevada: U.S. Geological Survey Open-File Report 84-90, p. 29.

Chesterman, C.W., 1968, Volcanic geology of the Bodie Hills, Mono County, California, *in* Coats, R.R., Hay, R.L., and Anderson, C.A., eds., Studies in volcanology: Geological Society of America Memoir 116, p. 45-68.

Clark, M.M., 1972, Collapse fissures along the Coyote Creek fault, *in* The Borrego Mountain earthquake of April 9, 1968: U.S. Geological Survey Professional Paper 787, p. 190-207.

_____1973, Map showing recently active breaks along the Garlock and associated faults, California: U.S. Geological Survey Miscellaneous Geologic Investigations Map I-741, scale 1:24,000.

_____1975, Faulted deformation in the upper drainage of the West Walker River near Sonora Junction, California: California Geology, v. 28, p. 103-104.

Clark, M.M., and Gillespie, A.R., 1981, Record of late Quaternary faulting along the Hilton Creek fault in the Sierra Nevada, California [abs.]: Seismological Society of America, 76th Annual Meeting, Earthquake Notes, v. 52, no. 1, p. 46.

Clark, M.M., and Lajoie, K.R., 1974, Holocene behavior of the Garlock fault: Geological Society of America Abstracts with Programs, v. 6, p. 156-157.

Clark, M.M., Harms, K.K., Lienkaemper, J.J., Harwood, D.S., Lajoie, K.R., Matti, J.C., Perkins, J.A., Rymer, M.J., Sarna-Wojcicki, A.M., Sharp, R.V., Sims, J.D., Tinsley, J.C., III, and Ziony, J.I., 1984, Preliminary slip-rate table and map of late-Quaternary faults of California: U.S. Geological Survey Open-File Report 84-106, 13 p. 5 pl.

Colman, S.M., and Watson, Ken, 1983, Ages estimated from a diffusion equation model for scarp degradation: Science, v. 221, p. 263-265.

Cramer, C.H., and Toppozada, T.R., 1980, A seismological study of the May, 1980, and earlier earthquake activity near Mammoth Lakes, California, *in* Sherburne, R.W., ed., Mammoth Lakes, California earthquakes of May 1980: California Division of Mines and Geology Special Report 150, p. 91-130.

Crittenden, M.D., 1963, New data on the isostatic deformation of Lake Bonneville: U.S. Geological Survey Professional Paper 454-E, p. 31.

Currey, D.R., and Burr, T.N., 1988, Linear model of threshold-controlled shorelines of Lake Bonneville, *in* Machette, M.N., ed., In the footsteps of G.K. Gilbert--Lake Bonneville and neotectonics of the eastern Basin and Range province, guidebook for field trip twelve: Utah Geological and Mineral Survey Miscellaneous Publication 88-1, p. 104-110.

Currey, D.R., Oviatt, C.G., and Plyler G.B., 1983, Lake Bonneville stratigraphy, geomorphology, and isostatic deformation in west-central Utah, *in* Gurgel, K.D., ed., Geologic excursions in neotectonics and engineering geology in Utah, Guidebook - Part IV: Utah Geological and Mineral Survey Special Studies 62, p. 63-82.

Currey, D.R., Atwood, G., and Mabey D.R., 1984, Major levels of Great Salt Lake and Lake Bonneville: Utah Geological and Mineral Survey Map 73, scale 1:750,000.

Curry, R.R., 1966, Glaciation approximately 3,000,000 B.P. in the Sierra Nevada, California: Science, v. 154, p. 770-771.

_____1971, Glacial and Pleistocene history of the Mammoth Lakes Sierra--A geologic guidebook: Missoula, Montana University of Montana Department of Geology, Geological Series Publication no. 11, 49 p., 4 pl.

Dalrymple, G.B., 1963, Potassium-argon dates of some Cenozoic volcanic rocks of the Sierra Nevada, California: Geological Society of America Bulletin, v. 74, p. 379-390.

Dalrymple, G.B., Cox, A., and Doell, R.R., 1965, Potassium-argon age and paleomagnetism of the Bishop Tuff, California: Geological Society of America Bulletin, v. 76, p. 665-674.

Davis, G.A., and Burchfiel, B.C., 1973, Garlock fault--An intracontinental transform structure, southern California: Geological Society of America Bulletin, v. 84, p. 1407-1422.

Davis, T.L., and Lagoe, M.B., 1987, The Arvin-Tchachapi earthquake (M=7.6) and its relationship to the White Wolf fault and the Pleito thrust system: Geological Society of America Abstracts with Programs, v. 19, p. 370.

Davis, W.M., 1903, The mountain ranges of the Great Basin: Harvard College Museum of Comparative Zoology Bulletin, Geology Series, v. XLII, no. 3, p. 129-177.

dePolo, C.M., Clark, D.G., Slemmons, D.B., and Aymard W.H., 1989, Historical Basin and Range province surface faulting and fault segmentation, *in* Schwartz, D.P., and Sibson, R.H., eds., Proceedings of Conference XLV--Fault segmentation and controls on rupture initiation and termination: U.S. Geological Survey Open-File Report 89-315, p. 131-162.

Dibblee, T.W., Jr., 1952, Geology of the Saltdale Quadrangle, California: California Division of Mines and Geology Bulletin 160, p. 43.

_____1980, Geology along the San Andreas fault from Gilroy to Parkfield, *in* Streitz, R., and Sherburne, R., eds., Studies of the San Andreas fault zone in northern California: California Division of Mines and Geology Special Report 140, p. 3-18.

Dickinson, W.R., 1981, Plate tectonics and the continental margin of California, *in* Ernst, W.G., ed., The geotectonic development of California (Rubey volume 1): Englewood Cliffs, New Jersey, Prentice-Hall, p. 1-28.

Dickinson, W.R., and Rich, E.I., 1972, Petrologic intervals and petrofacies in the Great Valley Sequence, Sacramento Valley, California: Geological Society of America Bulletin, v. 83, p. 3007-3024.

Dohrenwend, J.C., 1977, Late Cenozoic geology of a segment of the San Andreas fault system, Paicines to Lonoak, California: Final Technical Report of Grant #14-08-0001-G227, U.S. Geological Survey, 49 p.

Dorn, R.I., Turrin, B.D., Jull, A.J.T., Linick, T.W., and Donahue, D.J., 1987, Radiocarbon and cation-ratio ages for rock varnish on Tioga and Tahoe morainal boulders of Pine Creek, eastern Sierra Nevada, California, and their paleoclimatic implications: Quaternary Research, v. 28, p. 38-49.

Doser, D.I., 1986, Earthquake processes in the Rainbow Mountain-Fairview Peak-Dixie Valley, Nevada, region 1954-1959: Journal of Geophysical Research, v. 91, p. 12,572-12,586.

Doser, D.I., 1988, Source parameters of earthquakes in the Nevada seismic zone: Journal of Geophysical Research, v. 93, p. 15,001-15,015.

Dunn, J.R., 1953, The origin of the deposits of tufa in Mono Lake: Journal of Sedimentary Petrology, v. 23, p. 18-23.

Eardley, A.J., 1962, Gypsum dunes and evaporite history of the Great Salt Lake desert: Utah Geological and Mineral Survey Special Studies 2, 27 p.

Eaton, G.P., 1979, A plate-tectonic model for late Cenozoic crustal spreading in the Western United States, *in* Riecker, R.E., ed., Rio Grande Rift--Tectonics and magmatism: Washington, D.C., American Geophysical Union, p. 7-32.

_____1982, The Basin and Range province--Origin and tectonic significance: Annual Review of Earth and Planetary Sciences, v. 10, p. 409-440.

Eaton, J.P., O'Neill, M.E., and Murdock, J.N., 1970, Aftershocks of the 1966 Parkfield-Cholame, California, earthquake--A detailed study: Seismological Society of America Bulletin, v. 60, p. 1151-1197.

Eichelberger, J.C., Vogel, T.A., Younker, L.W., Miller, C.D., Heiken, G.H., and Wohletz, K.H., 1988, Structure and stratigraphy beneath a young phreatic vent--South Inyo Crater, Long Valley caldera, California: Journal of Geophysical Research, v. 93, p. 13,208-13,220.

Erickson, R.L., and Marsh, S.P., 1974, Geologic map of the Golconda quadrangle, Humboldt County, Nevada: U.S. Geological Survey Geologic Quadrangle Map GQ-1174, scale 1:24,000.

Ernst, W.G., 1970, Tectonic contact between the Franciscan melange and the Great Valley sequence, crustal expression of a late Mesozoic Benioff zone: Journal of Geophysical Research, v. 75, p. 886-902.

_____ed., 1981, The geotectonic development of California (Rubey volume 1): Englewood Cliffs, New Jersey, Prentice-Hall, 706 p.

Fonseca, J., 1988, The Sou Hills--A barrier to faulting in the central Nevada seismic belt: Journal of Geophysical Research, v. 93, p. 475-489.

Gale, H.S., 1914, Salines in the Owens, Searles, and Panamint basins, southeastern California: U.S. Geological Survey Contributions to Economic Geology, 1913, pt. I-L, Bulletin 580-L, 323 p.

Gilbert, C.M., 1938, Welded tuff in eastern California: Geological Society of America Bulletin, v. 49, p. 1829-1862.

Gilbert, G.K., 1883, Earthquakes: The Daily Tribune [Salt Lake City, Utah].

_____1890, Lake Bonneville: U.S. Geological Survey Monograph 1, 438 p.

Hall, N.T., 1984, Holocene history of the San Andreas fault between Crystal Springs Reservoir and San Andreas Dam, San Mateo County, California: Seismological Society of America Bulletin, v. 74, p. 281-299.

Hanks, T.C., and Andrews, D.J., 1989, Effect of far-field slope on morphologic dating of scarplike landforms: Journal of Geophysical Research, v. 94, p. 565-573.

Hanks, T.C., Bucknam, R.C., Lajoie, K.R., and Wallace R.E., 1984, Modification of wave-cut and faulting-controlled landforms: Journal of Geophysical Research, v. 89, p. 5771-5790.

Hamilton, Warren, 1988, Tectonic setting and variations with depth of some Cretaceous and Cenozoic structural and magmatic systems of the Western United States, *in* Ernst, W.G., ed., Metamorphism and crustal evolution of the Western United States: Englewood Cliffs, New Jersey, Prentice Hall, p. 1-40.

Harrill, J.R., Gates, J.S., and Thomas, J.M., 1988, Major ground-water flow systems in the Great Basin region of Nevada, Utah, and adjacent states: Hydrologic Investigations Atlas HA-694-C scale 1:1,000,000.

Hart, E.W., Bryant, W.A., and Smith, T.C., 1984, Summary of faults evaluated--Faults evaluation program 1983 area Sierra Nevada region: California Division of Mines and Geology, Open-File Report 84-52 SF, 2 sheets, scale 1:500,000.

Hecker, S., 1985, Timing of Holocene faulting in part of a seismic belt, west-central Nevada [unpub. M.S. manuscript]: Tucson, Arizona, University of Arizona, 42 p.

Heller, P.L., Bowdler, S.S., Chambers, H.P., Coogan, J.C., Hagen, E.S., Shuster, M.W., Winslow, N.S., and Lawton, T.F., 1986, Time of initial thrusting in the Sevier orogenic belt, Idaho-Wyoming and Utah: Geology, v. 14, p. 388-391.

Hildreth, W., and Mahood, G.A., 1984, Ring-fracture eruptions of the Bishop Tuff indicated by accidental lithic fragments: EOS Transactions, American Geophysical Union, v. 65, p. 1149.

Hill, D.P., and Eaton, J.P., 1987, Seismicity and seismotectonic fabric of California and western Nevada, *in* Jacobson, M.L., and Rodriguez, T.R., compilers, National Earthquake Hazards Reduction Program, Summaries of Technical Reports, Volume XXIV: U.S. Geological Survey Open-File Report 87-374, p. 246-250.

Hill, D.P., Bailey, R.A., and Ryall, A.S., 1985, Active tectonic and magmatic processes beneath Long Valley caldera, eastern California--An overview: Journal of Geophysical Research, v. 90, p. 11,111-11,120.

Hill, M., 1975, Living glaciers of California--A picture story: California Geology, v. 28, p. 171-177.

Hill, M.L., and Dibblee, T.W., 1953, San Andreas, Garlock, and Big Pine faults--A study of the character, history, and significance of their displacements: Geological Society of America Bulletin, v. 64, p. 443-458.

Hoots, H.W., Bear, T.L., and Kleinspell, W.D., 1954, Geological summary of the San Joaquin Valley, California, *in* Jahns, R.H., ed., Geology of southern California: California Division of Mines and Geology Bulletin 170, p. 113-129.

Hopson, C.A., Mattinson, J.M., and Pessagno, E.A., Jr., 1981, Coast Range ophiolite, western California, *in* Ernst, W.G., ed., The geotectonic development of California (Rubey volume 1): Englewood Cliffs, New Jersey, Prentice-Hall, p. 418-510.

Huber, N.K., and Rinehart, C.D., 1967, Cenozoic volcanic rocks of the Devils Postpile Quadrangle, eastern Sierra Nevada California: U.S. Geological Survey Professional Paper 554-D, p. D1-D21.

Irelan, William, Jr., 1888a, The Owens Valley earthquake: Eighth Annual Report of the State Mineralogist, California State Mining Bureau, p. 288-309.

_____1888b, Bodie district: Eighth annual report of the state mineralogist, California State Mining Bureau, p. 382-401.

Irwin, W.P., and Barnes, I., 1975, Effect of geologic structure and metamorphic fluids on seismic behavior of the San Andreas fault system in central and northern California: Geology, v. 3, p. 713-716.

Izett, G.A., Obradovich, J.D., and Mehnert, H.H., 1988, The Bishop ash bed (middle Pleistocene) and some older (Pliocene and Pleistocene) chemically and mineralogically similar ash beds in California, Nevada, and Utah: U.S. Geological Survey Bulletin 1675, 37 p.

Jahns, 1954, Investigations and problems of southern California geology, *in* Jahns, R.H., ed., Geology of southern California, General features, chapter 1: California Division of Mines and Geology Bulletin 170, p. 5-29.

Jayko, A.S., Blake, M.C., Jr., and Harms, T., 1987, Attenuation of the Coast Range ophiolite by extensional faulting, and nature of the Coast Range "thrust," California: Tectonics, v. 6, p. 475-488.

Jennings, C.W., compiler, 1975, Fault map of California with locations of volcanoes, thermal springs and thermal wells: California Division of Mines and Geology, Geologic Data Map No. 1, scale 1:750,000.

Jennings, J.D., 1957, Danger Cave: Salt Lake City, Utah, University of Utah Department of Anthropology, Anthropological Papers, no. 27, 328 p.

Keaton, J.R., Currey, D.R., and Olig, S.J., 1987, Paleoseismicity and earthquake hazards evaluation of the West Valley fault zone, Salt Lake City urban area, Utah: U.S. Geological Survey Contract Report, Contract No. 14-08-0001-22048, p. 55.

Knopf, A., 1918, A geologic reconnaissance of the Inyo Range and the eastern slope of the southern Sierra Nevada, California: U.S. Geological Survey Professional Paper 110, 130 p., 23 pl.

Lajoie, K.R., 1968, Late Quaternary stratigraphy and geologic history of Mono Basin, eastern California [unpub. Ph.D. dissertation]: Berkeley, California, University of California, 271 p.

Lawson, A.C., 1893, The post-Pliocene diastrophism of the coast of southern California: California University, Department of Geology Bulletin, v. 1, p. 115-160.

_____1895, Sketch of the geology of the San Francisco Peninsula: U.S. Geological Survey 15th Annual Report, p. 405-476.

_____1908, The California earthquake of April 18, 1906, Report of the State Earthquake Commission, Volume I: Washington, D.C., Carnegie Institution of Washington, 451 p.

_____1912, The recent fault scarps at Genoa, Nevada: Seismological Society of America Bulletin, v. II, p. 193-200.

Leadabrand, Russ, 1966, A guidebook to the Mojave Desert of California--Including Death Valley, Joshua Tree National Monument, and Antelope Valley: Los Angeles, California, The Ward Ritchie Press, 180 p.

Lipshie, S.R., 1976, Geologic guidebook to the Long Valley-Mono Craters region of eastern California, Field guide no. 5: Los Angeles, California, Geological Society of University of California Los Angeles (GSUCLA), 181 p.

Lienkaemper, J.J., 1987, Slip on the San Andreas fault southeast of Cholame, California [abs.]: Eos, Transactions, American Geophysical Union, v. 68, p. 1345.

Lisowski, M., and Prescott, W.H., 1981, Short-range distance measurements along the San Andreas fault system in central California, 1975-1979: Seismological Society of America Bulletin, v. 71, p. 1607-1624.

Louderback, G.D., 1947, Central California earthquakes of the 1830's: Seismological Society of America Bulletin, v. 37, p. 33-74.

Louie, J., Allen, C., Johnson, D., Haase, P., and Cohn, S., 1985, Fault slip in southern California: Seismological Society of America Bulletin, v. 75, p. 811-833.

Lubetkin, L.K.C., 1980, Late Quaternary activity along the Lone Pine fault, Owens Valley fault zone, California [unpub. M.S. thesis]: Stanford, California, Stanford University, 85 p.

Lubetkin, L.K.C., and Clark, M.M., 1988, Late Quaternary activity along the Lone Pine fault, eastern California: Geological Society of America Bulletin, v. 100, p. 755-766.

Mabey, D.R., 1960, Gravity survey of the western Mojave desert, California: U.S. Geological Survey Professional Paper 316-D, p. 51-73.

_____1987, The end of the wet cycle: Utah Geological and Mineral Survey, Survey Notes, p. 8-9.

Machette, M.N., ed., 1988, In the footsteps of G.K. Gilbert -- Lake Bonneville and neotectonics of the eastern Basin and Range province, guidebook for field trip twelve: Utah Geological and Mineral Survey Miscellaneous Publication 88-1, 120 p.

_____1989, Slope-morphometric dating, *in* Forman, S.L., ed., Dating methods applicable to Quaternary geologic studies in the Western United States: Utah Geological and Mineral Survey Special Publication, in press.

Machette, M.N., and Scott, W.E., 1988, Field trip introduction--A brief review of research on lake cycles and neotectonics of the eastern Basin and Range province, *in* Machette, M.N., ed., In the footsteps of G.K. Gilbert--Lake Bonneville and neotectonics of the eastern Basin and Range province, guidebook for field trip twelve: Utah Geological and Mineral Survey Miscellaneous Publication 88-1, p. 6-14.

Machette, M.N., Personius, S.F., Nelson, A.R., Schwartz, D.P., and Lund, W.R., 1989, Segmentation models and Holocene movement history of the Wasatch fault zone, Utah: U.S. Geological Survey Open-File Report, in press.

Martel, S.J., Harrison, T.M., and Gillespie, A.R., 1987, Late Quaternary vertical displacement rate across the Fish Springs fault, Owens Valley fault zone, California: Quaternary Research, v. 27, p. 113-129.

Mastin, L.G., and Pollard, D.D., 1988, Surface deformation and shallow dike intrusion processes at Inyo Craters, Long Valley, California: Journal of Geophysical Research, v. 93, p. 13,221-13,235.

Matthews, V.I., 1976, Correlation of Pinnacles and Neenach volcanic formations and their bearing on San Andreas fault problem: American Association of Petroleum Geologists Bulletin, v. 60, p. 2128-2141.

Maurer, D.K., 1985, Gravity survey and depth to bedrock in Carson Valley, Nevada-California: U.S. Geological Survey Water-Resources Investigations Report 84-4202, 20 p., 2 pl.

Mayo, E.B., 1934, The Pleistocene Long Valley Lake in eastern California: Science, v. 80, no. 2065, p. 95-96.

McCaffrey, W.F., and Hollett, K.J., 1988, Structure and depositional history of Owens Valley, California: Geological Society of America Abstracts with Programs, v. 20, p. 211.

Metz, J.A., and Mahood, G.A., 1985, Precursors to the Bishop Tuff eruption--Glass Mountain, Long Valley, California: Journal of Geophysical Research. v. 90, p. 11,121-11,126.

Miller, C.D., 1985, Holocene eruptions at the Inyo volcanic chain, California--Implications for possible eruptions in Long Valley caldera: Geology, v. 13, p. 14-17.

Miller, C.D., Mullineaux, D.R., Crandell, D.R., and Bailey, R.A., 1982, Potential hazards from volcanic eruptions in the Long Valley-Mono Lake area, east-central California and southwest Nevada--A preliminary assessment: U.S. Geological Survey Circular 877, 10 p.

Minster, J.B., and Jordan, T.H., 1978, Present-day plate motions: Journal of Geophysical Research, v. 83, p. 5331-5354.

Morrison, R.B., 1964, Lake Lahontan--Geology of southern Carson Desert, Nevada: U.S. Geological Survey Professional Paper 401, 156 p. 12 pl.

Naeser, C.W., Bryant, B.R., Crittenden, M.D., and Sorenson M.L., 1980, Fission-track dating in the Wasatch Mountains, Utah--An uplift study, *in* Evernden, J.F., compiler, Proceedings of conference X, Earthquake

hazards along the Wasatch and Sierra Nevada frontal fault zones: U.S. Geological Survey Open-File Report 80-801, p. 634-646.

Namson, J., and Davis, T., 1988, Structural transect of the western Transverse Ranges, California--Implications for lithospheric kinematics and seismic risk evaluation: Geology, v. 16, p. 675-679.

Nash, D.B., 1980, Morphologic dating of degraded normal fault scarps: Journal of Geology, v. 88, p. 353-360.

National Oceanic and Atmospheric Administration, 1982, Climate of Utah, Climatography of the United States No. 60: Asheville, North Carolina, National Climatic Center, 17 p.

Nelson, A.R., 1988, The northern part of the Weber segment of the Wasatch fault zone near Ogden, Utah, *in* Machette, M.N., ed., In the footsteps of G.K. Gilbert--Lake Bonneville and neotectonics of the eastern Basin and Range province, guidebook for field trip twelve: Utah Geological and Mineral Survey Miscellaneous Publication 88-1, p. 33-37.

Nilsen, T.H., 1984, Offset along the San Andreas fault of Eocene strata from the San Juan Bautista area and San Emigdio Mountains, California: Geological Society of America Bulletin, v. 95, p. 599-609.

Nilsen, T.H., and Stewart, J.H., 1980, The Antler orogeny--Mid-Paleozoic tectonism in western North America: Geology, v. 8, p. 298-302.

Noble, D.C., Slemmons, D.B., Korringa, M.K., Dickinson, W.R., Al-Rawi, Yehya, and McKee, E.H, 1974, Eureka Valley Tuff, east-central California and adjacent Nevada: Geology, v. 2, p. 139-142.

Oakeshott, G.B., Greensfelder, R.W., and Kahle, J.E., 1972, One hundred years later: California Geology, v. 25, no. 3, p. 55-61.

Page, B.M., 1981, The Southern Coast Ranges, *in* Ernst, W.G., ed., The geotectonic development of California (Rubey volume 1): Englewood Cliffs, New Jersey, Prentice-Hall, p. 329-417.

Pakiser, L.C., and Kane, M.F., 1965, Gravity study of Owens Valley, *in* Bateman, P.C., Geology and tungsten mineralization of the Bishop District, California: U.S. Geological Survey Professional Paper 470, p. 191-195.

Pampeyan, E.H., Holzer, T.L., and Clark, M.M., 1988, Modern ground failure in the Garlock fault zone, Fremont Valley, California: Geological Society of America Bulletin, v. 100, p. 677-691.

Parry, W.T., and Bruhn, R.L., 1986, Pore fluid and seismogenic characteristics of fault rock at depth on the Wasatch fault, Utah: Journal of Geophysical Research, v. 91, p. 730-744.

Pease, R. C., 1979a, Scarp degradation and fault history south of Carson City, Nevada [unpub. M.S. thesis]: Reno, Nevada, University of Nevada Reno, 90 p.

_____1979b, Earthquake hazards map, Genoa quadrangle: Nevada Bureau of Mines and Geology Map 1Ci, 1 sheet, scale 1:24,000.

_____1980, Genoa quadrangle geologic map: Nevada Bureau of Mines and Geology Map 1Cg, 1 sheet, scale 1:24,000.

Pearthree, P.A., and Demsey, K., 1987, Patterns of Holocene faulting and the rate of extension in central Nevada: Geological Society of America Abstracts with Programs, v. 19, p. 802.

Phillips, F.M., Smith, S.S., and Zreda, M.G., 1988, Cosmogenic ^{36}Cl buildup dating of the eastern Sierra Nevada glacial sequence--Preliminary results: Geological Society of America Abstracts with Programs, v. 20, no. 7, p. A53-A54.

Poley, C.M., Lindh, A.G., Bakun, W.H., and Schulz, S.S., 1987, Temporal changes in microseismicity and creep near Parkfield, California: Nature, v. 327, p. 134-137.

Power, W.L., and Tullis, T.E., 1989, Relationship between slickenside surfaces in fine-grained quartz and the seismic cycle: Journal of Structural Geology, [in press].

Prescott, W.H., Lisowski, M., and Savage, J.C., 1981, Geodetic measurement of crustal deformation on the San Andreas, Hayward, and Calaveras faults near San Francisco, California: Journal of Geophysical Research, v. 86, p. 10,853-10,869.

Putnam, W.C., 1949, Quaternary geology of the June Lake district, California: Geological Society of America Bulletin, v. 60, p. 1281-1302.

_____1960, Faulting and Pleistocene glaciation in the eastern Sierra Nevada of California, U.S.A.: International Geologic Congress, 21st Session, part 21, p. 270-274.

Radbruch, D.H., and Rogers, T.H., 1969, Field trip 2A and 2B--Hayward and Calaveras fault zones: Field Trips, 1969 National Meeting of the Association of Engineering Geologists, p. B1-B25.

Radtke, A.S., 1985, Geology of the Carlin gold deposit: U.S. Geological Survey Professional Paper 1267, 124 p.

Reid, H.F., 1910, The California earthquake of April 18, 1906, Report of the State Earthquake Commission, Volume II, The mechanics of the earthquake: Washington, D.C., Carnegie Institution of Washington, 192 p.

Rogers, A.M., Harmsen, S.C., Corbett, E.J., Priestley, K., and dePolo, D., 1989, The seismicity of Nevada and some adjacent parts of the Great Basin, *in* Slemmons, D.B., Engdahl, E.R., Blackwell, D., and Schwartz, D.P., eds., Neotectonics of North America: Boulder, Colorado, Geological Society of America, [in press].

Roquemore, G.R., 1988, Revised estimates of slip rate on the Little Lake fault, California: Geological Society of America Abstracts with Programs, v. 20, p. 225.

Ross, D.C., 1970, Quartz gabbro and anorthositic gabbro--Markers of offset along the San Andreas fault in the California Coast Ranges: Geological Society of America Bulletin, v. 81, p. 3647-3662.

_____1978, The Salinian block--A Mesozoic granitic orphan in the California Coast Ranges, *in* Howell, D.G., and McDougall, K.A., eds., Mesozoic paleogeography of the Western United States: Pacific Section, Society of Economic Paleontologists and Mineralogists, Pacific Coast Paleogeography Symposium 2, p. 509-522.

Russell, I.C., 1885, Geological history of Lake Lahontan, a Quaternary lake of northwestern Nevada: U.S. Geological Survey Monograph 11, 288 p.

_____1889, Quaternary history of Mono Valley, California: U.S. Geological Survey Eighth Annual Report of the Director, part 1, p. 261-394.

Ryall, A., and Ryall, F., 1980, Spacial-temporal variations in seismicity preceding the May, 1980, Mammoth Lakes, California, earthquakes, *in* Sherburne, R.W., ed., Mammoth Lakes, California earthquakes of May 1980: California Division of Mines and Geology Special Report 150, p. 27-39.

Ryall, A., Slemmons, D.B., and Gedney L.D., 1966, Seismicity, tectonism, and surface faulting in the Western United States during historic time: Seismological Society of America Bulletin, v. 56, p. 1105-1135.

Rymer, M.J., 1981, Geologic map along a 12 kilometer segment of the San Andreas fault zone, southern Diablo Range, California: U.S. Geological Survey Open-File Report 81-1173, scale 1:12,000.

_____1982, Structural framework of the San Andreas fault zone along Mustang Ridge, Monterey County, California: Geological Society of America Abstracts with Programs, v. 14, p. 229.

Saint-Amand, P., Gaines, C., and Saint-Amand, D., 1987, Owens Lake, an ionic soap opera staged on a natric playa, *in* Hill, M.L., ed., Cordilleran Section of the Geological Society of America, Decade of North American Geology Centennial Field Guide, v. 1: Boulder, Colorado, Geological Society of America, p. 145-150.

Sanders, C.O., and Slemmons, D.B., 1979, Recent crustal movements in the central Sierra Nevada-Walker Lane region of California-Nevada--Part III, the Olinghouse fault zone: Tectonophysics, v. 52, p. 585-597.

Savage, J.C., 1988, Principal component analysis of geodetically measured deformation in Long Valley caldera, eastern California, 1983-1987: Journal of Geophysical Research, v. 93, p. 13,297-13,305.

Savage, J.C., and Clark, M.M., 1982, Magmatic resurgence in Long Valley caldera, California--Possible cause of the 1980 Mammoth Lakes earthquakes: Science, v. 217, p. 531-532.

Savage, J.C., and Hastie, L.M., 1969, A dislocation model for the Fairview Peak, Nevada, earthquake: Seismological Society of America Bulletin, v. 59, p. 1937-1948.

Scholl, D.W., and Taft, W.H., 1964, Algae, contributors to the formation of calcareous tufa, Mono Lake, California: Journal of Sedimentary Petrology, v. 34, p. 309-319.

Schulz, S.S., Mavko, G.M., Burford, R.O., and Stuart, W.D., 1982, Long-term fault creep observations in central California: Journal of Geophysical Research, v. 87, p. 6977-6982.

Schwartz, D.P., and Coppersmith, K.J., 1984, Fault behavior and characteristic earthquakes--Examples from the Wasatch and San Andreas fault zones: Journal of Geophysical Research, v. 89, p. 5681-5698.

_____1986, Seismic hazards--New trends in analysis using geologic data, *in* Active Tectonics: Washington, D.C., National Research Council, National Academy Press, p. 215-230.

Scott, W.E., 1988, G.K. Gilbert's observations of post-Bonneville movement along the Warm Springs fault, Salt Lake County, Utah, *in* Machette, M.N., ed., In the footsteps of G.K. Gilbert--Lake Bonneville and neotectonics of the eastern Basin and Range province, guidebook for field trip twelve: Utah Geological and Mineral Survey Miscellaneous Publication 88-1, p. 44-46.

Scott, W.E., McCoy, W.D., Shroba, R.R., and Rubin, M., 1983, Reinterpretation of the exposed record of the last two cycles of Lake Bonneville, Western United States: Quaternary Research, v. 20, p. 261-285.

Shackleton, N.J., and Opdyke, N.D., 1973, Oxygen isotope and paleomagnetic stratigraphy of equatorial Pacific core V28-238--Oxygen isotope temperatures and ice volumes on a 10^5 year and 10^6 year scale: Quaternary Research, v. 3, p. 39-55.

Sharp, R.P., 1968, Sherwin till-Bishop Tuff geological relationships, Sierra Nevada, California: Geological Society of America Bulletin, v. 79, p. 351-364.

_____1969, Semiquantitative differentiation of glacial moraines near Convict Lake, Sierra Nevada, California: Journal of Geology, v. 77, p. 68-91.

_____1976, Field guide to southern California: Dubuque, Iowa, Kendall/Hunt Publishing Company, 208 p.

Sharp, R.P., and Birman, J.H., 1963, Additions to classical sequence of Pleistocene glaciations, Sierra Nevada, California: Geological Society of America Bulletin, v. 74, p. 1079-1086.

Shedlock, K.M., Brocher, T.M., and Harding, S.T., 1989, Shallow structure and deformation along the San Andreas fault in Cholame Valley, California, based on high-resolution reflection profiling: Journal of Geophysical Research, [in press].

Sieh, K., and Bursik, Marcus, 1986, Most recent eruption of the Mono Craters, eastern central California: Journal of Geophysical Research, v. 91, p. 12,539-12,571.

Sieh, K., and Wallace, R.E., 1987, The San Andreas fault at Wallace Creek, San Luis Obispo County, California, *in* Hill, M.L., ed., Cordilleran Section of the Geological Society of America, Decade of North American Geology Centennial Field Guide, v. 1: Boulder, Colorado, Geological Society of America, p. 193-198.

Sieh, K.E., 1978a, Central California foreshocks of the great 1857 earthquake: Seismological Society of America Bulletin, v. 68, p. 1731-1749.

_____1978b, Slip along the San Andreas fault associated with the great 1857 earthquake: Seismological Society of America Bulletin, v. 68, p. 1421-1428.

Sieh, K.E., and Jahns, R.H., 1984, Holocene activity of the San Andreas fault at Wallace Creek, California: Geological Society of America Bulletin, v. 95, p. 883-896.

Silberling, N.J., and Roberts, R.J., 1962, Pre-Tertiary stratigraphy and structure of northwestern Nevada: Geological Society of America Special Paper 72, p. 58.

Sims, J. D., 1987, Late Holocene slip rate along the San Andreas fault near Cholame, California: Geological Society of America Abstracts with Programs, p. 451.

_____1989, Chronology of displacement on the San Andreas fault in central California--Evidence from reversed positions of exotic rock bodies near Parkfield, California: U.S. Geological Survey Open-File Report, [in press].

Sims, J.D., and Hamilton, J.C., 1989, Tectonic control of Pleistocene drainage patterns by the San Andreas fault, central California: Geological Society of America Abstracts with Programs, v. 21, p.144.

Sims, J.D., Yarnold, J.A., and Hamilton, J.C., 1988, Holocene fault activity west of the San Andreas fault in the Parkfield-Cholame area, central California [abs.]: Eos, Transactions, American Geophysical Union, v. 69, p. 1419.

Slemmons, D.B., 1957, Geological effects of the Dixie Valley-Fairview Peak, Nevada, earthquakes of December 16, 1954: Seismological Society of America Bulletin, v. 47, p. 353-375.

Slemmons, D.B., and Bell, J.W., 1987, 1954 Fairview Peak earthquake area, Nevada, *in* Hill, M.L., ed., Cordilleran Section of the Geological Society of America, Decade of North American Geology Centennial Field Guide, v. 1: Boulder, Colorado, Geological Society of America, p. 73-76.

Slemmons, D.B., Steinbrugge, K.V., Tocher, D., Oakeshott, G.B., and Gianella, V.P., 1959, Wonder, Nevada, earthquake of 1903: Seismological Society of America Bulletin, v. 49, p. 251-265.

Slemmons, D.B., Van Wormer, Douglas, Bell, E.J., and Silberman, M.L., 1979, Recent crustal movements in the Sierra Nevada-Walker Lane region of California-Nevada--Part I, Rate and style of deformation: Tectonophysics, v. 52, p. 561-570.

Smith, G.I., 1962, Large lateral displacement on Garlock fault, California, as measured from offset dike swarm: American Association of Petroleum Geologists Bulletin, v. 46, p. 85-104.

_____1989, IGC field trip T117--Quaternary geology of the Great Basin: Washington, D.C., American Geophysical Union, 78 p.

Smith, G.I., and Street-Perrott, F.A., 1983, Pluvial lakes of the Western United States, *in* Porter, S.C., ed., The late Pleistocene, v. 1 of Wright, H.E., Jr., ed., Late-Quaternary environments of the United States: Minneapolis, Minnesota, University of Minnesota Press, p. 190-212.

Smith, R.B., and Arabasz, W.J., 1979, Seismicity, tectonics, and crustal structure in Utah--Important aspects from new data: Special Publication, University of Utah Seismograph Stations, Department of Geology and Geophysics, p. 395-408.

Smith, R.B., and Bruhn, R.L., 1984, Intraplate extensional tectonics of the eastern Basin-Range--Inferences on structural style from seismic reflection data, regional tectonics, and thermal-mechanical models of brittle-ductile deformation: Journal of Geophysical Research, v. 89, p. 5733-5762.

Stahl, S.D., 1987, Mesozoic structural features in Sonoma Canyon, Sonoma Range, Humboldt and Pershing Counties, Nevada, *in* Hill, M.L., ed., Cordilleran Section of the Geological Society of America, Decade of North American Geology Centennial Field Guide, v. 1: Boulder, Colorado, Geological Society of America, p. 85-90.

Stein, R.S., and Thatcher, W., 1981, Seismic and aseismic deformation associated with the 1952 Kern County, California, earthquake and relationship to the Quaternary history of the White Wolf fault: Journal of Geophysical Research, v. 86, p. 4913-4928.

Stein, R.S., and Yeats, R.S., 1989, Hidden earthquakes: Scientific American, v. 260, p. 48-57.

Stewart, J.H., 1971, Basin and Range structure--A system of horsts and grabens produced by deep-seated extension: Geological Society of America Bulletin, v. 82, p. 1019-1044.

_____1972, Initial deposits of the Cordilleran geosyncline--Evidence of a late Precambrian (850 m.y.) continental separation: Geological Society of America Bulletin, v. 83, p. 1345-1360.

_____1980, Regional tilt patterns of late Cenozoic basin-range fault blocks, Western United States: Geological Society of America Bulletin, Part 1, v. 91, p. 460-464.

Sturm, P.A., 1980, The Great Salt Lake brine system, *in* Gwynn, J.W., ed., Great Salt Lake--A scientific, historical and economic overview: Utah Geological and Mineral Survey Bulletin 116, p. 147-162.

Suppe, J., 1985, Principles of structural geology: Englewood Cliffs, New Jersey, Prentice-Hall, 537 p.

Swan, F.H., III., Schwartz, D.P., and Cluff, L.S., 1980, Recurrence of moderate to large magnitude earthquakes produced by surface faulting on the Wasatch fault zone, Utah: Seismological Society of America Bulletin, v. 70, p. 1431-1462.

Taylor, G.C., and Bryant, W.A., 1980, Surface rupture associated with the Mammoth Lakes earthquakes of 25 and 27 May, 1980, *in* Sherburne, R.W., ed., Mammoth Lakes, California earthquakes of May 1980: California Division of Mines and Geology Special Report 150, p. 49-67.

Thatcher, W., 1975a, Strain accumulation and release mechanism of the 1906 San Francisco earthquake: Journal of Geophysical Research, v. 80, p. 4862-4872.

_____1975b, Strain accumulation on the northern San Andreas fault zone since 1906: Journal of Geophysical Research, v. 80, p. 4873-4880.

Thatcher, W., and Lisowski, M., 1987, Long-term seismic potential of the San Andreas fault southeast of San Francisco, California: Journal of Geophysical Research, v. 92, p. 4771-4784.

Thenhaus, P.C., and Barnhard, T.P., 1989, Regional termination and segmentation of Quaternary fault belts in the Great Basin, Nevada and Utah: Seismological Society of America Bulletin, v. 79, p. [in press].

Thompson, G.A., and Burke, D.B., 1973, Rate and direction of spreading in Dixie Valley, Basin and Range province, Nevada: Geological Society of America Bulletin, v. 84, p. 627-632.

Thompson, R.S., Benson, L., and Hattori, E.M., 1986, A revised chronology for the last Pleistocene lake cycle in the central Lahontan Basin: Quaternary Research, v. 25, p. 1-9.

Tocher, D., 1956, Movement on the Rainbow Mountain fault: Seismological Society of America Bulletin, v. 46, p. 10-14.

Van Horn, R., 1975, Largest known landslide of its type in the United States--A failure by lateral spreading in Davis County, Utah: Utah Geology, v. 2, p. 83-88.

Vedder, J.G., and Wallace, R.E., 1970, Map showing recently active breaks along the San Andreas and related faults between Cholame Valley and Tejon Pass, California: U.S. Geological Survey Miscellaneous Geologic Investigations Map I-574, scale 1:24,000.

Wahrhaftig, C., Morrison, R.B., and Birkeland, P.W., eds., 1965, Guidebook for field conference I--Northern Great Basin and California, International Association for Quaternary Research VIIth Congress; Lincoln, Nebraska, Nebraska Academy of Sciences, 165 p.

Wallace, R.E., 1978, Patterns of faulting and seismic gaps in the Great Basin province, *in*, Isacks, B.L., and Plafker, G., co-organizers, and Evernden, J.F., convener, Proceedings of Conference VI, Methodology for identifying seismic gaps and soon-to-break gaps, May 25-27, 1978: U.S. Geological Survey Open-File Report 78-943, p. 858-868.

_____1979, Map of young fault scarps related to earthquakes in north central Nevada: U.S. Geological Survey Open-File Report 79-1554, scale 1:125,000.

_____1984a, Patterns and timing of late Quaternary faulting in the Great Basin province and relation to some regional tectonic features: Journal of Geophysical Research, v. 89, p. 5763-5769.

_____1984b, Fault scarps formed during the earthquakes of October 2, 1915, in Pleasant Valley, Nevada, and some tectonic implications: U.S. Geological Survey Professional Paper, v. 1274-A, 33 p.

Wallace, R.E., and Whitney, R.A., 1984, Late Quaternary history of the Stillwater seismic gap, Nevada: Seismological Society of America Bulletin, v. 74, p. 301-314.

Weber, G.E., and Lajoie, K.R., 1977, Late Pleistocene and Holocene tectonics of the San Gregorio fault zone between Moss Beach and Point Ano Nuevo, San Mateo County, California: Geological Society of America Abstracts with Programs, v. 9, p. 524.

Wheeler, R.L., and Krystinik, K.B., 1988, Segmentation of the Wasatch fault zone, Utah--Summaries, analyses, and interpretations of geological and geophysical data: U.S. Geological Survey Bulletin 1827, p. 47.

Whitney, J.D., 1865, Geological survey of California, report of progress and synopsis of the field work from 1860 to 1864: California Geological Survey, Geology, v. 1, 498 p.

_____1872, The Owens Valley earthquake: Overland Monthly, v. 9, p. 120-140.

Wood, S.H., 1977, Distribution, correlation, and radiocarbon dating of late Holocene tephra, Mono and Inyo Craters, eastern California: Geological Society of America Bulletin, v. 88, p. 89-95.

Working Group on California Earthquake Probabilities, 1988, Probabilities of large earthquakes occurring in California on the San Andreas fault: U.S. Geological Survey Open-File Report 88-392, 62 p.

Zepeda, R.L., Keller, E.A., and Rockwell, T.K., 1986, Rates of active tectonics at Wheeler Ridge, southern San Joaquin Valley, California: Geological Society of America Abstracts with Programs, v. 18, p. 126.

Zischinsky, U., 1969, Uber Sackungen: Rock Mechanics, v. 2, p. 30-52.

Zoback, M.L., 1983, Structure and Cenozoic tectonism along the Wasatch fault zone, Utah, *in* Miller, D.M., Todd, V.R., and Howard, K.A., eds., Tectonics and stratigraphy of the eastern Great Basin: Geological Society of America Memoir 157, p. 3-27.

_____1987, Superimposed late Cenozoic, Mesozoic, and possible Proterozoic deformation along the Wasatch fault zone in central Utah, *in* Gori, P.L., and Hays, W.W., eds., Assessment of regional earthquake hazards and risk along the Wasatch front, Utah, volume I: U.S. Geological Survey Open-File Report 87-585, p. E-1 - E-43.

Zoback, M.L., Anderson, R.E., and Thompson, G.A., 1981, Cainozoic evolution of the state of stress and style of tectonism of the Basin and Range province of the Western United States: Philosophical Transactions of the Royal Society of London, v. A 300, p. 407-434.

Zoback, M.L., and Zoback, M.D., 1980, State of stress in the conterminous United States: Journal of Geophysical Research, v.85, p. 6113-6156.

Zones, C.P., 1957, Changes in hydrologic conditions in the Dixie Valley and Fairview Valley areas, Nevada, after the earthquake of December 16, 1954: Seismological Society of America Bulletin, v. 47, p. 387-396.